Technische Universität München
TUM School of Natural Sciences

Investigation of prokaryotic adrenergic protein targets in *Vibrio campbellii* & investigation of the catechol-reactive proteome

von

Angela-Maria Weigert Muñoz

München 2022

Technische Universität München
TUM School of Natural Sciences

Investigation of prokaryotic adrenergic protein targets in *Vibrio campbellii* & investigation of the catechol-reactive proteome

Angela-Maria Weigert Muñoz

Vollständiger Abdruck der von der TUM School of Natural Sciences
der Technischen Universität München zur Erlangung des akademischen Grades
einer

Doktorin der Naturwissenschaften (Dr. rer. nat.)

genehmigten Dissertation.

Vorsitz:	Prof. Dr. Cathleen Zeymer
Prüfer*innen der Dissertation:	1. Prof. Dr. Stephan A. Sieber
	2. Prof. Dr. Matthias Feige
	3. Assoc. Prof. Dr. Megan Wright

Die Dissertation wurde am 29.12.2022 bei der Technischen Universität München eingereicht
und durch die TUM School of Natural Sciences am 03.03.2023 angenommen.

You don´t have to see the whole staircase. Just take the first step.

- Martin Luther King

Danksagung

Zu allererst möchte ich mich bei meinem Doktorvater Prof. Stephan A. Sieber für die Betreuung meiner Arbeit bedanken, insbesondere für sein Vertrauen und seinen Rückhalt. In meiner Promotion hatte ich die Möglichkeit, ein methodisch vielseitiges und inhaltlich spannendes Thema zu bearbeiten, wobei ich die Freiheit hatte, viele eigene Ideen einzubringen. Meinen Horizont durfte ich auf Konferenzen und während eines kurzen Aufenthaltes an der Emory University in Atlanta, USA, erweitern. Für seine fortwährende fachliche wie außerfachliche Unterstützung bin ich sehr dankbar.

Weiterhin danke ich der Prüfungskommission dafür, dass sie sich die Zeit genommen hat, meine Arbeit zu begutachten.

Diese Arbeit wäre nicht möglich gewesen ohne den großartigen Beitrag einiger Kooperationspartner. Vor allem Elisabeth Hoyer, Kilian Schumacher und Prof. Kirsten Jung haben Expertise und eine Menge Arbeit in das Epinephrinprojekt fließen lassen. In diesem Projekt wurde ich weiterhin unterstützt durch Prof. Katja M. Taute und Dr. Marianne Grognot. Für ihre Arbeit bin ich allen sehr dankbar.
Annerose Kurz-Drexler und Dr. Daniela Vogt-Weisenhorn danke ich für die Präparierung der Mausneuronen. Kevin Meighen-Berger und Prof. Matthias Feige danke ich für die Durchführung der ER Stressassays. Lukas Niederegger und Prof. Corinna Hess danke ich für die Hilfe bei den CV Messungen. Diese Arbeiten waren für das Catecholprojekt unerlässlich.
Für diverse Auswertungen von Daten des „Hacker Workflows“ danke ich Dr. Stephan M. Hacker, dies war in beiden Projekten sehr hilfreich.

Auch innerhalb der Arbeitsgruppe gab es Kooperationen. Für seine Beharrlichkeit in den Alginatassays danke ich Patrick Allihn. Ricky Wirawan danke ich für die Fortsetzung dieses Projektes innerhalb einer herausragenden Masterarbeit und Markus Schwarz für dessen Übernahme. Jonas Drechsel danke ich für die großzügige Spende des Überfliegers DJ-1.
Für das kritische Lesen dieser Arbeit und ihre wertvollen Anmerkungen danke ich Till Reinhardt, Robert Macsics, Konstantin Eckel, Dietrich Mostert und Michael Zollo.
Für die gemeinsame Betreuung der HPLCs danke ich Thomas Gronauer, Max Bottlinger und Barbara Eyermann. Ines Hübner und Alexandra Geissler danke ich für die unkomplizierte Zusammenarbeit bei der Messung der HRMS Proben.
Mona Wolff, Katja Bäuml, Barbara Seibold und Christina Brumer danke ich dafür, dass sie jeden Tag den Doktoranden im Labor und der Bürokratie immens das Leben erleichtern.

Die Betreuung meiner Forschungspraktikanten hat mir großen Spaß gemacht, ich danke Juanita Ferreira Olmos, Larissa Tröbelsberger, Pedro Aragón Fernández und Elena Kratz für ihren Beitrag zu dieser Arbeit.

Meine Promotion begann in Lab C, in dem nur gelegentlich der Chickensong oder Vogelgesang den Freezerlärm übertönten. Dennoch hat es mit Theresa „the other ThAngela“ Rauh, Martin Pfanzelt, Pavel Kielkowski und Jan-Niklas Dienemann immer etwas zu lachen gegeben. Nach dem Umzug ins CPA war Till Reinhardt zunächst mein einziger Sitznachbar, zu dem ich mich gerne häufig für ein bestätigendes „wird schon passen“ umgedreht habe. Hin und wieder sorgten Fetzen von Denglisch von Stuart Ruddell, Meetings von Josef Braun, oder ein lautes „sooooo“ von Michael Zollo für Erheiterung in dieser Ecke der Auswertezone.
Dietrich Mostert, Ines Hübner, Jonas Drechsel, Patrick Allihn, Patrick Zanon, Robert Macsics und Till Reinhardt danke ich für bitterernste Spielerunden, das regelmäßige gemeinsame Versumpfen in der Kaffeeküche oder anderswo, das nächtliche Hüte basteln, oder andere Aktionen zum ästhetischen Nachteil Zanis.
Allen anderen Kollegen danke ich für die vielen fachlich relevanten sowie die nicht fachlich relevanten Gespräche beim Mittagessen, Kaffeerunden oder nach Feierabend, sowie für ihre Kollegialität und Hilfsbereitschaft im Labor. Dass über so viele Jahre eine so positive Arbeitsatmosphäre besteht, ist nicht selbstverständlich.

Schließlich danke ich meinen Eltern und meiner Schwester, die mich ständig unterstützen und mir während dieser Zeit den Rücken freigehalten haben. Mein größter Dank gilt Jonas, der mich fortwährend motiviert und der mich versteht wie niemand sonst.

Abstract

Catecholamine hormones are important mediators of stress and neurological signalling in eukaryotes. Beyond that, catecholamines are specifically sensed by bacteria and they trigger a variety of prokaryotic responses that are crucial for virulence and host colonisation, e.g., increased motility. Despite great research effort, the precise mode of action and the molecular targets of catecholamine hormones in bacteria are not well understood. The aim of the first part of this thesis was to identify protein targets of catecholamines in the aquatic pathogen *Vibrio campbellii* and to elucidate the cellular pathways modulated by these hormones. Initial bioactivity assays demonstrated a bipartite mode of action which consists of promotion of bacterial growth under iron-limited conditions and enhanced colony expansion on soft agar. The catecholamine hormone epinephrine, which carries a catechol group, promoted both growth under iron limitation and motility on soft agar. The clinical adrenergic drug phenylephrine, on the other hand, had no effect on growth as it does not contain an intact catechol group, but it still promoted motility. Moreover, catecholamine-dependent motility on soft agar was blocked by the adrenergic antagonist labetalol. To enable the identification of prokaryotic adrenergic protein targets by chemical proteomics, photoreactive probes were synthesised based on the structural scaffold of the catecholamine hormone epinephrine and the clinical drug phenylephrine. The identification of protein targets of both chemical probes in live *V. campbellii* by mass spectrometry revealed the chemotaxis coupling protein CheW as a major adrenergic target. *In vitro* analyses confirmed binding of epinephrine, phenylephrine, and labetalol with affinity constants in the sub-micromolar range. Consistent with these results, adrenergic compounds influenced the chemotaxis of *V. campbellii* towards glucose. Therefore, the results of this study highlight CheW as an as yet unknown adrenergic prokaryotic target. Moreover, they point toward a potential novel regulatory mechanism in which the chemotactic control is modulated by small molecule binding to CheW.

Besides catecholamines, many other biologically relevant compounds including drugs and plant secondary metabolites carry catechol moieties. The catechol group is prone to oxidation, leading to the formation of quinones which react with nucleophilic amino acid residues in proteins. Therefore, catechol compounds can post-translationally modify proteins and thus alter their activity. However, the scope of catechol protein reactivity is poorly understood. The aim of the second part of this thesis was to elucidate the proteome targeted by structurally diverse catechol compounds using competitive chemical proteomics. First, a broadly reactive minimalist catechol probe was designed based on dopamine. Labelling experiments in live

human cells confirmed broad protein reactivity of the probe. Next, labelling was performed in competition with the catecholamine hormone dopamine to reveal protein targets of the parent compound. Analysis of the modification introduced by the probe on the proteome revealed a previously unknown cysteine-selective protein modification by an *O*-methylated probe metabolite. This finding provides an explanation for the cysteine reactivity of 3-*O*-methyl catechols such as capsaicin. Labelling was performed in competition with a suite of structurally diverse catechols from drugs and plant secondary metabolites as well as capsaicin to identify their protein targets. These experiments revealed stark differences in protein binding across the catechol compounds as some demonstrated broad protein reactivity whereas others showed no binding. Proteins of the endoplasmic reticulum were overrepresented among proteins targeted by the probe and certain competitors. Specifically, protein disulphide isomerases and proteins involved in the unfolded protein response were targeted by the probe and by dopamine. Thus, a chemical proteomics strategy was developed to reveal the protein target scope of a suite of structurally diverse catechols with biological relevance.

Zusammenfassung

Katecholaminhormone sind wichtige Botenstoffe in der eukaryotischen Stressantwort und in neurologischen Signalprozessen. Darüber hinaus werden Katecholamine spezifisch von Bakterien erkannt und sie stimulieren unterschiedliche prokaryotische Antworten, die essentiell sind für Virulenz und Wirtsbesiedelung, wie z.B. Motilität. Trotz großen Forschungsaufwands ist die genaue Wirkungsweise von Katecholaminen in Bakterien nicht vollständig aufgeklärt. Das Ziel des ersten Teils dieser Arbeit war es, Zielproteine von Katecholaminen im aquatischen Erreger *Vibrio campbellii* zu identifizieren und die zellulären Signalwege aufzuklären, die durch diese Hormone aktiviert werden. Erste Bioaktivitätstests zeigten einen zweiseitigen Wirkmechanismus. Einerseits verstärkten Katecholamine bakterielles Wachstum unter Eisenlimitierung, andererseits förderten sie die Ausbreitung von Kolonien auf weichem Agar. Das Katecholaminhormon Epinephrin, das eine Katecholgruppe besitzt, förderte sowohl das Wachstum unter Eisenlimitierung, als auch die Motilität auf weichem Agar. Der klinisch eingesetzte adrenerge Agonist Phenylephrin dagegen hatte keinen Einfluss auf das Wachstum aber verstärkte dennoch die Motilität. Für die Identifizierung prokaryotischer adrenerger Zielproteine mittels chemischer Proteomik wurden photoreaktive Sonden basierend auf den Strukturen des Katecholaminhormons Epinephrin und des klinischen Arzneimittels Phenylephrin synthetisiert. Über Massenspektrometrie wurde das Chemotaxis-Kopplungsprotein CheW als eines der Hauptinteraktoren beider Sonden in lebenden *V. campbellii* ermittelt. *In vitro* Bindungsstudien mit aufgereinigtem CheW bestätigten die Wechselwirkung des Proteins mit Epinephrin, Phenylephrin und Labetalol mit Affinitätskonstanten im sub-mikromolaren Bereich. Damit übereinstimmend beeinflussten die adrenergen Substanzen die Chemotaxis zu Glukose. Somit stellen die Ergebnisse dieser Studie CheW als einen bisher unbekannten adrenergen prokaryotischen Rezeptor heraus. Darüber hinaus deuten sie auf einen möglicherweise neuartigen Regulationsmechanismus hin, in welchem die chemotaktische Kontrolle durch die Bindung chemischer Liganden an CheW beeinflusst wird.

Neben Katecholaminen enthalten viele weitere biologisch relevante Verbindungen wie zum Beispiel Arzneimittel und sekundäre Pflanzenstoffe Katecholgruppen. Die Katecholgruppe neigt zur Oxidation zum Chinon, welches mit nukleophilen Aminosäureresten in Proteinen reagieren kann. Daher können Katecholverbindungen Proteine posttranslational modifizieren und so ihre Aktivität verändern. Das Ausmaß der Proteinreaktivität von Katecholverbindungen ist jedoch nur unzureichend bekannt. Das Ziel des zweiten Teils dieser Arbeit war es, mithilfe

kompetitiver chemischer Proteomik das durch Katechole modifizierte Proteom zu entschlüsseln. Zunächst wurde, basierend auf der Struktur von Dopamin, eine minimalistische Katecholsonde mit umfangreicher Proteinreaktivität entwickelt. Diese umfangreiche Reaktivität wurde in Markierungsexperimenten in lebenden humanen Zellen bestätigt. Anschließend wurde die Markierung in Kompetition mit dem Katecholaminhormon Dopamin durchgeführt, wodurch Zielproteine der Ausgangsverbindung ermittelt werden konnten. Die Untersuchung der durch die Sonde im Proteome eingeführten Modifikation offenbarte eine bisher unbekannte cysteinselektive Proteinmodifikation durch einen *O*-methylierten Sondenmetaboliten. Diese Erkenntnis liefert eine Erklärung für die Cystein-Reaktivität von 3-*O*-Methylkatecholen wie zum Beispiel Capsaicin. Die Markierungsexperimente wurden in Kompetition mit einer Reihe strukturell verschiedener Katecholverbindungen aus Arzneimitteln und sekundären Pflanzenstoffen durchgeführt, sowie mit Capsaicin, um deren Zielproteine zu identifizieren. Bei diesen Experimenten zeigten sich deutliche Unterschiede im Ausmaß der Proteinmodifikation zwischen den verschiedenen Verbindungen, wobei einige Verbindungen eine breite Proteinreaktivität aufwiesen, während andere keine Bindung zeigten. Proteine des endoplasmatischen Retikulums waren unter den durch die Sonde und bestimmte Kompetitoren gebundenen Proteine überrepräsentiert. Insbesondere Proteindisulfidisomerasen und Proteine, die an der Antwort auf ungefaltete Proteine beteiligt sind, wurden von der Sonde und von Dopamin modifiziert. Zusammenfassend wurde eine Strategie entwickelt, um mithilfe chemischer Proteomik die Zielproteine einer Reihe strukturell unterschiedlicher Katechole mit biologischer Relevanz zu ermitteln.

Introductory remarks

Results of this thesis have been published as follows:

Weigert Muñoz, A.; Hoyer, E.; Schumacher, K.; Grognot, M.; Taute, K. M.; Hacker, S. M.; Sieber, S. A.;* Jung, K.,* Eukaryotic catecholamine hormones influence the chemotactic control of *Vibrio campbellii* by binding to the coupling protein CheW. *Proc Natl Acad Sci USA* **2022**, *119* (10), e2118227119.

Weigert Muñoz, A.; Meighen-Berger, K.; Hacker, S. M.; Feige, M. J.; Sieber, S. A., A chemical probe unravels the reactive proteome of health-associated catechols. *Manuscript in preparation.*

Journal publications not highlighted in this thesis:

Weigert Muñoz, A.; Zhao, W.;* Sieber, S.A.,* Monitoring host-pathogen interactions via chemical proteomics. *Manuscript in preparation.*

Schlagintweit, J. F.; Jakob, C. H. G.; Meighen-Berger, K.; Gronauer, T. F.; **Weigert Muñoz, A.**; Weiß, V.; Feige, M. J.; Sieber, S. A.; Correia, J. D. G.; Kühn, F. E., Fluorescent palladium(II) and platinum(II) NHC/1,2,3-triazole complexes: antiproliferative activity and selectivity against cancer cells. *Dalton Trans* **2021**, *50* (6), 2158-2166.

Jakob, C. H. G.;* **Weigert Muñoz, A.;*** Schlagintweit, J. F.; Weiß, V.; Reich, R. M.; Sieber, S. A.; Correia, J. D. G.; Kühn, F. E., Anticancer and antibacterial properties of trinuclear Cu(I), Ag(I) and Au(I) macrocyclic NHC/urea complexes. *J Organomet Chem* **2021**, *932*, 121643.

Zhao, W.; Cross, A. R.; Crowe-McAuliffe, C.; **Weigert Muñoz, A.**; Csatary, E. E.; Solinski, A. E.; Krysiak, J.; Goldberg, J. B.; Wilson, D. N.; Medina, E.; Wuest, W. M.; Sieber, S. A., The Natural Product Elegaphenone Potentiates Antibiotic Effects against *Pseudomonas aeruginosa*. *Angew Chem Int Ed Engl* **2019**, *58* (25), 8581-8584.

Karunakaran, S. C.; Cafferty, B. J.; **Weigert Muñoz, A.**; Schuster, G. B.; Hud, N. V., Spontaneous Symmetry Breaking in the Formation of Supramolecular Polymers: Implications for the Origin of Biological Homochirality. *Angew Chem Int Ed Engl* **2019**, *58* (5), 1453-1457.

Wright, M. H.; Tao, Y.; Drechsel, J.; Krysiak, J.; Chamni, S.; **Weigert Muñoz, A.**; Harvey, N. L.; Romo, D.; Sieber, S. A., Quantitative chemoproteomic profiling reveals multiple target interactions of spongiolactone derivatives in leukemia cells. *Chem Comm* **2017**, *53* (95), 12818-12821.

* authors contributed equally

Conference presentations:

Eukaryotic catecholamine hormones influence the chemotactic control of *Vibrio campbellii* by binding to the coupling protein CheW
Poster presentation, Gordon Research Seminar and Conference on Bioorganic Chemistry, 11th–17th June 2022, Proctor Academy, Andover, New Hampshire, United States

Investigation of interkingdom adrenergic signalling in bacteria using chemical proteomics
Poster presentation, Helmholtz Institute for Pharmaceutical Research Saarland (HIPS) Symposium, 20th May 2021, online

Investigation of interkingdom adrenergic signalling in bacteria using chemical proteomics
Poster presentation, EMBO Workshop: Chemical Biology, 3rd–5th September 2020, online

Table of contents

I – Background 1
1 Catechols – broad biological activity from chemical versatility 2
2 Chemical proteomics for the identification of small molecule protein targets 3
2.1 Characteristics of chemical probes for target identification 3
2.2 Click chemistry in chemical proteomics 4
2.3 Workflow variations 6
II – Investigation of prokaryotic adrenergic protein targets in *V. campbellii* 7
1 Catecholaminergic interkingdom signalling 8
1.1 The catecholaminergic endocrine system 8
1.2 Catechol compounds in bacteria 10
1.2.1 Catechols in siderophores 10
1.2.2 Catecholamines as interkingdom signals 11
1.2.2.1 Sensing via two-component systems 11
1.2.2.2 Catecholamines in bacterial chemotaxis 13
1.2.2.3 Catecholamines in iron supply 14
1.3 Aim of the project – identification of prokaryotic adrenergic targets 15
2 Results and discussion 16
2.1 Synthesis of chemical probes 16
2.1.1 First generation probe **EPI-P1** 16
2.1.2 Second generation probes 16
2.2 Bioactivity assays 18
2.2.1 Colony spread on soft agar 18
2.2.2 Investigation of siderophore properties 20
2.3 Target identification by chemical proteomics 21
2.3.1. Gel-based photoaffinity labelling 21
2.3.2 MS-based photoaffinity labelling with **EPI-P1** 22
2.3.3 MS-based photoaffinity labelling with **PE-P** and competition with **PE** 23
2.3.4 MS-based photoaffinity labelling with **PE-P** in competition with **EPI** and clinical antagonists 25
2.4 Investigation of the mechanism of **PE-P** binding 29
2.4.1 Labelling in presence of radical scavengers 29
2.4.2 Labelling in lysate of different strains 29
2.4.3 MS-based analysis of **PE-P** modification 30
2.4.4 Identification of CheW binding sites 31
2.5 Validation of CheW as adrenergic target 33
2.5.1 Catecholamine binding to purified CheW 33
2.5.2 Analysis of the CheW interaction network 33
2.5.3 Effects of **EPI** and **PE** on the VC proteome 35
2.5.4 Investigation of mechanisms behind catecholamine-dependent colony spread 36
2.6 Conclusion and outlook 40
3 Experimental procedures 43

3.1 Chemical synthesis 43
3.1.1 General remarks 43
3.1.2 Synthesis of 3-(but-3-yn-1-yl)-3-(2-iodoethyl)-3*H*-diazirine (**PCL-I**) 43
3.1.3 Synthesis of (*R*)-4-(2-((2-(3-(but-3-yn-1-yl)-3*H*-diazirin-3-yl)ethyl)amino)-1-hydroxyethyl)-benzene-1,2-diol (**EPI-P1**) 44
3.1.4 Amide coupling general protocol (second generation probes) 45
3.1.5 Synthesis of (*R*)-*N*-(2-(3,4-dihydroxyphenyl)-2-hydroxyethyl)hept-6-ynamide (**EPI-P2**) 45
3.1.6 Synthesis of *N*-(2-hydroxy-2-(3-hydroxyphenyl)ethyl)hept-6-ynamide (**PE-P**) 46
3.1.7 Synthesis of *N*-(2-hydroxy-2-(4-hydroxyphenyl)ethyl)hept-6-ynamide (**OA-P**) 46
3.2 Biochemical methods 48
3.2.1 General information 48
3.2.1.1 Chemical compounds 48
3.2.1.2 Bacterial culture 48
3.2.2 Bioactivity assays 51
3.2.2.1 Soft agar colony expansion assay 51
3.2.2.2 Growth assays 51
3.2.2.3 3D motility assay 51
3.2.2.4 3D chemotaxis assays 52
3.2.2.5 Data acquisition and analysis of 3D trajectories 52
3.2.2.6 Chemotaxis capillary assay 53
3.2.3 Proteomics methods 54
3.2.3.1 Preparative photolabelling with **PE-P** 54
3.2.3.2 Preparative photolabelling with **EPI-P1** 54
3.2.3.3 *In situ* analytical scale photolabelling 55
3.2.3.4 CuAAC for preparative scale photolabelling 55
3.2.3.5 CuAAC for analytical scale photolabelling 55
3.2.3.6 Analytical photolabelling in lysate with radical scavengers 56
3.2.3.7 Analytical photolabelling in lysate of different strains 56
3.2.3.8 SDS-PAGE 56
3.2.3.9 Enrichment, alkylation, and digest for photoaffinity labelling experiments 57
3.2.3.10 Chemoproteomics experiments with isoDTB tags 57
3.2.3.11 Co-IP 58
3.2.3.12 Whole proteome analysis 60
3.2.3.13 Peptide reconstitution (all proteomics experiments) 61
3.2.3.14 LC-MS/MS measurements 61
3.2.3.15 MS data analysis (photoaffinity labelling, co-IP, and full proteome experiments) 62
3.2.3.16 Analysis of isoDTB data 63
3.2.3.17 AlphaFold structure prediction 64
3.2.4 Biochemical and biotechnological methods 64

3.2.4.1 Construction of a plasmid coding for N-terminally His6-tagged CheW ... 64
3.2.4.2 Purification of 6His-CheW ... 64
3.2.4.3 Microscale thermophoresis ... 65
3.2.4.4 Strain construction ... 65
III – Investigation of the catechol-reactive proteome ... 67
1 Covalent protein modifications by catechols ... 68
1.1 Dopamine as a post-translational protein modification ... 68
1.1.1 Dopamine reactivity ... 68
1.1.2 Protein dopamination in Parkinson´s disease ... 70
1.2 Plant secondary metabolites ... 72
1.3 Aims – investigation of the catechol-reactive proteome ... 74
2 Results and discussion ... 76
2.1 Probe synthesis and evaluation ... 76
2.1.1 Probe design ... 76
2.1.2 Chemical synthesis ... 77
2.1.3 Evaluation of protein binding ... 77
2.2 Labelling in live cells ... 79
2.2.1 Labelling in Hek293 cells ... 79
2.2.2 Investigation of proteome-wide probe modification ... 81
2.2.3 Labelling in neuronal cells ... 82
2.2.4 Labelling in competition with different catechol compounds ... 85
2.3 Measurement of flavonoid redox potentials ... 91
2.4 Conclusion and outlook ... 93
3 Experimental procedures ... 95
3.1 Chemical methods ... 95
3.1.1 Chemical Synthesis ... 95
3.1.1.1 General remarks ... 95
3.1.1.2 Amide coupling general protocol ... 95
3.1.1.3 Synthesis of *N*-(3,4-dihydroxyphenethyl)pent-4-ynamide (**DA-P1**) ... 95
3.1.1.4 Synthesis of *N*-(3,4-dihydroxyphenethyl)hex-5-ynamide (**DA-P2**) ... 96
3.1.1.5 Synthesis of *N*-(3,4-dihydroxyphenethyl)hept-6-ynamide (**DA-P3**) ... 96
3.1.1.6 Synthesis of *N*-(4-hydroxyphenethyl)hex-5-ynamide **(DA-P4)** ... 97
3.1.2 Cyclic voltammetry ... 97
3.2 Biochemical Methods ... 98
3.2.1 General information ... 98
3.2.1.1 Chemical compounds ... 98
3.2.1.2 Cell culture ... 98
3.2.1.3 Preparation of primary mouse neurons ... 98
3.2.2 Intact protein mass spectrometry ... 99
3.2.3 Proteomics methods ... 100
3.2.3.1 Preparative scale labelling in Hek293 cells ... 100
3.2.3.2 Analytical scale labelling in Hek293 ... 100
3.2.3.3 Preparative and analytical scale labelling in primary mouse neurons 101
3.2.3.4 Labelling in heat-denatured lysate ... 101

3.2.3.5 CuAAC 101
3.2.3.6 SDS-PAGE 101
3.2.3.7 Enrichment, alkylation, and digest for target identification 102
3.2.3.8 Chemoproteomics experiments with isoDTB tags 102
3.2.3.9 Peptide reconstitution (all proteomics experiments) 102
3.2.3.10 LC-MS/MS measurements 103
3.2.3.11 Analysis of MS data from target identification experiments 103
3.2.3.12 Analysis of isoDTB data 103
3.2.3.13 GO term enrichment analyses 104
3.2.3.14 Heat maps 104
IV References 105
V Abbreviations 127
VI Appendix 131
1 NMR spectra 132
2 Protein tables 141

I – Background

1 Catechols – broad biological activity from chemical versatility

The 1,2-dihydroxybenzene moiety, also known as catechol, forms part of a breadth of natural products with biological relevance for plants, animals, and bacteria. Due to their chemical versatility, the cellular effects and biological modes of actions of catechols span a wide range (Figure I-1). As part of catecholamines, they are involved in animal stress response and neurological processes. Consequently, medicinal drugs that target these pathways often carry a catechol moiety. Its propensity to oxidation makes catechols antioxidative agents which are beneficial for cell physiology in general – however, oxidation products of dopamine (**DA**), for instance, are reactive and can post-translationally modify proteins leading to cell death, if excessive. In plants, the catechol group is part of polyphenol secondary metabolites which humans and animals consume regularly, and which impact their cell biology. Bacteria, on the other hand, use catechols to scavenge iron from the environment, making them indispensable for growth under nutrient limitation. Finally, catecholamines act as interkingdom signals between animal hosts and associated bacteria. This work focusses on different modes of actions of catechols in two biological kingdoms. In the first part, biological effects and protein targets of catecholamine hormones and related adrenergic drugs are investigated in bacteria. The second part explores covalent post-translational protein modifications (PTMs) by **DA** and plant secondary metabolites in human cells.

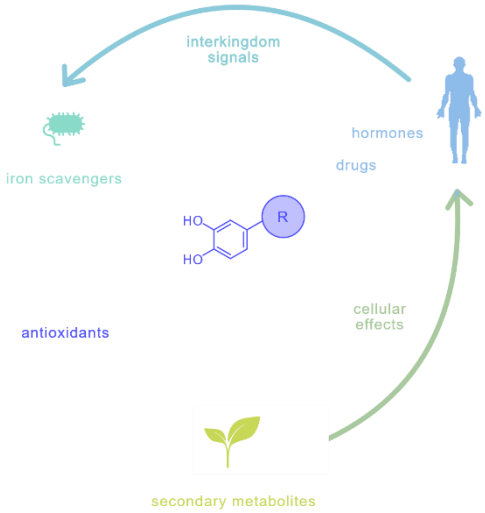

Figure I-1. Catechols exert diverse functions across biological kingdoms. R = residue.

2 Chemical proteomics for the identification of small molecule protein targets

Chemical proteomics is a versatile method to study the interaction of small molecules or larger biomolecules with proteins or whole proteomes in a global, unbiased way.[1-5] A compound of interest is derivatised to a chemical probe that enables the analysis of protein binding by visual or mass spectrometry (MS) methods. Small molecules are key players in cell physiology where they are critical for the function of proteins and the coordination of multicellular communities. Chemical proteomics has helped reveal previously unknown protein interactions with small molecules such as organic co-factors,[6-9] PTMs,[10,12-15] and hormone receptors.[11,16] Furthermore, chemical proteomics is frequently applied to understand the mode of action of natural products with antibacterial or anticancer activities,[17-21] or to characterise enzyme functions.[3]

2.1 Characteristics of chemical probes for target identification

To reveal protein interaction partners, the compound of interest is derivatised to a chemical probe that binds proteins irreversibly and can be ligated in a second step, for example, to a fluorescence reporter or an affinity handle. The fluorophore enables analysis of labelled proteins following SDS-PAGE separation by in-gel fluorescence scanning and the affinity handle facilitates enrichment and subsequent MS-based identification of target proteins (Figure I-2 A). For the probes to retain the protein targets of their parent compounds, it is essential that they display largely the same biological activity, therefore, modifications need to be minimal. One key feature of a chemical probe is the ability to form an irreversible bond to the protein interaction partner that is stable throughout the workflow. Intrinsically reactive compounds, typically electrophiles, or metabolically incorporated molecules such as PTMs require no further modification. Non-covalent binders on the other hand need to be equipped with photoreactive groups that generate broadly reactive species upon irradiation with UV light (Figure I-2 B). Conventional photocrosslinkers include benzophenones, aryl azides, and diazirines.[22] Their activation yields a diradical, a nitrene, and a carbene, respectively (Figure I-2 C). These species are extremely reactive and their selectivity for target proteins is achieved by proximity. As a large number of proteins in human cells has high propensity to interact with the photocrosslinker moiety largely independent of the probe structure,[23] it is indispensable to use adequate controls in photolabelling experiments to discriminate against unspecific off-targets. Typically, competition of the probe by the parent compound, enrichment

of probe-treated proteins compared to a negative control (e.g. a biologically inactive but structurally related small molecule) as well as biological validation of the identified targets are performed.

The second characteristic of chemical probes is a reporter tag, most typically a fluorescent dye or an affinity handle for the enrichment of labelled proteins. Historically, tags such as rhodamine dyes or biotin were directly incorporated in the probe,[4] however, these compounds suffered from poor cell permeability and were more likely to interfere with protein binding due to steric hindrance. More recent probes carry latent tags that perturb cell permeability to a lesser extent and can be chemically derivatised after cell lysis in the presence of detergents. Most commonly, probes are derivatised with an alkyne or azide to enable copper-catalysed azide-alkyne cycloaddition (CuAAC), also known as copper-catalysed click chemistry.

2.2 Click chemistry in chemical proteomics

The term *click chemistry* was coined for modular reactions that have very high yields, are wide in scope, and proceed at simple reaction conditions (e.g., in the presence of water and oxygen).[24] Their characteristically high driving force facilitates rapid, highly efficient, and selective reactions.[24] A prime example for click reactions is the 1,3-dipolar cycloaddition of an alkyne and an azide to form 1,2,3-triazoles,[24] which was developed by Rolf Huisgen,[25] although, it requires elevated temperatures, long reaction times, and lacks regioselectivity. These pitfalls were circumvented by the addition of a Cu(I) catalyst discovered by Morten Meldal and K. Barry Sharpless which enabled the selective formation of 1,4-disubstituted 1,2,3-triazole products in excellent yields, at room temperature, and in a variety of solvents including water (Figure I-2 D).[26-27] Whilst probe labelling may be performed in live cells provided the probes are cell-permeable, non-toxic, and metabolically stable enough, ligation of probe-labelled proteins to a reporter tag by CuAAC needs to be performed after lysis as Cu(I) is cytotoxic. This two-step approach is compatible with typical chemoproteomics experiments where labelling is read out by in-gel fluorescence or by MS methods. It should be noted that for projects that require ligation in live cells, for instance to track labelling by fluorescence microscopy,[12] the Bertozzi lab developed bioorthogonal chemistries such as the strain-promoted azide-alkyne cycloaddition (SPAAC) and the Staudinger ligation.[28] However, for gel- and MS-based chemoproteomics, the synthetic tractability and the fast, oxygen-tolerant reaction make CuAAC superior to SPAAC and Staudinger ligation, respectively. Notably, the

merit of click chemistry and its expansion to bioorthogonal chemistry was acknowledged with this year´s Nobel Prize in chemistry awarded to Barry Sharpless, Morten Meldal, and Carolyn Bertozzi.

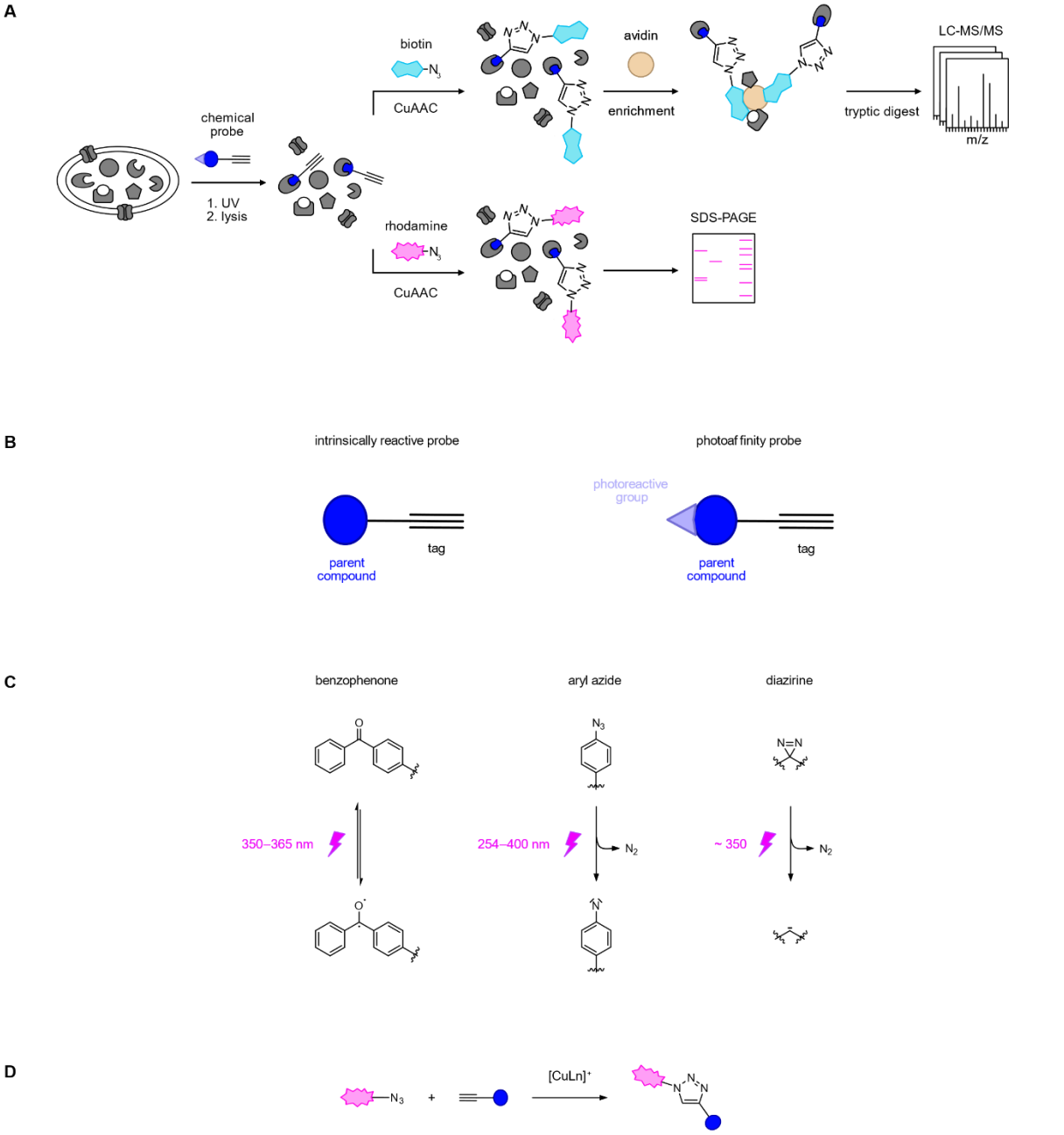

Figure I-2. Target identification by chemical proteomics. (A) Typical chemoproteomics workflow with photoaffinity labelling. The probe is added to live cells, incubated, and irradiated with UV light to enable covalent target engagement. For intrinsically reactive probes, irradiation is omitted. Following cell lysis, labelled proteins are ligated to reporter tags by copper-catalysed azide-alkyne cycloaddition (CuAAC). The tag can be a biotin affinity handle for avidin enrichment and MS-based identification of protein hits (top) or a rhodamine dye for in-gel fluoresce detection (bottom). (B) Schematic representation of an intrinsically reactive probe (left) and a photoaffinity probe (right). (C) Commonly used photoreactive groups and photoactivation. (D) Reaction scheme of CuAAC; Ln = ligand.[4,22,29-30]

2.3 Workflow variations

A valuable variation of chemoproteomics is a competitive approach where a covalent broad-spectrum probe labels an enzyme class or a specific amino acid residue. [2-3,31] This way, protein binding of larger numbers of (typically intrinsically reactive) compounds can be monitored by screening for a decrease in probe labelling rather than derivatising several molecules to chemical probes. Furthermore, this set-up enables the direct comparison of different structures and can give insights into different reactivities and selectivities.

Another variant uses isotopically labelled desthiobiotin[32] or biotin coupled to a TEV-cleavable linker[33] as affinity tags. Probe-modified peptides can be released from the affinity resin by elution with organic solvent or by proteolytic digest, respectively, and directly analysed and quantified by MS thanks to the isotopic labels. This is a very powerful method as it can give insights into the nature of modification and points to the protein-reactive species of the probe.

II – Investigation of prokaryotic adrenergic protein targets in *V. campbellii*

This chapter is based on the publication:

Weigert Muñoz, A.; Hoyer, E.; Schumacher, K.; Grognot, M.; Taute, K. M.; Hacker, S. M.; Sieber, S. A.; Jung, K., Eukaryotic catecholamine hormones influence the chemotactic control of *Vibrio campbellii* by binding to the coupling protein CheW. *Proc Natl Acad Sci USA* **2022**, *119* (10), e2118227119.

Contributions:

AW planned and conducted probe synthesis, growth assays, and all proteomics experiments and selected compounds for bioactivity assays. EH performed soft agar assays, CheW purification, and MST assays. KS performed capillary chemotaxis assays. MG and KMT planned, performed, and analysed 3D motility data. SMH analysed isoDTB data. SAS and KJ supervised the project. The CheW AlphaFold structure prediction was kindly provided by Dr. Anthe Janssen and Prof. Gerard van Westen from Leiden University.

1 Catecholaminergic interkingdom signalling

1.1 The catecholaminergic endocrine system

For humans and animals, arguably the most relevant catechol compounds are the catecholamines epinephrine (**EPI**), norepinephrine (**NE**), and **DA**, which regulate diverse processes in the brain and the peripheral nervous system. They share a common structure containing a catechol motif linked to a side-chain amine and are biosynthetically derived from tyrosine. **EPI** and **NE** act as hormones which are produced by the adrenal glands and secreted into the bloodstream from where they affect nearly all tissues. **NE** is furthermore a neurotransmitter which is also synthesised and released in the central nervous system. **DA** is largely produced in neuronal cell bodies where it acts as a neurotransmitter, although it is also present in the bloodstream. Their cognate receptors are G protein-coupled receptors (GPCRs), which are localised in the cellular membrane. Adrenergic receptors (or adrenoceptors) regulate the sympathetic nervous system and their activation by **NE** or **EPI** stimulates the so-called "fight or flight" response, which is characterised by an increase in heart rate, energy mobilisation, and redistribution of blood, amongst others. **DA**, on the other hand, is sensed by **DA** receptors which are primarily located in the brain. Thus, the dopaminergic system controls mainly neurological processes including motivation, motor control, and cognition.

The pharmacological activation of catecholaminergic GPCRs generally consists of non-covalent ligand binding to the extracellular receptor domain. This brings about a change of the receptor conformation inside the cells[34] which activates G proteins in the cytoplasm and results in altered levels of intracellular messengers such as cAMP or signalling lipids. Catecholaminergic antagonists are frequently used clinical drugs that block the activation by endogenous ligands.[35] Human adrenergic receptors are classified as α-type or β-type receptors, which are further divided into two to three subtypes. Similarly, there are two major classes of **DA** receptors, the D_1-like and the D_2-like family, each with several subtypes.[36] The subtypes transfer the signal to different signal relay pathways via varying G proteins which increases the variety of physiological effects and fine-tunes catecholaminergic signalling across tissues.

Both the adrenergic and dopaminergic systems are pharmaceutical targets of many clinical drugs that have varying selectivity for the receptor subtypes. Often, adrenergic drugs share a certain structural similarity with the catecholamines by retaining the catechol moiety (Figure II-1). Examples for this are dobutamine (**DB**) and isoprenaline (**IP**), both of which activate adrenoceptors, but also drugs that act on enzymes such as carbidopa (**CD**), or levodopa

(**LD**), a **DA** prodrug, and more. Interestingly, non-catechol analogues that carry only one hydroxy group can also have agonistic effects on adrenergic receptors, such as phenylephrine (**PE**) and octopamine (**OA**). **PE** is a clinically applied agonist of the α_1-adrenergic receptor. **OA** is a neurotransmitter in invertebrates where it is sensed by specific GPCRs. Beyond that, trace amounts are also present in mammals and pharmacological activity on adrenergic receptors has been observed.[37-38] Similarly, in the α- and β-antagonist labetalol (**LAB**) the catechol group is replaced by a hydroxybenzamide and in the β-blocker propranolol (**PRO**) by a naphthyl group. This demonstrates that the catechol group is common not only in hormones but also in clinical drugs. However, some examples shown in this section illustrate that an intact catechol group is not strictly required for protein receptor binding.

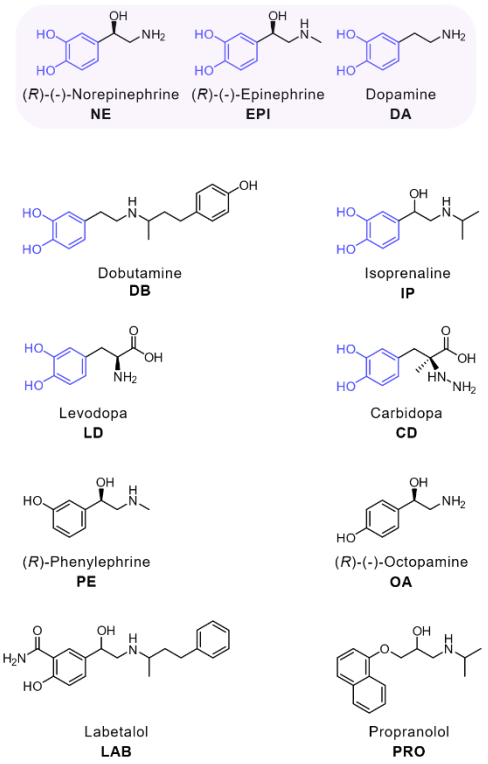

Figure II-1. Structures of catecholamines and related drugs. The catechol moiety is highlighted in blue. Note that **DB**, **IP**, **LAB**, and **PRO** are clinically applied as stereoisomeric mixtures.

1.2 Catechol compounds in bacteria

1.2.1 Catechols in siderophores

Iron is essential for the growth of any organism and bacteria require 10^{-5}–10^{-7} M ferric iron. As in most habitats the iron concentration is magnitudes lower,[39] bacteria rely on diffusible iron chelating small molecules, termed siderophores, to obtain it from their environment. Ferric siderophore complexes are sensed by bacterial receptors and taken up to release the iron into the cytosol. Among the typical iron-chelator motifs in bacterial siderophores are hydroxamates and catechols.[39] Common siderophores of Gram-negative bacteria such as *Escherichia coli* and *Salmonella enterica* are enterochelin (also known as enterobactin), a triscatechol that forms a hexadentate ligand with iron,[40-41] and its glucosylated derivative salmochelin.[42] More examples of catechol siderophores include corynebactin (*Corynebacterium glutamicum*, *Bacillus subtilis*),[43-44] vibriobactin from *Vibrio cholerae*,[45] azotochelin,[46] protochelin,[47] aminochelin (all three from *Azotobacter vinelandii*),[48] and itoic acid (*B. subtilis*, Figure II-2).[49]

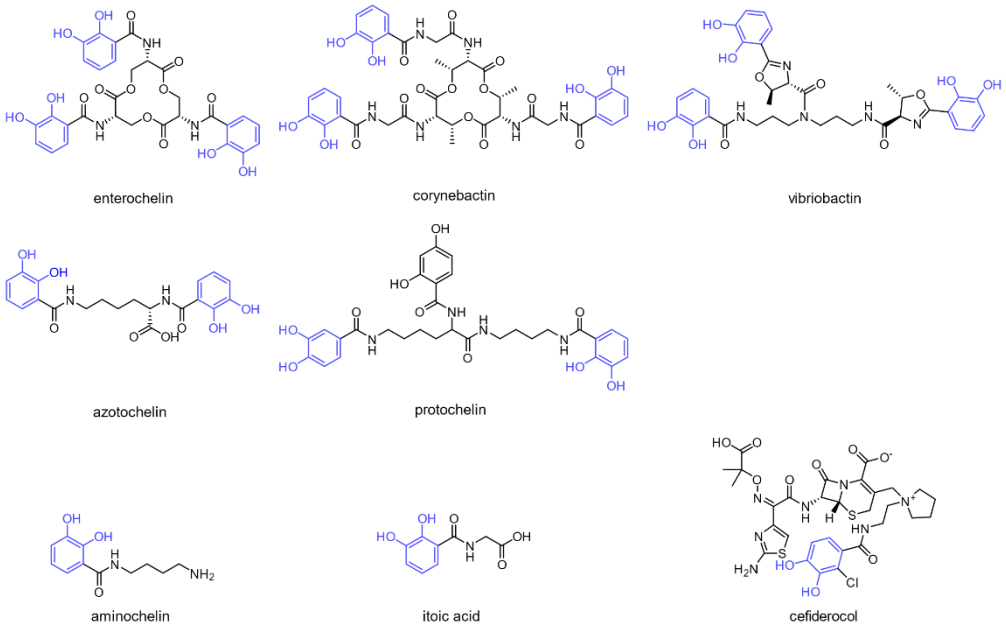

Figure II-2. Examples of catechol siderophores. The catechol group (blue) is a common motif in bacterial siderophores.[40-50]

Bacteria further enhance their competitive advantages by utilising other iron chelators from the environment in addition to their own siderophores. These so-called *xenosiderophores* may be scavenged from other species,[51] plant catechol polyphenols,[52] or host catecholamine hormones.[53-54] In the body fluids of eukaryotes, high-affinity iron-binding proteins such as transferrin maintain extremely low levels of available iron to restrict bacterial growth, a strategy termed *nutritional immunity*.[55] To circumvent this challenge, bacteria use enterobactin,

structurally related catechols, and even host catecholamines to remove iron from transferrin to restore growth despite iron limitation.[53,56-57]

It is noteworthy that the range of molecules taken up as xenosiderophores appears to be quite broad. This is exploited in the design of *Trojan horse* antibiotics, where a siderophore moiety is conjugated to a drug to improve its cellular permeability. The marketed antibiotic cefiderocol, for instance, is a cephalosporin-catechol conjugate (*Fetroja*®) that is taken up via the siderophore-iron transport pathway of Gram-negative aerobic bacteria.[50] These examples highlight how the iron-binding properties make catechols an important bioactive molecule at the interface of bacteria and their environment.

1.2.2 Catecholamines as interkingdom signals

Interkingdom signalling refers to the chemical communication between organisms belonging to different biological kingdoms. As **EPI** and **NE** modulate intestinal physiology, these hormones are present at high concentrations (micromolar) in the gastrointestinal tract, where a great number of bacteria is constantly exposed to them.[58] In general, the co-evolution of eukaryotic organisms and microbes has fostered a breadth of small molecule-based interactions that facilitate the bidirectional molecular crosstalk across the two biological kingdoms and are essential for successful host colonisation by both symbiotic and pathogenic bacteria.[58] Evidence that host-associated animal hormones can be sensed by opportunistic bacterial pathogens as signals to adjust the expression of specific virulence genes,[59] for example, via specific receptors,[11,15,60-61] has sparked major interest in this field of research. Specifically, catecholamine hormones modulate a variety of biological processes in prokaryotes, that are often associated with virulence.[53,62-64] The mode of action of prokaryotic adrenergic signalling most likely involves different molecular mechanisms that shall be discussed in the following.

1.2.2.1 Sensing via two-component systems

There is evidence that certain opportunistic pathogens such as *Pseudomonas aeruginosa* and enterohaemorrhagic *E. coli* (EHEC) sense host hormones via two-component systems.[11,15,60-61] Two-component systems are widespread signalling sensors in bacteria and consist of a transmembrane sensor domain and a cytoplasmic response regulator (Figure II-3).[65] They commonly sense signals in the periplasm or extracellular space and trigger the activation or

repression of gene transcription. The typically dimeric sensor is connected to an intracellular histidine kinase domain which autophosphorylates upon ligand binding and relays the phosphoryl group to an aspartyl residue of the response regulator. The latter commonly has a DNA-binding domain which acts as a transcription factor and thus directly regulates gene expression.[65]

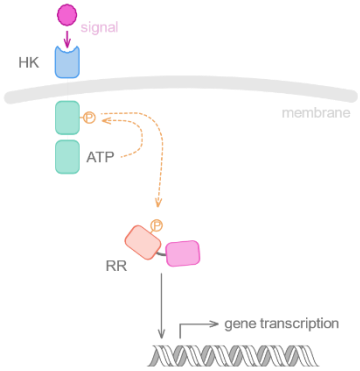

Figure II-3. Schematic representation of a prototypical two-component system. The binding of an extracellular signal (pink circle) to the histidine kinase (HK) sensory domain (blue) triggers its autophosphorylation at the cytoplasmic side (green rectangles). The phosphoryl group (orange circle) is transferred to the receiver domain (red rectangle) of the response regulator (RR). Phosphorylated RR binds to the DNA and initiates the transcription of target genes. Dashed, orange arrows indicate phosphoryl transfers. Adapted with modifications from Capra and Laub[66] and Allihn *et al*.[15]

The notion that catecholamines are sensed by a specific prokaryotic adrenergic receptor is corroborated by the observation that certain antagonists of the human receptors also antagonise adrenergic effects in bacteria.[60,67-68] Early work from the Sperandio group identified two two-component systems, QseBC and QseEF, as potential prokaryotic adrenoceptors in EHEC. In vitro autophosphorylation assays using the purified histidine kinase QseC in liposomes revealed activation by **EPI** and **NE** that could be blocked by the α-adrenergic antagonist phentolamine but not by the β-blocker **PRO**.[60] Congruently, EHEC activated transcription of flagella and motility genes in response to **EPI** but no longer in the *qseC* knock-out mutant,[68] although it should be noted that deletion of *qseC* lead to an overall loss of virulence in animal models.[60] In an analogous experimental approach, QseE, was also discovered to respond to **EPI**.[61] QseBC and QseEF are global regulators of the expression of genes related to flagella, motility, and many more that are critical for EHEC virulence.[58,61] Moreover, QseBC also senses the quorum sensing signal AI-3,[60,69] therefore, QseBC is a potential intersection of interkingdom and bacterial signalling.

These reports entailed a suite of studies seeking to corroborate QseC and QseE as global prokaryotic adrenergic receptors and claiming that homologues mediate adrenergic responses also in other species, sometimes generating inconclusive results. For instance, increased *V. cholerae* motility was observed in the presence of **EPI** and **NE**.[70] The authors proclaimed a

protein with 29% sequence identity of *E. coli* QseC as adrenergic receptor, although these effects were not abolished in a knockout mutant of the corresponding gene.[70] A similar study in *V. campbellii* found that **NE** and **DA** promoted motility and other virulence-associated processes but could not identify a receptor.[71] Moreira *et al*. reported that catecholamines promoted *S. enterica* serovar Typhimurium virulence via QseC by comparing the transcription of QseC-dependent genes after infection of **EPI**/**NE**-free mice compared to wild-type.[72] Another study in *S.* Typhimurium showed an increase in soft agar motility in the presence of **NE** and reduced virulence when the QseC homologue was deleted, however, both observations could not functionally be correlated.[73] A follow-up study seeking to do so found that mutants of every component of the QseBC two-component system as well as QseE still responded to **NE** with increased motility.[74] This was supported by others reporting that several species including EHEC were still responsive to catecholamines after these genes were knocked out.[70,75-77] It is plausible that the prokaryotic adrenergic response could be mediated by multiple receptors.[62] Furthermore, it is conceivable that there are other, as yet unexplored bacterial pathways that contribute to catecholamine signalling and virulence independent of two-component systems.

1.2.2.2 Catecholamines in bacterial chemotaxis

Others have observed a role of catecholamines in chemotaxis, a process in which bacteria navigate along chemical gradients towards attractants and away from repellents.[78-80] Importantly, chemotaxis can substantially contribute to host invasion and infectivity of pathogens.[81-83] The individual components of the chemotaxis signalling cascades can vary largely across bacterial species but typically, the core of the chemotaxis complex is constituted by a transmembrane chemoreceptor (methyl-accepting chemotaxis protein, MCP) and a cytoplasmic histidine kinase CheA, which are bridged by the coupling protein CheW (Figure II-4).[84] The MCP senses extracellular stimuli and triggers the autophosphorylation of CheA in response. In *E. coli,* the phosphoryl group is ultimately transferred to the response regulator CheY which induces clockwise rotation of the flagellar motor resulting in an increase of the tumbling frequency that reorients the cell.[84] Unphosphorylated CheY, on the other hand, disconnects from the flagellar motor which promotes counter-clockwise rotation and minimises bacterial tumbling, leading to prolonged periods of straight swimming. In most species, CheA phosphorylation is inhibited by attractants (straight swimming) and stimulated by repellents (tumbling).[84]

A study from the Sourjik group[85] found that **NE** was a weak attractant at low concentrations but behaved as a repellent at higher concentrations (≥ 1 mM) in *E. coli*. Furthermore, the two major MCPs, Tar and Tsr, mediated opposite responses, which contrasts with the behaviour of conventional chemotactic signals that specifically bind to the periplasmic sensor domain.[84] The authors therefore proposed that catecholamines might be sensed indirectly, although they emphasised that the response was specific and discriminated against chemically related compounds.[85]

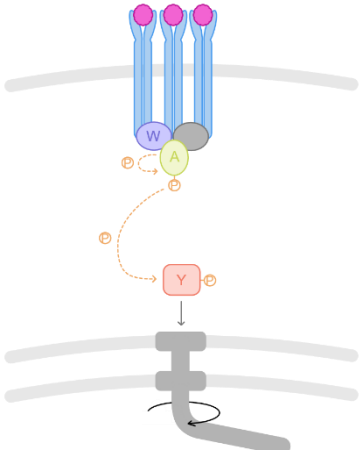

Figure II-4. Core components of a typical chemotaxis complex. Transmembrane chemoreceptors (blue) canonically sense extracellular signals (pink circles) that bind to the sensory domain. Intracellularly, chemoreceptors are connected to the histidine kinase CheA (green oval) via the scaffold protein CheW (purple oval). Receptor stimulation triggers a change in conformation that is transmitted to CheA via CheW. This results in CheA autophosphorylation and consequent transfer of the phosphoryl group (orange circle) to CheY (red rectangle). Phosphorylated CheY binds to the flagellar motor and induces clockwise flagellar rotation and increases bacterial tumbling rate. Note that details such as default rotation direction vary across species. Dashed, orange arrows indicate phosphoryl transfers. Simplified adaptation from Bi *et al.*[84]

1.2.2.3 Catecholamines in iron supply

Catechols in general and specifically catecholamines are known to act as surrogate siderophores (see section II-1.2.1). As a consequence, they promote bacterial growth under iron-restricted conditions as they are encountered in the host. Experimentally, these conditions are typically mimicked by the addition of serum to the bacterial growth medium which contains high-affinity iron binding proteins such as transferrin.[71,86-87] Since iron in general has extensive effects on the cell[62] and siderophores can be critical for pathogenicity,[88] it is plausible that the modulation of cellular iron might also contribute to catecholaminergic responses other than growth.

This section highlights that adrenergic responses in bacteria are most likely multi-layered and it is crucial to consider the different effects and chemical properties of catechols (e.g., iron binding, covalent protein modification) in experiment design.

1.3 Aim of the project – identification of prokaryotic adrenergic targets

The two-component systems QseBC and QseEF are considered prokaryotic adrenergic receptors in EHEC,[60-61] however, uncertainties remain as to whether there are additional receptors,[62] or about the role of homologues in other species.[73] One example is *Vibrio campbellii* (previously *Vibrio harveyi*) ATCC BAA-1116,[89] a marine, motile, bioluminescent γ-proteobacterium, and an opportunistic pathogen for fish, shrimp, squid, and other marine invertebrates.[90] Catecholamines not only promoted its growth under iron-limited conditions but also other biological processes with relevance for virulence such as siderophore production, biofilm formation, and swimming motility.[71] As observed in other species,[60,67-68] effects were reversible by clinical antagonists of human adrenoceptors. In this case, α-blockers including **LAB** but not the β-blocker **PRO** inhibited motility promotion by **NE**, suggesting that catecholamines act via a specific receptor.[71] However, the identity of an adrenergic receptor in this species was not revealed.

The first part of this thesis aims to elucidate the cellular pathways behind catecholamine-promoted motility in *V. campbellii* and to identify the associated protein receptor using chemical proteomics. The focus was set on motility because it is crucial for symbiotic as well as pathogenic bacteria to colonise their host and required for *Vibrio* to establish virulence.[91] The choice of organism was based on work by the Sperandio group, which proposed that adrenergic effects intersect with quorum sensing via QseC binding[60] as *V. campbellii* is an important model organism in this area of research.[92-94]

More precisely, the goal was to apply chemical proteomics to identify a protein that acts as a prokaryotic adrenergic receptor in a pharmacological sense. Therefore, the protein in question should show affinity to catecholamine hormones as well as to clinical antagonists that block motility enhancement by the hormones. Moreover, it was important to disentangle the effects associated with the potential protein of interest from those resulting from altered iron supply. As outlined in section II-1.1, **PE**, and potentially **OA**, target adrenergic receptors although they do not contain a catechol group. Therefore, this study focussed on catecholamines, adrenergic antagonists, and the non-catechol agonists **PE**, and **OA**.

2 Results and discussion

2.1 Synthesis of chemical probes

2.1.1 First generation probe **EPI-P1**

In order to perform target identification by chemical proteomics, synthesis of a chemical probe was required. To facilitate the identification of non-covalent protein interactors, a photoreactive group and an alkyne were incorporated. Since *V. campbellii* (VC) responded to both **NE** and **EPI** in preliminary bioactivity assays (see section II-2.2.1), the photocrosslinker was attached by alkylation of the **NE** amino group.[95] For this, a commercially available minimalist photocrosslinker was converted from an alcohol **PCL-OH** to the iodide **PCL-I** via *Appel* reaction following a published protocol.[29] The iodination product **PCL-I** was obtained in 62% yield. Next, **NE** was alkylated with **PCL-I**. This reaction was performed in DMF at 70 °C for 17 h in the absence of base to avoid decomposition of **NE**. **EPI-P1** was obtained in 62% yield (Scheme II-1 A). Purification was performed by flash column chromatography in the presence of acetic acid to stabilise the product which resulted in residual acid (42% [w/w]) in the final product that could not be removed without decomposition of the probe.

2.1.2 Second generation probes

Catecholamines are prone to oxidation to reactive *ortho*-quinones which are subject to an intra- or intermolecular nucleophilic attack by the side chain amine. This can be avoided by converting the amine to an unreactive derivative. A second-generation probe was obtained attaching an alkyne handle by acylation of the **NE** amino group which indeed resulted in more stable products and more facile purification (Scheme II-1 B). Amide coupling was performed using EDC·HCl and HOBt in the presence of TEA and yielded **EPI-P2** in 16% yield.

To obtain structure-activity data in subsequent biological assays, probes were also synthesised based on **OA** and **PE** analogously to **EPI-P2**. It was important to apply probes that cannot act as siderophores to reveal iron-independent adrenergic effects. Non-catechol probes were synthesised by acylation of norphenylephrine (**NP**) to **PE-P** and of **OA** to **OA-P** using the same conditions as for **EPI-P2**. **PE-P** and **OA-P** were obtained in 65% and 54% yield, respectively. The yield of the non-catechol probes was higher in comparison to **EPI-P2**, probably due to increased stability of the starting material.

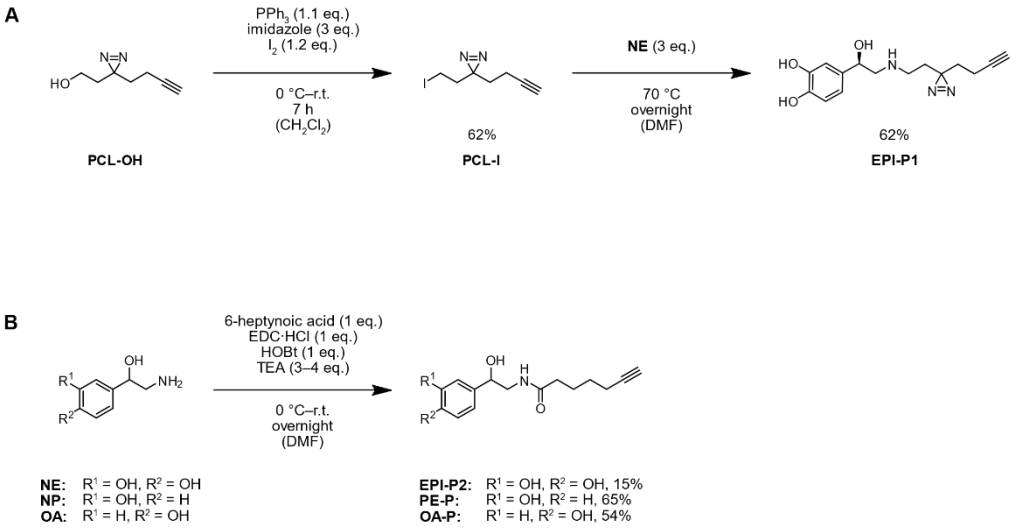

Scheme II-1. Synthesis of adrenergic probes. (A) Synthesis of first-generation probe **EPI-P1**. (B) Synthesis of second-generation probes **EPI-P2**, **PE-P**, and **OA-P**. PPh_3 = triphenylphosphine; eq. = equivalents; DMF = *N*,*N*-dimethylformamide; EDC·HCl = 1-(3-dimethylaminopropyl)-3-ethylcarbodiimide hydrochloride; HOBt = hydroxybenzotriazole; TEA = triethylamine.

2.2 Bioactivity assays

2.2.1 Colony spread on soft agar

Yang *et al*. observed that **NE** promoted VC motility by measuring the diameter of a bacterial colony incubated on semisolid agar containing **NE**.[71] This protocol provided a quick first read-out of potential catecholaminergic effects. Therefore, VC was incubated on semisolid agar containing **NE**, **EPI**, **PE**, or **OA** (50 µM, Figure II-5 A and B). Consistent with the literature, **NE** slightly increased the swimming halo to 1.08 ± 0.02 compared to the solvent control (average of six independent replicates ± standard deviation). The effect of **EPI** was stronger as the diameter was increased to 1.27 ± 0.01. **PE**, although lacking one hydroxy group, had a comparably strong effect (1.22 ± 0.01), which had not been reported previously. This finding was especially intriguing as it opened up the possibility to make a **PE**-derived active chemical probe incapable of complexing iron but still promoting motility. Furthermore, it indicates that motility is enhanced independently of the siderophore properties of catecholamines in this experimental set up. Interestingly, **OA** did not significantly change the colony diameter (0.93 ± 0.03), highlighting the importance of the position of the hydroxyl group.

Prokaryotic catecholaminergic responses are often reported to be sensitive to certain adrenergic antagonists, which corroborates that they are mediated via a specific receptor. Yang *et al*. observed that the α- and β-antagonist **LAB** blocks **NE** activity but not the β-blocker **PRO**.[71] Therefore, **LAB** and **PRO** were tested (50 µM, Figure II-5 C). **LAB** alone slightly reduced the motility halo relative to the solvent control (0.92 ± 0.01). Bacteria treated with **LAB** in combination with either **EPI**, **NE**, or **PE** (50 µM each), swam to 0.92 ± 0.01, 0.99 ± 0.02, and 0.97 ± 0.01 compared to the solvent control. The difference of **LAB** alone compared to **LAB** plus agonist was statistically not significant (one-way ANOVA with Tukey's post hoc test), suggesting that **LAB** indeed blocked catecholamine activity and, hence, acted as an antagonist. **PRO** (50 µM) alone did not affect the halo diameter compared to the solvent control (1.01 ± 0.00). **PRO** in combination with either **EPI**, **NE**, or **PE** (50 µM each) showed a comparable increase in colony halo as in the absence of **PRO** as the halo was increased to 1.20 ± 0.13, 1.11 ± 0.03, and 1.27 ± 0.02 compared to the solvent control, respectively. These values were significantly different from samples treated with **PRO** alone, pointing out that **PRO** is not an antagonist of catecholamine-dependent motility.

Finally, the chemical derivatives **EPI-P1**, **EPI-P2**, **PE-P**, and **OA-P** were studied (50 µM except **EPI-P1** at 60 µM, Figure II-6 D). Satisfyingly, **EPI-P1** and **PE-P** largely retained the activity of the parent compound (1.29 ± 0.02 and 1.12 ± 0.01 halo increase, respectively).

EPI-P2 and **OA-P** only showed a weak increase (1.04 ± 0.01 and 1.06 ± 0.01, respectively). Interestingly, **OA-P** gained some activity compared to its parent compound, possibly resulting from the derivatisation at the amino group. **EPI-P1** and **PE-P** therefore provided suitable probes for the identification of target proteins.

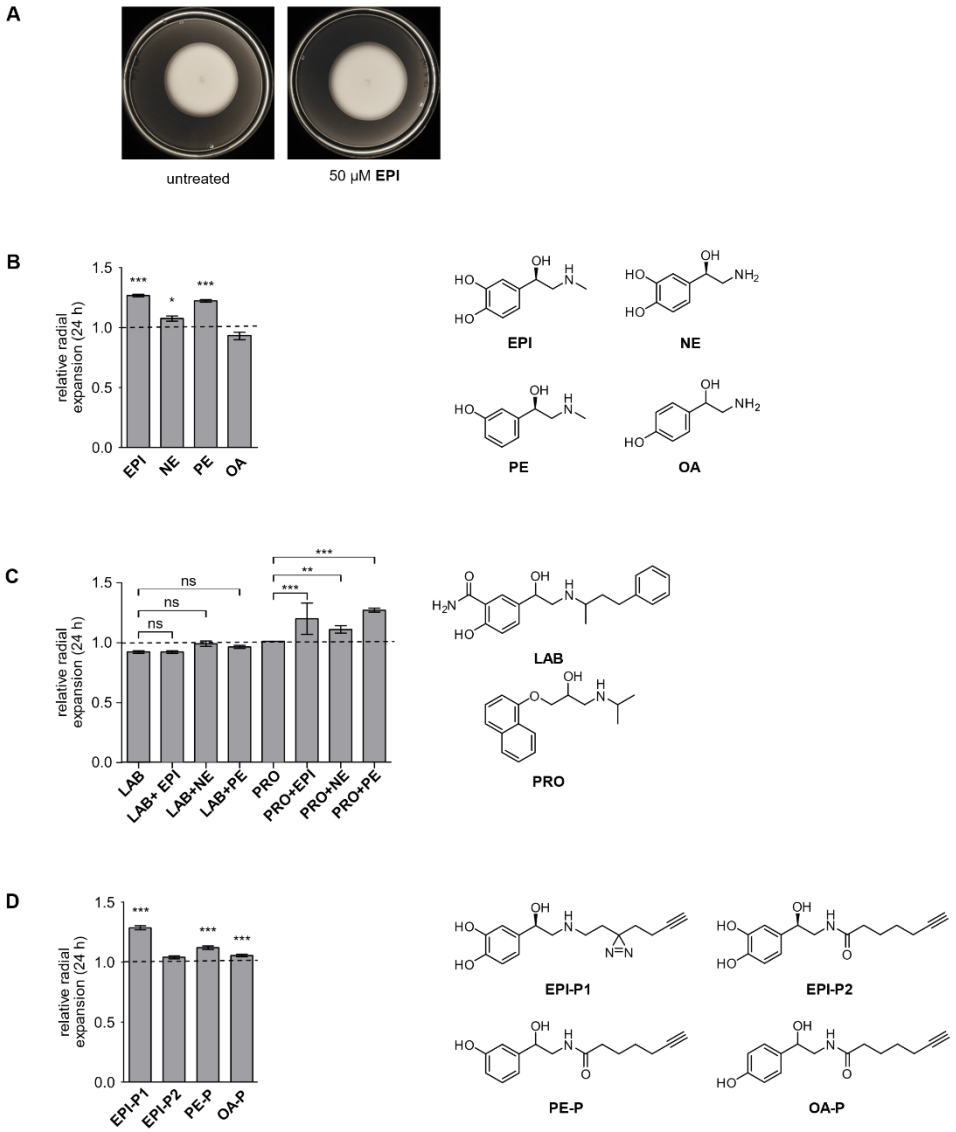

Figure II-5. Effects of catecholamines and related compounds on soft agar colony expansion. (A) Images show VC colonies treated with 50 µM **EPI** and an untreated control. (B) Swimming halo diameters of VC treated with parent compounds **EPI**, **NE**, **PE**, and **OA**. Significance is indicated relative to the respective solvent control. (C) Swimming halo diameters of VC treated with adrenergic antagonists **LAB** and **PRO** alone or in combination with **EPI**, **NE**, or **PE**. Significance is indicated relative to treatment with the respective antagonist alone. (D) Swimming halo diameters of VC treated with chemical probes **EPI-P1**, **EPI-P2**, **PE-P**, and **OA-P**. Significance is indicated relative to the respective solvent control. All compounds were added at 50 µM except **EPI-P1** at 60 µM. Radial expansions were normalized to an untreated control. Error bars represent standard deviation, n = 6 independent experiments. Significance was determined performing a one-way ANOVA with Tukey's post hoc test (ns = not significant, * = $p < 0.05$, ** = $p < 0.01$, *** = $p < 0.001$). Experiments were performed by E. Hoyer (LMU). Adapted from Weigert Muñoz *et al.*[16]

2.2.2 Investigation of siderophore properties

Catecholamines promote bacterial growth under iron-limited condition by acting as surrogate siderophores which restore cellular iron supply. **EPI**, **PE**, and the chemical probes **EPI-P1**, **EPI-P2**, **PE-P**, and **OA-P** were next tested for their siderophore properties in VC grown in full growth medium (LB35) supplemented with 30% (v/v) adult bovine serum. The latter contains high-affinity iron binding proteins such as transferrin that restrict bacterial growth.

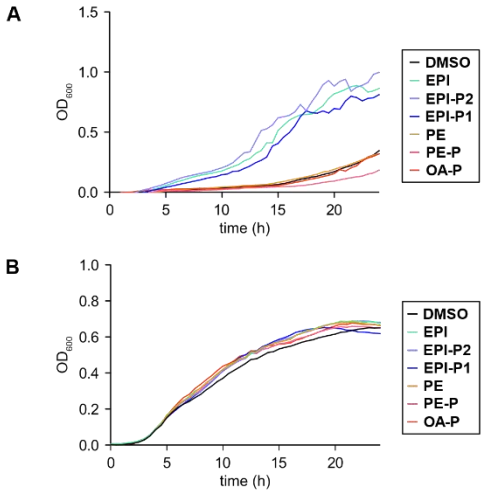

Figure II-6. Effects of catecholamines and related compounds on VC growth under iron-limited conditions. (A) Growth in LB35 medium supplemented with 30% (v/v) adult calf serum and in (B) serum-free LB35. VC was grown in a 96-well microtiter plate with interval shaking at 30 °C in the presence of compounds (50 µM). Data show the average of triplicates. Adapted from Weigert Muñoz *et al.*[16]

In the presence of serum, VC treated with DMSO, **PE**, **PE-P**, or **OA-P** (50 µM) showed greatly compromised growth and reached OD 0.09–0.19 after 20 h. The catechol compounds **EPI**, **EPI-P1**, and **EPI-P2** enabled bacterial growth to OD 0.70–0.88 after 20 h (Figure II-6 A) which was comparable to growth in serum-free medium (OD 0.62–0.68, 20 h) (Figure II-6 B). Furthermore, no such stark differences in growth were observed in the absence of serum.

These observations corroborate that a catechol moiety is required to overcome iron limitation. The lack of growth promotion in the iron rich medium furthermore indicates that this is primarily driven by improved iron supply. The ability of **PE** to promote motility on soft agar whilst showing no effect on growth under iron limitation illustrates that the adrenergic response of VC is likely multi-faceted and mediated via parallel mechanisms. The presence of **EPI-P1** and **PE-P** enhanced the colony diameter on soft agar, therefore, both probes were suitable for target identification. Growth assays indicated that **EPI-P1** has siderophore properties in contrast to **PE-P**. Therefore, the latter was the most fitting probe to selectively reveal VC adrenergic targets that promote motility independent of iron uptake.

2.3 Target identification by chemical proteomics

2.3.1. Gel-based photoaffinity labelling

General labelling quality of the probes was analysed by gel-based photoaffinity labelling. Stationary phase VC was incubated with **EPI-P1**, **EPI-P2**, **PE-P**, or **OA-P** (50 µM), and irradiated. Next, cells were lysed in PBS and insoluble proteins were separated and resuspended in 1% SDS. Both soluble and insoluble fractions were ligated to rhodamine-azide by CuAAC and separated by SDS-PAGE. Fluorescence scanning revealed labelling in both fractions by all four probes, indicating good cell permeability (Figure II-7). **EPI-P1** and **EPI-P2** labelled independent of UV irradiation. Both probes carried a catechol group that labelled proteins most likely following oxidation to an *ortho*-quinone or to reactive radical species. Irradiation increased labelling intensities for both probes but this was especially pronounced for **EPI-P2**, even though it did not carry a diazirine. This indicates that UV promoted the decomposition to reactive species. Surprisingly, both **PE-P** and **OA-P** showed UV-dependent labelling although they did not carry a conventional photocrosslinker. Labelling intensity of **OA-P** was relatively weak, consistent with its low activity in the motility assays.

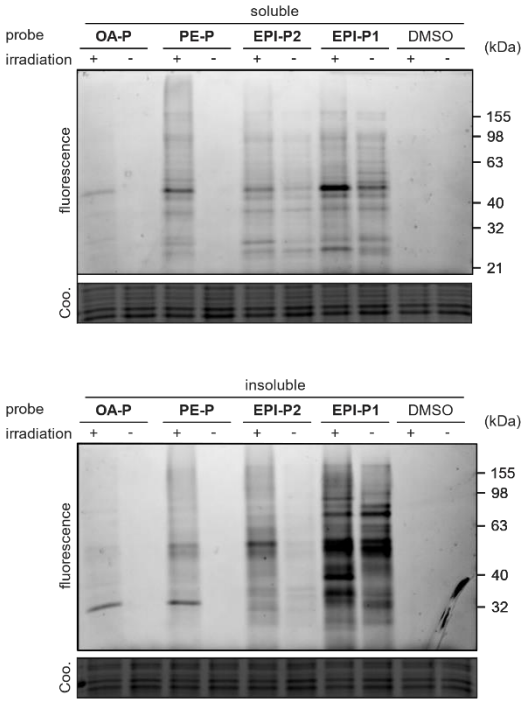

Figure II-7. Photoaffinity labelling in live VC. Probes (50 µM) or DMSO were added to live VC, incubated and irradiated. Following lysis, separation into soluble and insoluble (PBS) proteins, CuAAC to rhodamine-azide, and separation by SDS-PAGE, labelled proteins were visualised by fluorescence imaging. Gels were Coomassie-stained (Coo.) to reveal total protein load (15 µg per lane). Adapted from Weigert Muñoz *et al.*[16]

2.3.2 MS-based photoaffinity labelling with **EPI-P1**

Stationary VC was labelled with **EPI-P1** (7.5 µM), irradiated, and lysed in 1% (v/v) triton X-100 (TX100). Labelled proteins were ligated to a biotin-containing linker by CuAAC. Following enrichment on avidin beads, proteins were digested, and the peptides analysed by liquid chromatography with tandem MS (LC-MS/MS).

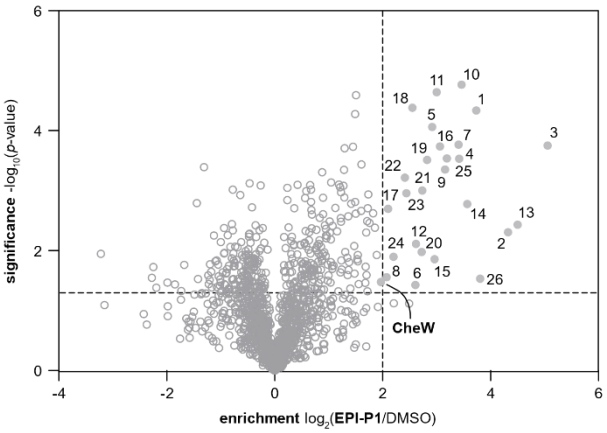

legend	UniProt	gene	protein name
CheW	**A7MS42**	**VIBHAR_03137**	**CheW-like domain-containing protein**
1	A7MSY4	VIBHAR_00007	Iron-hydroxamate ABC transporter substrate-binding protein
2	A7MT36	VIBHAR_01351	Succinate dehydrogenase cytochrome b556 subunit
3	A7MUH3	VIBHAR_03044	Protease 4
4	A7MV17	VIBHAR_01530	Transporter
5	A7MWN4	VIBHAR_00869	Outer membrane channel protein TolC
6	A7MWW5	grpE	Protein GrpE
7	A7MX99	VIBHAR_00062	Peptidyl-prolyl cis-trans isomerase
8	A7MXZ7	frr	Ribosome-recycling factor
9	A7MY24	upp	Uracil phosphoribosyltransferase
10	A7MY64	VIBHAR_01273	OmpA-like domain-containing protein
11	A7MY66	VIBHAR_01269	Porin_4 domain-containing protein
12	A7MYY0	VIBHAR_03442	PNPLA domain-containing protein
13	A7MZS4	VIBHAR_01404	Colicin I receptor
14	A7N0S3	VIBHAR_02285	Putrescine-binding periplasmic protein
15	A7N146	VIBHAR_03705	Single-stranded DNA-binding protein
16	A7N1M5	VIBHAR_01558	Porin_4 domain-containing protein
17	A7N1N3	VIBHAR_01548	Lipoprotein
18	A7N1T8	VIBHAR_03287	Outer membrane protein OmpK
19	A7N283	VIBHAR_06741	Porin_4 domain-containing protein
20	A7N3X4	VIBHAR_05367	Phasin_2 domain-containing protein
21	A7N5U4	VIBHAR_04785	Peptidase M16
22	A7N6I6	VIBHAR_06262	OmpA-like domain-containing protein
23	A7N7I3	VIBHAR_05401	FtsX domain-containing protein
24	A7N7I4	VIBHAR_05402	ABC transporter permease
25	A7N7K9	VIBHAR_07111	ABC transporter ATP-binding protein
26	A7N8H3	VIBHAR_05966	HTH tetR-type domain-containing protein

Figure II-8. Volcano plot of photoaffinity labelling with EPI-P1. Live VC was treated with **EPI-P1** (7.5 µM) or DMSO, irradiated, and lysed in 1% (v/v) TX100 (without fractionation). Labelled proteins were ligated to biotin by CuAAC, enriched on avidin, and enzymatically digested. Resulting peptides were analysed by LC-MS/MS with label-free quantification using MaxLFQ,[96] filtered for proteins identified in three replicates, and missing values were imputed. Samples were compared using a two-sided two-sample *t*-test. The volcano plot shows proteins enriched by **EPI-P1** compared to the DMSO control. Proteins enriched above the cut-off ($-\log_{10}(p\text{-value}) > 1.3$, $\log_2(\text{enrichment}) > 2$) are considered significant and listed in the table. The experiment was performed in three independent replicates. Adapted from Weigert Muñoz *et al.*[16]

In total, 27 proteins were enriched above the cut-off (p-value ≤ 0.05, enrichment ≥ 4), revealing broad reactivity (Figure II-8). Strikingly, an iron-hydroxamate ABC transporter substrate-binding protein (A7MSY4, VIBHAR_00007)[97] and the colicin I receptor (A7MZS4, VIBHAR_01404)[98] were among the top hits. A7MZS4 is annotated as outer membrane receptor

for ferrienterochelin and colicins in the KEGG database.[99-102] In *E.* coli, the colicin receptor I is encoded by the *cirA* gene, which transports catechol siderophores such as dihydroxybenzoyl serine.[103-104] A BLAST search (blastp)[105] of the VC proteome for *E. coli* CirA yielded A7MZS4 as top hit (7e-105, 34.31%), as also reported by others.[106] This indicates that **EPI-P1** indeed acted as siderophore. Among the significant hits were two OmpA-like domain-containing proteins (A7MY64 and A7N6I6) which were annotated with the GO terms "porin activity" (GOMF) and "ion transport" (GOBP) in UniProt.[107-109] Three protein hits designated as "porin_4 domain-containing protein" (A7MY66, A7N1M5, and A7N283) were annotated with the GO terms "porin activity" (all three) and "ion transmembrane transport" (A7MY66).[110-112] Unfortunately, annotation of these proteins is poor, therefore, it cannot be said whether the substantial representation of porins has a biological relevance or whether it stems from unspecific association. Intriguingly, OmpA has been hypothesised to be a potential entry point for catecholamine-iron complexes in *E. coli*.[87] The chemotaxis protein CheW (A7MS42)[113] was enriched 3.9-fold in this dataset and was not among the most prominent hits. Nevertheless, it was an intriguing finding as it is directly related to motility and constitutes the core of the chemotaxis complex.[114]

2.3.3 MS-based photoaffinity labelling with **PE-P** and competition with **PE**

It is conceivable that the abundance of iron-uptake proteins interfered with the identification of further adrenergic targets using **EPI-P1**. Moreover, the tendency of **EPI-P1** to oxidise to highly reactive species might have further contributed to unspecific labelling. **PE-P**, devoid of the catechol moiety, was therefore promising to label proteins associated with motility more selectively. VC was treated with **PE-P** (10 µM), irradiated, and lysed. Control samples were treated with DMSO. A second control was treated with a 25-fold excess of **PE** before addition of the probe. Comparison of **PE-P** treated samples to DMSO-treated samples reveals targets of **PE-P**. Comparison of **PE-P** treated samples to 25-fold excess plus probe reveals which proteins are also bound by the parent compound when the excess of **PE** outcompetes binding by the probe. The target protein should thus be significantly enriched in both comparisons. To further improve protein coverage of potential protein targets localised in the membrane, the lysate was separated into a PBS-soluble and PBS-insoluble fraction and both fractions were processed separately. Insoluble proteins were redissolved in 1% SDS.

In the insoluble fraction, 23 proteins were significantly enriched and outcompeted by **PE** compared to 32 in the soluble (Figure II-9).

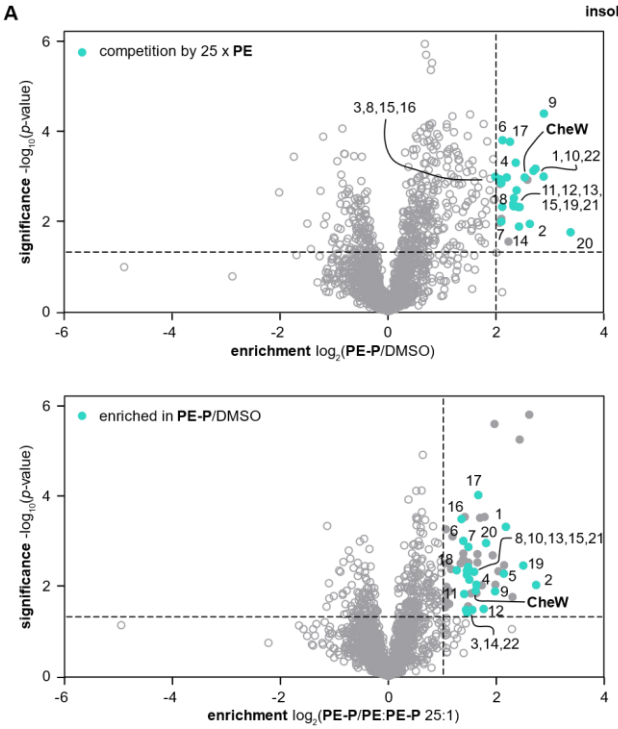

legend	UniProt	gene	protein name
CheW	**A7MS42**	**VIBHAR_03137**	**CheW-like domain-containing protein**
1	A7MSA8	VIBHAR_03672	UPF0307 protein VIBHAR_03672
2	A7MT63	VIBHAR_01308	HPr domain-containin g protein
3	A7MTV7	yihI	Der GTPase-activating protein Y ihI
4	A7MUD0	VIBHAR_02658	DNA-binding response regulator
5	A7MUJ3	VIBHAR_03027	UPF0352 protein VIBHAR_03027
6	A7MV84	tig	Trigger factor
7	A7MWU1	nusB	Transcription antitermination prot. NusB
8	A7MWW5	grpE	Protein GrpE
9	A7MWX0	VIBHAR_011 26	UPF0125 protein VIBHAR_011 26
10	A7MX55	groS	10 kDa chaperonin
11	A7MXE6	nusG	Transcr. termin./antitermin. prot. NusG
12	A7MXS1	VIBHAR_00356	uncharacterised
13	A7MYT1	VIBHAR_01892	Phosphatidylinositol kinase
14	A7MYT3	csrA	Translational regulator CsrA
15	A7MZ63	rpsG	30S ribosomal protein S7
16	A7MZI4	rbfA	Ribosome-binding factor A
17	A7N1J5	VIBHAR_01583	Two-component system response regulator TorR
18	A7N1L7	infA	Translation initiation factor IF-1
19	A7N2H7	VIBHAR_05151	Restriction endonuclease subunit S
20	A7N3V9	VIBHAR_05396	CSD domain-containing protein
21	A7N3X4	VIBHAR_05367	Phasin_2 domain-containing protein
22	A7N8F2	VIBHAR_06507	DUF2058 domain-containing protein

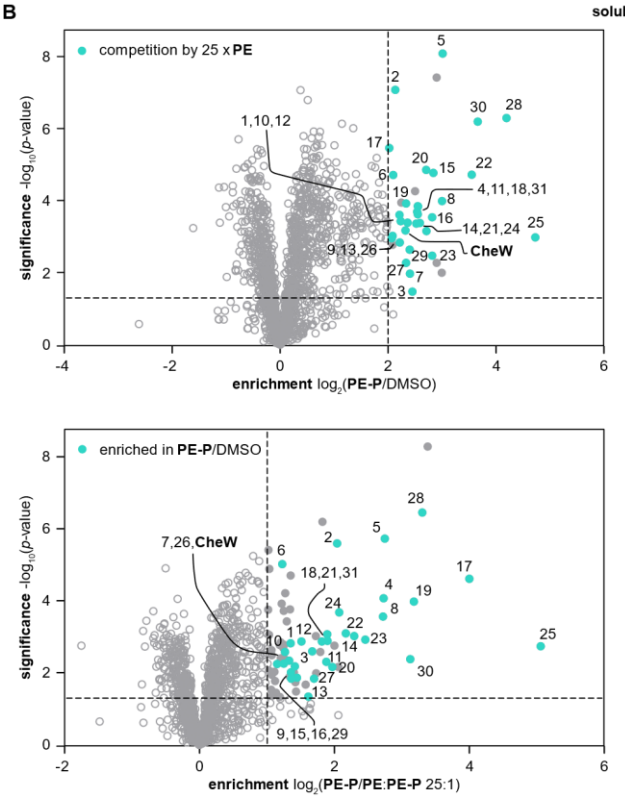

legend	UniProt	gene	protein name
CheW	**A7MS42**	**VIBHAR_03137**	**CheW-like domain-containing prot.**
1	A7MSA8	VIBHAR_03672	UPF0307 prot. VIBHAR_03672
2	A7MSM3	VIBHAR_00684	Caps_synth_GfcC domain-containing prot.
3	A7MT63	VIBHAR_01308	HPr domain-containing protein
4	A7MTX7	VIBHAR_00542	Bacteriocin immunity protein
5	A7MU88	VIBHAR_02715	Peptidase_M75 domain-containing prot.
6	A7MUH2	msrB	Peptide methionine sulfoxide reductase MsrB
7	A7MUJ3	VIBHAR_03027	UPF0352 protein VIBHAR_03027
8	A7MV11	VIBHAR_01537	UPF0434 protein VIBHAR_01537
9	A7MV80	VIBHAR_01439	Tim44 domain-containing protein
10	A7MV84	tig	Trigger factor
11	A7MWM7	VIBHAR_00879	DUF1043 family protein
12	A7MWW5	grpE	Protein GrpE
13	A7MWX0	VIBHAR_01126	UPF0125 protein VIBHAR_01 126
14	A7MWX4	smpB	SsrA-binding protein
15	A7MX55	groES	Co-chaperonin GroES
16	A7MXS1	VIBHAR_00356	uncharacterised
17	A7MXY8	btuB	Vitamin B12 transporter BtuB
18	A7MYV0	rimM	Ribosome maturation factor RimM
19	A7MZ56	VIBHAR_00081	LTD domain-containing protein
20	A7MZE3	VIBHAR_01069	Ancillary SecYEG translocon subunit
21	A7N0U9	VIBHAR_02259	DUF2960 domain-containing protein
22	A7N1Q4	VIBHAR_03306	Multidrug DMT transporter permease
23	A7N1U9	VIBHAR_03260	Chemotaxis protein
24	A7N2H7	VIBHAR_05151	Restriction endonuclease subunit S
25	A7N3V9	VIBHAR_05396	CSD domain-containing protein
26	A7N3X4	VIBHAR_05367	Phasin_2 domain-containing protein
27	A7N6H7	VIBHAR_06294	Protein YecA
28	A7N757	VIBHAR_06143	AI 2-binding periplasmic prot. LuxP
29	A7N8F2	VIBHAR_06507	DUF2058 domain-containing protein
30	A7N8S0	VIBHAR_p08260	Exported protein
31	A7N8T0	VIBHAR_p08234	KfrA_N domain-containing protein

Figure II-9. Volcano plots of competitive photoaffinity labelling experiments with PE-P and PE. Live VC was treated with **PE-P** (10 µM), DMSO, or a 25-fold excess of **PE** prior to addition of **PE-P**. Bacteria were irradiated, lysed, separated into soluble (PBS) and insoluble proteins, ligated by CuAAC to biotin-azide, enriched on avidin beads, and digested, and peptides were analysed by LC-MS/MS. MS data were analysed by MaxLFQ,[96] filtered for proteins identified in four replicates, and missing values were imputed. Samples were compared using a two-sided two-sample *t*-test. Top plot shows proteins enriched by **PE-P** compared to the DMSO control. Bottom plot shows proteins enriched by **PE-P** alone compared to samples treated with **PE-P** plus a 25-fold excess of **PE**. Proteins overlapping in both plots are highlighted in cyan. Tables show UniProt[108] identifiers of proteins enriched in both comparisons. (A) Insoluble fraction. (B) Soluble fraction. Experiments were performed in five independent replicates. Adapted from Weigert Muñoz *et al.*[16]

Consistent with the lack of growth promotion under iron limitation, **PE-P** did not enrich proteins associated with iron uptake. CheW (A7MS42) was significantly enriched in both fractions and, especially in the insoluble fraction, among the most prominent hits. Overall, the labelling was quite broad which required more experiments to further narrow down the hits to a potential receptor.

2.3.4 MS-based photoaffinity labelling with **PE-P** in competition with **EPI** and clinical antagonists

Colony spread was strongly increased in the presence of **EPI**. Therefore, **EPI** was anticipated to outcompete probe binding to a potential receptor involved in catecholamine-dependent motility. Labelling was performed with **PE-P** with a 10-fold excess of **EPI**. Competitor concentration was lower than in the **PE** experiment to minimise potential protein modification and precipitation by **EPI** oxidation products. Similar to **PE** competition experiments, 33 and 18 proteins were enriched and outcompeted in the insoluble and soluble fraction, respectively (Figure II-10).

To narrow down the potential hits even further, competition was also performed with **LAB** or **PRO**. **LAB** blocked catecholamine-dependent motility, indicating it might bind to the same protein as **EPI** and **PE**. As **PRO** showed no antagonism, outcompeted hits should therefore be considered unspecific off-targets. At a 10-fold excess, 35 proteins were enriched and outcompeted by **LAB** out of which only one was also outcompeted by **PRO** in the insoluble fraction (Figure II-11 A). In the soluble fraction, 32 proteins were enriched and outcompeted by **LAB**, out of which two were outcompeted also by **PRO** (Figure II-11 B).

The comparison of hits that were enriched and outcompeted by **PE**, **EPI**, and **LAB** but not by **PRO** yielded eight proteins in the insoluble fraction (Figure II-12 A) and five in the soluble fraction (Figure II-12 B). In the insoluble fraction, the der GTPase-activating protein YihI (A7MTV7),[115] the 30S ribosomal protein S7 (A7MZ63),[116] the translation initiation factor IF-1 (A7N1L7),[117] a phosphatidylinositol kinase (A7MYT1),[118] a DNA-binding response regulator (A7MUD0),[119] and two poorly characterised proteins (A7MXS1 and A7N8F2)[120-121] were significant across all experiments. In the soluble fraction, A7MZ56 was also outcompeted by **PRO** and therefore considered unspecific. Two proteins were poorly annotated (A7MXS1 and A7N8F2),[120-121] the third was a restriction endonuclease subunit S (A7N2H7),[122] and the last was CheW. Notably, of all differentially outcompeted proteins in both fractions, CheW was the

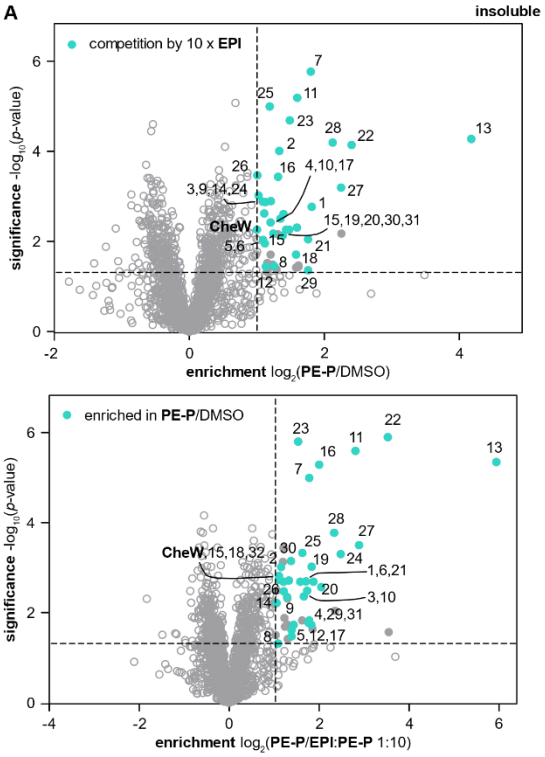

legend	UniProt	gene	protein name
CheW	**A7MS42**	**VIBHAR_03137**	**CheW-like domain-containing protein**
1	A7MRS9	VIBHAR_01641	Lipoprotein
2	A7MSM3	VIBHAR_00684	Caps_synth_GfcC domain-containing protein
3	A7MSV2	VIBHAR_01872	Phage shock protein PspA
4	A7MTV7	yihI	Der GTPase-activating protein YihI
5	A7MU88	VIBHAR_02715	Peptidase_M75 domain-containing protein
6	A7MUD0	VIBHAR_02658	DNA-binding response regulator
7	A7MWY7	VIBHAR_01876	Biotin_lipoyl_2 domain-containing protein
8	A7MX37	VIBHAR_01812	Heat shock protein HtpX
9	A7MX55	groES	Co-chaperonin GroES
10	A7MXS1	VIBHAR_00356	uncharacterised
11	A7MXY8	btuB	Vitamin B12 transporter BtuB
12	A7MYT1	VIBHAR_01892	Phosphatidylinositol kinase
13	A7MZ56	VIBHAR_00081	LTD domain-containing protein
14	A7MZ63	rpsG	30S ribosomal protein S7
15	A7MZR7	VIBHAR_01426	5'-deoxynucleotidase VIBHAR_01426
16	A7N0D8	VIBHAR_02497	TSPc domain-containing protein
17	A7N0E8	VIBHAR_02489	Phage protein
18	A7N0U9	VIBHAR_02259	DUF2960 domain-containing protein
19	A7N1L7	infA	Translation initiation factor IF-1
20	A7N1N3	VIBHAR_01548	Lipoprotein
21	A7N1Q4	VIBHAR_03306	Multidrug DMT transporter permease
22	A7N1T8	VIBHAR_03287	Outer membrane protein OmpK
23	A7N4I9	VIBHAR_06577	Isochorismatase domain-containing protein
24	A7N4M9	VIBHAR_05881	Endo/exonuclease/phosphatase domain-containing protein
25	A7N503	VIBHAR_05789	TonB-dep. hemoglobin/transferrin/lactoferrin family receptor
26	A7N5C3	gcvH	Glycine cleavage system H protein
27	A7N5L8	VIBHAR_06895	Alpha-glucosidase
28	A7N5R2	VIBHAR_04824	Aamy domain-containing protein
29	A7N6B5	VIBHAR_05162	DUF11 domain-containing protein
30	A7N757	VIBHAR_06143	Autoinducer 2-binding periplasmic protein LuxP
31	A7N8F2	VIBHAR_06507	DUF2058 domain-containing protein
32	A7N8H3	VIBHAR_05966	HTH tetR-type domain-containing protein

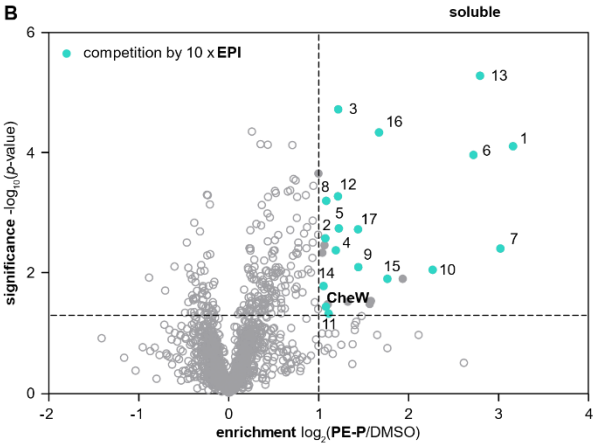

legend	UniProt	gene	protein name
CheW	**A7MS42**	**VIBHAR_03137**	**CheW-like domain-containing protein**
1	A7MSM3	VIBHAR_00684	Caps_synth_GfcC domain-containing protein
2	A7MSV2	VIBHAR_01872	Phage shock protein PspA
3	A7MU88	VIBHAR_02715	Peptidase_M75 domain-containing protein
4	A7MUD0	VIBHAR_02658	DNA-binding response regulator
5	A7MXS1	VIBHAR_00356	uncharacterised
6	A7MXY8	btuB	Vitamin B12 transporter BtuB
7	A7MZ56	VIBHAR_00081	LTD domain-containing protein
8	A7MZ63	rpsG	30S ribosomal protein S7
9	A7N0D8	VIBHAR_02497	TSPc domain-containing protein
10	A7N0Y0	atpC	ATP synthase epsilon chain
11	A7N146	VIBHAR_03705	Single-stranded DNA-binding protein
12	A7N1J5	VIBHAR_01583	Two-component system response regulator TorR
13	A7N1T8	VIBHAR_03287	Outer membrane protein OmpK
14	A7N1Y0	VIBHAR_03240	UPF0325 protein VIBHAR_03240
15	A7N2H7	VIBHAR_05151	Restriction endonuclease subunit S
16	A7N4I9	VIBHAR_06577	Isochorismatase domain-containing protein
17	A7N8F2	VIBHAR_06507	DUF2058 domain-containing protein

Figure II-10. Volcano plots of competitive photoaffinity labelling experiments with PE-P and EPI. Live VC was treated with **PE-P** (10 µM), DMSO, or a 10-fold excess of **EPI** prior to addition of **PE-P**. Bacteria were irradiated, lysed, separated into soluble (PBS) and insoluble proteins, ligated by CuAAC to biotin-azide, enriched on avidin beads, digested, and peptides were analysed by LC-MS/MS. MS data were analysed by MaxLFQ,[96] filtered for proteins identified in three replicates, and missing values were imputed. Samples were compared using a two-sided two-sample *t*-test. (A) Insoluble fraction. Top plot shows proteins enriched by **PE-P** compared to the DMSO control. Bottom plot shows proteins enriched by **PE-P** alone compared to samples treated with **PE-P** plus a 10-fold excess of **EPI**. Proteins overlapping in both plots are highlighted in cyan. (B) Soluble fraction. Plot shows proteins enriched by **PE-P** alone compared to the DMSO control. Proteins outcompeted by a 10-fold excess of **EPI** are highlighted in cyan. Tables show UniProt[108] identifiers of proteins enriched in both comparisons. Experiments were performed in four independent replicates. Adapted from Weigert Muñoz *et al.*[16]

only protein that was also significantly enriched by **EPI-P1**. A closer inspection of the label-free quantification (LFQ) values of CheW (insoluble fraction) treated with either **PE-P** alone, **PE-P** plus competitor, or DMSO showed that **PE-P** binding was indeed outcompeted by **PE**, **EPI**, and **LAB**, but not by **PRO** (Figure II-12 C). Therefore, from all the photoaffinity labelling experiments combined, CheW emerged as top hit and was prioritised for subsequent validation studies.

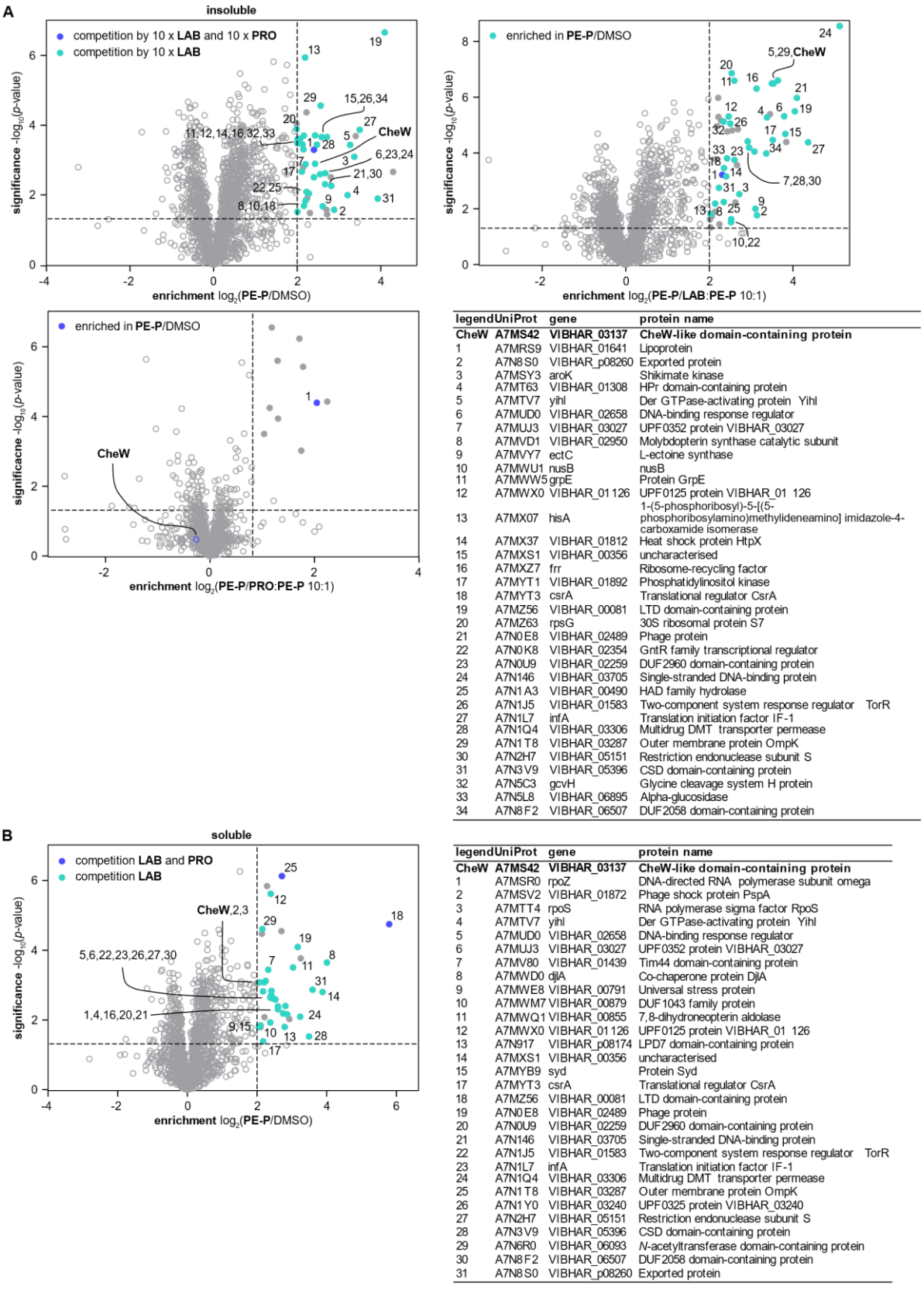

legend	UniProt	gene	protein name
CheW	**A7MS42**	**VIBHAR_03137**	**CheW-like domain-containing protein**
1	A7MRS9	VIBHAR_01641	Lipoprotein
2	A7N8S0	VIBHAR_p08260	Exported protein
3	A7MSY3	aroK	Shikimate kinase
4	A7MT63	VIBHAR_01308	HPr domain-containing protein
5	A7MTV7	yihI	Der GTPase-activating protein YihI
6	A7MUD0	VIBHAR_02658	DNA-binding response regulator
7	A7MUJ3	VIBHAR_03027	UPF0352 protein VIBHAR_03027
8	A7MVD1	VIBHAR_02950	Molybdopterin synthase catalytic subunit
9	A7MVY7	ectC	L-ectoine synthase
10	A7MWU1	nusB	nusB
11	A7MWW5	grpE	Protein GrpE
12	A7MWX0	VIBHAR_01126	UPF0125 protein VIBHAR_01126
13	A7MX07	hisA	1-(5-phosphoribosyl)-5-[(5-phosphoribosylamino)methylideneamino] imidazole-4-carboxamide isomerase
14	A7MX37	VIBHAR_01812	Heat shock protein HtpX
15	A7MXS1	VIBHAR_00356	uncharacterised
16	A7MXZ7	frr	Ribosome-recycling factor
17	A7MYT1	VIBHAR_01892	Phosphatidylinositol kinase
18	A7MYT3	csrA	Translational regulator CsrA
19	A7MZ56	VIBHAR_00081	LTD domain-containing protein
20	A7MZ63	rpsG	30S ribosomal protein S7
21	A7N0E8	VIBHAR_02489	Phage protein
22	A7N0K8	VIBHAR_02354	GntR family transcriptional regulator
23	A7N0U9	VIBHAR_02259	DUF2960 domain-containing protein
24	A7N146	VIBHAR_03705	Single-stranded DNA-binding protein
25	A7N1A3	VIBHAR_00490	HAD family hydrolase
26	A7N1J5	VIBHAR_01583	Two-component system response regulator TorR
27	A7N1L7	infA	Translation initiation factor IF-1
28	A7N1Q4	VIBHAR_03306	Multidrug DMT transporter permease
29	A7N1T8	VIBHAR_03287	Outer membrane protein OmpK
30	A7N2H7	VIBHAR_05151	Restriction endonuclease subunit S
31	A7N3V9	VIBHAR_05396	CSD domain-containing protein
32	A7N5C3	gcvH	Glycine cleavage system H protein
33	A7N5L8	VIBHAR_06895	Alpha-glucosidase
34	A7N8F2	VIBHAR_06507	DUF2058 domain-containing protein

legend	UniProt	gene	protein name
CheW	**A7MS42**	**VIBHAR_03137**	**CheW-like domain-containing protein**
1	A7MSR0	rpoZ	DNA-directed RNA polymerase subunit omega
2	A7MSV2	VIBHAR_01872	Phage shock protein PspA
3	A7MTT4	rpoS	RNA polymerase sigma factor RpoS
4	A7MTV7	yihI	Der GTPase-activating protein YihI
5	A7MUD0	VIBHAR_02658	DNA-binding response regulator
6	A7MUJ3	VIBHAR_03027	UPF0352 protein VIBHAR_03027
7	A7MV80	VIBHAR_01439	Tim44 domain-containing protein
8	A7MWD0	djlA	Co-chaperone protein DjlA
9	A7MWE8	VIBHAR_00791	Universal stress protein
10	A7MWM7	VIBHAR_00879	DUF1043 family protein
11	A7MWQ1	VIBHAR_00855	7,8-dihydroneopterin aldolase
12	A7MWX0	VIBHAR_01126	UPF0125 protein VIBHAR_01126
13	A7N917	VIBHAR_p08174	LPD7 domain-containing protein
14	A7MXS1	VIBHAR_00356	uncharacterised
15	A7MYB9	syd	Protein Syd
17	A7MYT3	csrA	Translational regulator CsrA
18	A7MZ56	VIBHAR_00081	LTD domain-containing protein
19	A7N0E8	VIBHAR_02489	Phage protein
20	A7N0U9	VIBHAR_02259	DUF2960 domain-containing protein
21	A7N146	VIBHAR_03705	Single-stranded DNA-binding protein
22	A7N1J5	VIBHAR_01583	Two-component system response regulator TorR
23	A7N1L7	infA	Translation initiation factor IF-1
24	A7N1Q4	VIBHAR_03306	Multidrug DMT transporter permease
25	A7N1T8	VIBHAR_03287	Outer membrane protein OmpK
26	A7N1Y0	VIBHAR_03240	UPF0325 protein VIBHAR_03240
27	A7N2H7	VIBHAR_05151	Restriction endonuclease subunit S
28	A7N3V9	VIBHAR_05396	CSD domain-containing protein
29	A7N6R0	VIBHAR_06093	*N*-acetyltransferase domain-containing protein
30	A7N8F2	VIBHAR_06507	DUF2058 domain-containing protein
31	A7N8S0	VIBHAR_p08260	Exported protein

Figure II-11. Volcano plots of competitive photoaffinity labelling experiments with PE-P and clinical antagonists. Live VC was treated with **PE-P** (10 µM), DMSO, or a 10-fold excess of **LAB** or **PRO** prior to addition of **PE-P**. Bacteria were irradiated, lysed, separated into soluble (PBS) and insoluble proteins, ligated by CuAAC to biotin-azide, enriched on avidin beads, digested, and peptides were analysed by LC-MS/MS. MS data were analysed by MaxLFQ,[96] filtered for proteins identified in three replicates, and missing values were imputed. Samples were compared using a two-sided two-sample *t*-test. (A) Insoluble fraction. Top left plot shows proteins enriched by **PE-P** compared to the DMSO control. Top right plot shows proteins enriched by **PE-P** alone compared

to samples treated with **PE-P** plus a 10-fold excess of **LAB**. Bottom plot shows proteins enriched by **PE-P** alone compared to samples treated with **PE-P** plus a 10-fold excess of **PRO**. Proteins overlapping in **PE-P**/DMSO and **PE-P**/**LAB** are highlighted in cyan, proteins overlapping in all three plots in blue. (B) Soluble fraction. Plot shows proteins enriched by **PE-P** compared to the DMSO control. Proteins outcompeted by a 10-fold excess of **LAB** are highlighted in cyan, proteins outcompeted by both **LAB** and **PRO** in blue. Tables show UniProt[108] identifiers of proteins enriched in **PE-P**/DMSO and **PE-P**/**LAB**. Experiments were performed in four independent replicates. Adapted from Weigert Muñoz *et al*.[16]

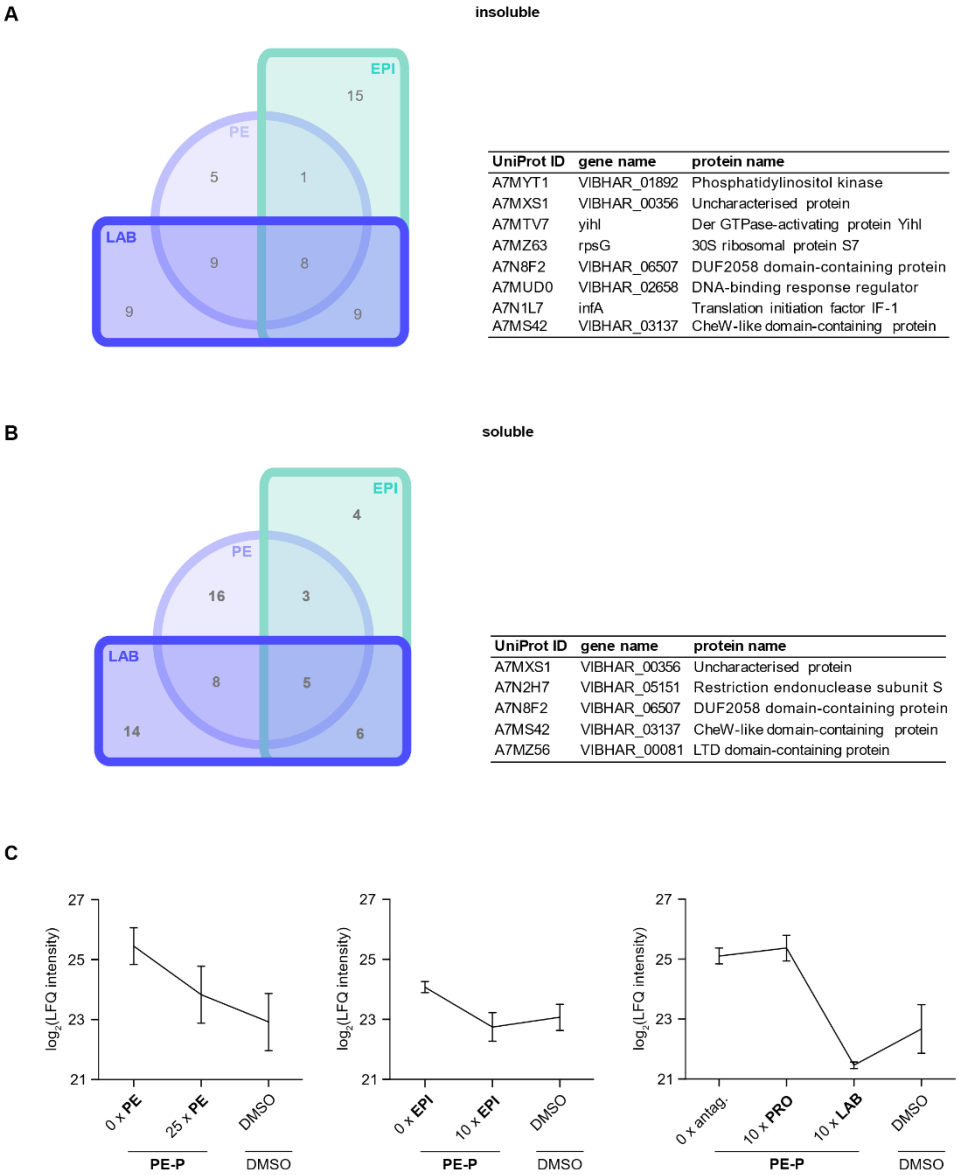

UniProt ID	gene name	protein name
A7MYT1	VIBHAR_01892	Phosphatidylinositol kinase
A7MXS1	VIBHAR_00356	Uncharacterised protein
A7MTV7	yihI	Der GTPase-activating protein YihI
A7MZ63	rpsG	30S ribosomal protein S7
A7N8F2	VIBHAR_06507	DUF2058 domain-containing protein
A7MUD0	VIBHAR_02658	DNA-binding response regulator
A7N1L7	infA	Translation initiation factor IF-1
A7MS42	VIBHAR_03137	CheW-like domain-containing protein

UniProt ID	gene name	protein name
A7MXS1	VIBHAR_00356	Uncharacterised protein
A7N2H7	VIBHAR_05151	Restriction endonuclease subunit S
A7N8F2	VIBHAR_06507	DUF2058 domain-containing protein
A7MS42	VIBHAR_03137	CheW-like domain-containing protein
A7MZ56	VIBHAR_00081	LTD domain-containing protein

Figure II-12. Comparison of proteins outcompeted by PE, EPI, and LAB. For each condition, only proteins were considered that were also enriched compared to the DMSO control. (A) Insoluble fraction. (B) Soluble fraction. (C) LFQ intensities of CheW in samples treated with either **PE-P** alone, **PE-P** plus competitors, or DMSO (insoluble fraction). Adapted from Weigert Muñoz *et al*.[16]

2.4 Investigation of the mechanism of **PE-P** binding

2.4.1 Labelling in presence of radical scavengers

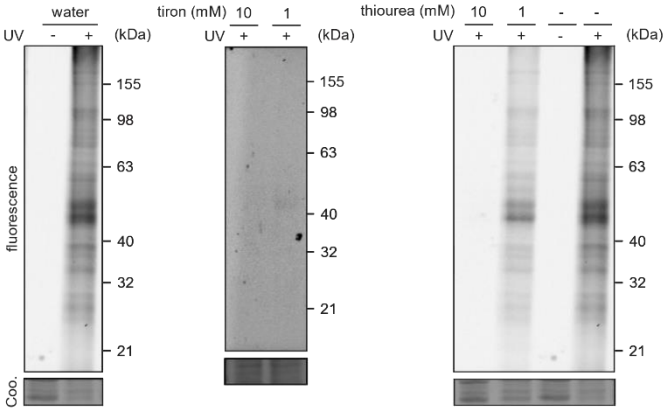

Figure II-13. Labelling in the presence of radical scavengers. In-gel fluorescence analysis of VC lysate treated with **PE-P** (50 µM) in the presence of thiourea or tiron (with irradiation). Proteins were precipitated in acetone to remove radical scavengers before CuAAC to rhodamine-azide. Coo. = Coomassie. Adapted from Weigert Muñoz *et al.*[16]

Next, the unexpected UV-dependent labelling by **PE-P** was explored. To interrogate whether the labelling was based on a radical mechanism, labelling was performed in VC lysate with **PE-P** (50 µM) in the presence of different radical scavengers (Figure II-13). Labelled proteins were precipitated in acetone and washed with methanol before CuAAC to remove radical scavengers that could interfere with the reaction. Thiourea quenched labelling slightly at 1 mM and completely at 10 mM. In the presence of 1 mM tiron (sodium 4,5-dihydroxybenzene-1,3-disulfonate hydrate), no labelling was detectable. This indicates that UV induces fragmentation of the probe to reactive radical species which covalently bind to proteins.

2.4.2 Labelling in lysate of different strains

Next, labelling was compared in the lysates of VC and three other bioluminescent strains *Photorhabdus asymbiotica*, *Photorhabdus luminescens*, and *Aliivibrio fischeri*. Non-luminescent *Vibrio parahaemolyticus* and *S.* Typhimurium were included for comparison (Figure II-14). Labelling by **PE-P** (50 µM) in the lysates of *V. parahaemolyticus*, *P. asymbiotica*, *P. luminescens*, and *A. fischeri* was distinct, although weaker than in VC, while it was absent in *S.* Typhimurium. Since labelling was performed in lysate, differences in uptake can be ruled out. Therefore, probe reactivity must be promoted by certain cellular components that are not specifically linked to bioluminescence and are most abundant in VC. The exact activation mechanism and whether the reactivity is promoted by a small molecule, a protein, or

another specific chemical condition present in these strains, are interesting subjects for further studies.

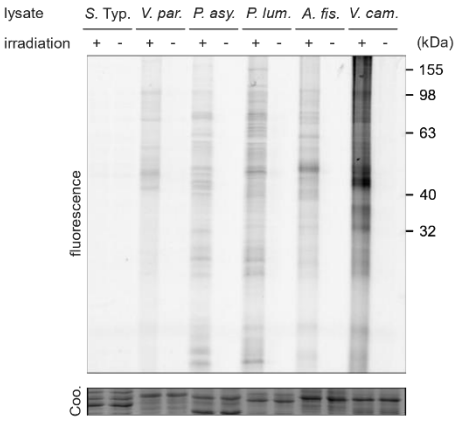

Figure II-14. Photoaffinity labelling in lysates of different strains. Lysates (1 µg/µL protein in PBS) were treated with **PE-P** (50 µM), irradiated, clicked to rhodamine-azide, and proteins were separated by SDS-PAGE. Total protein load (15 µg per lane) was visualized by Coomassie staining (Coo.). *S*. Typ. = *S*. Typhimurium; *V. par*. = *V. parahaemolyticus*; *P. asy*. = *P. asymbiotica*; *P. lum*. = *P. luminescens*; *A. fis.* = *A. fischeri*; *V. cam*. = VC.

Enzymatic conversion of phenol derivatives to radicals can be catalysed, for instance, by an engineered ascorbate peroxidase (APEX).[123] The resulting phenol radicals are highly reactive, short-lived, and covalently react with electron-rich amino acids.[123-127] As APEX is activated in the presence of H_2O_2, it is used as a tool to map proteins in close proximity, e.g. by targeting APEX to an organelle of interest[123] or by fusing it to a bait protein.[128] A similar enzymatic activation of **PE-P** by an unknown enzyme upon UV irradiation is plausible.

2.4.3 MS-based analysis of **PE-P** modification

To further corroborate this hypothesis, recently developed isotopically labelled desthiobiotin-azide (isoDTB) tags[32] were used to inspect the modification of CheW and other proteins by **PE-P**. VC lysate was labelled with **PE-P** (10 µM) and labelled proteins were ligated to heavy or light isoDTB tags in a 1:1 ratio and enriched. Following tryptic digest, unbound peptides were washed off the resin and modified peptides were eluted and detected by LC-MS/MS (Figure II-15 A). An unbiased analysis[31] revealed modified peptides with the added mass corresponding to **PE-P** plus the light or heavy isoDTB tag (Figure II-15 B). Consistent with a radical binding mechanism, the modification was highly selective for tyrosine which constituted 90% of detected modified residues (Figure II-15 C and D).

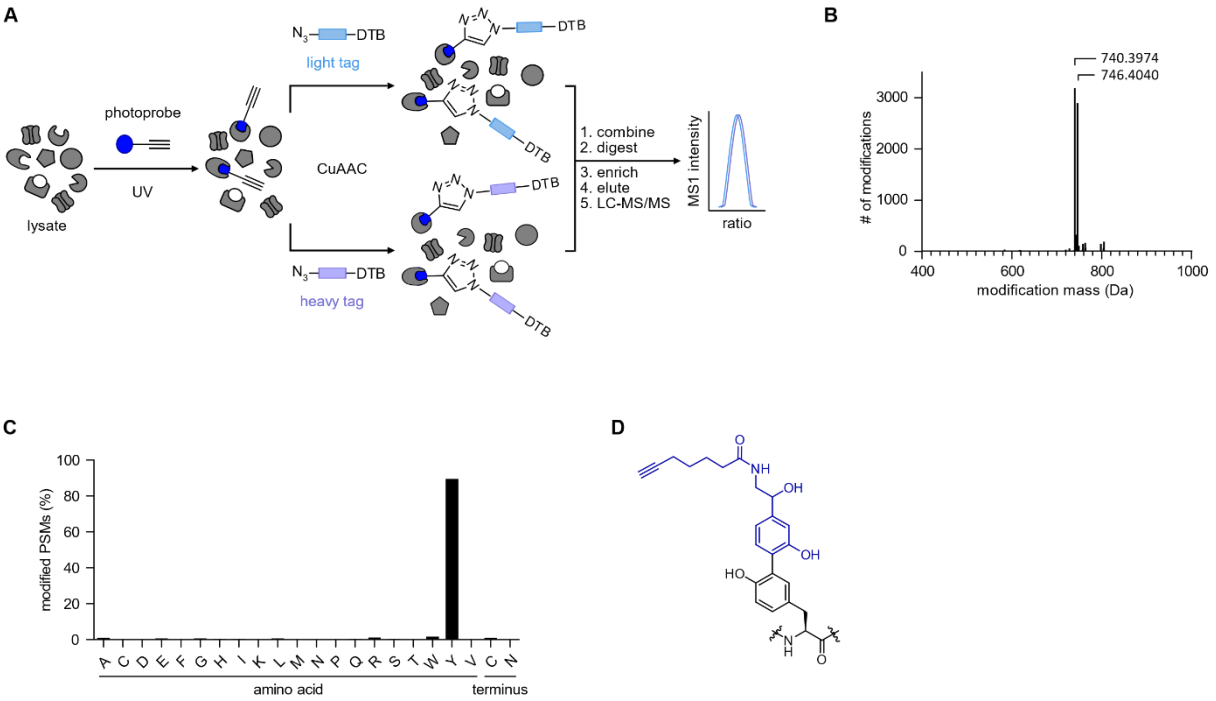

Figure II-15. Proteome-wide analysis of PE-P modifications. (A) Schematic representation of workflow utilising isoDTB tags.[31-32] Labelling with **PE-P** (blue circle, 10 µM) in VC lysate was followed by irradiation, then samples were split in two and subjected to CuAAC with either light- (blue rectangle) or heavy-labelled (purple rectangle) isoDTB-azide. Differentially labelled lysates were combined in a ratio of 1:1, and proteins were digested. Following enrichment on avidin, modified peptides were eluted and analysed by LC-MS/MS. Peptides detected with a ratio of ~1:1 heavy:light tag were considered true hits. (B) Analysis of the masses of modification introduced by **PE-P** plus the light or heavy isoDTB tag, respectively, by an unbiased, proteome-wide search. (C) Analysis of the amino acid selectivity of **PE-P** labelling. (D) Potential structure (or regioisomer) of a **PE-P**-modified tyrosine corresponding to the observed modification mass. The analysis was performed in technical duplicates. PSM = peptide spectrum match. Adapted from Weigert Muñoz *et al.*[16]

2.4.4 Identification of CheW binding sites

In CheW, two tyrosine residues, Y_{44} and Y_{112}, were modified by the probe (Figure II-16 A–B). Mapping these residues into the predicted structure (AlphaFold,[129] kindly provided by Dr. Anthe Janssen and Prof. Gerard van Westen, Leiden University) revealed that the two tyrosines are in the vicinity of a conserved arginine, R_{64}, which is assumed to be involved in modulating CheA activity (Figure II-16 C).[130] Based on this structure, it is conceivable that ligand binding in this region may affect the interaction between CheA and CheW, although this requires further investigation.

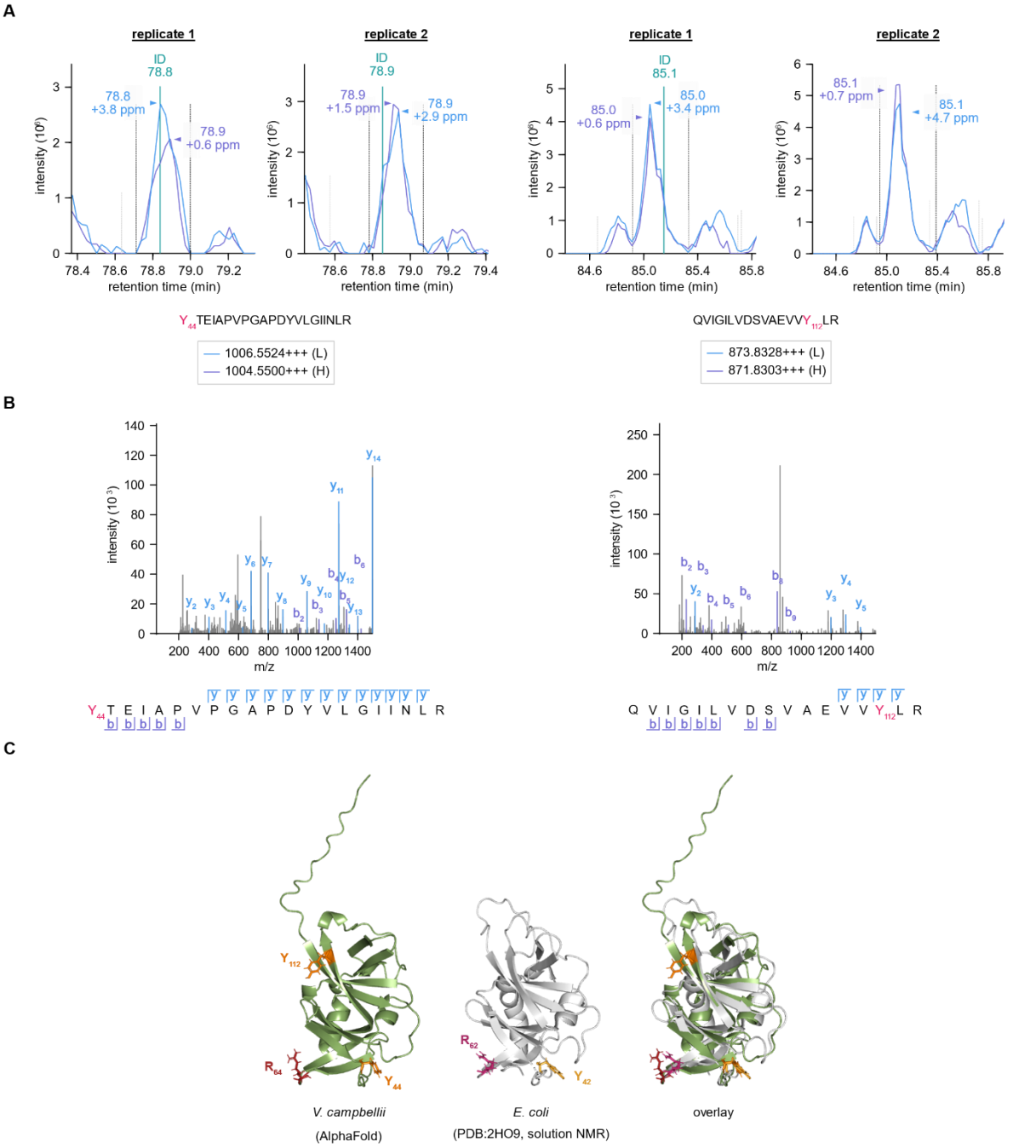

Figure II-16. Identification of PE-P binding sites in CheW. (A) Extracted MS1 ion chromatograms of the two CheW peptides labelled by **PE-P** containing the Y_{44} and the Y_{112} binding site, respectively. Two replicates are shown of each peptide. Dashed lines define the quantified MS1 peaks and the expected m/z of the detected charge state is shown in the box. Peaks are labelled with the retention time (in min) and the deviation of the detected mass from the expected mass of the modified peptide (in ppm). ID denotes that an MS2 scan was acquired at the indicated retention time. (B) MS2 spectra with identified b- and y-ions. (C) Structure of VC CheW predicted with AlphaFold[129] and visualised with PyMOL.[131] **PE-P** binding sites Y_{44} and Y_{112} are marked in orange, R_{64} in red. The *E. coli* CheW structure (PDB:2HO9[132], solution NMR) is shown for comparison (grey). CheW from *E. coli* and VC were overlayed in PyMOL, RMSD = 2.217 (1448 to 1448 atoms of 1771 total). R_{62} and Y_{42} are conserved in the *E. coli* protein; an orthologue of Y_{112} is absent. MS data analysis was performed by S. M. Hacker (TUM/Leiden University). The VC structure was kindly provided by A. Janssen and G. van Westen (Leiden University). Adapted from Weigert Muñoz *et al.*[16]

2.5 Validation of CheW as adrenergic target

2.5.1 Catecholamine binding to purified CheW

Binding of adrenergic compounds to CheW was next investigated by microscale thermophoresis (MST), which measures temperature-induced changes in fluorescence as a function of ligand concentration. **EPI**, **NE**, and **PE** were included as they promoted colony spread on soft agar, and the antagonist **LAB**. **PRO** could not be tested due to interference of its intrinsic fluorescence. **OA**, which had shown no activity, was included as a negative control. Concentration-dependent effects on the fluorescently labelled CheW were observed in the presence of **EPI**, **NE**, **PE**, and **LAB**, and dissociation constants K_d were determined ranging from 300 to 740 nM, indicating strong affinity binding (Figure II-17). It is especially noteworthy that **LAB** displayed affinity as it had no effect on motility by itself, indicating that it does indeed act like an antagonist. Consistent with its lack of activity in the soft agar assays, no binding could be observed for **OA**.

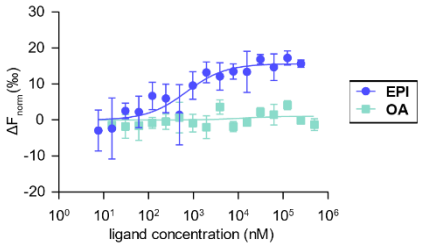

ligand	K_d (µM)
EPI	0.68 ± 0.34
NE	0.74 ± 0.42
PE	0.30 ± 0.25
LAB	0.64 ± 0.56

Figure II-17. Binding of adrenergic compounds to purified CheW. Binding affinities of adrenergic compounds to purified CheW (50 nM) were measured by MST. K_d values were determined from the Thermophoresis + T-Jump signal for data analysis (n = 3 independent measurements, error bars represent standard deviation). Experiments were performed by E. Hoyer (LMU). Adapted from Weigert Muñoz *et al.*[16]

2.5.2 Analysis of the CheW interaction network

Since binding of catecholamines to CheW could be verified *in vitro*, the next step was to investigate this in the cellular context. Therefore, co-immunoprecipitation (co-IP) of CheW in presence and absence of **EPI** was performed to reveal potential effects on protein-protein interactions. Moreover, this experiment was expected to corroborate the central role of CheW in the chemotaxis protein network by revealing its association with core chemotaxis proteins. Live VC was treated with 100 µM **EPI** or DMSO. Next, disuccinimidyl sulfoxide (DSSO) was added to crosslink interacting proteins.[133] Following lysis, proteins of both **EPI**- and DMSO-treated samples were enriched by a CheW-specific antibody or by an equivalent amount of an unspecific isotype control, digested, and analysed by LC-MS/MS. Comparison of proteins

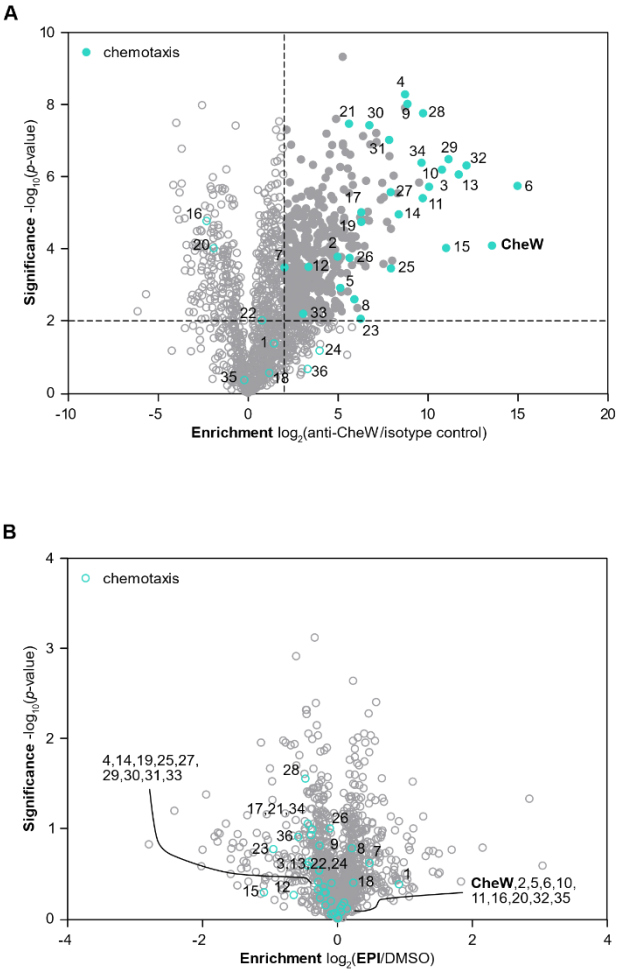

C

legend	UniProt	gene	protein name
CheW	**A7MS42**	**VIBHAR_03137**	**CheW-like domain-containing protein**
1	A7MRW7	VIBHAR_02788	Chemotaxis protein
2	A7MS23	VIBHAR_03153	Flagellar motor switch protein FliN
3	A7MS30	VIBHAR_03143	Response regulatory domain-containing protein
4	A7MS43	VIBHAR_03138	CheW-like domain-containing protein
5	A7MS45	cheB	Protein-glutamate methylesterase/ protein-glutamine glutaminase
6	A7MS46	VIBHAR_03141	Chemotaxis protein CheA
7	A7MS47	VIBHAR_03142	Protein phosphatase CheZ
8	A7MSY8	VIBHAR_0001 1	CheX domain-containing protein
9	A7MUA2	VIBHAR_02691	Methyl-accepting chemotaxis protein
10	A7MUN5	VIBHAR_02869	Chemotaxis protein CheV
11	A7MV20	VIBHAR_01518	Methyl-accepting chemotaxis protein
12	A7MWN1	VIBHAR_00866	Methyl-accepting chemotaxis protein
13	A7MWX6	VIBHAR_01884	Methyl-accepting chemotaxis protein
14	A7MX68	VIBHAR_001 19	Methyl-accepting chemotaxis protein
15	A7MY50	VIBHAR_01282	Chemotaxis protein CheV
16	A7MY53	VIBHAR_01283	Protein-glutamate *O*-methyltransferase
17	A7MZ15	VIBHAR_01753	Methyl-accepting chemotaxis protein
18	A7MZL8	VIBHAR_02418	Methyl-accepting chemotaxis protein
19	A7MZM4	VIBHAR_02368	Chemotaxis protein
20	A7N1J3	VIBHAR_01599	Methyl-accepting transducer domain-containing protein
21	A7N1Z9	VIBHAR_06258	Chemotaxis protein
22	A7N2G1	VIBHAR_05214	Maltodextrin-binding protein
23	A7N2H6	VIBHAR_05150	Methyl-accepting chemotaxis protein
24	A7N349	VIBHAR_05097	Methyl-accepting chemotaxis protein
25	A7N3F7	VIBHAR_04784	Chemotaxis protein
26	A7N3I2	VIBHAR_04747	Methyl-accepting transducer domain-containing protein
27	A7N3U3	VIBHAR_05406	Methyl-accepting chemotaxis protein
28	A7N3W8	VIBHAR_05387	Methyl-accepting chemotaxis protein
29	A7N4M2	VIBHAR_05890	Chemotaxis protein CheV
30	A7N579	VIBHAR_05691	Chemotaxis protein
31	A7N5E2	VIBHAR_05936	Methyl-accepting chemotaxis protein
32	A7N639	VIBHAR_05250	Chemotaxis protein CheV
33	A7N6C7	VIBHAR_05136	Methyl-accepting chemotaxis protein
34	A7N6F4	VIBHAR_06314	Chemotaxis protein
35	A7N757	VIBHAR_06143	Autoinducer 2-binding periplasmic protein LuxP
36	A7N839	VIBHAR_07022	Chemotaxis protein

Figure II-18. Identification of CheW interaction partners by co-IP. Live VC was treated with **EPI** (100 µM) or DMSO and proteins chemically crosslinked. Lysates were pulled down with an anti-CheW antibody or an isotype control. (A) Comparison of proteins enriched by the anti-CheW antibody to proteins enriched by the isotype control in both DMSO controls to identify CheW interaction partners. (B) Comparison of proteins enriched by the anti-CheW antibody in samples treated with **EPI** to DMSO controls. (C) UniProt[108] identifiers of proteins with the annotation "chemotaxis" in the GOBP[26, 27] or KEGG[100,102,134] database. Experiments were performed in four independent replicates. Samples were analysed by LC-MS/MS with label-free quantification,[96] filtered for proteins identified in three replicates, and samples were compared using a two-sided two-sample *t*-test. Adapted from Weigert Muñoz *et al*.[16]

enriched by the CheW antibody against the isotype control (both DMSO-treated) revealed interaction partners of CheW (Figure II-18 A). Among the significantly enriched proteins were several hits that are annotated to be involved in chemotaxis in the GO[135-136] or KEGG[100,102,134] database including CheA, CheZ, several MCPs, and a number of CheVs,[130] confirming the validity of the antibody and the methodology. Comparison of **EPI**-treated with DMSO-treated samples (both CheW antibody) revealed no changes in the protein interaction network in the presence of **EPI** (Figure II-18 B). The catecholamines might therefore act by inducing conformational changes rather than affecting the associated protein network, however, this requires more detailed research. The lack of change in the protein network is in line with the

observation that chemotaxis receptor arrays remain intact upon activation.[137] Moreover, these data strongly corroborate the central role of the identified target (A7MS42) in chemotaxis.

2.5.3 Effects of **EPI** and **PE** on the VC proteome

To reveal potential proteomic effects behind increased motility in the presence of **PE** and **EPI**, VC colonies from swimming assays were harvested off agar plates containing **EPI** (100 µM), **PE** (50 µM), or a DMSO control after 7 h or 24 h. Following lysis, the proteome was prepared for LC-MS/MS analysis (with LFQ). The analysis of dysregulated proteins was complicated by the poor annotation of proteins in VC. After 7 h exposition to **EPI**, six proteins were strongly upregulated (Figure II-19 A). Two of them, A7N237 and A7N8H5 are not well annotated.[138-139] The other four, A7N0E3,[140] A7MS66,[141] A7MZS8,[142] and A7N8L7,[143] most likely have oxidoreductase activity. Two are even explicitly assumed to act on catechols or quinones, e.g. the A7N8L7 is annotated as "quercetin 2,3-dioxygenase" (UniProt)[108,143] and A7N0E3 is a "FMN-dependent NADH:quinone oxidoreductase" acting as a "quinone reductase that provides resistance to thiol-specific stress caused by electrophilic quinones" (UniProt).[108,140] In the 24 h samples, A7MS66, A7MZS8, A7N8H5, A7N8L7, and A7N0E3 were still strongly upregulated whilst A7N237 was no longer significantly dysregulated (Figure II-19 B). None of these hits were up- or downregulated in **PE**-treated samples. In general, **PE** seemed to elicit a weaker effect on the proteome and no clear-cut response could be observed (Figure II-19 C and D). The effect of **EPI** most likely is a cellular defence against oxidative stress caused by oxidised **EPI** species. Although the bacteria were harvested from a set-up in which a clear response to **EPI** and **PE** was observed, this was the only specific response on the proteome level. As it was not caused by **PE**, it is likely not the driver of colony spread. The lack of responsiveness on the protein abundance level is consistent with CheW as the major adrenergic target and indicates that catecholamines may affect colony spread without major alterations in the overall proteome.

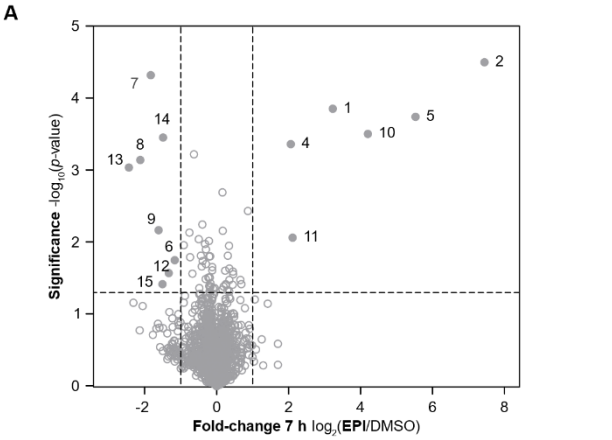

legend	UniProt	gene	protein name
1	A7MS66	VIBHAR_03109	FMN_red domain-containing protein
2	A7MZS8	VIBHAR_02944	GST C-terminal domain-containing protein
4	A7N8H5	VIBHAR_05924	UPF0312 protein VIBHAR_05924
5	A7N8L7	VIBHAR_06417	Quercetin 2,3-dioxygenase
6	A7MSE4	VIBHAR_03634	Lipopolysaccharide export system permease protein LptF
7	A7MVS2	VIBHAR_02204	CYTH domain-containing protein
8	A7MXU4	VIBHAR_00313	Adenyl_cycl_N domain-containing protein
9	A7MYN5	VIBHAR_01932	DUF3019 domain-containing protein
10	A7N0E3	azoR	FMN dependent NADH:quinone oxidoreductase
11	A7N237	VIBHAR_06786	DUF2721 domain-containing protein
12	A7N459	VIBHAR_05601	Polyketide cyclase
13	A7N5X0	VIBHAR_06993	CENP-V/GFA domain-containing protein
14	A7N640	VIBHAR_05251	PpiC domain-containing protein
15	A7N888	VIBHAR_06435	DUF2007 domain-containing protein

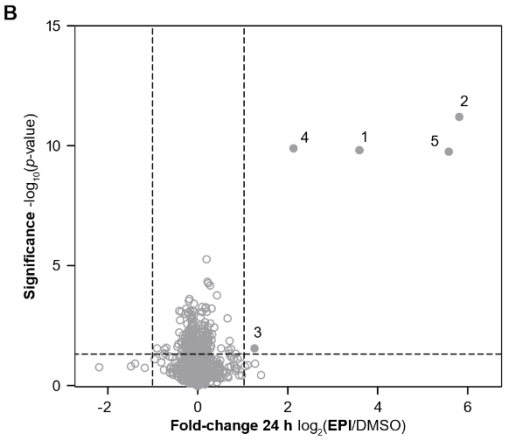

legend	UniProt	gene	protein name
1	A7MS66	VIBHAR_03109	FMN_red domain-containing protein
2	A7MZS8	VIBHAR_02944	GST C-terminal domain-containing protein
3	A7N2I5	VIBHAR_05120	DUF1722 domain-containing protein
4	A7N8H5	VIBHAR_05924	UPF0312 protein VIBHAR_05924
5	A7N8L7	VIBHAR_06417	Quercetin 2,3-dioxygenase

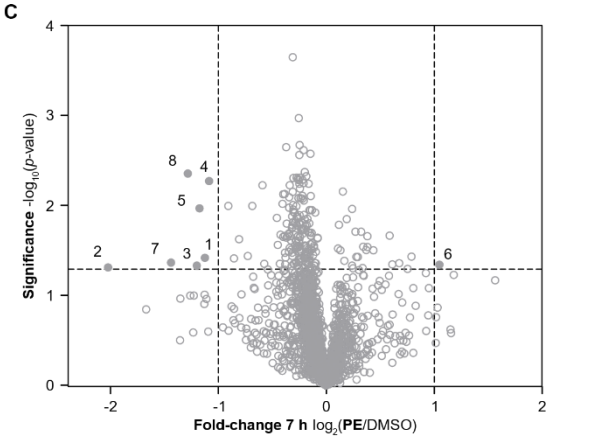

legend	UniProt	gene	protein name
1	A7MW55	VIBHAR_02383	GGDEF domain-containing protein
2	A7MWV4	VIBHAR_01141	Aminobenzoyl-glutamate transporter
3	A7MX10	hisF	Imidazole glycerol phosphate synthase subunit HisF
4	A7MXW0	VIBHAR_00292	Cystatin domain-containing protein
5	A7MXY0	VIBHAR_00278	Cell division protein FtsX
6	A7MY01	rnhB	Ribonuclease HII
7	A7MZV0	VIBHAR_02884	WxL domain-containing protein
8	A7N0B5	VIBHAR_02524	Multidrug ABC transporter permease/ATP-binding protein

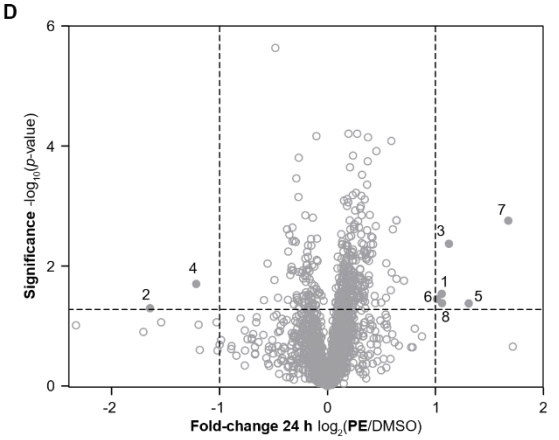

legend	UniProt	gene	protein name
1	A7MSY0	VIBHAR_00025	Site-spec. DNA-methyltransferase
2	A7MWF9	VIBHAR_00761	*N*-acetyltransferase domain-containing protein
3	A7MXF6	VIBHAR_00205	OKR_DC_1 domain-containing protein
4	A7MYT8	VIBHAR_03514	CinA domain-containing protein
5	A7N0C9	VIBHAR_02521	GTP-binding protein
6	A7N2P9	betA	Oxygen-dependent choline dehydrogenase
7	A7N3D4	VIBHAR_04996	Aminotran_5 domain-containing protein
8	A7N6V0	VIBHAR_06035	Exoribonuclease R

Figure II-19. Whole proteome analysis of VC treated with adrenergic compounds. VC was harvested from soft agar plates containing compounds as indicated. Volcano plots show fold-change of protein abundance in VC treated (A) 7 h with **EPI** (100 µM) or (B) treated 24 h compared to a DMSO control. Protein abundance in samples treated (C) 7 h with **PE** (50 µM) or (D) treated 24 h compared to a DMSO control. Peptides were analysed by LC-MS/MS with LFQ, filtered for proteins identified in two (7 h) or four (24 h) replicates, and missing values were imputed. Samples were compared using a two-sided two-sample *t*-test; n = 3 (7 h) or n = 5 (24 h) independent replicates. Significantly dysregulated proteins ($-\log_{10}(p\text{-value}) > 1.3$, $\log_2(\text{enrichment}) > 2$) are shown as full circles and are listed in the tables.

2.5.4 Investigation of mechanisms behind catecholamine-dependent colony spread

Colony expansion on soft agar is frequently reported as an assay to determine swimming motility, though the underlying biological processes are more complex. Besides motility

behaviour, the colony diameter is further influenced by a combination of chemosensing, chemoattractant consumption, and growth.[144-145] Therefore, a more thorough analysis of potential mechanisms behind catecholamine-promoted colony expansion was required. First, 3D trajectories of VC motility were measured in the presence or absence of **EPI**. For this, the movement of individual bacteria were microscopically tracked.

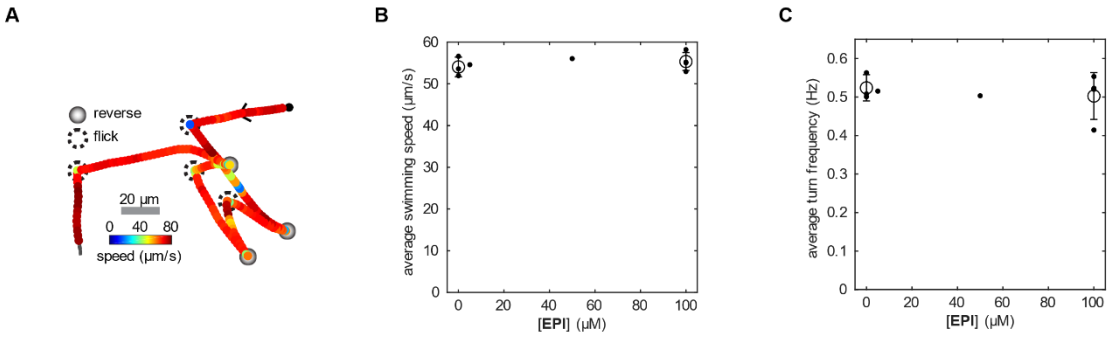

Figure II-20. 3D tracking of VC motility. (A) Example VC 3D trajectory shows run-reverse-flick motility turns alternating between reversals and flicks. (B) Average motile swimming speed in the presence of varying **EPI** concentrations; bacteria with an average swimming speed of at least 20 µm/s were defined as motile. (C) Average turning frequency in the presence of varying **EPI** concentrations. Points represent technical replicates; open circles denote average with error bars as standard deviation. The analysis was performed for motile bacteria with a minimum trajectory duration of 1 s. Experiments were performed by M. Grognot and K. M. Taute (Harvard University). Adapted from Weigert Muñoz *et al.*[16]

VC motility followed a run-reverse-flick pattern (Figure II-20 A) with swimming speeds of 54 ± 2 µm/s (Figure II-20 B) and a steady-state turning frequency of $0.52 \pm 0.03\ s^{-1}$ (Figure II-20 C). Both the swimming speed and turning frequency were not altered in the presence of **EPI**.

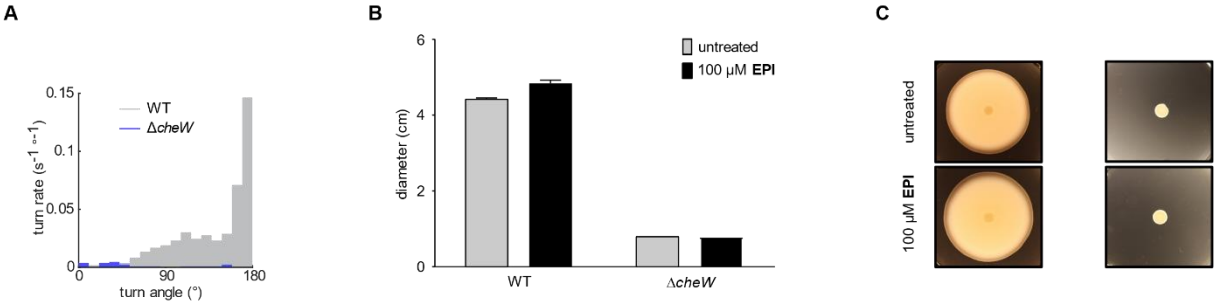

Figure II-21. Effects of *cheW* deletion on VC motility. (A) Rate of turn events as a function of turn angle in wild-type VC and the Δ*cheW* mutant determined from 3D motility tracking. Rates were determined based on 1,447 turn events detected in 1,295 s trajectory time (wild-type) and 29 events in 3,250 s (Δ*cheW*). (B) Motility halo diameters from soft agar assays of VC wild-type and Δ*cheW* mutant after 24 h incubation with or without **EPI** (100 µM). Error bars represent standard deviation (wild-type n = 7 and mutant n = 6 independent replicates). (C) Soft agar plate showing wild-type and Δ*cheW* after 24 h incubation. Experiments were performed by M. Grognot and K. M. Taute (Harvard University) and by E. Hoyer (LMU). Adapted from Weigert Muñoz *et al.*[16]

The protein components of the chemotaxis cascade can vary greatly across species and some are known to encode more than one chemotaxis system,[144] therefore, it was important to inspect the motility of a deletion mutant of the identified CheW (A7MS42). While the swimming speed

was in a similar range as determined for the wild-type (48 ± 4 µm/s), Δ*cheW* displayed a smooth swimming behaviour with a much lower turning frequency (Figure II-21 A). Interestingly, the mutant was severely compromised in its ability to spread on soft agar both in the presence and absence of **EPI** (Figure II-21 B and C). It has been observed previously that the Δ*cheW* mutant of another *Vibrio* species, which was unable to chemotact, could no longer spread on soft agar.[146] On soft agar, bacteria need to navigate through a lose agar mesh and smooth swimmers get stuck as they are unable to reorient themselves by tumbling.[144] These observations highlight that the identified protein (A7MS42) is indeed central for VC chemotaxis and its deletion severely impacts motility in general and also specifically affects spread in soft agar assays.

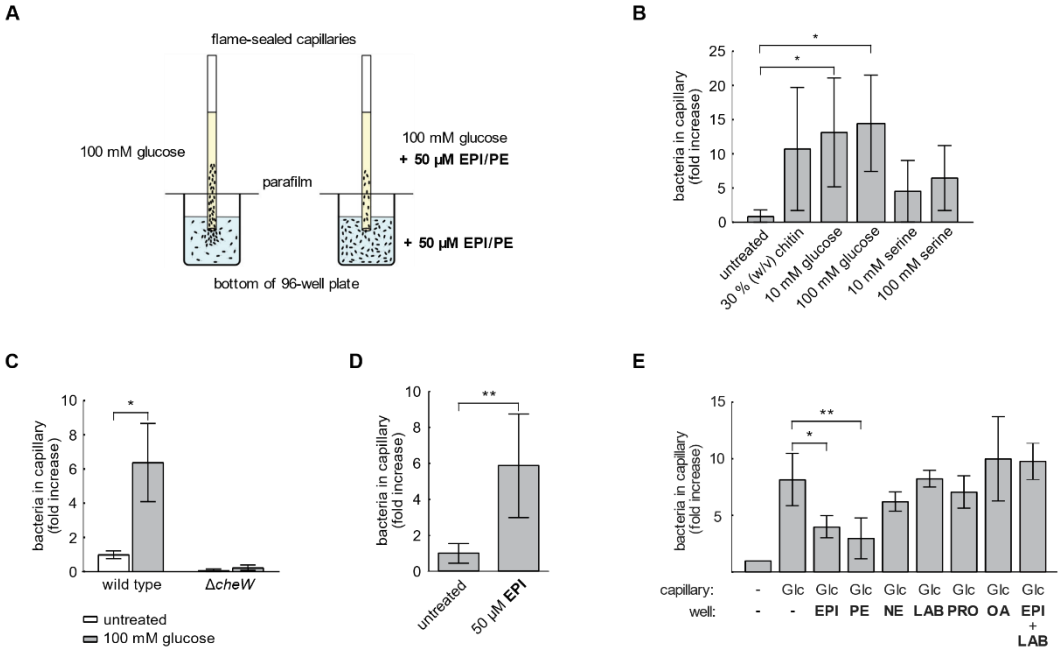

Figure II-22. Effects of adrenergic compounds on VC chemotaxis. (A) Experimental set-up of capillary-based assay. A capillary containing chemoattractant was inserted into a reservoir where the signal was absent, generating a diffusion gradient and causing bacteria to swim from the reservoir into the glass capillary. Bacterial numbers in the capillary were determined after 60 min. (B) Number of wild-type VC determined in capillary filled with different chemical attractants. (C) Number of Δ*cheW* VC determined in a capillary filled with glucose compared to the wild-type. (D) Number of wild-type VC determined in capillary filled with **EPI**. (E) Number of wild-type VC in capillaries filled with glucose (100 mM) in the presence of adrenergic compounds (50 µM, homogenous concentration). Experiments were performed in HEPES-buffered artificial seawater. Bacterial numbers were normalised to an untreated control. Error bars denote standard deviation, n = 4 biological replicates. Statistical significance was determined using an unpaired two-tailed *t*-test (* = $p < 0.05$, ** = $p < 0.01$). Glc = glucose. Experiments were performed by K. Schumacher (LMU). Adapted from Weigert Muñoz *et al.*[16]

Finally, a closer look was taken on chemotaxis. Chemotaxis is the directional movement along the gradient of a chemical stimulus that allows bacteria to find optimum conditions. The role of adrenergic compounds in chemotaxis was studied in a capillary-based assay.[147] To a well with VC, a glass capillary containing a solution of the chemotactic signal was introduced, thus generating a gradient by diffusion (Figure II-22 A). The number of bacteria accumulated in the capillary after a given time compared to a control containing only medium reflected whether

the substance of interest elicits chemotaxis. Satisfyingly, a significant increase in the number of bacteria was observed in capillaries containing chitin (30% w/v) or glucose (10–100 mM) after 1 h, validating the methodology. Chemotaxis towards serine (10–100 mM) was less pronounced (Figure II-22 B). The Δ*cheW* mutant was drastically impaired in its ability to swim into the capillary both in the presence and absence of attractant, indicating disrupted chemotaxis signalling (Figure II-22 C). A gradient of **EPI** (50 µM in capillary) also led to an increased cell number in the capillary compared to the control, demonstrating that VC senses **EPI** as a chemoattractant (Figure II-22 D).

In *E. coli*, **NE** elicited a biphasic chemotactic response which contrasted with the behaviour of conventional chemotactic signals.[85] This response was similar to unconventional chemotactic signals which are not sensed by a specific periplasmic sensor domain,[84] although the response was specific and discriminated against chemically related compounds.[85] These observations are consistent with a specific sensor protein or protein domain that is located downstream of the MCP´s periplasmic sensor in the chemotaxis complex, such as CheW. Being a central component of the core chemotaxis complex, interaction of CheW with small molecules might have more global implications for the entire chemotactic process compared to a conventional chemotactic signal and result in an overall modulation of chemotaxis. To explore this hypothesis, chemotaxis to attractants was monitored in the presence of adrenergic compounds. For this, bacteria were exposed to a gradient of the strong chemoattractant glucose whilst the concentration of adrenergic compounds in the medium was homogenous (in both the well and the capillary). Intriguingly, the number of bacteria in a glucose-containing capillary was significantly lower in the presence of a homogenous background of **EPI** or **PE**, indicating that these compounds indeed modulated chemotactic control (Figure II-22 E). **NE** had no significant effect, which is in line with its weak activity in the soft agar assays. Furthermore, the presence of **OA**, **LAB**, and **PRO** did not alter bacterial numbers in the glucose capillary, consistent with their lack of activity in the plate-based assays. Moreover, an equimolar combination of **LAB** with **EPI** suppressed the effects of the latter, demonstrating that also in this assay, **LAB** acted as an adrenergic antagonist. Hence, the specific effects of adrenergic compounds in the chemotaxis assay largely reflected the results from the soft agar assays and suggest that binding of **EPI** or **PE** to CheW affects the swimming behaviour of VC in chemical gradients.

2.6 Conclusion and outlook

The aim of this project was to elucidate the cellular processes behind catecholamine-dependent colony spread in VC. The key findings were the following:

- First, it was shown that catecholamine-promoted spread on soft agar is likely independent of altered iron supply as it could be observed for both **EPI** and **PE**, the latter of which carries no catechol group and should not act as siderophore, as was shown by the lack of growth stimulation in iron-deprived medium. Furthermore, **EPI** and **PE** were antagonised by the clinical adrenergic antagonist **LAB** in the soft agar assay. These observations pointed to a specific receptor that mediates adrenergic motility responses in VC.
- Second, CheW (A7MS42), which constitutes the core of the chemotaxis complex,[114] was identified as a major adrenergic target as it was enriched in an untargeted chemical proteomics approach using two probes based on **EPI** and **PE**, respectively. It was demonstrated that **EPI**, **PE**, and **LAB** bind to CheW as they outcompeted binding of the chemical probe *in situ* and affinity constants in the nanomolar range were determined *in vitro*.
- Third, while adrenergic compounds did not seem to affect swimming speed or turning frequency of VC, chemotaxis to glucose was strongly reduced in the presence of **EPI** or **PE**. Again, this effect was antagonised in the presence of **LAB**. These findings are consistent with a modulation of VC chemotactic control by **EPI** and **PE**.

The extremely low turning frequency and loss of chemotaxis of a Δ*cheW* mutant proved the central role of the identified target protein in VC motility. Therefore, it is in fact plausible that small molecule binding to CheW can have extensive effects on chemotaxis and swimming behaviour.

The data illustrated in this thesis point towards CheW as a potential receptor protein which modulates chemotaxis in response to small molecule binding. These results are unexpected, considering that canonically, chemical stimuli are sensed by the periplasmic sensory domain of chemoreceptors.[84] However, non-conventional sensing mechanisms are reported in the literature, in which regulation occurs downstream of the sensory domain. For instance, cytoplasmic parts of chemoreceptors are involved in the sensing of certain physicochemical stimuli and repellents such as phenol.[84] Beyond that, uptake of sugars lowers the phosphorylation state of intracellular proteins of the phosphotransferase system (PTS). This causes PTS proteins to alter the activity of CheA, which acts directly downstream of CheW.

These examples highlight that chemotaxis is indeed significantly regulated by processes independent of the periplasmic sensory domain. It has previously been observed that *E. coli* chemotaxis to **NE** appears to follow a non-conventional mechanism and that it may be sensed indirectly.[85] Another consideration is that regulation of chemotaxis at the level of CheW appears in fact plausible. Certain bacterial species encode several coupling proteins, which enables a more fine-tuned control of chemotaxis.[114,130] For instance, the coupling protein CheV consists of a CheW domain fused to a receiver domain and phosphorylation of the latter is assumed to modulate coupling efficiency.[130] Yet, the exact molecular mechanism behind the modulation of chemotactic control by adrenergic compounds remains to be unravelled.

Another open question is the physiological role of adrenergic modulation of chemotactic control. Chemotaxis and swimming motility overall are crucial for host colonisation and the infectivity of pathogens.[83,144] Bacteria use chemotaxis to navigate along chemical gradients searching for the best environmental conditions. In many cases, chemotaxis reflects metabolic preferences, i.e., nutrients are sensed as chemoattractants and toxins as chemorepellents. In other cases, chemoattractants merely serve as cues indicating supportive environmental conditions. Host-associated chemicals are often sensed as chemoattractants[148] to guide the bacteria towards their host or to a specific site of infection.[144,149] As a consequence, the regulation of chemotaxis in the physiological context of bacteria-host interaction is highly complex and not yet well understood.[144] Swimming motility entails a large energetic cost and may even negatively impact bacterial growth, therefore, bacteria need to gauge chemotactic activity according to their surroundings. It is assumed that *E. coli* invests energy in motile behaviour depending on the anticipated benefits.[144] For instance, during growth in poor carbon sources, motility is upregulated to promote chemotaxis towards potential additional nutrient sources, whilst motility is downregulated in a nutritionally rich environment.[144] These trade-offs require multiple regulatory strategies.[144] Interestingly, the downregulation of chemotaxis appears favourable under certain conditions. For instance, a non-chemotactic, smooth swimming mutant of *V. cholerae* was found to outcompete wild-type bacteria in an infection model because the disability to chemotact likely allowed it to more widely spread out into the host.[83] The observation that *V. cholerae* from human stool is more infective compared to when grown *in vitro* was associated with improved motility and concurrent lack of chemotaxis.[150-151] Intriguingly, this was accompanied by reduced expression of CheW.[151]

In conclusion, it is tempting to speculate that chemotaxis towards glucose is reduced in the presence of **EPI** to prioritise localisation within the host over nutritional interests and that small molecule binding to CheW is an as yet unknown regulatory strategy. In this case, colonisation

of a specific niche within an animal host may be preferential over nutrient acquisition. Follow-up studies should examine chemotaxis in the presence of **EPI** or **PE** more closely, e.g., by elucidating whether adrenergic compounds reduce chemotaxis in global way or if this is specific for chemoattractants, or even specific signals. Another pressing point is whether CheW acts as an adrenergic sensor in other species and whether the modulation of chemotactic activity via ligand binding to CheW is a global mechanism.

3 Experimental procedures

3.1 Chemical synthesis

3.1.1 General remarks

Chemicals with reagent or higher grade as well as dry solvents were purchased from *Sigma Aldrich*, *Acros Organics*, or *Alfa Aesar*. 2-(3-But-3-ynyl-3*H*-diazirin-3-yl)-ethanol was purchased from *Ark Pharm Inc*.

Analytical thin layer chromatography was performed on aluminium-coated TLC silica gel plates (silica gel 60, F254, *Merck KGaA*) with visualisation by UV light (λ = 254 nm) or $KMnO_4$-stain (3.0 g $KMnO_4$, 20.0 g K_2CO_3, and 5 mL 5% [w/v] NaOH in 300 mL ddH_2O). Column chromatography was carried out using silica gel (40–63 µm (Si 60), *Merck KGaA*). High-resolution mass spectra (HRMS) were measured on a LTQ-FT Ultra (*Thermo Fisher*) equipped with an ESI ion source.

NMR spectra were measured at room temperature on Avance-III HD NMR systems with 300, 400, or 500 MHz (*Bruker Co.*). Chemical shifts are reported in parts per million (ppm) and residual proton signals of deuterated solvents were used as internal reference (^{1}H NMR: $CDCl_3$ δ = 7.26 ppm, DMSO-d_6 δ = 2.50 ppm, 0.04% [v/v] DCl in D_2O referenced to D_2O δ = 4.79 ppm. ^{13}C-NMR: $CDCl_3$ δ = 77.16 ppm, DMSO-d_6 δ = 39.52 ppm, 50% [v/v] AcOD in D_2O referenced to AcOD δ = 178.990 ppm). Coupling constants (*J*) are reported in Hertz (Hz). Signal multiplicities are denoted with the following abbreviations: s – singlet, d – doublet, dd – doublet of doublets, dt – doublet of triplets, ddd – doublet of doublet of doublets, t – triplet, td – triplet of doublets, p – pentet, and m – multiplet. NMR data were analysed using MestReNova (*Mestrelab Research*).

3.1.2 Synthesis of 3-(but-3-yn-1-yl)-3-(2-iodoethyl)-3*H*-diazirine (**PCL-I**)[95]

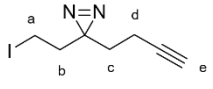

PCL-I
$C_7H_9IN_2$
248.07 g/mol

The reaction was carried out following a published protocol.[29] A solution of imidazole (74 mg, 1.08 mmol, 3.0 eq.) and triphenylphosphine (104 mg, 0.398 mmol, 1.1 eq.) in anhydrous CH_2Cl_2 (2 mL) was cooled to 0 °C. Pestled iodine (110 mg, 0.434 mmol, 1.2 eq.) was added

and the solution was stirred at 0 °C for 5 min. 2-(3-(But-3-ynyl)-3*H*-diazirin-3-yl)ethanol (50 mg, 0.361 mmol, 1.0 eq.) was added in CH_2Cl_2 (~1 mL) and the reaction mixture was stirred 7 h under the exclusion of light. The reaction was quenched with saturated aqueous $Na_2S_2O_3$ (2 mL) and the aqueous layer was extracted with EtOAc (2 x 5 mL). Combined organic layers were washed with brine (1 x 5 mL) and dried over Na_2SO_4. Solvents were removed under reduced pressure (≥ 50 mbar) and the residue was purified by column chromatography (EtOAc/n-hexane 1:20). Solvents were removed under reduced pressure (≥ 50 mbar) and the product was obtained as a colourless liquid (55 mg, 0.222 mmol, 62%).

TLC: R_f = 0.53 (EtOAc/n-hexane 1:20) [UV/$KMnO_4$]. **^{1}H-NMR** (500 MHz, $CDCl_3$) δ [ppm]: 2.89 (t, *J* = 7.6 Hz, 2H, H-a), 2.12 (t, *J* = 7.6 Hz, 2H, H-d), 2.06-2.00 (m, 3H, H-b, H-e), 1.69 (t, *J* = 7.2 Hz, 2H, H-c). **^{13}C-NMR** (75 MHz, $CDCl_3$) δ [ppm]: 82.56, 69.57, 37.66, 31.96, 28.73, 13.39, -3.88. Analytical data are in accordance with literature reports.[29]

3.1.3 Synthesis of (*R*)-4-(2-((2-(3-(but-3-yn-1-yl)-3*H*-diazirin-3-yl)ethyl)amino)-1-hydroxyethyl)-benzene-1,2-diol (**EPI-P1**)[95]

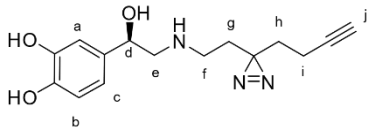

EPI-P1
$C_{15}H_{19}N_3O_3$
289.34

NE (105 mg, 0.621 mmol, 3.5 eq.) was added to a solution of **PCL-I** (44 mg, 0.177 mmol, 1.0 eq.) in anhydrous DMF (6 mL) and it was stirred at 70 °C (with reflux) under argon for 17 h. Solvents were removed under reduced pressure and the residue was purified by column chromatography (MeOH/AcOH/CH_2Cl_2 1:3:10) and solvents were removed under reduced pressure with toluene co-evaporation. The product **EPI-P1** was obtained as a mixture with acetic acid (**EPI-P1**:AcOH 1:3.5) as a brown solid (53 mg, 0.106 mmol, 62%).

TLC: R_f = 0.43 (MeOH/AcOH/CH_2Cl_2 1:3:7) [UV/$KMnO_4$]. **^{1}H-NMR** (500 MHz, DCl/D_2O 38:962) δ [ppm]: 6.66–6.63 (m, 2H, H-a and H-b), 6.57 (dd, *J* = 8.2, 2.1 Hz, 1H, H-c), 4.63 (dd, *J* = 7.9, 5.2 Hz, 1H, H-d), 3.01–2.95 (m, 2H, H-e), 2.78 (td, *J* = 8.7, 2.1 Hz, 2H, H-f), 2.10 (t, *J* = 2.7 Hz, 1H, H-j), 1.80–1.74 (m, 13H, AcOH + H-i), 1.59 (ddd, *J* = 10.6, 6.4, 2.7 Hz, 2H, H-g), 1.42 (t, *J* = 7.1 Hz, 2H, H-h). **^{13}C-NMR** (101 MHz, AcOD/D_2O 1:1) δ [ppm]: 147.11, 147.04, 134.59, 120.99, 118.78, 116.23, 86.08, 72.85, 71.27, 56.17, 45.43, 33.56, 32.06, 29.07, 15.19. **HRMS:** (ESI) $C_{15}H_{20}N_3O_3^+$ $[M+H]^+$ calculated: 290.1499; found: 290.1499.

3.1.4 Amide coupling general protocol (second generation probes)

To a solution of 6-heptynoic acid (127 µL, 0.950 mmol, 1.0 eq.) in DMF (10 mL), EDC·HCl (182 mg, 0.95 mmol, 1.0 eq.) and HOBt (128 mg, 0.95 mmol, 1.0 eq.) was added. The clear solution was stirred at 0 °C for 30 min and then at room temperature for 4 h. Anhydrous TEA (395 µL, 2.85 mmol, 3.0 eq.; or 4 eq. if amine was HCl salt) was added followed by the amine (0.95 mmol, 1.0 eq.). The mixture was stirred overnight. Water (100 mL) was added, the mixture was extracted with 3 x EtOAc (30 mL), and combined organic phases were washed with brine (30 mL) and dried over Na_2SO_4. Solvents were removed under reduced pressure and the crude mixture was purified by SiO_2 chromatography ($MeOH/CH_2Cl_2$ 8:92).

3.1.5 Synthesis of (*R*)-*N*-(2-(3,4-dihydroxyphenyl)-2-hydroxyethyl)hept-6-ynamide (**EPI-P2**)

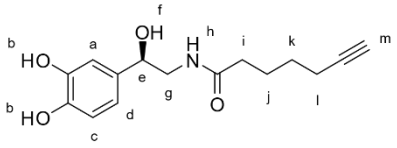

EPI-P2
$C_{15}H_{19}NO_4$
277.32

The reaction was performed with L-norepinephrine (161 mg, 0.950 mmol, 1.0 eq.) and the product was obtained as a pale orange amorphous solid (86 mg, 0.310 mmol, 16%).

TLC: R_f = 0.37 ($MeOH/CH_2Cl_2$ 8:92) [UV/$KMnO_4$]. **^{1}H-NMR:** (500 MHz, DMSO-d_6) δ [ppm]: 8.78 (s, 1H, H-b), 8.68 (s, 1H, H-b), 7.77 (t, J = 5.6 Hz, 1H, H-h), 6.71 (d, J = 1.7 Hz, 1H, H-a), 6.65 (d, J = 8.0 Hz, 1H, H-c), 6.54 (dd, J = 8.0, 1.7 Hz, 1H, H-d), 5.18 (d, J = 4.1 Hz, 1H, H-f), 4.39 (dt, J = 8.3, 4.4 Hz, 1H, H-e), 3.23–3.17 (m, 1H, H-g), 3.00 (ddd, J = 13.1, 7.9, 5.1 Hz, 1H, H-g), 2.74 (t, J = 2.6 Hz, 1H, H-m), 2.13 (td, J = 7.0, 2.6 Hz, 2H, H-l), 2.08–2.04 (m, 2H, H-i), 1.54 (p, J = 7.4 Hz, 2H, H-j), 1.39 (p, J = 7.1 Hz, 2H, H-k). **^{13}C-NMR:** (101 MHz, DMSO-d_6) δ [ppm]: 172.10, 144.83, 144.19, 134.87, 116.88, 115.05, 113.46, 84.43, 71.29, 71.20, 46.96, 34.69, 27.52, 24.42, 17.48. **HRMS:** (ESI) $C_{15}H_{20}NO_4^+$ $[M+H]^+$ calculated: 278.1387, found: 278.1388.

3.1.6 Synthesis of *N*-(2-hydroxy-2-(3-hydroxyphenyl)ethyl)hept-6-ynamide (**PE-P**)

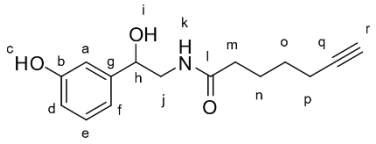

The reaction was performed with DL-norphenylephrine·HCl (180 mg, 1.00 mmol, 1.0 eq.) and the product was obtained as a white powder (169 mg, 0.648 mmol, 65%).

TLC: R_f = 0.63 (MeOH/CH_2Cl_2 8:92) [UV/$KMnO_4$]. **^{1}H-NMR:** (500 MHz, DMSO-d_6) δ [ppm]: 9.27 (s, 1H, H-c), 7.83 (t, *J* = 5.8 Hz, 1H, H-k), 7.09 (t, *J* = 7.8 Hz, 1H, H-e), 6.74 (s, 1H, H-a), 6.71 (d, *J* = 7.6 Hz, 1H, H-f), 6.61 (dd, *J* = 8.0, 2.5 Hz, 1H, H-d), 5.35 (d, *J* = 4.3 Hz, 1H, H-i), 4.48 (dt, *J* = 8.5, 4.5 Hz, 1H, H-h), 3.28–3.22 (m, 1H, H-j), 3.06–3.00 (m, 1H, H-j), 2.75 (t, *J* = 2.6 Hz, 1H, H-r), 2.13 (td, *J* = 7.0, 2.6 Hz, 2H, H-p), 2.07 (t, *J* = 7.4 Hz, 2H, H-m), 1.55 (p, *J* = 7.4 Hz, 2H, H-n), 1.38 (p, *J* = 7.1 Hz, 2H, H-o). **^{13}C-NMR:** (101 MHz, DMSO-d_6) δ [ppm]: 172.56, 157.62, 145.83, 129.35, 117.08, 114.35, 113.29, 84.86, 71.90, 71.68, 47.31, 35.12, 27.97, 24.85, 17.93. **HRMS:** (ESI) $C_{15}H_{12}NO_3^+$ $[M+H]^+$ calculated: 262.1438, found: 262.1438.

3.1.7 Synthesis of *N*-(2-hydroxy-2-(4-hydroxyphenyl)ethyl)hept-6-ynamide (**OA-P**)

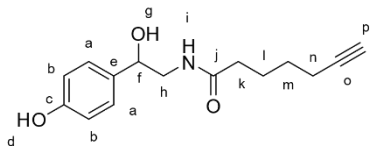

The reaction was performed with DL-octopamine·HCl (241 mg, 1.27 mmol, 1.0 eq.) and the product was obtained as a white powder (189 mg, 0.723 mmol, 54%).

TLC: R_f = 0.47 (MeOH/CH_2Cl_2 9:91) [UV/$KMnO_4$]. **^{1}H-NMR:** (300 MHz, DMSO-d_6) δ [ppm]: 9.22 (s, 1H, H-d), 7.76 (t, *J* = 5.7 Hz, 1H, H-i), 7.15–7.04 (m, 2H, H-a), 6.75–6.64 (m, 2H, H-b), 5.22 (d, *J* = 4.2 Hz, 1H, H-g), 4.47 (dt, *J* = 8.6, 4.6 Hz, 1H, H-f), 3.26–3.01 (m, 2H, H-h), 2.74 (t, *J* = 2.7 Hz, 1H, H-p), 2.13 (td, *J* = 7.0, 2.7 Hz, 2H, H-n), 2.06 (t, *J* = 7.3 Hz, 2H, H-k), 1.60–1.48 (m, 2H, H-l), 1.44–1.32 (m, 2H, H-m). **^{13}C-NMR:** (75 MHz, DMSO-d_6)

δ [ppm]: 172.01, 156.34, 134.06, 127.10, 114.68, 84.37, 71.18, 71.14, 46.81, 34.63, 27.48, 24.38, 17.43. **HRMS:** (ESI) $C_{15}H_{18}NO_3^-$ [M-H]$^-$ calculated: 260. 1292; found: 260.1292.

3.2 Biochemical methods

3.2.1 General information

3.2.1.1 Chemical compounds

For proteomics experiments, synthesised probes were stored as DMSO stocks at -20 °C; unmodified parent compounds were dissolved in DMSO on the day of the experiment.

Table II-1. Compounds used in this study.

abbreviation	substance	supplier
EPI	DL-epinephrine hydrochloride	*TCI Chemicals*
NE	L-norepinephrine	*Alfa Aesar*
PE	(*R*)-(-)-phenylephrine hydrochloride	*Sigma*
LAB	labetalol hydrochloride	*Sigma*
PRO	propranolol hydrochloride	*Sigma*

3.2.1.2 Bacterial culture

Bacteria were stored as 50% (v/v) glycerol stocks at -80 °C. Unless otherwise specified, overnight cultures for growth assays, photolabelling, and co-IP experiments were grown from 50% (v/v) glycerol stocks inoculated 1:1000 into 20 mL medium for 15 h at the indicated temperatures and 200 rpm. Overnight cultures were then diluted 1:100 into fresh medium (60 mL) and grown to early stationary phase. For 3D motility and chemotaxis assays, overnight cultures were inoculated from individual *V. campbellii* colonies, grown on 2% (w/v) MB agar plates streaked from a glycerol stock, and grown to saturation in 2 mL MB at 30 °C, 200 rpm. Day cultures were inoculated with the overnight cultures at 1:200 dilution in 10 mL MB and grown at 30 °C, 250 rpm, until they reached OD_{600} 0.3.

Table II-2. Bacterial culture conditions.

strain	medium	temperature
Vibrio campbellii (all strains)	LB35, MB, TMN	30 °C
Escherichia coli (all strains)	LB	37 °C
Photorhabdus asymbiotica	CASO	30 °C
Photorhabdus luminescens	CASO	30 °C
Aliivibrio fischeri	Medium 514c	25 °C
Vibrio parahaemolyticus	LB30	30 °C
Salmonella enterica serovar Typhimurium	LB	37 °C

Table II-3. Media used in this study.

medium	ingredients
LB	1% (w/v) peptone, 0.5% (w/v) NaCl, 0.5% (w/v) yeast extract, pH 7.5
LB35	LB containing 3.5% (w/v) NaCl
MB	Difco Marine Broth 2216
TMN	50 mM Tris-HCl, 300 mM NaCl, 5 mM $MgCl_2$, 5 mM glucose, pH 7.5
LB30	LB containing 3% (w/v) NaCl
CASO	1.7% (w/v) peptone from casein, 0.3% (w/v) peptone from soybean, 0.25% (w/v) K_2HPO_4, 0.5% (w/v) NaCl, 0.25% (w/v) glucose, pH 7.3
MB	Difco Marine Broth 2216
Medium 514c	Marine Bouillon (*Carl Roth* CP73)
TMN	50 mM Tris-HCl, 300 mM NaCl, 5 mM $MgCl_2$, 5 mM glucose, pH 7.5

Table II-4. Strains and plasmids used in this study.

strain or plasmid	relevant genotype or description	reference
	Escherichia coli	
DH5__αλpir	*endA1 hsdR17 glnV44 (= supE44) thi-1 recA1 gyrA96 relA1* φ80'*lac*Δ*(lacZ)*M15 Δ*(lacZYA-argF)*U169 *zdg*-232::Tn10 *uidA::pir+*	[152]
WM3064	*thrB*1004 *pro thi rpsL hsdS lacZ*ΔM15 RP4-1360 Δ(*araBAD*)567 Δ*dapA*1341::[*erm pir*]	W. Metcalf, Univ. of Illinois, Urbana
BL21(DE3)	F^- *ompT gal dcm lon hsdSB*(rB^- mB^-) λ(DE3)	[153]
	Vibrio campbellii	
V. campbellii ATCC BAA-1116	wild-type	[89]
V. campbellii Δ*cheW*	clean deletion of *cheW*	This work[16]
	Photorhabdus asymbiotica	
ATC43949	wild-type	[154]
	Photorhabdus luminescens	
TT01	wild-type	[155]
	Aliivibrio fischeri	
DSM507	wild-type	[156]
	***Salmonella enterica* serovar Typhimurium**	
LT2	wild-type	[157]
	Vibrio parahaemolyticus	
RIMD 2210633	wild-type	T. Iida and T. Honda, Osaka University

plasmids		
pET28a	Vector for expression of N-terminally 6xHis-tagged proteins with a thrombin site, Km^R	*Novagen*
pET28a-*cheW*	*cheW* cloned in the BamHI and XhoI sites of pET28a, Km^R	This work[16]
pNTPS138-R6KT	*mobRP4*$^+$ *ori*-R6K *sacB*; suicide plasmid for in-frame deletions, Km^R	[158]
pNPTS138-R6KT-*cheW*	pNPTS-138-R6KT-derived suicide plasmid for clean deletion of *cheW* in *V. campbellii*, Km^R	This work[16]

Table II-5. Oligonucleotides used in this study.

name	sequence (restriction site in blue)	description
fwd_BamHI_up_cheW	TAGCCGGATCCTTGAACAGCACACTGAGACAGC	Generation of the **pNPTS138-R6KT *cheW*** plasmid for clean deletion of *cheW* in *V. campbellii*
rev_EcoRI_down_cheW	GCGTAGAATTCGCGAGAGGAATATGTCGGGTC	
rev_start cheW _up	TGAGCCATAAAAGCTTGAGACATAGTTAATCCTCGTTAATG	
fwd_start cheW _down	AAGCTTTTATGGCTCACCTGTAATTGGCTGATGAATCATGG	
fwd_BamHI_cheW	TAGCCGGATCCATGTCTCAAGCTTTTGAAG	Generation of the overexpression plasmid **pET28a-*cheW*** coding for N-terminal His_6-tagged *cheW*
rev_cheW_Stop_XhoI	TAGCCCTCGAGTTACAGGTGAGCCATCTCATC	

3.2.2 Bioactivity assays

3.2.2.1 Soft agar colony expansion assay

Soft agar colony expansion assays were performed as described previously on LB35 plates containing 0.3% (w/v) agar.[71] Catecholamines and antagonists were dissolved in water and added as supplements directly to the autoclaved medium before pouring plates. As control, the appropriate volume of water was added to the plates. A *V. campbellii* overnight culture was diluted in fresh LB35 (OD_{600} 1.0) and 5 µL culture was dropped in the centre of the plate with six independent replicates for each condition. After an incubation of 24 h at 30 °C, the colony diameter was measured. Radial expansions were normalized to an untreated control and significance was determined performing a one-way ANOVA with Tukey´s post hoc test.

3.2.2.2 Growth assays

A *V. campbellii* overnight culture was diluted 1:100 in fresh LB35 medium (60 mL) and grown until early stationary phase (8 h, OD_{600} ~5.0). Compounds (1 µL 10 mM stock in DMSO for 50 µM final concentration) were dispensed into a clear flat-bottom 96-well plate (*Thermo Scientific*) and 199 µL of bacterial culture previously diluted to OD_{600} 0.005 in LB35 or in LB35 supplemented with 30% (v/v) of adult bovine serum (*Sigma*) was added. The plate was incubated in an Infinite® M200 Pro plate reader (*Tecan*) at 30 °C with 20 s shaking every 5 min. The absorbance at 600 nm was measured every 30 min. Blank values (only medium) were subtracted from data values and data were plotted in GraphPad Prism 5.03.

3.2.2.3 3D motility assay

Bacterial culture (20 µL) was added to TMN (1 mL) containing **EPI** at the specified concentrations, mixed gently, and left on the bench for 30 min. The solutions were then flowed into sample chambers, consisting of three layers of parafilm as spacers between a microscopy slide and a #1 coverslip that had been heated and pressed to seal. After filling, the ends of the filled chamber were sealed with molten valap (a mixture of vaseline, lanolin, and paraffin) and immediately brought to the microscope for recording, all within 60 min of dilution from the day culture. **EPI** was diluted into TMN from a 50 mM stock solution in DMSO stored at -20 °C, within 3 h before the experiment.

3.2.2.4 3D chemotaxis assays

3D chemotaxis experiments were performed using a high-throughput chemotaxis assay[159] using a commercially available microfluidic device (*Ibidi*) consisting of two 65 µL reservoirs connected by a 1 mm-long channel with a height of 70 µm and a width of 1 mm. *V. campbellii* cultures were diluted into chemotaxis buffer without (creating solution A) or with the putative chemoattractant (creating solution B) to OD_{600} 0.008 for **EPI** gradients or OD_{600} 0.005 for serine and glucose gradients. Chemotaxis buffer consisted of TMN, with an added background of **EPI** or **PE** for some experiments as specified, and without glucose for glucose gradients. Chemoattractants included **EPI**, L-serine, and D-glucose at the specified concentrations. First, the entire microfluidic device was overfilled with solution A. Then, the content of one reservoir was exchanged by solution B. A linear chemical gradient was established in the narrow channel between reservoirs within approximately 30 min and was stable for several hours. About 40–60 min after closing the device, 3D bacterial trajectories were acquired in the middle of this gradient. For experiments with **EPI** gradients, **EPI** was prepared as a 40 mM stock in TMN within 3 h before the experiment. For serine chemotaxis experiments, **EPI** was prepared as 20 mM stock in TMN within 3 h before the experiments. For glucose chemotaxis experiments, **EPI** and **PE** were prepared as 60 mM stock in water, within 3 h before the experiment.

3.2.2.5 Data acquisition and analysis of 3D trajectories

Phase contrast microscopy recordings were obtained at room temperature (~21 °C) on a Nikon Ti-E inverted microscope using an sCMOS camera (PCO Edge 4.2) and a 40x objective lens (Nikon CFI SPlan Fluor ELWD 40x ADM Ph2, correction collar set to 1.2 mm to induce spherical aberrations).[160] For motility experiments, it was focused 135 µm above the bottom surface of the sample chamber. One to four 1 or 1.5-min long recordings were obtained at 30 fps per condition in motility experiments, alternating between conditions. A typical 1.5-min motility recording yields 1,500–2,000 bacterial trajectories. For chemotaxis experiments, it was focused at the centre of the 70 µm-tall channel in all three dimensions. Two to three 2–2.5-min long recordings were obtained at 30 fps per condition in chemotaxis experiments. Three biological replicates were performed for chemotaxis in a 100 µM/mm **EPI** gradient, one otherwise. Biological replicates used cultures grown from different colonies.

3D trajectories were extracted from phase contrast recordings using a high-throughput 3D tracking method based on image similarity between bacteria and a reference library.[160] Trajectories shorter than 5 frames were discarded. Positions were smoothed using 2nd order

ADMM-based trend-filtering with regularisation parameter $\lambda = 0.3$, and speeds computed as forward differences in positions divided by the time interval between frames. All trajectories with an average speed below a 20 µm/s threshold were considered non-motile and discarded. The range of 3D bacterial trajectories was ~350 µm x 300 µm laterally (*x*, *y*) and 200 µm (*z*) in motility chambers, or the entire 70 µm height (*z*) of the channel in the chemotaxis device.

For motility experiments, trajectories with a minimum duration of 1 s were analysed for turn events. The turn event detection was based on the local rate of angular change of direction, computed from the dot product between the sums of the two consecutive velocity vectors preceding and subsequent to a time point. The threshold for a turn to begin was an α-fold rate relative to the median rate of angular change rate of the run segments, as determined in three iterations of the procedure. It was determined by visual inspection of trajectories that a factor $\alpha = 10$ gave satisfactory results. A new run begins with at least two time points (at least 0.066 s) below this threshold.

For chemotaxis experiments, the *z* position of the top and bottom of the chemotaxis chambers were identified by visual inspection of trajectory data, and all trajectory segments within 10 µm of the top or bottom of the central channel were removed to avoid surface interaction effects. The drift velocity is the average of the *x* component of all instantaneous 3D speed vectors from all bacteria, *x* being the gradient direction. The noise on the drift measurement was estimated by a jack-knife resampling procedure consisting of dividing the data into subsets of 150 trajectories and computing the standard error of the mean drift obtained for different subsets.

3.2.2.6 Chemotaxis capillary assay

The capillary assay was performed following a published protocol[147] adapted for *Vibrio* species.[161-162] Briefly, *V. campbellii* overnight cultures were diluted into LB35 medium (1:100) and grown to OD_{600} 0.5. The cells were gently washed three times (10 min, 2,000 x *g*) and resuspended in HEPES-buffered artificial seawater (H-ASW: 100 mM $MgSO_4$, 20 mM $CaCl_2$, 20 mM KCl, 400 mM NaCl, and 50 mM HEPES, pH 7.5).[163] The OD_{600} was adjusted to 0.1, and 200 µL culture was transferred into a 96-well plate. The plate was covered with three layers of parafilm and the open end of a flame-sealed 1 µL capillary (64 mm, *Drummond Scientific*) was inserted into the bacterial suspension. The capillaries were filled with either H-ASW alone or with attractants dissolved in H-ASW. Solutions containing attractants and cell suspensions were supplemented with catecholamines and antagonists as indicated. The hormones were either dissolved in H-ASW or diluted from a 100-fold concentrated stock solution in 0.1 M HCl

prepared immediately before the experiment (**EPI** and **NE**) and added directly after the wash steps. After 60 min incubation at room temperature, the contents of the capillaries were expelled and plated in appropriate dilutions on LB agar plates containing carbenicillin. The plates were incubated at 30 °C overnight and colony forming units were enumerated. Each experiment was conducted at least three times with four technical replicates per condition. Statistical significance was determined using an unpaired two-tailed *t*-test (* = $p < 0.05$, ** = $p < 0.01$).

3.2.3 Proteomics methods

3.2.3.1 Preparative photolabelling with **PE-P**

Overnight cultures of *V. campbellii* were diluted 1:100 into 60 mL fresh medium and grown until early stationary phase (30 °C, 200 rpm, 7 h, OD_{600} ~5.0–5.2). Bacteria were harvested by centrifugation (6,000 x *g*, 10 min, 4 °C), washed with PBS (10 mL), and adjusted to OD_{600} 4.0 in 10 mL PBS. Competitors **PE**, **EPI**, **LAB**, **PRO** or DMSO were added from 1,000-fold concentrated DMSO stocks to the final concentrations as indicated and the suspensions were incubated 15 min, 30 °C, 200 rpm in 50 mL falcons with the lids fixed loosely. Next, DMSO or the photoprobe **PE-P** was added from a 1,000-fold concentrated stock (10 mM) to a final concentration of 10 µM and incubated 1 h, 30 °C, 200 rpm. Samples were transferred to 10 cm dishes and irradiated for 10 min with UV light (UV low-pressure mercury-vapour fluorescent lamp, *Philips* TL-D 18W BLB, 360 nm maximum) on a cooling pack. Labelled bacteria were centrifuged (6,000 x *g*, 10 min, 4 °C) and the pellet was washed twice with cold PBS (1 mL). Pellets were flash frozen and stored at -80 °C. Pellets were resuspended in 1 mL PBS + EDTA-free protease inhibitor (*Roche*) and sonicated 2 x 15 s, 60% intensity, on ice. Following centrifugation (16,060 x *g*, 30 min, 4 °C), the supernatant was removed ("soluble") and the pellet was resuspended in 1% (w/v) SDS/PBS with sonication for 2 x 15 s, 40% intensity. Cell debris was pelleted (16,060 x *g*, 10 min, r.t.) and the supernatant was transferred into a new tube ("insoluble").

3.2.3.2 Preparative photolabelling with **EPI-P1**

Preparative scale photolabelling experiments with **EPI-P1** were performed as with **PE-P** with the following exceptions: Labelling was performed in 5 mL culture and **EPI-P1** was added to 7.5 µM (25 µL from a 1.5 mM DMSO stock), the same volume of 5.25 mM acetic acid in DMSO was added as control. Samples were incubated for 30 min at 30 °C, 200 rpm and cultures

were irradiated for 5 min in 6 cm dishes. Bacteria were lysed in 450 µL PBS + protease inhibitor with sonication (2 x 15 s, 60% intensity), then TX100 was added to 1% (v/v) and sonicated (1 x 10 s, 10% intensity) and samples were incubated for 30 min on ice. Insoluble debris was removed by centrifugation (16,060 x *g*, 20 min, 4 °C).

3.2.3.3 *In situ* analytical scale photolabelling

Analytical scale photolabelling experiments were performed as preparative scale experiments with the following exceptions: Probe concentration was 50 µM (0.5% [v/v] DMSO). Irradiation of 1 mL labelled bacteria was performed in a 12-well dish. Lysis and fractionation into soluble and insoluble proteins was performed as for preparative experiments with **PE-P** (in 200 µL).

3.2.3.4 CuAAC for preparative scale photolabelling

Protein concentration was determined using the Roti®-Quant kit (*Carl Roth*) and adjusted to ~1 µg/µL in 500 µL. SDS was added to 0.8% (w/v) in the "soluble" samples. Click reagents were added to the lysate from a premix to the following concentrations: 100 µM rhodamine-biotin-azide tag[164] (10 mM stock in DMSO), 1 mM $CuSO_4$ (50 mM stock in water), 1 mM tris(2-carboxyethyl)phosphine hydrochloride (TCEP, 52 mM stock in water), and 100 µM tris((1-benzyl-4-triazolyl)methyl)amine (TBTA, 1.667 mM stock in 20% [v/v] DMSO/*t*-BuOH) and incubated 1 h, 25 °C, 400 rpm. Proteins were precipitated in 2 mL acetone at -20 °C overnight, pelleted (20,450 x *g*, 15 min, 4 °C), and washed twice with 1 mL ice-cold methanol with sonication (1 x 10 s, 10% intensity). Pellets were air-dried, proteins resolubilized in 1 mM dithiothreitol (DTT), 0.2% (w/v) SDS/PBS with sonication (1 x 10 s, 10% intensity), and transferred to LoBind microcentrifuge tubes.

3.2.3.5 CuAAC for analytical scale photolabelling

CuAAC for analytical labelling experiments was performed with rhodamine-azide (tetramethylrhodamine 5-carboxamido-(6-azidohexanyl), 5-isomer, *Base Click*). The click reaction was quenched by addition of the same volume of 2 x sample loading buffer (63 mM Tris/HCl, 10% [v/v] glycerol, 2% [w/v] SDS, 0.0025% [w/v] bromophenol blue, 5% [v/v] 2-mercaptoethanol).

3.2.3.6 Analytical photolabelling in lysate with radical scavengers

Lysate (in PBS) was adjusted to a protein concentration of 1 mg/mL and DMSO or **PE-P** was added to 50 µM (0.1% [v/v] DMSO) in 60–100 µL lysate in a 96-well plate. Samples were incubated for 1 h at 30 °C, 200 rpm and radical scavengers were added to 1 mM or 10 mM as indicated (11 µL from a freshly made 10 mM or 100 mM stock in water), mixed thoroughly, and irradiated for 10 min. Proteins were precipitated in acetone and washed with methanol to remove the radical scavengers (as described above), resuspended in 1% (w/v) SDS/PBS (with vortexing and sonication) to the same protein concentration, and subjected to CuAAC with rhodamine-azide.

3.2.3.7 Analytical photolabelling in lysate of different strains

Overnight cultures were grown from colonies in 5–20 mL medium, diluted in fresh medium (20–60 mL), and grown for 8–9 h (*P. luminescens*: OD_{600} 4.17; *P. asymbiotica*: OD_{600} 4.18; *A. fischeri*: OD_{600} 1.81). Bacteria were harvested and washed as for photolabelling experiments and the pellets were frozen. Bacteria were resuspended in 2 mL PBS and lysed (3 x 15 s, 60% intensity) on ice, the suspension was centrifuged (21,000 x *g*, 30 min, 4 °C), and the supernatant transferred to a new tube. Protein concentration was adjusted to 1 µg/µL and labelling was performed as described above at 50 µM **PE-P** (1% [v/v] DMSO) but at room temperature and without shaking. No radical scavengers were added and CuAAC was performed directly after irradiation without acetone precipitation.

3.2.3.8 SDS-PAGE

Stacking gels consisted of 4% (w/v) acrylamide (in 50 mM Tris, pH 6.8) and resolving gels of 12.5% (w/v) acrylamide (in 300 mM Tris, pH 8.8) and were run in a Tris-glycine buffer (25 mM Tris, 192 mM glycine, 0.1% (w/v) SDS, pH 8.3). Typically, 30 µL sample (~15 µg protein), 8 µL fluorescent marker (BenchMark™ Fluorescent Protein Standard, *Thermo Fisher*), and 12 µL protein marker (Roti®-Mark Standard, *Carl Roth*) were loaded and gels were run at 150–300 V (depending on gel size) on a EV265 Consort power supply (*Hoefer*). Fluorescence was scanned in a LAS-4000 imaging system equipped with a Fujinon VRF43LMD3 lens and a 575DF20 filter (*Fujifilm*). Gels were stained in Coomassie staining solution (0.25% [w/v] Coomassie Brilliant Blue R-250, 9.2% [v/v] concentrated acetic acid, 45.4% [v/v] ethanol) overnight and destained in 10% (v/v) acetic acid, 40% (v/v) ethanol).

3.2.3.9 Enrichment, alkylation, and digest for photoaffinity labelling experiments

Protein LoBind microcentrifuge tubes and MS-grade reagents were used throughout MS sample preparation. Per sample, 50 µL avidin slurry (*Sigma*) was dispensed into a microcentrifuge tube and washed 3 x with 0.2% (w/v) SDS/PBS (3 min, 400 x *g*). Protein samples were centrifuged (21 000 x *g*, 10 min, r.t.) to remove particulates, then added to the beads, and incubated at room temperature under constant rotation for 1–2 h. Beads were pelleted, the supernatant discarded, and beads were washed with 0.5–1 mL of the following solutions: 2 x 1% (w/v) SDS/PBS, then 3 x 4 M urea/PBS, and 3 x 50 mM triethylammonium bicarbonate buffer (TEAB). The beads were resuspended in 100 µL 50 mM TEAB and reduced with 10 mM DTT (from 250 mM stock in water) at 55 °C for 30 min with shaking. Next, beads were washed with 0.5 mL TEAB, resuspended in 100 µL TEAB and thiols were alkylated with 20 mM iodoacetamide (from 500 mM stock in TEAB) at 25 °C from 30 min with shaking. Beads were washed twice with 100 µL TEAB, resuspended in 100 µL TEAB, and 1 µg trypsin was added (from 0.5 µg/µL in 50 mM acetic acid, *Promega*). Proteins were digested at 37 °C for 14 h under vigorous shaking. The digest was quenched with formic acid (1% [v/v] final concentration, pH 2–3), beads were washed twice with 100 µL 0.1% (v/v) formic acid, and the washes were combined with the supernatant.

Samples were desalted on stage tips consisting of three layers of C-18 material (Empore C18 disk-C18, 47 mm, *Agilent Technologies*) plunged into p200 tips which were inserted into holes in the lids of microcentrifuge tubes. The following solutions were added, and the stage tips were centrifuged (≤ 1–2 min, 500 x *g*) after every addition: stage tips were washed with 1 x 80 µL methanol and then equilibrated with 1 x 80 µL 80% (v/v) acetonitrile, 0.5% (v/v) formic acid and with 2 x 100 µL 0.5% (v/v) formic acid. Next, peptides were loaded and desalted with 1 x 150 µL 0.1% (v/v) formic acid. Stage tips were transferred to fresh LoBind microcentrifuge tubes and the peptides were eluted with 100 µL 80% (v/v) acetonitrile, 0.5% (v/v) formic acid. Solvents were removed in a speed vac and dry peptides were stored at -80 °C until analysis.

3.2.3.10 Chemoproteomics experiments with isoDTB tags

A pellet of *V. campbellii* grown to stationary phase (OD_{600} ~5.0, ~24 mL) was washed 3 x with PBS, stored at -80 °C, and lysed in 1.5 mL PBS with sonication (5 x 15 s, 60% intensity, on ice). Insoluble proteins were removed by centrifugation (16,060 x *g*, 30 min, 4 °C). Protein concentration was adjusted to 1 mg/mL, and 2 mL lysate was labelled with 10 µM **PE-P** (2 µL of a 10 mM stock in DMSO) at 30 °C for 1 h, 200 rpm. Following 10 min UV-irradiation (UV

low-pressure mercury-vapour fluorescent lamp, *Philips* TL-D 18W BLB, 360 nm maximum) in a 6-well plate (*Thermo Scientific*), the lysate was split into 2 x 800 µL and adjusted to 1% (w/v) SDS (from a 10% (w/v) stock in PBS) before adding the click reagents as for the photoaffinity labelling experiments except using either heavy or light labelled isoDTB azide (100 µM final from a 5 mM DMSO stock, isoDTB azide synthesised as reported previously[32]). After the click reaction, heavy- and light-labelled lysates (800 µL each) were combined in 8 mL cold acetone and precipitated overnight at -20 °C. Precipitated proteins were centrifuged (10,178 x *g*, 10 min, 4 °C), the supernatant decanted, the pellet resuspended in 1 mL cold methanol with sonication (10% intensity), and pelleted again. The methanol wash was repeated, and protein pellets were air-dried and resuspended in 300 µL 8 M urea in 0.1 M TEAB with sonication (10% intensity). Samples were centrifuged (16,249 x *g*, 3 min) and reduced with 10 mM DTT (15 µL of 201 mM stock in water) for 45 min at 37 °C, 850 rpm. Next, thiols were alkylated with 20 mM iodoacetamide (15 µl from a 400 mM stock in water) for 30 min at 25 °C, 850 rpm (protected from light) and remaining iodoacetamide was quenched with 10 mM DTT for 30 min at 25 °C, 850 rpm. Then, 900 µL 0.1 M TEAB was added (to achieve pH ~8 and 2 M urea) and proteins were digested with 20 µg trypsin (40 µL from 0.5 µg/µL in 50 mM acetic acid, *Promega*) overnight at 37 °C with intense shaking. Per sample, 2 x 25 µL avidin slurry (*Sigma*) in Protein LoBind tubes was washed with 3 x 1 mL 1% (v/v) Nonidet P-40 (NP-40) in PBS with centrifugation (400 x *g*, 2 min). The tryptic digest was split into two portions, added to 600 µL 0.2% (v/v) NP-40 and then to the avidin beads and incubated for 2.5 h with constant rotation. Beads were then centrifuged (1,000 x *g*, 2 min), the supernatant discarded, and the beads were resuspended in 600 µL 0.1% (v/v) NP-40, and transferred to a centrifuge column (*Fisher Scientific*) recombining the two portions of one sample. Beads were washed with 2 x 600 µL 0.1% (v/v) NP-40, then with 3 x 600 µL PBS, and with 3 x 600 µL water, after every washing step the solutions were removed by suction. The columns were transferred into LoBind tubes and peptides were eluted with 400 µL (in 3 batches) 50% (v/v) acetonitrile, 0.1% (v/v) on (5,000 x *g*, 3 min). Solvents were removed in a speed vac and dry peptides were stored at -80 °C until analysis.

3.2.3.11 Co-IP

A customised polyclonal rabbit antibody against 6His-CheW was obtained from *Kaneka Eurogentec*. For this purpose, heterologously produced and purified 6His-CheW was supplied as antigen in a Speedy 28-day immunisation programme with two rabbits as hosts. Polyclonal

IgG antibodies were obtained from 5 mL crude rabbit serum after the immunisation by affinity purification. Specificity of the antibody against CheW was verified by Western blot analyses.

V. campbellii from an overnight culture were diluted in LB35 medium and grown until early stationary phase, pelleted, washed with PBS, and resuspended in PBS to OD_{600} 4.0 as for preparative photolabelling experiments with **PE-P**. Four replicates were used starting from independent overnight cultures. Next, 10 mL suspension in a 50 mL falcon was treated with 100 µM **EPI** (from 100 mM stock in DMSO) or DMSO and incubated 30 min, 30 °C, 200 rpm. Bacteria were harvested (6,000 x *g*, 5 min, r.t.) and resuspended in 2 mL PBS containing 100 µM **EPI** or the equivalent volume of DMSO. The DSSO crosslinker was added to 2 mM (from a 100 mM stock in DMSO, DSSO synthesised as described previously[133]), and samples were incubated at 30 °C, 200 rpm for 30 min. Bacteria were pelleted (6,000 x *g*, 10 min, 4 °C), washed with 2 x 1 mL cold 50 mM Tris/HCl, pH 8.0 to quench the DSSO, and the pellet was flash-frozen and stored at -80 °C. The pellet was resuspended in 1 mL lysis buffer (50 mM Tris/HCl, pH 7.4, 150 mM NaCl, 5% [v/v] glycerol, 0.1% [v/v] NP-40) and sonicated 3 x 15 s, 60% intensity, on ice. The lysate was cleared by centrifugation (21,000 x *g*, 30 min, 4 °C) and the supernatant was sterile filtered (0.2 µm). Protein amount was adjusted to 1 mg (1 µg/µL). Per sample, 30 µL protein A/G bead slurry (*Pierce Biotechnology*, *Thermo Fisher Scientific*) in LoBind microcentrifuge tubes was equilibrated with 1 x 1 mL cold wash buffer (50 mM Tris/HCl, pH 7.4, 150 mM NaCl, 5% [v/v] glycerol, 0.05% [v/v] NP-40) and centrifuged (1,000 x *g*, 1 min, 4 °C). The supernatant was discarded and the lysate was added to the beads. Next, 2.5 µg antibody (167 µL from a 0.015 µg/µL stock in 50% [v/v] glycerol) or a rabbit mAb IgG XP® isotype control (1 µL, 2.5 µg/µL, *Cell Signaling Technology*) was added and incubated overnight at 4 °C under constant rotation. Samples were centrifuged (30 s, 500 x *g*, 4 °C), the supernatant discarded, and the beads washed with 2 x 1 mL cold wash buffer and 3 x 1 mL cold basic buffer (50 mM Tris/HCl, pH 7.4, 150 mM NaCl, 5% [v/v] glycerol). Proteins were reduced and digested by the addition of 25 µL IP elution buffer I (50 mM Tris/HCl, pH 8.0, 5 ng/µL trypsin, 2 M urea, 1 mM DTT) at 25 °C, 1,000 rpm for 30 min. To alkylate cysteines, 100 µL IP elution buffer II (50 mM Tris/HCl, pH 8.0, 2 M urea, 5 mM iodoacetamide) was added, and the samples were incubated overnight (~16 h) at 37 °C, 1,000 rpm. Formic acid was added to 1% (v/v) (pH 2–3) to quench the digestion and samples were desalted on stage tips.

Desalting was performed as for photolabelling experiments with slight modifications: two layers of C-18 material were used and stage tips were equilibrated with 1 x 80 µL methanol, then 1 x 80 µL 80% (v/v) acetonitrile, 0.5% (v/v) formic acid, and with 3 x 70 µL 0.5% (v/v)

formic acid. Samples were centrifuged (16,249 x *g*, 2 min) and loaded, the beads were washed with 2 x 150 µL 0.5% (v/v) formic acid and washes were loaded too. Peptides were desalted with 3 x 70 µL 0.5% (v/v) formic acid and eluted with 2 x 30 µL 80% (v/v) acetonitrile, 0.5% (v/v) formic acid. Solvents were removed in a speed-vac and dry samples were stored at -80 °C.

3.2.3.12 Whole proteome analysis

Bacteria were grown on soft agar motility plates as described above containing 100 µm **EPI**, 50 µM **PE**, or the appropriate volume of solvent as control. The plates were incubated at 30 °C for 7 h or 24 h and bacteria were harvested as previously described with minor changes.[165] Cells were washed off the surface with 2 ml ice-cold PBS, centrifuged (10,000 x *g*, 20 min, 4 °C), washed twice, and the pellets were frozen and stored at -80 °C. Bacterial pellets were lysed in 200 µL 100 mM Tris/HCl, pH 7.4 with sonication (3 x 15 s, 60% intensity, on ice). Next, 80 µL 10% (w/v) SDS, 1.25% (w/v) deoxycholic acid was added and samples were vortexed and incubated at 90 °C for 10 min. Nucleic acids were sheared by sonication (1 x 20 s, 10% intensity), insoluble debris removed by centrifugation (16,060 x *g*, 30 min) and the supernatant was transferred to a LoBind tube. The protein amount was adjusted across all replicates of a condition (20–200 µg) and samples were precipitated overnight with 1.2 mL acetone at -20 °C. Precipitated proteins were pelleted (21,000 x *g*, 15 min, 4 °C) and resuspended in 0.5–1 mL ice-cold methanol. Methanol washes were performed twice. Pellets were air-dried, resuspended in 200 µL denaturation buffer (7 M urea, 2 M thiourea in 20 mM HEPES, pH 7.5) with sonication (10% intensity) and reduced with 1 mM DTT (1 µL from 200 mM stock in water) for 1 h at 37 °C, 600 rpm. Thiols were alkylated with 5.5 mM iodoacetamide (2 µL from 550 mM stock in 50 mM TEAB) for 30 min at 25 °C, 600 rpm (protected from light) and excessive iodoacetamide was quenched with 4 mM DTT for 30 min at 25 °C, 600 rpm. Proteins were digested with LysC (1:200 LysC:total protein, 0.5 µg/µL, MS-grade, *Wako*) for 2 h at 25 °C, 600 rpm, then samples were diluted by adding 800 µL 50 mM TEAB and further digested with trypsin (1:100 trypsin:total protein, from 0.5 µg/µL in 50 mM acetic acid, *Promega*) for 16 h at 37 °C, 1000 rpm.

The digestion was quenched with 3% (v/v) formic acid (pH ~2.5) and samples were desalted on 50 mg SepPak C-18 columns (*Waters*). For this, columns were washed with 1 x 1 mL acetonitrile and 1 x 1 mL elution buffer (80% [v/v] acetonitrile, 0.5% [v/v] formic acid) and equilibrated with 3 x 1 mL 0.1% (v/v) trifluoroacetic acid (TFA). Peptides were added on the columns and washed with 3 x 1 mL 0.1% (v/v) TFA and with 1 x 500 µL 0.5% (v/v) formic

acid. Finally, peptides were eluted into 2 mL LoBind tubes with 3 x 250 µL elution buffer, solvents were removed in a speed vac and dry peptides were stored at -20 °C.

3.2.3.13 Peptide reconstitution (all proteomics experiments)

Dry peptides were reconstituted in 30 µL 1% (v/v) formic acid with vortexing and in a sonication bath (10 min) and filtered through centrifugal filters (0.22 µm, Durapore, PVDF, *Merck KGaA*) pre-equilibrated with 300 µL 1% (v/v) formic acid (16,249 x *g*, 2 min, r.t.). For full proteome experiments, peptides were reconstituted in a volume corresponding to a protein concentration of 1 µg/µL.

3.2.3.14 LC-MS/MS measurements

Whole proteome peptide samples were analysed on an UltiMate 3000 nano HPLC system (Dionex) equipped with an Acclaim C18 PepMap100 (75 µm ID × 2 cm) trap column and an Aurora Series Emitter Column with Gen2 nanoZero fitting (75 µm ID × 25 cm, 1.6 µm FSC C18) separation column (column oven heated to 40 °C) coupled to an Orbitrap Fusion (Thermo Fisher) in EASY-spray setting. Peptides were loaded on the trap column and washed with 0.1% (v/v) TFA before being transferred to the analytical column and separated in a 152 min gradient (buffer A: 0.1% [v/v] formic acid in water, buffer B: 0.1% [v/v] formic acid in acetonitrile, gradient: 5–22% [v/v] buffer B in 112 min, then to 32% [v/v] buffer B in 10 min, then to 90% [v/v] buffer B in 10 min and hold 90% [v/v] buffer B for 10 min, then to 5% [v/v] buffer B in 0.1 min and hold 5% [v/v] buffer B for 9.9 min) with a flow rate of 400 nL/min. The Orbitrap Fusion was operated in a TOP10 data dependent mode and full scan acquisition in the orbitrap was performed with a resolution of 120,000 and an AGC target of 2e5 (maximum injection time of 50 ms) in a scan range of 300−1,500 m/z. Monoisotopic precursor selection as well as dynamic exclusion (exclusion duration: 60 s) was enabled. Most intense precursors with charge states of 2–7 and intensities greater than 5e3 were selected for fragmentation. Isolation was performed in the quadrupole using a window of 1.6 m/z. Precursor ions were collected to an AGC target of 1e4 (maximum injection time of 35 ms). Fragments were generated using higher-energy collisional dissociation (HCD, normalized collision energy: 30%) and detected in the ion trap operating at a rapid scan rate.

Co-IP samples were measured on the Orbitrap Fusion with the same parameters as whole proteome samples except that precursors were selected with a maximum injection time of 100 ms.

Photoaffinity labelling peptide samples were analysed on an UltiMate 3000 nano HPLC system (*Dionex*) equipped with an Acclaim C18 PepMap100 (75 µm ID × 2 cm) trap column and a 25 cm Aurora Series emitter column (25 cm × 75 µm ID, 1.6 µm FSC C18) (*Ionopticks*) separation column (column oven heated to 40 °C) coupled to a Q Exactive Plus (*Thermo Fisher*) in EASY-spray setting. Peptides were loaded on the trap column and washed with 0.1% (v/v) TFA before being transferred to the analytical column and separated using a 152 min gradient (buffer A: 0.1% [v/v] formic acid in water, buffer B: 0.1% [v/v] formic acid in acetonitrile. Gradient of buffer B: 5% [v/v] for 7 min, increase to 22% [v/v] in 105 min, then to 32% [v/v] in 10 min, then to 90% [v/v] in 10 min, hold at 90% [v/v] for 10 min, decrease to 5% [v/v] in 0.1 min and hold at 5% [v/v] for 9.9 min) with a flow rate of 400 nL/min. The Q Exactive Plus was operated in a TOP10 data dependent mode and full scan acquisition in the orbitrap was performed with a resolution of 140 000 and an AGC target of 3e6 (maximum injection time of 80 ms) in a scan range of 300−1,500 m/z. Most intense precursors with charge states of > 1, a minimum AGC target of 1e3, and intensities greater than 1e4 were selected for fragmentation. Peptide fragments were generated using higher-energy collisional dissociation (HCD, normalized collision energy: 27%) and detected in the orbitrap with a resolution of 17 500 m/z. The AGC target was set to 1e5 (maximum injection time 100 ms) and the dynamic exclusion duration to 60 s. Isolation in the quadrupole was performed with a window of 1.6 m/z.

Differential isotopic labelling samples were measured on a Q Exactive Plus spectrometer with a different gradient (buffer B: 5% [v/v] for 7 min, increase to 40% [v/v] in 105 min, then to 60% [v/v] B in 10 min, and to 90% [v/v] B in 10 min, hold at 90% [v/v] for 10 min, then decrease to 5% [v/v] in 0.1 min and hold at 5% [v/v] for another 9.9 min) at the same flow rate. All parameters were the same as for photoaffinity labelling experiments except full MS scans were collected at a resolution of 70 000.

3.2.3.15 MS data analysis (photoaffinity labelling, co-IP, and full proteome experiments)

MS data were analysed using MaxQuant[166-167] version 1.6.5.0 and peptides were searched against the UniProt database for *Vibrio campbellii* ATCC BAA-1116 / BB120 (taxon identifier 338187, downloaded on 17.02.2020). Cysteine carbamidomethylation was set as fixed

modification and methionine oxidation and N-terminal acetylation as variable modifications. Trypsin (without N-terminal cleavage to proline) was set as proteolytic enzyme with a maximum of two allowed missed cleavages. LFQ mode[96] was performed with a minimum ratio count of 2. The "match between runs" (0.7 min match and 20 min alignment time window) and second peptide identification options were activated. All other parameters were used as pre-set in the software. LFQ intensities were further processed with Perseus[168] version 1.6.1.1. Peptides of the categories "only identified by site", "reverse", or "potential contaminant" were removed and LFQ intensities were $\log_2$-transformed.

Data were filtered to retain only protein groups identified in at least 3/4 valid values (experiments: competitive labelling **PE-P** vs. **EPI**; competitive labelling **PE-P** vs. **PRO**/**LAB**; co-IP), 4/5 valid values (competitive labelling **PE-P** vs. **PE;** full proteome **PE**; full proteome **EPI**, 24 h), 2/3 valid values (full proteome **EPI**, 7 h), or 3/3 valid values (labelling with **EPI-P1**) in at least one group and missing values were imputed (width 0.3, downshift 1.8, total matrix). A two-sided two-sample Student´s *t*-test with permutation-based FDR (FDR 0.05) was performed and the significance cut-off was set at *p*-value = 0.05 ($-\log_{10}$(*p*-value) = 1.3) and an enrichment factor of 2 ($\log_2(x) = 1$) or 4 ($\log_2(x) = 2$) as indicated in the plots. Protein IDs were matched to annotations downloaded from annotations.perseus-framework.org on 18.02.2020. Proteins with the annotation "chemotaxis" in the GOBP or KEGG database were highlighted in the co-IP plots.

The BLAST (blastp) search for siderophore transporters was conducted in GenBank[169] (November 2022) using the CirA (WP_000489247) *E. coli* sequence as query as previously reported.[106]

3.2.3.16 Analysis of isoDTB data

Analysis software was set up as previously described[31] using the MSconvert tool (version: 3.0.19172-57d620127) of the ProteoWizard software (version: 3.0.19172 64bit),[170] the FragPipe interface (version: 14.0),[171-172] MSFragger (version: 3.1.1),[171-172] Philosopher (version: 3.3.10),[173] IonQuant (version 1.4.6),[174] and Python (version: 3.7.3). The FASTA file (*Vibrio campbellii* ATCC BAA-1116/BB120; taxon identifier 338187, downloaded on 17.02.2020) was modified by adding the reverse sequences manually. Modifications were analysed as previously described.[31] Amino acid selectivity was analysed and data were evaluated and filtered as previously published[31] performing an Offset Search in

MSFragger[171-172] with mass offsets set as 740.3974 or 746.4040. Run MS1 quant was enabled with Labelling based quant with masses set as 740.3974 or 746.4040. Specific amino acids were quantified and data were evaluated and filtered as previously published[31] performing a Closed Search in MSFragger with variable modifications set to 740.3974 or 746.4040 on Tyr. Run MS1 quant was enabled with Labelling based quant with masses set as 740.3974 or 746.4040.

3.2.3.17 AlphaFold structure prediction

The sequence of CheW was retrieved from UniProt (Uniprot Code: A7MS42) and used as basis for the AlphaFold prediction on a local installation of the AlphaFold algorithm as released by Jumper *et al*.[129] Visualisation and alignment with the CheW structure from *E. coli* (PDB:2HO9, solution NMR) was done using the open source version of PyMOL 2.4.[131]

3.2.4 Biochemical and biotechnological methods

3.2.4.1 Construction of a plasmid coding for N-terminally His6-tagged CheW

The *cheW* gene of *V. campbellii* (VIBHAR_RS14640; old locus tag VIBHAR_03137) was cloned into vector pET28a using BamHI and XhoI as restriction sites, resulting in an extension of the sequence by codons for a N-terminal His_6 tag.

3.2.4.2 Purification of 6His-CheW

To purify CheW of *V. campbellii*, *E. coli* BL21(DE3) carrying the plasmid pET28a-*cheW* was cultivated in LB supplemented with kanamycin (50 mg/mL) at 37 °C. At OD_{600} 0.6, 0.4 mM isopropyl β-D-1-thiogalactopyranoside (IPTG) was added to the culture to induce *cheW* expression at 30 °C for 4 h. Cells were harvested (20 min, 5,000 x *g*, 4 °C), resuspended, and disrupted by high-pressure cell disrupter (*Constant Systems Limited*) in ice-cold disruption buffer (20 mM Tris/HCl pH 7.5, 500 mM NaCl, 10 mM imidazole, 3 mg DNase, and 0.5 mM phenazine methosulfate [PMSF] in double-distilled water [ddH_2O]). After removal of intact cells and cells debris via centrifugation (5,000 x *g*, 30 min, 4 °C), membrane vesicles were removed by ultracentrifugation (45,000 x *g*, 60 min, 4°C), and the cell lysate was loaded onto a Ni-nitrilotriacetic acid (NTA) column (*Qiagen*). After a washing step (20 mM Tris/HCl

pH 7.5, 500 mM NaCl, 50 mM imidazole), the recombinant protein was eluted with elution buffer (20 mM Tris/HCl pH 7.5, 500 mM NaCl, 250 mM imidazole).

3.2.4.3 Microscale thermophoresis

PD-10 desalting columns packed with Sephadex G-25 resin (*GE Healthcare*) were used to exchange 6His-CheW protein buffer to MST buffer (PBS with 0.05% [v/v] Tween 20). Purified CheW was labelled using the RED-tris-NTA Labelling kit (*NanoTemper Technologies*) following the manufacturer´s instructions. Ligands were dissolved in MST buffer and serially diluted. Fluorescently labelled 6His-CheW (50 nM) was mixed with ligand concentrations in a range of 7.63 nm–500 µM. After 10 min incubation at room temperature, followed by centrifugation (10,000 x *g*, 10 min) to remove aggregates, the solution was soaked into Monolith NT. 115 Series Standard Treated Capillaries. MST measurements were carried out using a Monolith NT.115 instrument (*NanoTemper Technologies*) with 60% LED/ excitation power and medium MST power (40%). Three independent measurements were analysed (*NT Analysis software version 1.5.41, NanoTemper Technologies*) using the signal from Thermophoresis + T-Jump.

3.2.4.4 Strain construction

Construction of the Δ*cheW* marker-less in-frame deletion in *V. campbellii* ATCC-BAA 1116 was achieved using the suicide plasmid pNPTS138-R6KT-*cheW* as described previously.[175] Briefly, 600 bp upstream and downstream of *cheW* were amplified by PCR using *V. campbellii* ATCC-BAA 1116 genomic DNA as template. After PCR product purification, the fragments were fused by overlap PCR. The overlap PCR fragment was cloned into plasmid pNPTS138-R6KT using BamHI and EcoRI as restriction sites. The resulting plasmid pNPTS138-R6KT-Δ*cheW* was introduced into *V. campbellii* ATCC-BAA 1116 by conjugative mating using *E. coli* WM3064 as a donor in LB medium containing 2,6-diaminopimelic acid (DAP). Single-crossover integration mutants were selected on LB plates containing kanamycin but lacking DAP. Single colonies were grown over a day without antibiotics and plated onto LB plates containing 10% (w/v) sucrose to select for plasmid excision. Kanamycin-sensitive colonies were checked for targeted deletion by colony PCR using primers bracketing the site of the deletion.

III – Investigation of the catechol-reactive proteome

This chapter is based on a manuscript in preparation.

Contributions:

All experiments were planned and performed by AW except for the following: Preparation of mouse neurons was performed by Annerose Kurz-Drexler with supervision by Dr. Daniela Vogt-Weisenhorn (Helmholtz Zentrum München); redox potentials were measured in collaboration with Lukas Niederegger with supervision by Prof. Dr. Corinna R. Hess (Technical University of Munich). Dr. Stephan M. Hacker (Technical University of Munich/Leiden University) analysed isoDTB data.

1 Covalent protein modifications by catechols

1.1 Dopamine as a post-translational protein modification

1.1.1 Dopamine reactivity

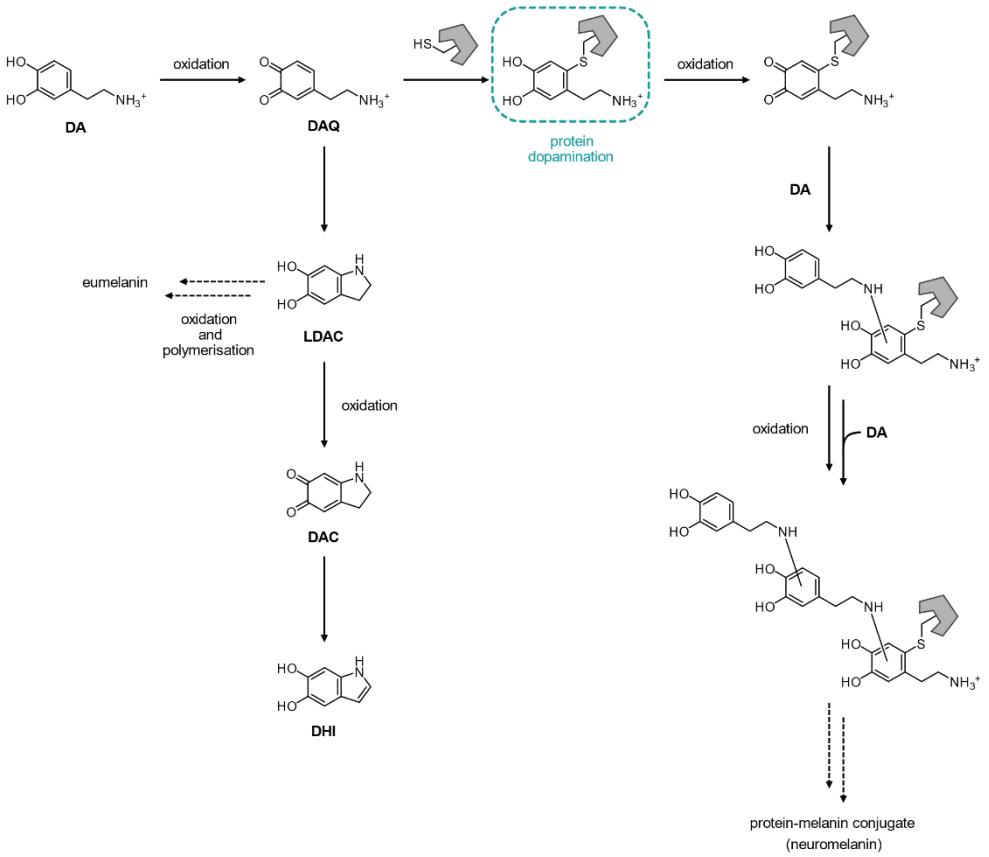

Figure III-1. Reaction trajectories of DA oxidation leading to protein modification and competing processes. **DA** is oxidised to **DA** quinone (**DAQ**) which undergoes intramolecular nucleophilic attack to form leukodopaminochrome (**LDAC**). **LDAC** oxidation and polymerisation yields the pigment eumelanin. **LDAC** oxidation to dopaminochrome (**DAC**) is followed by rearrangement to 5,6-dihydroxyindole (**DHI**). Nucleophilic protein side chains such as cysteine attack **DAQ** in a Michael-type addition. Protein-**DA** adducts may be further oxidised and react with additional **DA** molecules forming a protein-melanin conjugate termed neuromelanin. Adapted from Monzani *et al.*[176] with modifications. Note that other oxidation products such as **DA**-semiquinone radicals[176] or the **DHI** quinone[177] can also be protein-reactive (not shown for simplicity).

Under aqueous conditions at physiological pH, the catechol group is prone to rapid oxidation to a radical (following a one-electron oxidation) or to an *ortho*-quinone (two-electron oxidation).[176] **DA** oxidation is especially favoured at basic pH, in the presence of metal ions such as iron or copper, or under increased cellular oxidative stress.[176,178] The oxidation products are reactive species that may undergo further chemical reactions or covalently modify cellular structures. **DA** quinone (**DAQ**), for instance, can cyclise via intramolecular nucleophilic attack by the amine side chain to form leukodopaminochrome (**LDAC**), a precursor of the natural pigment melanin.

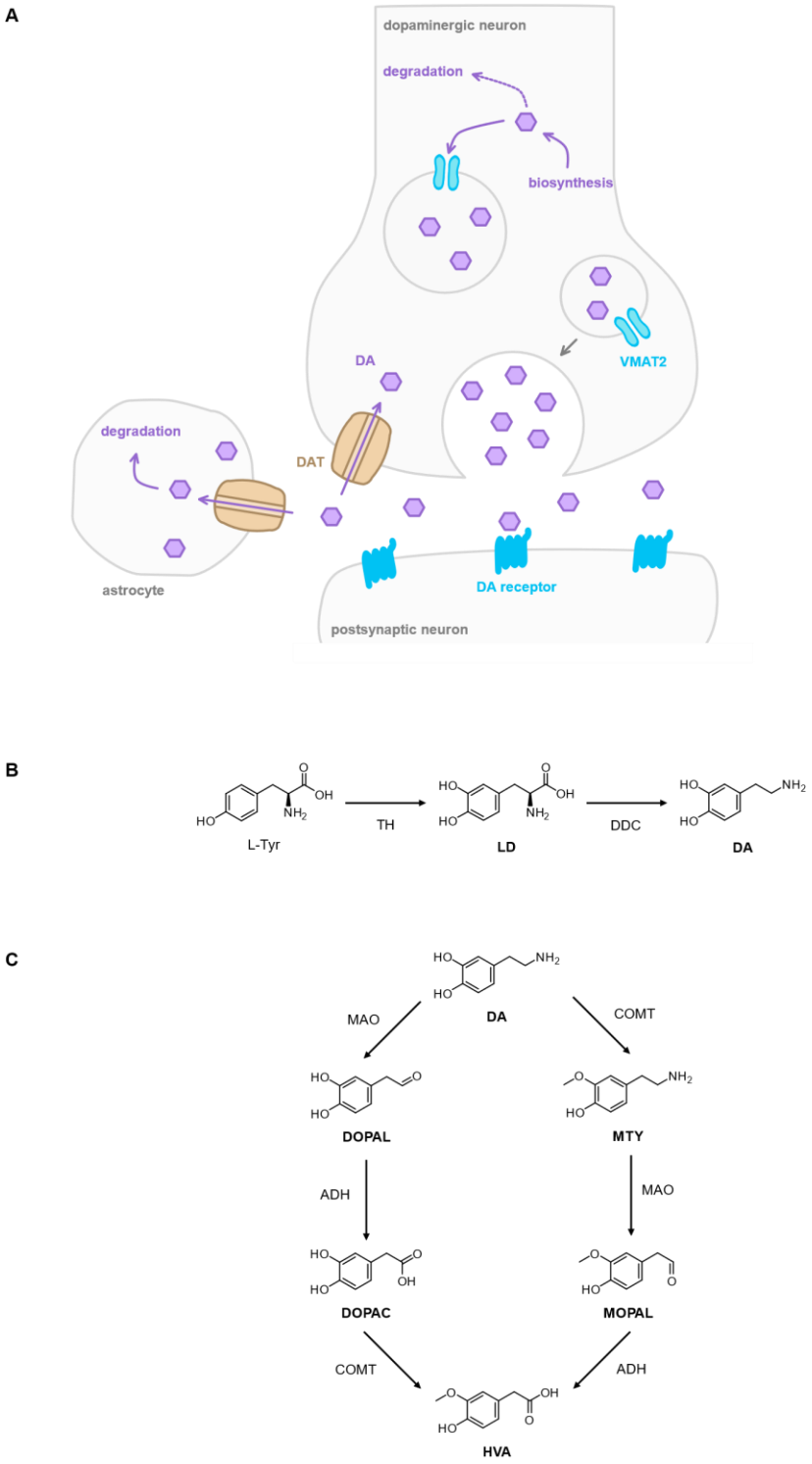

Figure III-2. DA biosynthesis, storage, and metabolisation in dopaminergic neurons. (A) Pre-synaptic dopaminergic neurons produce **DA** in the cytosol and transfer it to designated vesicles via the VMAT2 transporter. Upon stimulation, **DA** is released into the synaptic cleft where it binds to postsynaptic **DA** receptors. To terminate the signal, **DA** is taken back up via the **DA** transporter (DAT). Astrocytes can also take up **DA** for degradation. (B) **DA** is synthesised from L-tyrosine via hydroxylation by the tyrosine hydroxylase (TH) to **LD** which is then decarboxylated to **DA** by the DOPA decarboxylase (DDC). (C) **DA** metabolisation involves deamination by a monoaminooxidase (MAO), oxidation by an aldehyde dehydrogenase (ADH), and hydroxymethylation by the catechol-*O*-methyltransferase (COMT). Adapted with modifications from Monzani *et al.*[176]

DAQ may also be subjected to nucleophilic attack by protein side chains such as cysteine in a Michael-type addition and result in PTMs which can deactivate enzyme activity and cause

protein aggregation.[176] Protein-bound **DA** may be oxidised again and add to further **DA** molecules, forming a protein-melanin conjugate termed neuromelanin (Figure III-1).[176]

Confining **DA** from the cytosol is crucial to avoid excessive modification of cellular structures[179] and the biosynthesis, storage, and degradation of **DA** need to be tightly regulated. **DA** is produced by dopaminergic neurons that store it in designated vesicles where pH ~5.6 is maintained.[178] Low pH minimises catechol oxidation[178] and prevents **DA** cyclisation and polymerisation by keeping the amine group protonated, thus abrogating its nucleophilicity. Upon neuronal stimulation, **DA** is released into the synaptic cleft where it binds to post-synaptic **DA** receptors and is then taken back up through the **DA** transporter (DAT) to terminate the signal (Figure III-2 A). The biosynthetic precursors are L-tyrosine and **LD**. **LD** is the standard treatment for PD as it passes the blood-brain barrier (Figure III-2 B). Inside the cell, **DA** is transferred back into the vesicles or otherwise degraded by two different pathways which both involve deamination by monoamine oxidases and methylation of the hydroxy group by the catechol-*O*-methyltransferase (COMT) (Figure III-2 C). **DA** precursors as well as metabolites are also protein-reactive.[176,180]

1.1.2 Protein dopamination in Parkinson´s disease

The accumulation of **DA** oxidation products is associated with both hereditary and sporadic forms of Parkinson´s disease (PD).[181] This neurological disorder is characterised by a loss of dopaminergic neurons and a consequent reduction of **DA** levels in the brain, resulting in impaired motoric and cognitive functions. It is known that covalent binding of **DA** or **DA** metabolites to particular proteins results in their functional inactivation.[176] Specifically, proteins with critical functions in the pathogenesis of PD have been studied in this context. Although the pathogenesis of PD is largely not understood and often idiopathic, the mutation of certain proteins is associated with hereditary forms of PD. Most commonly implicated are loss-of-function mutations in the E3 ubiquitin-protein ligase parkin (encoded by the *PARK2* gene) which result in the selective degeneration of catecholaminergic neurons. A study seeking to shed light on sporadic, nonhereditary forms of PD revealed that parkin is modified by **DA** rendering it insoluble and abrogating its activity.[182] Congruently, reduced solubility of parkin was observed in the brains of PD patients, thereby providing a potential mechanism of parkin inactivation in dopaminergic neurons with age.[182] PD is furthermore characterised by the formation of Lewy bodies in the brain, consisting of insoluble protein aggregates (inclusion bodies). A major constituent of Lewy bodies is α-synuclein, which has been found to form toxic

oligomers upon interaction with **DA** or structurally related catechols, although only a fraction of this interaction appeared to be covalent.[176,183-184] Elevated oxidative stress is a further major contributor to PD development, and indeed, loss-of-function mutations of the protein deglycase DJ-1 (encoded by the *PARK7* gene), a redox-sensitive chaperone that regulates antioxidant gene expression, are associated with hereditary early-onset PD.[181,185-187] Moreover, DJ-1 protects neurons from **DA** toxicity.[185] Modification of DJ-1 using radiolabelled **DA** has been revealed, however, the functional consequences were not elucidated.[188] Dopamination of cysteine residues in the active site of another PD risk factor, the glucocerebrosidase, was observed during elevated mitochondrial stress.[181] The consequent inactivation of this lysosomal enzyme promoted lysosomal dysfunction and the accumulation of α-synuclein, two hallmarks of PD.[181]

Other proteins with critical functions not necessarily previously implicated in PD development are subject to **DA** post-translational modification. For instance, the **DA** metabolite 5,6-dihydroxyindole (**DHI**) modifies Nurr1, a transcription factor that regulates genes critical for dopaminergic neuron survival and maintenance and is critical for **DA** homeostasis.[177] Moreover, the glutathione-disulphide oxidoreductase glutaredoxin (Grx) is covalently modified by the **LD**-derived quinone leading to its inactivation.[180] Grx reduces glutathionylated proteins (Protein-SSG) to the free thiol form to restore protein function and its inhibition by **LD** was concomitant with increased apoptosis.[180] Similarly, a recent study found that **DA** modifies and functionally inhibits a member of the protein disulphide isomerases (PDIs), PDIA3.[189] PDIs are typically (but not exclusively) localised to the endoplasmic reticulum (ER), where they are involved in oxidative protein folding and are therefore critical to maintain cellular protein homeostasis. Interestingly, inhibition of PDIs can be neuroprotective,[190] although this effect might be context-dependent, as higher levels of PDI are required for examples under circumstances of elevated ER stress.

Overall, post-translational modification by **DA** is not well understood. It is a complex process as it is not limited to oxidation products of **DA** alone but also involves its metabolites and precursors. Furthermore, due to the reactivity of the generated electrophiles, the chemical selectivity of protein dopamination is likely to be poor. It is therefore substantial to study these processes in a cellular context and in an unbiased manner.

1.2 Plant secondary metabolites

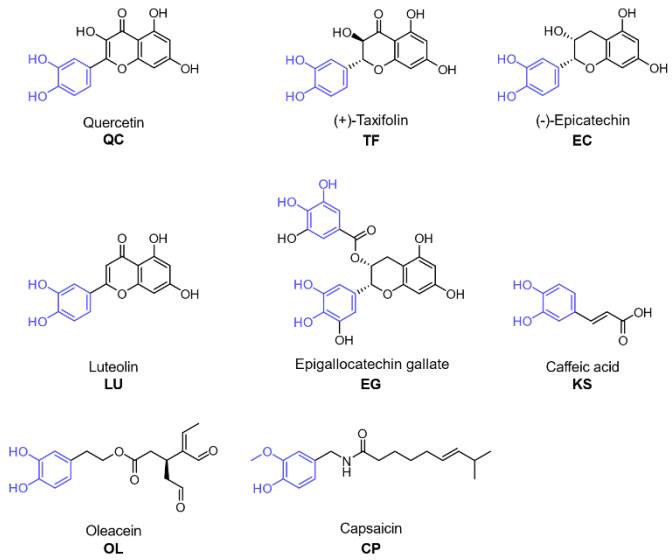

Figure III-3. Examples of catechol plant secondary metabolites.

Secondary metabolites are organic molecules that are not directly involved in the growth and development of an organism, but are important in ecological interactions. Plants use secondary metabolites for example as pigments, for defence, or as UV protection. The most abundant secondary metabolites in plants are phenolic compounds[191] which include numerous catechols. Flavonoids such as quercetin (**QC**), taxifolin (**TF**), (-)-epicatechin (**EC**), and luteolin (**LU**), epigallocatechin gallate (**EG**), among many more, are contained in a large number of plant-based foods and drinks such as fruits, vegetables, herbs, nuts, wine, tea and cocoa.[192] Examples of non-flavonoid catechols are caffeic acid (**KS**) from diverse sources, oleacein (**OL**) from olive oil, or capsaicin (**CP**), an *O*-methylated catechol derivative from chili peppers (Figure III-3).

The consumption of flavonoids and other plant polyphenols is generally considered beneficial for human health due to their antioxidative properties.[193] However, the biological effects go beyond antioxidation[194] and an extensive selection of literature reports biological effects that are mediated by specific interference with a particular enzymatic activity or metabolic pathway. Catechol phytochemicals are associated, for example, with anticancer,[31,35,36] anti-inflammatory,[195-196] antiangiogenesis,[197-198] and neuroprotective effects.[194] Oral administration of the flavonoid isoquercetin (quercetin-3-*O*-glucopyranosid) has shown antithrombotic effects in a phase II clinical study by inhibition of extracellular PDIs.[199] Binding of **EG** to the 67-kDa laminin receptor,[200] the urokinase,[201] and the inhibition of matrixmetalloproteases (MMP-2 and MMP-9)[202] have been proposed to mediate anticarcinogenic effects. Further cellular pathways targeted by plant catechols include fatty acid biosynthesis,[203] NF-κB signalling,[204-205] mitosis,[206]

and a large number of kinases.[206-207] Furthermore, some flavonoids are reported to interfere with steroid hormone signalling,[207] e.g. by activating the oestrogen receptor α.[195,208] These examples of reported bioactivities are not exhaustive[207,209] and a particular catechol may target multiple pathways.[198,210-211]

Overall, the biological effects of this compound class are not yet well understood. A host of animal studies reports the inhibition of carcinogenesis by plant polyphenols, however, the results are sometimes inconsistent.[193] Recent studies found that catechol compounds broadly inhibit the aggregation of tau and amyloid proteins and that this activity was promoted by their autooxidation.[212-213] This, together with the breadth of target pathways,[31,35,36] indicates that there is a general catechol target proteome that presumably highly depends on the biological context studied. To date, there is no clear consensus of the mode of action of plant polyphenols and related structures. The substantial number of reported target pathways indicates pleiotropic effects, therefore, an unbiased approach in live cells is needed to obtain a better understanding of catechol protein targets to functionally map catechol reactivity to different cell types, protein classes, and subcellular localisations.

1.3 Aims – investigation of the catechol-reactive proteome

The mode of action and the protein target scope of **DA** and plant catechols are not conclusively understood. Cellular effects and proteins modulated by catechols are quite diverse, indicating that the mode of action is broad and probably highly context-dependent. Therefore, the second part of this thesis aims to characterise the catechol-reactive proteome in a global, unbiased, and compound-centric manner using a broadly reactive chemical probe coupled with proteomics.

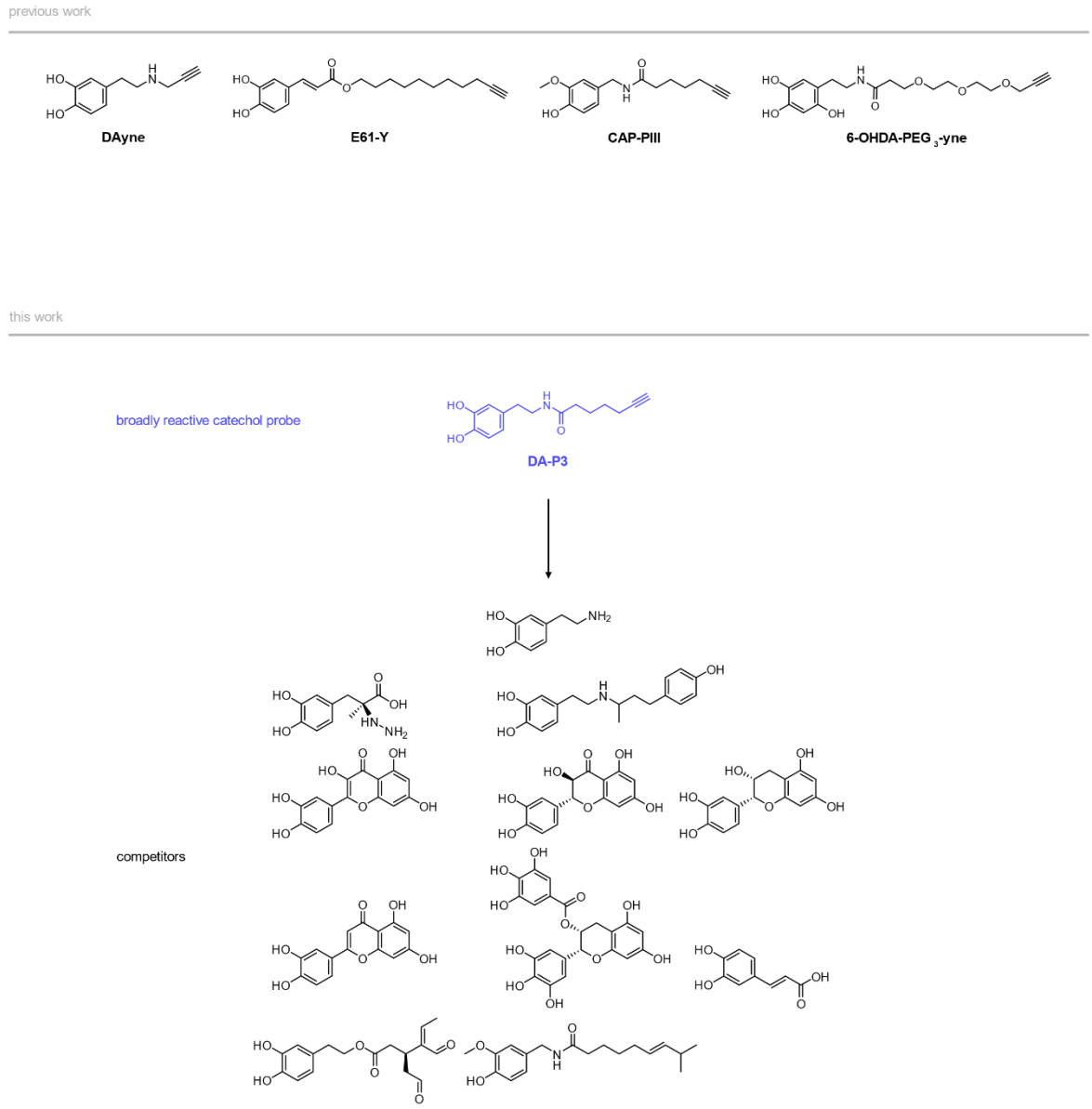

Figure III-4. Chemical proteomics strategies for the identification of catechol targets. Recently reported chemical probes based on **DA**,[189] n-octyl caffeate,[214] **CP**,[215] and 6-hydroxydopamine (**6-OHDA**)[216] (top) and competitive approach used in this work (bottom).

Recent studies have reported specific chemical probes of select catechols and related structures including **DA**,[189] **CP**,[215] n-octyl caffeate,[214] and 6-hdyroxydopamine (**6-OHDA**),[216] the latter being a neurotoxic oxidation product of **DA** (Figure III-4). In general, the analysis of protein

modification by **DA** using MS-based methods is challenged by the tendency of **DA**-protein adducts to precipitate,[182] which interferes with their detection.[176] Hurben *et al*. applied *N*-propargyl **DA** (**DAyne**) to study **DA** targets in the neuronal cell line SH-SY5Y by chemical proteomics.[189] However, no competition by the parent compound **DA** was shown for MS-based data. Moreover, due to the presence of both an electrophilic and a nucleophilic residue, this probe likely polymerises and forms insoluble aggregates with labelled proteins to some extent, as is known for the parent compound.[176] Thus, target proteins might be missed in the MS-based analysis. Farzam *et al*. designed a probe based on **6-OHDA**, which was not cell permeable and could only be applied in lysate.[216] Zhang *et al*. recently applied a **CP**-probe to show addition to cysteine residues but the binding mechanism remained unresolved.[215]

In this work, a broadly reactive chemical probe was designed based on **DA** with increased protein reactivity and cell permeability compared to the published **DA**-based probes.[189,216] Unlike the previously described probe **DAyne**,[189] this new chemical probe is unable to polymerise. Due to its broad protein reactivity it was applied in competition with a suite of structurally diverse catechols from plants and drugs with the goal to globally characterise and functionally categorise the catechol-reactive proteome. This approach facilitated the direct comparison of multiple substances and the characterisation of the reactivity and target scope of a number of catechols.

2 Results and discussion

2.1 Probe synthesis and evaluation

2.1.1 Probe design

To maintain protein reactivity of the catechol, **DA** was derivatised at the amino group with an alkyne handle to facilitate ligation to reporter tags. The modification was introduced via an amide bond as this had yielded more stable products in the **EPI** project (see section II-2.1.2). **DA** oxidation products are prone to inter- or intramolecular nucleophilic attack by the amine leading to cyclisation, polymerisation, and, ultimately, the formation of insoluble aggregates.[176,217] Polymerisation of **DA** oxidation products yields the skin pigment melanin. Sequential addition of **DA** can also occur on a protein, generating an insoluble protein-melanin conjugate known as neuromelanin, which physiologically forms in the brain (Scheme III-1).[176,179]

To facilitate MS-based detection of target proteins, it is convenient to counteract these side reactions by eliminating the nucleophilic side chain by acylation of the amine. Preventing polymerisation allows for more precise dosing of the probe improving experimental reproducibility. More importantly, sequential modification and consequent precipitation of target proteins is impeded, which would strongly interfere with MS-based identification. Lastly, attenuating side-reactions is expected to increase probe reactivity towards proteins.

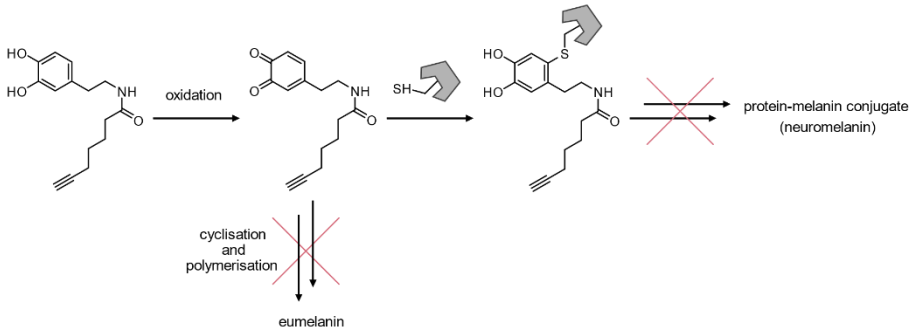

Scheme III-1: Proposed protein reactivity of DA probes.

2.1.2 Chemical synthesis

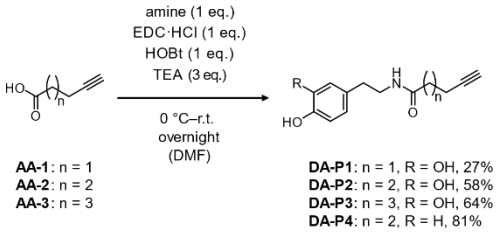

Scheme III-2: Synthesis of DA probes. eq. = equivalents; DMF = *N*,*N*-dimethylformamide; EDC·HCl = 1-(3-dimethylaminopropyl)-3-ethylcarbodiimide hydrochloride; HOBt = hydroxybenzotriazole; TEA = triethylamine.

DA probes were synthesised analogously to the second-generation **EPI** probes (see section II-2.1.2). A terminal alkyne was introduced by acylation of the **DA** amino group using EDC·HCl and HOBt in the presence of TEA (Scheme III-2). **DA** probes were synthesised with a chain length of five to seven carbon atoms, yielding **DA-P1**, **DA-P2**, and **DA-P3** in yields of 27%, 58%, and 64%, respectively. A negative control probe, **DA-P4**, was obtained from coupling of 5-hexynoic acid to tyramine in 81% yield. Superior yield compared to **DA-P1**–**DA-P3** is likely due to the better stability of the starting material.

2.1.3 Evaluation of protein binding

DJ-1 is a redox-sensitive chaperone containing three reactive cysteines. It is assumed to play a role in the pathogenesis of PD[185-186] and has been reported to be modified by **DA**.[188] To evaluate protein reactivity of the probes, purified DJ-1 was incubated exemplarily with **DA**, **DA-P2**, **DA-P3**, or **DA-P4** (100 equivalents) in PBS in the absence of any further catalyst and resulting adducts were analysed by HRMS (Figure III-5). DJ-1 was modified by two to three molecules of **DA-P2** and **DA-P3**, respectively. As expected, **DA-P4** showed no protein binding, corroborating the necessity for an intact catechol group.

However, no adducts of the parent compound **DA** could be observed. This is consistent with previous studies failing to detect **DA** modifications by MS methods.[176-177] It has been suggested that this is caused by reversibility or neutral loss during ionisation.[177] Intriguingly, the modification by the probes was stable enough for MS analysis, suggesting that catechol modifications per se should be detectable. However, it is conceivable that a cysteine modification by **DA** is reversible by intramolecular nucleophilic attack of the amine (at the quinone) resulting in a displacement of the thiol via an addition-elimination-type mechanism. The absence of a nucleophilic residue in the probe, on the other hand, would render the modification irreversible. Another consideration is that the probes should be more reactive

towards proteins than **DA** due to its inability to cyclise. Finally, **DA** modification is known to promote protein precipitation,[176] which would interfere with MS detection. To sum up, superior protein binding of amide probes might stem from increased protein reactivity, irreversibility of binding, or the lack of protein precipitation – or a combination of these factors.

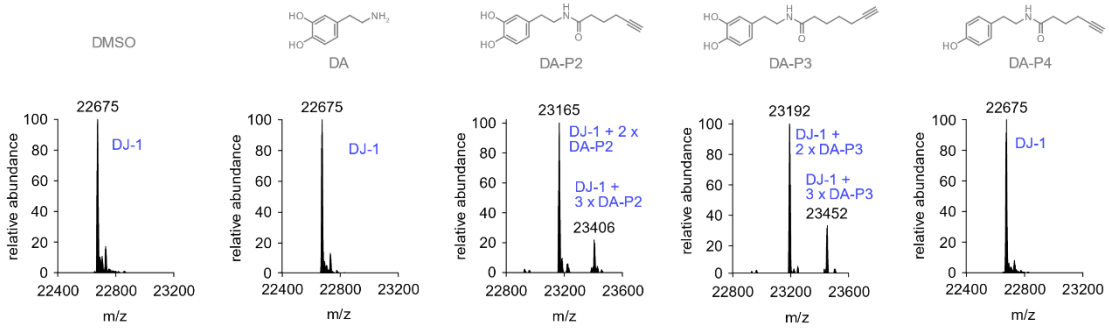

Figure III-5. Labelling of purified DJ-1. HRMS spectra of intact DJ-1 (5 µM) incubated with probes (100 equivalents) in PBS.

Therefore, labelling was next performed in a competitive way to monitor **DA** binding by probe displacement. A reduction in labelling should reflect binding by **DA** even if it is transient or causes protein precipitation. DJ-1 (1 µM) was pre-incubated with different concentrations of **DA** (12.5–200 µM) before addition of **DA-P3** (25 µM). The protein was precipitated by acetone to remove residual **DA** before CuAAC, as **DA** oxidation is promoted in the presence of copper.[176] Labelled protein was then ligated to rhodamine-azide, separated by SDS-PAGE, and fluorescence visualised (Figure III-6). Probe displacement was indeed visible with increasing **DA** concentrations. Subsequent Coomassie staining indicated protein precipitation at 100 µM **DA**, corroborating that this likely interferes with MS-based detection to some extent. Importantly, the amide probes form protein adducts that are stable enough for MS-based detection and are thus suitable for proteomics experiments using **DA** as competitor.

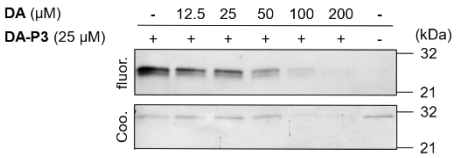

Figure III-6. Competitive labelling of DJ-1. DJ-1 (1 µM) was incubated with **DA** at different concentrations as indicated before addition of **DA-P3** (25 µM). Labelled DJ-1 was ligated to rhodamine azide, separated by SDS-PAGE, and scanned for fluorescence (fluor.). Full protein load was visualised by Coomassie staining (Coo.).

2.2 Labelling in live cells

2.2.1 Labelling in Hek293 cells

Next, probes were assessed in live cells. Hek293 are non-dopaminergic,[182,218] but reported to take up monoamine neurotransmitters including **DA**,[219] possibly via an organic cation transporter such as OCT1 (SLC22A1) which is expressed in this cell line (Human Protein Atlas version 21.1).[220-221]

Live Hek293 cells were treated with **DA-P1**, **DA-P2**, **DA-P3**, or DMSO, lysed, and labelled proteins were ligated to rhodamine azide for a gel-based fluorescence scan (Figure III-7). After 1 h treatment, distinct labelling was observed with all probes starting from 15 µM. While the overall labelling pattern was comparable, fluorescence intensity increased proportionally to the acyl chain length, which is known to influence cell permeability.[222] Even at the highest concentration (100 µM), no protein precipitation was apparent from the Coomassie stain.

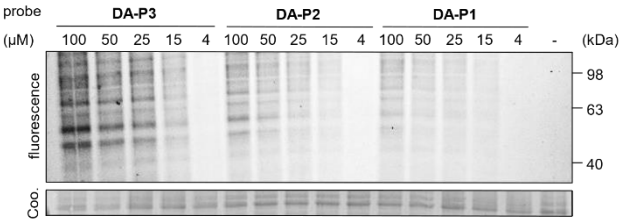

Figure III-7. Comparison of DA probes in live Hek293 cells. Cells were treated with **DA-P1**, **DA-P2**, **DA-P3**, or DMSO at different concentrations as indicated. Following lysis, labelled proteins were ligated to rhodamine azide, separated by SDS-PAGE, and imaged for fluorescence. Full protein load (15 µg per lane) was visualised with Coomassie stain (Coo.).

Protein targets were next analysed by MS using **DA-P3** (15 µM) as it had shown the strongest labelling in the gel. Hek293 cells were treated either with **DA-P3**, DMSO, or with a 30-fold excess of **DA** followed by **DA-P3**, and labelled proteins were ligated to biotin-azide after lysis. Proteins were enriched on avidin, digested, and analysed by LC-MS/MS with LFQ.

Comparison of proteins enriched by **DA-P3** to the DMSO control revealed 236 hits ($-\log_{10}(p\text{-value}) \geq 2$; 3946 identified, Figure III-8 A and Table VI-1). The enrichment of proteins in probe-treated samples compared to samples pre-treated with **DA** revealed 205 hits (~5% of 3948 identified proteins, Figure III-8 B and Table VI-2). Considering only proteins that were identified in all three conditions (DMSO, only probe, competition), 149 proteins (63%) enriched by **DA-P3** compared to DMSO were also significantly outcompeted by **DA**, with most of non-significant hits still close below the cut-off (Figure III-8 B and C). These data strongly support that **DA-P3** mimics the protein reactivity of **DA**/**DAQ**.

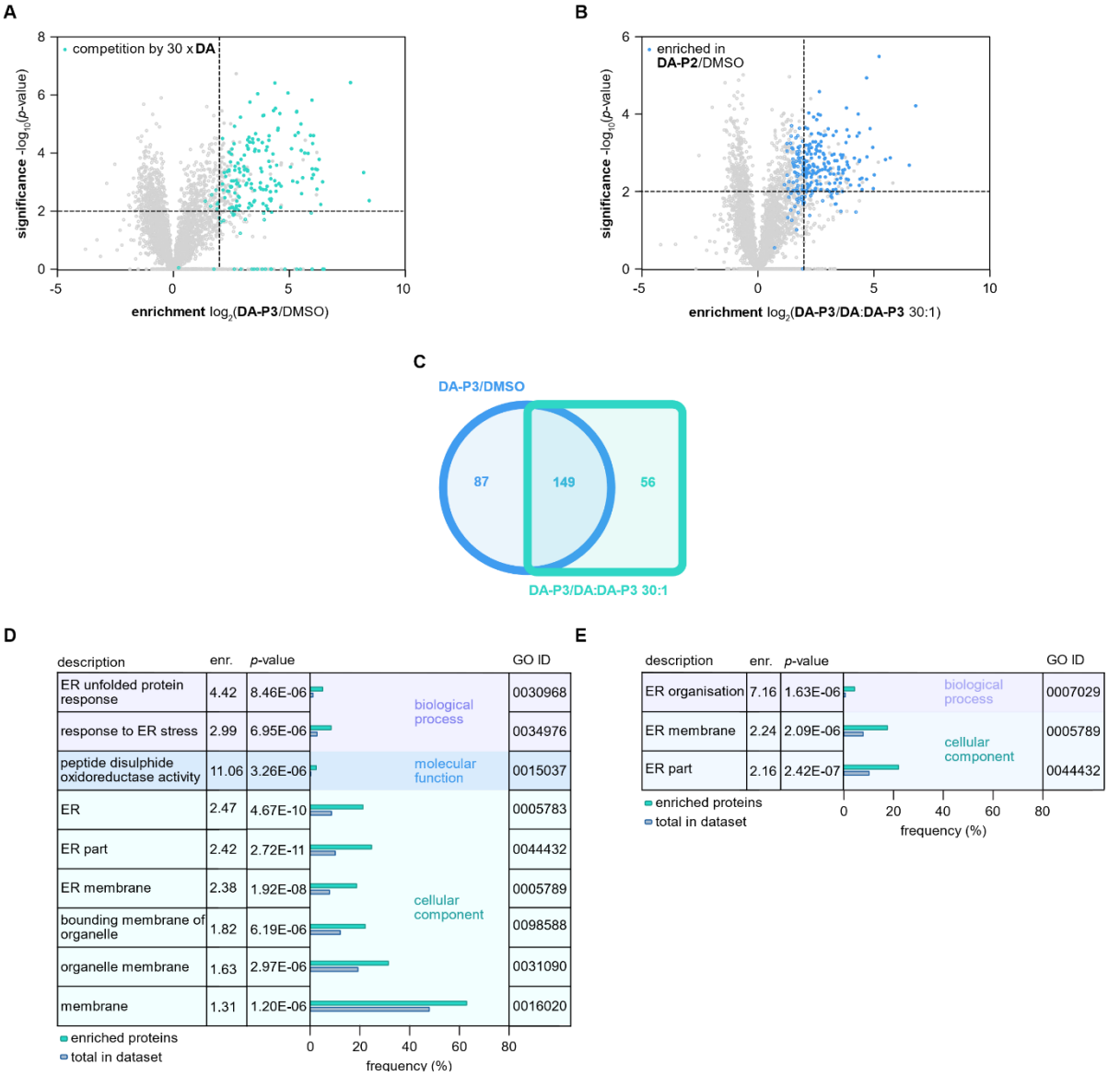

Figure III-8. Competitive labelling in Hek293 cells. Live cells were treated with **DA-P3** (15 µM), DMSO, or with a 30-fold excess of **DA** followed by **DA-P3**. Following lysis, labelled proteins were ligated to biotin-azide, enriched on avidin, digested, and peptides analysed by MS with LFQ.[96] LFQ data were filtered for proteins identified in three replicates in at least one condition and samples were compared using a two-sided two-sample *t*-test. (A) Volcano plot showing proteins enriched by **DA-P3** compared to the DMSO control. Proteins that were outcompeted by **DA** are highlighted in cyan. (B) Volcano plot showing proteins enriched by **DA-P3** compared to a 30-fold excess of **DA**. Proteins that were significant in **DA-P3** compared to DMSO are highlighted in blue to visualise the overlap. See Tables VI-1–2 for details on significant protein hits. Proteins with missing values are shown with $-\log_{10}(p\text{-value}) = 0$. (C) Overlap of proteins significantly enriched against DMSO (blue circle) and against a 30-fold excess of **DA** (cyan square). Only proteins that were identified in all samples of all three conditions were included. The tables show GO terms enriched among the significant proteins compared to proteins detected in total (p-value $\leq 10^{-5}$) in the comparison of **DA-P3** (D) to DMSO and (E) to a 30-fold excess of **DA**.

A GO term enrichment analysis using the GOrilla tool[223-224] revealed that terms related to the ER were strongly enriched in both comparisons (Figure III-8 D–E). In the enrichment against the DMSO control, specifically ER stress and unfolded protein response (UPR, "response to ER stress", "ER unfolded protein response") as well as peptide disulphide oxidoreductases ("peptide disulphide oxidoreductase activity") were affected and enriched at least 3-fold compared to the total dataset.

2.2.2 Investigation of proteome-wide probe modification

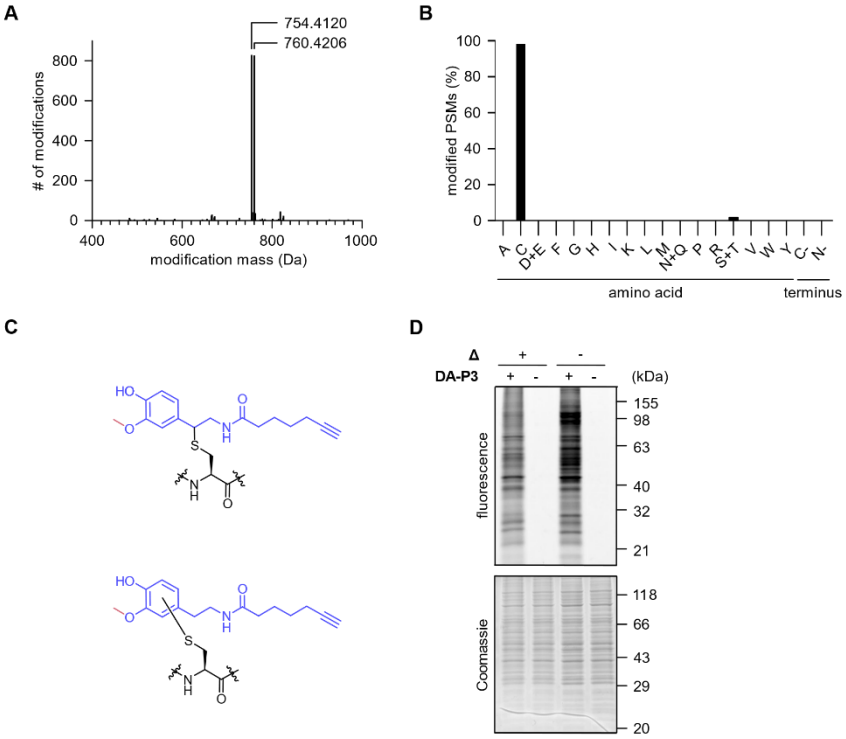

Figure III-9. Analysis of modifications introduced by DA-P3 proteome-wide. Lysate from Hek293 treated *in situ* with **DA-P3** (15 µM) was ligated to heavy- or light-labelled isoDTB-azide, combined in a 1:1 ratio, digested, and peptides enriched on avidin. Modified peptides were eluted and analysed by LC-MS/MS. (A) Unbiased analysis of modifications in the proteome. Modifications detected in a ratio of ~1:1 were considered true hits. (B) Amino acid selectivity of the detected modification. PSM = peptide spectrum matches. (C) Structures of potential regioisomers of cysteine modifications corresponding to the observed mass. (D) Labelling in heat-denatured Hek293 lysate (0.5% deoxycholic acid, 0.5% NP-40/PBS) with **DA-P3** (15 µM). Δ = heat-denatured. MS data were analysed by S. M. Hacker (TUM/Leiden University).

Next, the mass of modification and amino acid selectivity of **DA-P3** were investigated using isoDTB tags[32] to analyse probe-modified peptides from Hek293 cells by LC-MS/MS. In an unbiased analysis,[16,31] added masses of 754.4120 and 760.4206 were detected which corresponds to **DA-P3** plus the heavy or the light tag, respectively, as well as an additional methyl group (Figure III-9 A). In human cells, the COMT transfers a methyl group onto the catechol moiety of catecholamine neurotransmitters, catechol oestrogens, or xenobiotics as part of a degradation pathway.[225] Considering the large substrate range, methylation of **DA-P3** by COMT is plausible. Consistent with a Michael-type addition, 98% of all detected modified residues were cysteines (Figure III-9 B). The finding that an *O*-methylated catechol covalently modifies proteins was unexpected but consolidates a recent report describing protein modification by **CP**.[215] Likewise, **CP** modified cysteines. The authors could not provide a mechanistic explanation and hypothesised, that cysteine modification by **CP** was preceded by its conversion to a quinone.[215] The present results, however, strongly indicate that *O*-methylated catechols can directly modify cysteines, presumably via oxidation to the corresponding quinone

methide (Figure III-9 C). A comparable reaction is known between **CP** and glutathione.[226] Of note, these data furthermore reflect the propensity of catechols to undergo cellular metabolisation.

To investigate the impact of enzymatic *O*-methylation on protein modification, labelling was performed in heat-denatured Hek293 lysate containing detergents (0.5% deoxycholic acid, 0.5% NP-40/PBS). This should inactivate any methyl-transferring enzymes by denaturation. A control experiment was performed in lysate without heat denaturation but containing equal concentrations of detergents and total protein. In-gel fluorescence analysis revealed that heat and detergents did not abrogate labelling, indicating that no enzymatic activity is required to activate **DA-P3** (Figure III-9 D). Labelling in untreated lysate appeared more intense in the non-heated control and some additional bands were visible, however, this could be due to changes in protein abundance following heat treatment. Roughly 800 modifications were detected by MS, which is comparatively low (~3000 modifications in the **EPI** project with similar experimental conditions). Moreover, no methyl modification could be detected in the *in vitro* labelling of DJ-1, which was in any case performed in PBS in the absence of any potential methyl donor or corresponding enzymes. These observations indicate that *O*-methylated probes only constitute a subset of probe-modifications that could not entirely be detected by the MS workflow. Nevertheless, the reactivity of *O*-methylated catechols appears to be substantial and it is an interesting point for future research.

2.2.3 Labelling in neuronal cells

Elevated oxidative stress coupled to aberrant protein dopamination may be a driver in the pathogenesis of PD.[176,181] DJ-1 protects neurons against **DA** toxicity,[185] and, consistently, loss-of-function mutations are associated with hereditary forms of the disease. Hence, *DJ-1* knock-out rodent models are frequently used in PD research[181,185-187] To investigate dopamination in brain cells, labelling with **DA-P3** was performed in embryonic mouse neurons (cortex and hippocampus). Labelling was performed in both wild-type and *DJ-1* knock-out cells. A gel-based analysis with different concentrations of **DA-P3** displayed strong labelling at 15 µM in both cell types, therefore, this concentration was chosen for further MS-based analyses (Figure III-10 A). In the MS data, a similar number of proteins was significantly enriched compared to the DMSO control in wild-type and knock-out (279 out of 3736 in wild-type and 185 out of 3154 in knock-out, Figure III-10 B and D, Tables VI-3–4). *DJ-1* knock-out cells should experience higher oxidative stress.[181] In literature reports, increased **DA** oxidation in *DJ-1*

knock-out mutants was observed after several days.[181,227] Potentially, the time-scale of chemoproteomics labelling is too short to monitor these differences. The above findings may indicate that cellular oxidative stress does not immediately impact catechol reactivity significantly even if it may promote **DA** toxicity in the long term. An analysis of GO term overrepresentation[223-224] revealed significant enrichment of disulphide oxidoreductases and ER proteins in the wild type (Figure III-10 F). In the *DJ-1* knock-out cells, ER proteins and specifically proteins related to ER stress were overrepresented (Figure III-10 G). Hence, in this aspect, the results in primary neurons reproduced the findings from Hek293.

Labelling was also performed in competition with a 50- or a 100-fold excess of **DA** (750 µM and 1500 µM, respectively). Despite these high concentrations, competition of **DA-P3** compared to **DA** plus **DA-P3** was poor even at 100-fold excess, and only one protein was enriched above the cut-off in each cell type, namely the signal recognition particle 19 kDa protein (Srp19) in wild-type, and the holocytochrome *c*-type synthase (Hccs) in knock-out cells (Figure III-10 B and D). Srp19 and Hccs were closely below the cut-off in knock-out and wild-type samples, respectively. The LFQ intensities of Hccs and Srp19 decreased in proportion to the **DA** concentration in both wild-type and knockout, indicating that these proteins are indeed modified by **DA** (Figure III-10 C and E). Srp19 is a subunit of the signal recognition particle (SRP) complex, which targets secretory and membrane proteins to the ER during ribosomal translation.[228] This way, proteins are cotranslationally translocated into the ER through a specific transporter. The Srp19 subunit is essential for correct assembly of the eukaryotic SRP and the deregulation of SRP is associated with disease development.[229] Holocytochrome *c* is an electron carrier in oxidative phosphorylation and thus essential for eukaryotic mitochondrial respiration. Hccs is required to covalently attach the heme cofactor to apocytochrome[230-231] and loss of the Hccs leads to severe cell damage.[232] Both proteins play a crucial role in cellular function and their potential dysregulation by **DA** binding warrants future investigation. The overall poor competition may be due to neuron-specific differences in uptake, storage, or enzymatic degradation of **DA** compared to Hek293 cells and requires further studies.

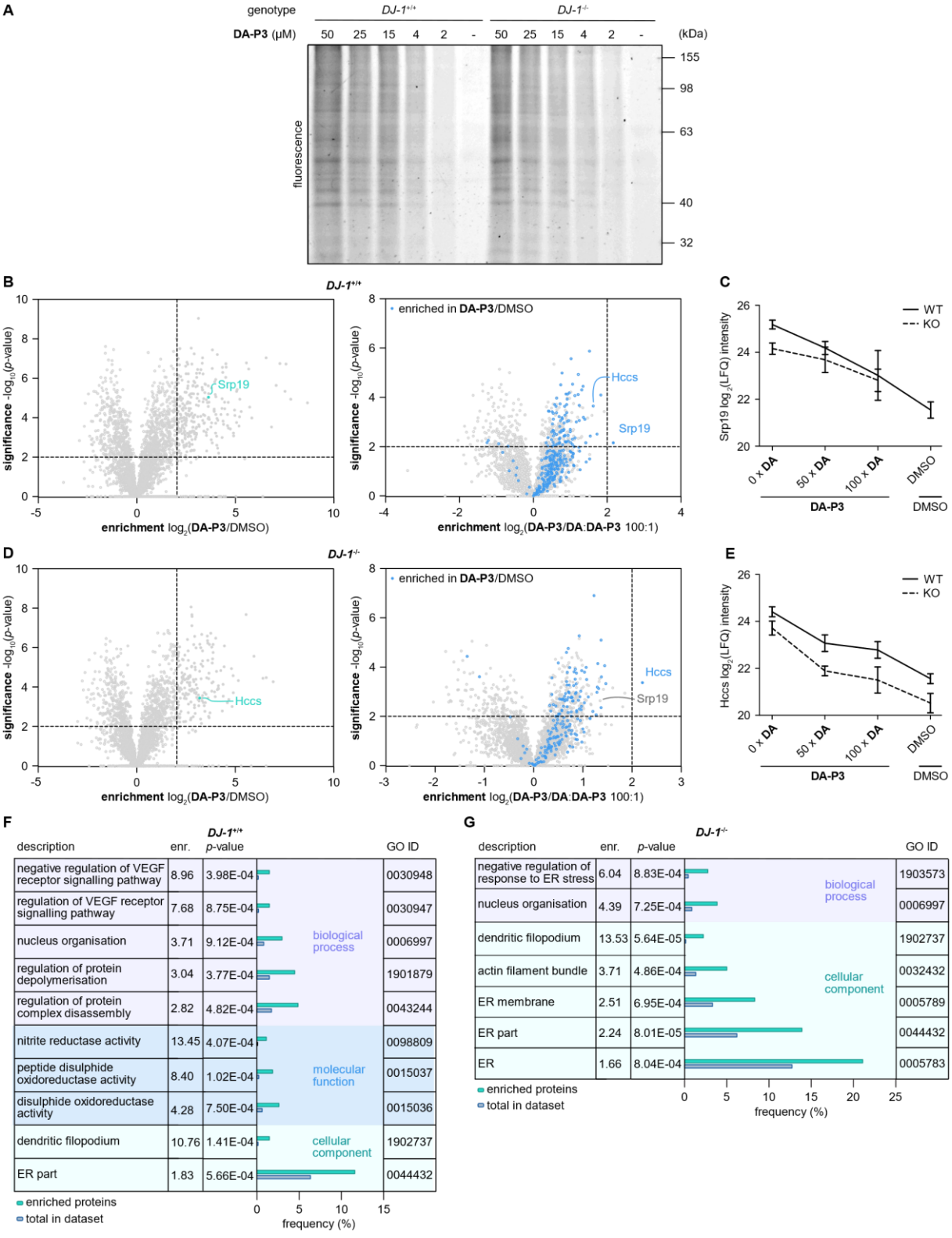

Figure III-10. Labelling with DA-P3 in live primary mouse neurons. (A) In-gel fluorescence detection of labelling with different concentrations of **DA-P3** as indicated. (B) Volcano plot of MS-based labelling in wild-type cells showing proteins enriched by **DA-P3** (15 µM) compared to a DMSO control (left) or to a 100-fold excess of **DA** (right). (C) Profile plot of Srp19 LFQ intensities in the presence of 50-fold and 100-fold **DA** excess. (D) Volcano plot of MS-based labelling in *DJ-1* knock-out cells showing proteins enriched by **DA-P3** compared to the DMSO control (left) or to a 100-fold excess of **DA** (right). (E) Profile plot of Hccs LFQ intensities in the presence of 50-fold and 100-fold **DA** excess. MS data from four biological replicates were analysed by MaxLFQ[96] and filtered for proteins identified in three replicates in at least one condition. Samples were compared using a two-sided two-sample *t*-test. Proteins were considered significant when they were enriched more than four-fold ($\log_2$(enrichment) ≥ 2) with a *p*-value of less than 0.01 ($-\log_{10}$(*p*-value) ≥ 2); proteins outcompeted by **DA** are

labelled in green; proteins that were above the cut-off in the enrichment experiment (against DMSO) are highlighted in blue; proteins with missing values are shown with -$\log_{10}$(*p*-value) = 0. (F) GO term enrichment analysis of proteins significantly enriched (against DMSO) in *DJ-1*$^{+/+}$ cells. G) GO term enrichment analysis of proteins significantly enriched (against DMSO) in *DJ-1*$^{-/-}$ cells. GO term enrichment analyses: *p*-value ≤ 10-3. See Tables VI-3–4 for details on significant protein hits. Neurons were prepared by A. Kurz-Drexler (Helmholtz Zentrum).

2.2.4 Labelling in competition with different catechol compounds

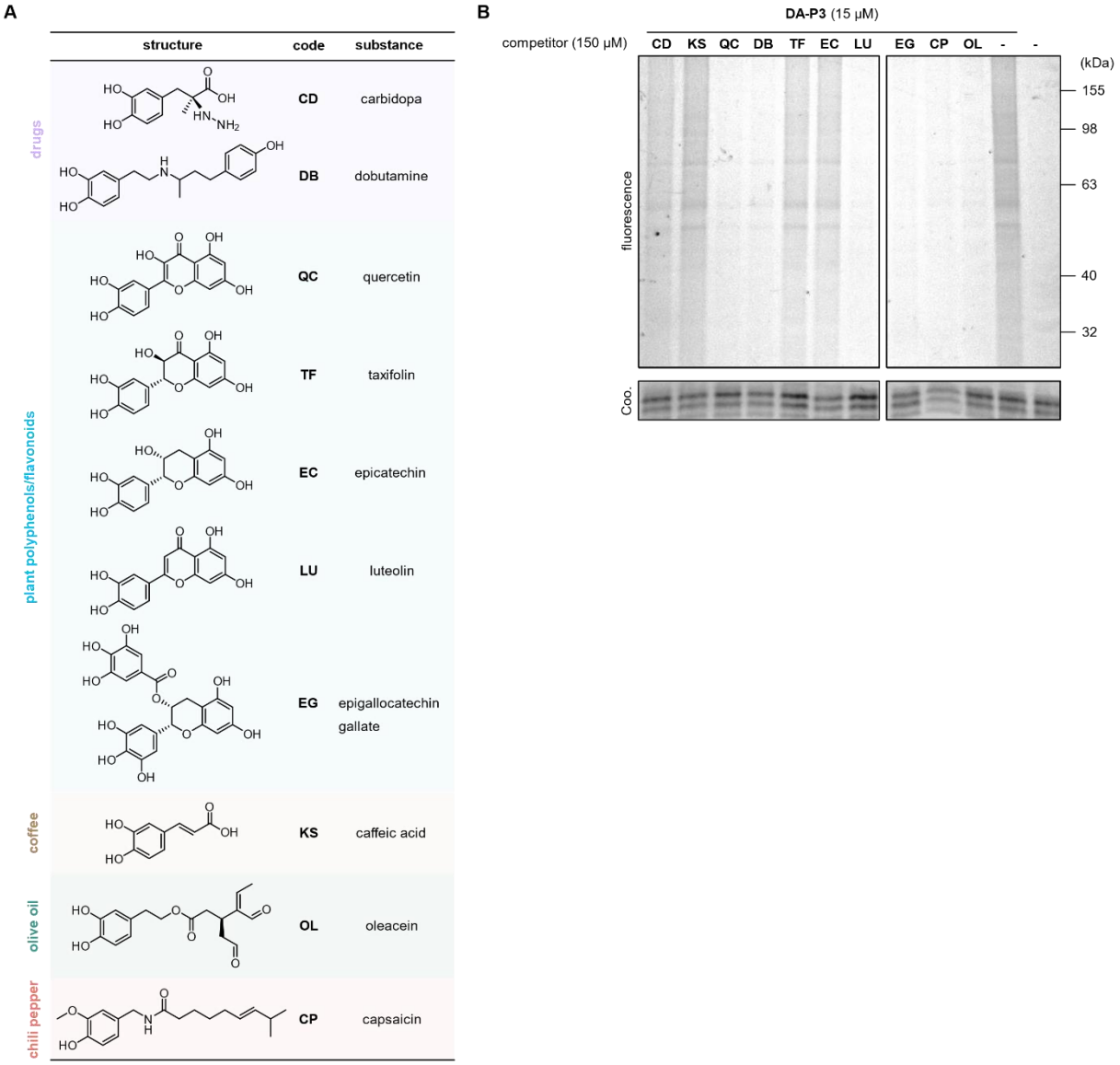

Figure III-11. Labelling in competition with diverse catechols. (A) Structures of catechol competitors. (B) In-gel fluorescence analysis of labelling in competition with catechols. Live Hek293 cells were treated with a 10-fold excess of catechols (150 µM) before addition of **DA-P3** (15 µM). Full protein load (15 µg per lane) was visualised by Coomassie staining (Coo.).

In light of the broad protein reactivity of **DA-P3**, labelling was next performed in competition with a suite of structurally diverse catechols to elucidate their protein target scope. A number of plant secondary metabolites (**QC**, **TF**, **EC**, **LU**, **EG**, **KS**) was included as well as medicinal drugs (**DB**, **CD**). Furthermore, **CP**, containing an *O*-methylated catechol group, was included

for comparison (Figure III-11 A). Hek293 cells were treated with a 10-fold probe excess (150 µM) before addition of **DA-P3** (15 µM). Gel-based analysis indicated that six catechols, namely **DB**, **QC**, **LU**, **EG**, **OL**, and **CP** outcompeted labelling to a large extent. In contrast, four compounds, namely **CD**, **TF**, **EC**, and **KS**, appeared much less reactive (Figure III-11 B).

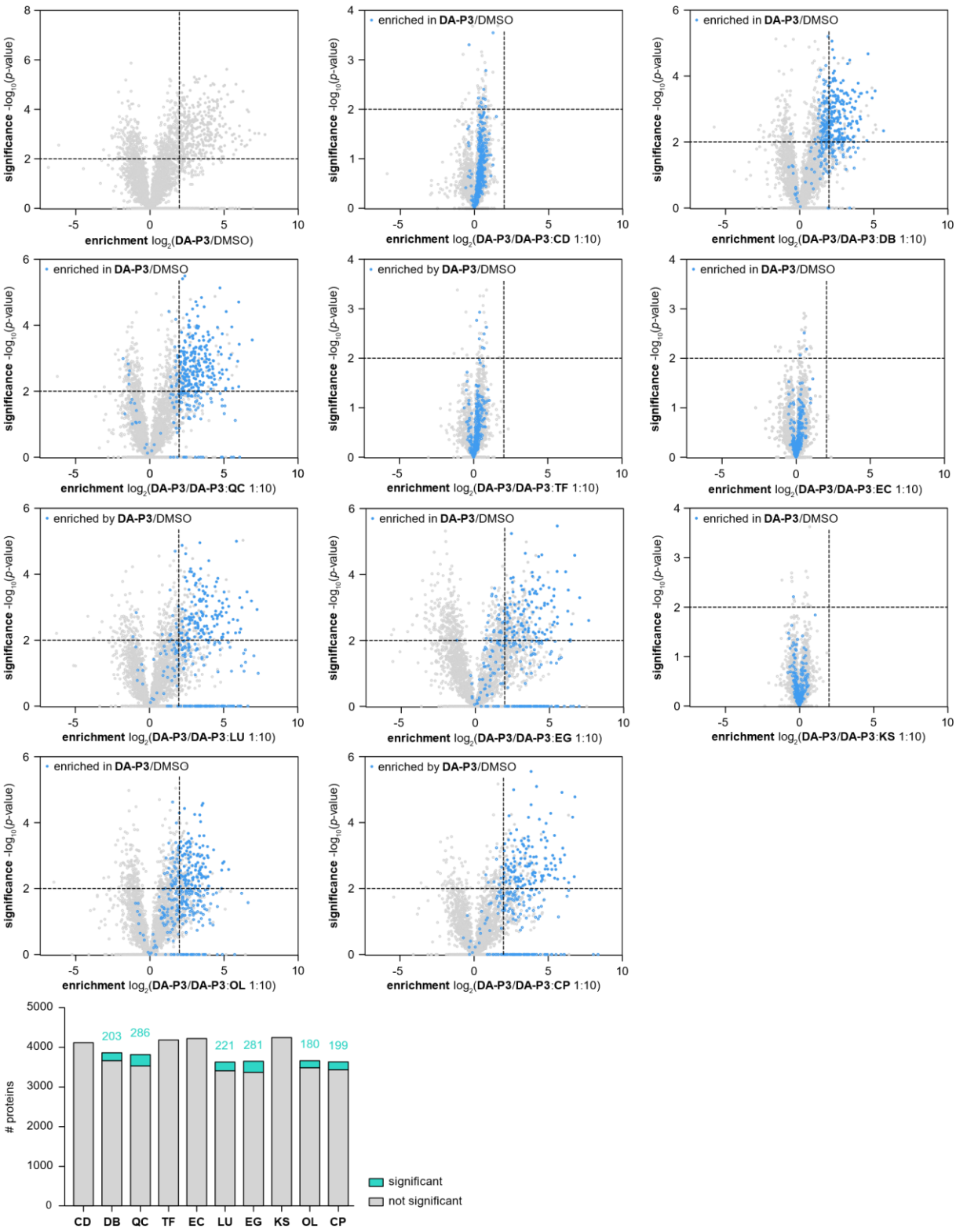

Figure III-12. Labelling in competition with diverse catechols. Volcano plots show enrichment of proteins by **DA-P3** (15 µM) compared to DMSO or to a 10-fold excess of different catechols as indicated. Labelling was performed in live Hek293 cells. LFQ[96] values were filtered for proteins identified in three replicates in at least one condition. Samples were compared using a two-sided two-sample *t*-test. Proteins that were above the cut-off in the enrichment experiment (against DMSO) are highlighted in blue; proteins with missing values are shown with $-\log_{10}(p\text{-value}) = 0$. The bar plot shows the number of proteins significantly outcompeted by each catechol (cyan) and non-significant hits (grey). The full bar represents the total number of detected proteins. The experiment was performed in three independent replicates. See Tables VI-5–10 for details on significant protein hits.

Indeed, this division of reactivity was also reflected by the MS data. **LU**, **CP**, **OL**, **QC**, **DB**, and **EG** showed strong competition with 180–286 proteins above the cut-off (with at least 3627 proteins quantified), whilst **CD**, **TF**, **EC**, and **KS**, did not outcompete binding to any protein (Figure III-12, Tables VI-5–10). It is worth highlighting that **CP**, carrying a 3-*O*-methylcatechol group, was among the reactive substances.

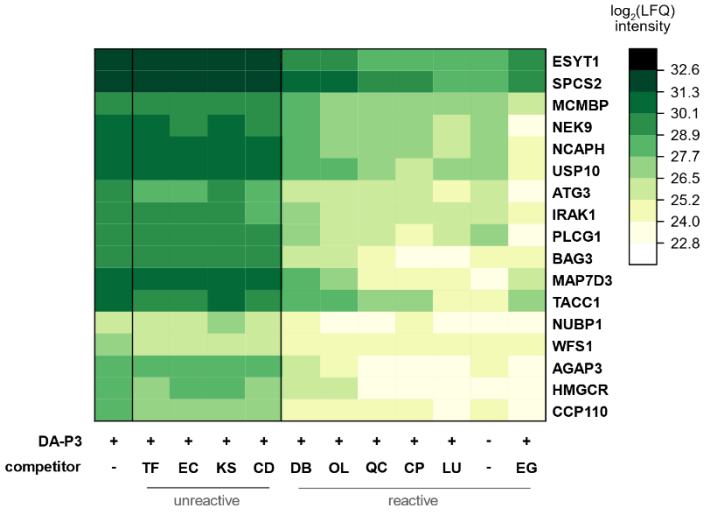

Figure III-13. Comparison of protein target scope of different catechols. Heat map shows LFQ intensities of proteins that were significantly outcompeted by all catechols categorised as reactive.

Interestingly, 17 proteins were consistently identified as significant hits in samples treated with **DB**, **OL**, **QC**, **CP**, **LU**, and **EG**, revealing an unanticipated broad overlap and indicating that some proteins may be susceptible to catechol modification largely independent of the structure (Figure III-13). Among them, four proteins were associated with the ER, namely ESYT1 (tethers the ER to the plasma membrane),[233-234] SPCS2 (contributes to cotranslational translocation of nascent proteins into the ER),[235] WFS1 (ER membrane glycoprotein involved in the regulation of cellular Ca^{2+} homeostasis),[236] and HMGCR. HMGCR is localised in the ER membrane where it catalyses the rate-determining step in the biosynthesis of cholesterol and other isoprenoids and is therefore the main target of cholesterol-lowering drugs (statins).[237-238] Interestingly, **EG** has previously been reported to act as a potent inhibitor of HMGCR activity *in vitro*.[239] The other hits are involved in DNA replication (MCM-BP),[240] mitosis (NCAPH),[241] microtubule assembly (MAP7D3),[242] regulation of nuclear receptor transcriptional activity (TACC1),[243] mitotic progression (Nek9),[244] regulation of p53 localisation and stability (USP10),[245] second messenger production (PLCG1),[246] modulation of Hsc70/Hsp70 chaperone activity (BAG3),[247] Fe/S protein maturation (NUBP1),[248] centriolar processes (CCP110),[249-250] immune response (IRAK1),[251-252] or have E2 enzyme activity (ATG3).[253] These results indicate that catechols may affect cellular pathways very broadly.

Figure III-14. Enrichment of GO term frequencies in proteins outcompeted by different catechols. Significant proteins were compared against total detected proteins (after filtering) using the GOrilla tool;[223-224] *p*-value ≤ 10^{-3}. Compounds for which no GO term was significantly enriched are not shown. Red, dashed boxes mark ER-associated terms. IMP = inosine monophosphate; regul. = regulation; neg. = negative; pos. = positive; biosyn. = biosynthetic; ER = endoplasmic reticulum; UPR = unfolded protein response; intramol. = intramolecular; membr. = membrane.

GO term enrichment analyses[223-224] of significantly outcompeted proteins (*p*-value ≤ 10^{-3}) by individual catechols yielded 57 biological processes, 21 molecular functions, and 27 cellular components in total (Figure III-14). Across all categories, terms related to structural proteins (e.g., microtubule, cytoskeleton, cell adhesion) were most prominent. Moreover, as already observed for **DA**, ER-associated terms were enriched in samples treated with **DB** and **QC** in the cellular compartment category. In the **DA** competition experiments in both Hek293 cells and neurons GO terms specifically related to ER stress and PDIs were enriched. ER stress is accompanied by an accumulation of unfolded proteins and the UPR is a cellular response aiming to relieve unfolded protein load, e.g., by reducing protein biosynthesis, or else initiate

apoptosis. PDIs maintain redox homeostasis and perform oxidative protein folding in the ER. Therefore, they are critical for cellular protein turnover. Interestingly, the inhibition of PDIs has been reported for catechols including **DA**, the flavonoid isoquercetin, and n-octyl caffeate.[189,199,214] PDIs are interesting targets as they are thought to be important in cancer progression and represent potential antitumour targets.[214,254] Moreover, cancer cells divide rapidly and have high protein turnover, resulting in constant ER stress. Therefore, they are more sensitive to PDI inhibition and perturbations of the UPR.[254] Interestingly, the inhibition of PDIs can also result in neuroprotection.[190,255] Altogether, future experiments should explore whether the modulation of ER-associated cellular processes accounts for some of the health-promoting biological effects attributed to catechols (see section III-1.2).

2.3 Measurement of flavonoid redox potentials

Strikingly, the flavonoids **QC**, **TF**, **EC**, and **LU** differed largely in their protein reactivity despite their structural similarity. In the flavonoid structure, two benzene rings are connected by a 3-carbon linker. In **QC** and **LU**, the C3 structure is unsaturated, generating a Michael acceptor. This feature is absent in **DB**, **EG**, **CP**, and **DA-P3**, all of which are very protein-reactive, indicating that this is most likely not the (sole) cause of reactivity. Since protein binding requires oxidation of the catechol moiety, redox potentials of the flavonoids were determined by cyclic voltammetry (CV, Figure III-15).

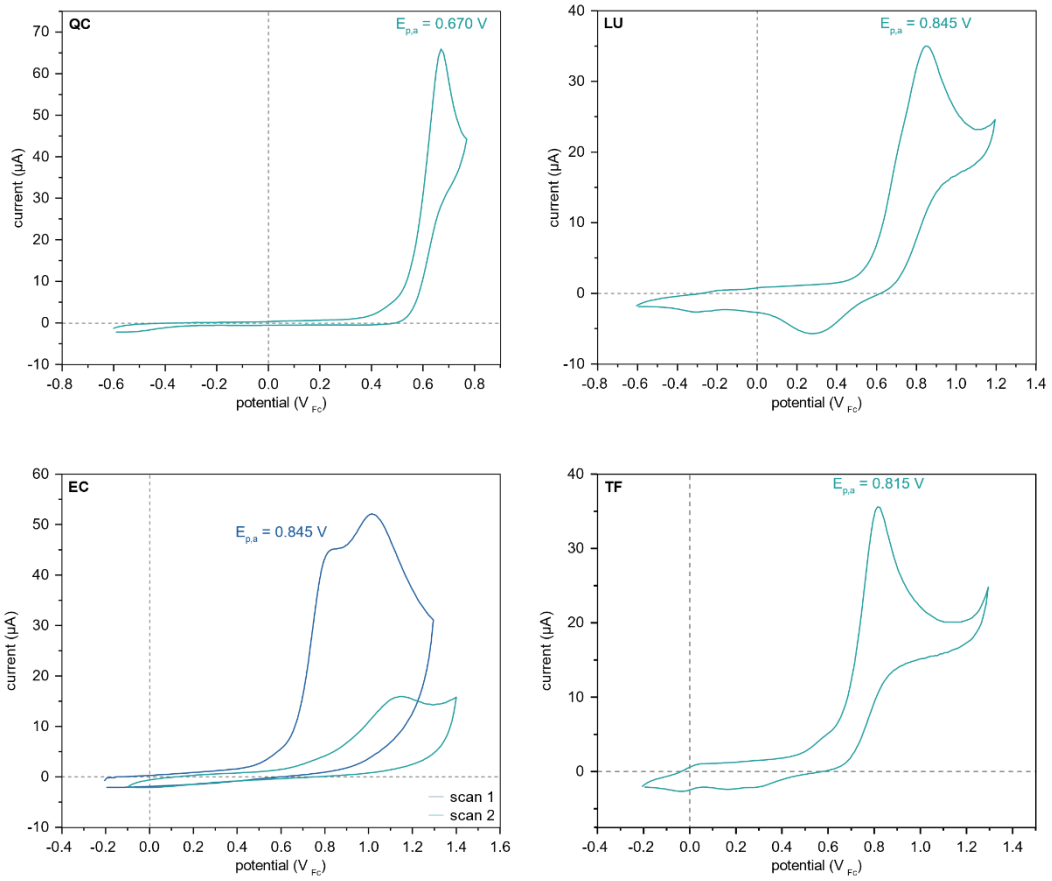

Figure III-15. Cyclic voltammograms of flavonoids. Plots show anodic peak potentials of the first oxidative events (second scan). Measurements were performed in a 0.1 M $TBAF_6$ acetonitrile solution under argon using glassy carbon as working and counter electrodes and $Ag/AgNO_3$ (10 mM $AgNO_3$) as reference electrode. For **EC**, the peak potential was determined from the first scan. V_{Fc} = Volt versus ferrocene$^{+/0}$. Measurements were performed in collaboration with L. Niederegger (TUM).

For **QC**, the first oxidative event was measured at an anodic peak potential $E_{p,a}$ = 0.670 V_{Fc} (V_{Fc} = Volt versus ferrocene$^{+/0}$). This was slightly lower than for the other flavonoids for which anodic peak potentials $E_{p,a}$ = 0.845 V_{Fc} (**LU**), $E_{p,a}$ = 0.845 V_{Fc} (**EC**), and 0.815 V_{Fc} (**TF**) were determined. **QC** and **LU** outcompeted probe binding to a large number of proteins (286 and 221, respectively), whereas **EC** and **TF** showed no competition. Therefore, redox potentials did

not correlate with protein reactivity. Conceivably, differences in protein binding stem from a combination of several factors such as uptake, subcellular distribution, and enzymatic (de)activation.

2.4 Conclusion and outlook

The biological effects of catechol natural products are manifold including anticancer,[197-198,200,202,256] antiangiogenic,[197] neuroprotective,[194,257-259] antithrombotic,[199] and anti-inflammatory.[215] Similarly, the proposed target proteins and pathways are diverse,[180,194,198-202,210-211,215,257-258,260] pointing to a broad mode of action and cellular target scope. In fact, some biological effects depend mainly on the presence of a catechol group.[212-213] Assuming broad protein reactivity of the catechol group, general protein reactivity of a suite of catechols was studied in a compound-centric, unbiased approach using competitive chemical proteomics. This approach enabled the direct comparison of multiple substances present in nutrition and drugs.

In this project, a **DA**-based probe was synthesised which allowed the detection of protein labelling by MS methods *in vitro* and in live cells. Competition of **DA-P3** labelling by **DA** could be proven on purified DJ-1 and in Hek293 cells. A major limitation of this approach is that competitive labelling with **DA** appeared not to be applicable to brain-derived cells. Nevertheless, it was still possible to identify targets of **DA-P3** in neurons. Moreover, Hccs and Srp19, which were outcompeted by **DA** in neurons, are intriguing potential targets and the physiological consequences of **DA** modification should be explored in future studies.

Analysis of the mass of modification introduced by **DA-P3** revealed cysteine modification by a presumably methylated probe metabolite. This type of modification has not been reported before and provides a rationale for the protein reactivity of 3-*O*-methylated catechols such as **CP**.[215] It furthermore implies that methylated **DA** metabolites may also post-translationally modify proteins.

In situ competitive proteomics experiments revealed broad protein labelling by some catechols, namely **DB**, **QC, LU**, **EG**, **OL**, and **CP**. Interestingly, the overlap of protein hits was substantial with 17 proteins that were consistently outcompeted. An overrepresentation of proteins linked to the ER was observed among targets of **DA-P3, DA**, **QC**, and **DB**. **DA-P3** and **DA** in particular targeted proteins specifically related to ER stress, the UPR, and some PDIs. This finding is intriguing as the interference with ER stress mechanisms could provide an explanation for some of the biological effects attributed to catechols such as their anti-cancer activity. In the literature, protein homeostasis is discussed as an intriguing oncology target. Strategies include the inhibition of molecular chaperones such as Hsp90,[261] the proteasome,[262] and PDIs.[263-265] Beyond cancer, PDIs have been implicated in the pathogenesis of neurological

and infectious diseases, amongst others.[266-267] Interestingly, the cellular effects resulting from PDI inhibition appear to be highly context-dependent. In experimental models of different neurological diseases, small molecule PDI inhibitors had neuroprotective effects.[190,255,268] It was observed that the mode of action involved the inhibition of apoptosis in response to certain stress stimuli and that these effects were independent of ER stress pathways.[268] In the context of cancer, on the other hand, PDI inhibition disrupts protein homeostasis, causes ER stress, and triggers cell death.[214,263] Intriguingly, targeting PDIs appears to have anti-cancer activity with minimal toxicity towards healthy cells.[214,264] Future experiments should therefore aim to better understand the role of catechol natural products in ER physiology and elucidate whether catechol natural products themselves induce ER stress or whether they disrupt the ER stress response. Furthermore, functional inhibition of PDIs by catechols should be investigated.

3 Experimental procedures

3.1 Chemical methods

3.1.1 Chemical Synthesis

3.1.1.1 General remarks

See section II-3.1.1.

3.1.1.2 Amide coupling general protocol[269]

To a solution of carboxylic acid (1.0 eq.) in DMF (24 mL), EDC·HCl (1.0 eq.) was added followed by HOBt (1.0 eq.). The solution was stirred at 0 °C for 30 min and then at room temperature for 1.5 h, and anhydrous TEA (3.0 eq.) was added dropwise. The amine (1.0 eq.) was added and the mixture was stirred at room temperature overnight protected from light. EtOAc (100 mL) was added and the mixture was washed three times with water (30 mL). The combined aqueous phases were reextracted with EtOAc (20 mL), washed with brine (50 mL), and dried over Na_2SO_4. Solvents were removed under reduced pressure and the crude mixture was purified by SiO_2 chromatography (0.5% AcOH, 1–3% MeOH/CH_2Cl_2).

3.1.1.3 Synthesis of *N*-(3,4-dihydroxyphenethyl)pent-4-ynamide (**DA-P1**)

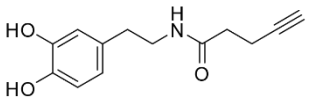

DA-P1
$C_{13}H_{15}NO_3$
233.27 g/mol

DA-P1 was obtained from dopamine·HCl (569 mg, 3.00 mmol, 1.0 eq.) and 4-pentynoic acid (**AA-1**, 294 mg, 3.00 mmol, 1.0 eq.) as a grey solid (186 mg, 0.798 mmol, 27%).

TLC: R_f = 0.26 (0.5% AcOH, 3% MeOH/CH_2Cl_2) [UV/$KMnO_4$]. **^{1}H-NMR:** (500 MHz, DMSO-d_6) δ [ppm]: 8.83–8.53 (m, 2H), 7.90 (t, J = 5.3 Hz, 1H), 6.65–6.60 (m, 1H), 6.58–6.54 (m, 1H), 6.45–6.40 (m, 1H), 3.20–3.13 (m, 2H), 2.75 (t, J = 2.6 Hz, 1H), 2.53–2.47 (m, 2H + DMSO), 2.36–2.30 (m, 2H), 2.27–2.21 (m, 2H). **^{13}C-NMR:** (75 MHz, DMSO-d_6) δ [ppm]: 170.05, 145.04, 143.52, 130.20, 119.21, 115.98, 115.49, 83.81, 71.26, 40.63, 34.70, 34.24, 14.26. **HRMS:** (ESI) $C_{13}H_{16}NO_3^+$ $[M+H]^+$ calculated: 234.1125; found: 234.1124.

3.1.1.4 Synthesis of *N*-(3,4-dihydroxyphenethyl)hex-5-ynamide (**DA-P2**)

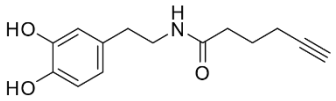

DA-P2
$C_{14}H_{17}NO_3$
247.29 g/mol

DA-P2 was obtained from dopamine·HCl (284 mg,1.50 mmol, 1.0 eq.) and 5-hexynoic acid (**AA-2**, 168 mg, 166 µL, 1.50 mmol, 1.0 eq.) as a brown oil (217 mg, 0.876 mmol, 58%).

TLC: R_f = 0.34 (0.5% AcOH, 3% MeOH/CH_2Cl_2) [UV/$KMnO_4$]. **^{1}H-NMR:** (400 MHz, DMSO-d_6) δ [ppm]: 8.65 (s, 2H), 7.81 (t, J = 5.6 Hz, 1H), 6.62–6.56 (m, 1H), 6.56–6.51 (m, 1H), 6.43–6.35 (m, 1H), 3.13 (dt, J = 8.1, 6.0 Hz, 2H), 2.73 (t, J = 2.7 Hz, 1H), 2.47 (t, J = 7.5 Hz, 2H), 2.10 (td, J = 7.2, 1.9 Hz, 4H), 1.62 (p, J = 7.3 Hz, 2H). **^{13}C-NMR:** (101 MHz, DMSO-d_6) δ [ppm]: 171.25, 145.03, 143.48, 130.27, 119.19, 115.94, 115.45, 84.14, 71.42, 40.53, 34.69, 34.20, 24.29, 17.41. **HRMS:** (ESI) $C_{14}H_{18}NO_3^+$ $[M+H]^+$ calculated: 248.1281; found: 248.1281.

3.1.1.5 Synthesis of *N*-(3,4-dihydroxyphenethyl)hept-6-ynamide (**DA-P3**)

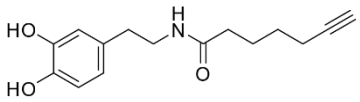

DA-P3
$C_{15}H_{19}NO_3$
261.32 g/mol

DA-P3 was obtained from dopamine·HCl (398 mg, 2.10 mmol, 1.0 eq.) and 6-heptynoic acid (**AA-3**, 265 mg, 280 µL, 2.10 mmol, 1.0 eq.) as a brown oil (352 mg, 1.35 mmol, 64%). **TLC:** R_f = 0.46 (5% MeOH/CH_2Cl_2) [UV/$KMnO_4$]. **^{1}H-NMR:** (400 MHz, DMSO-d_6) δ [ppm]: 8.67 (s, 2H), 7.79 (t, J = 5.5 Hz, 1H), 6.64–6.58 (m, 1H), 6.58–6.53 (m, 1H), 6.44–6.37 (m, 1H), 3.20–3.10 (m, 2H), 2.74 (t, J = 2.6 Hz, 1H), 2.53–2.46 (m, 2H + DMSO-d_6), 2.13 (td, J = 7.0, 2.6 Hz, 2H), 2.03 (t, J = 7.4 Hz, 2H), 1.61–1.49 (m, 2H), 1.44–1.32 (m, 2H). **^{13}C-NMR:** (101 MHz, DMSO-d_6) δ [ppm]: 171.64, 145.02, 143.47, 130.25, 119.17, 115.93, 115.43, 84.36, 71.20, 48.59, 40.47, 34.78/34.73 (rotamers), 27.50, 24.39, 17.43. **HRMS:** (ESI) $C_{15}H_{20}NO_3^+$ $[M+H]^+$ calculated: 262.1438; found: 262.1438.

3.1.1.6 Synthesis of *N*-(4-hydroxyphenethyl)hex-5-ynamide **(DA-P4)**

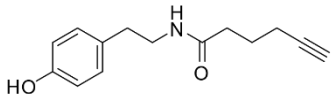

DA-P4
$C_{14}H_{17}NO_2$
231.30 g/mol

DA-P4 was obtained from 4-(2-aminoethyl)phenol (412 mg, 3.00 mmol, 1.0 eq.) and 5-hexanoic acid (**AA-2**, 336 mg, 331 µL, 3.00 mmol, 1.0 eq.) as an off-white amorphous solid (565 mg, 2.44 mmol, 81%). **TLC:** R_f = 0.42 (3% MeOH, 0.5% AcOH/CH_2Cl_2) [UV/$KMnO_4$]. **^{1}H-NMR:** (400 MHz, DMSO-d_6) δ [ppm]: 9.20 (s, 1H), 7.86 (t, *J* = 5.4 Hz, 1H), 6.97 (d, *J* = 8.4 Hz, 2H), 6.66 (d, *J* = 8.4 Hz, 2H), 3.18 (q, *J* = 6.5 Hz, 2H), 2.77 (t, *J* = 2.6 Hz, 1H), 2.57 (t, *J* = 7.4 Hz, 2H), 2.17–2.08 (m, 4H), 1.64 (p, *J* = 7.2 Hz, 2H). **^{13}C-NMR:** (101 MHz, DMSO-d_6) δ [ppm]: 171.25, 155.61, 129.52, 129.43, 115.06, 84.12, 71.40, 40.48, 34.39, 34.17, 24.28, 17.38. **HRMS:** (ESI) $C_{14}H_{18}NO_2^+$ $[M+H]^+$ calculated: 232.1332; found: 232.1332.

3.1.2 Cyclic voltammetry

Measurements were performed with a BioLogic SP200 potentiostat using 3 mm diameter glassy carbon disk electrodes as working and counter electrodes. $Ag/AgNO_3$ (10 mM) was used as a reference electrode. CV measurements were carried out in a five neck glass cell under argon atmosphere with 0.1 M $TBAPF_6$ in acetonitrile as electrolyte. The concentration of the flavonoids was 1 mM and a scan rate of 100 mV/s was applied. Potentials are reported with reference to an internal standard of ferrocenium/ferrocene ($Fc^{+/0}$, indicated by V_{Fc}). Unless otherwise stated, peak potentials were determined from the second scan.

3.2 Biochemical Methods

3.2.1 General information

3.2.1.1 Chemical compounds

Table III-1: Chemical compounds used in this study.

code	name	CAS number	supplier
DA	dopamine·HCl	62-31-7	*Alfa Aesar*
DB	dobutamine·HCl	49745-95-1	*TCI Chemicals*
CD	carbidopa monohydrate	38821-49-7	*Acros Organics*
CP	capsaicin	404-86-4	*Sigma Aldrich*
EC	(-)-epicatechin	490-46-0	*TCI Chemicals*
EG	epigallocatechin gallate	989-51-5	*Sigma Aldrich*
KS	caffeic acid	331-39-5	*Sigma Aldrich*
LU	luteolin	491-70-3	*TCI Chemicals*
TF	(+)-taxifolin	480-18-2	*TCI Chemicals*
OL	oleacein	149183-75-5	*Phytolab*
QC	quercetin	849061-97-8	*Cayman Chemical*

Catechol compounds were stored as indicated by the manufacturer and chemical probes as 100 mM DMSO stocks at -20 °C.

3.2.1.2 Cell culture

All cells were grown in a humidified incubator at 37 °C in a 5% CO_2 atmosphere. For subculturing of human cell lines, cells were washed with PBS, detached with accutase® solution (*Sigma*), and split in a ratio of 1:9.

3.2.1.3 Preparation of primary mouse neurons

Primary neurons were prepared from cortex of E13.5–E14 embryos derived from matings of homozygous wild-type mice and homozygous DJ-1 deficient mice,[270] respectively.

The day before isolating primary neurons, cell culture plates were coated with poly-D-lysin-hydrobromide (50 µg/mL, *Sigma*). Plates were washed once with PBS and coated additionally with laminin (1 µg/mL, *Sigma*) 3 h before seeding primary neurons.

The pregnant mother was killed by cervical fracture, the uteri were removed and transferred to cold dissection medium (HBSS [*Gibco*] + 1% [v/v] penicillin-streptomycin [10.000 U/mL, *Gibco*] + 0.7% [v/v] HEPES [1 M, *Thermo Fisher Scientific*], and the embryos were dissected out. The heads were cut off the embryos and the brains were isolated in fresh petri dishes filled with cold dissection buffer. Next, the two hemispheres were separated and the meninges were carefully pulled off. After removing the olfactory bulbs and the hippocampus, the cortex halves were transferred to a 15 mL falcon tube filled with 10 mL dissection medium, constantly chilled on ice. Cortices of 2 embryos were collected in one falcon. Subsequently, the dissection medium was removed under sterile conditions and the tissue was washed with 1 mL trypsin solution (100 mL 0.25% [w/v] trypsin [*Thermo Fisher Scientific*] + 0.8 mL HEPES [1 M, *Thermo Fisher Scientific*]). Next, 1.5 mL fresh trypsin solution was added and the tube was incubated for 20 min at 37 °C and shaken every 5 min. Next, trypsin was removed and cells were washed twice with 10 mL serum medium (DMEM + 5% [v/v] FCS). Cells were left in 1.5 mL serum medium and triturated with a fire-polished Pasteur pipette until the suspension was homogenous. After centrifugation (80 x *g*, 5 min), the cell pellet was resuspended in 5 mL neuron growth medium (Neurobasal™ Plus Medium [*Thermo Fisher Scientific*] supplemented with 2% [v/v] B-27™ Plus Supplement [*Thermo Fisher Scientific*], 0.25% [v/v] Glutamax [*Thermo Fisher Scientific*], and 100 U/mL penicillin/streptomycin [*Thermo Fisher Scientific*]), cells were counted and 1.5 x 10^6 cells were plated in the previously coated 60 mm plates. Per biological replicate, cells from two embryos were combined and seeded out on three plates to obtain different conditions (DMSO, only probe, competitor plus probe). Medium was partially exchanged (50:50) on day 2–3 and again after 7 days. Neurons were cultured for 14 days at 37 °C in a 5% CO_2 atmosphere before labelling.

3.2.2 Intact protein mass spectrometry

DJ-1 was kindly provided by Dr. Jonas Drechsel (purified as described previously[271]). Chemical probes (500 µM) were added to DJ-1 (5 µM) in PBS from DMSO stocks and samples were incubated at room temperature with mild shaking and protection from light for 15 h. HRMS analysis of 1 µL protein solution was carried out on a LTQ FT Ultra™ mass spectrometer (*Thermo Scientific*) equipped with an electro spray ionisation (ESI) source operated in positive

ionisation mode coupled to a Dionex Ultimate 3000 HPLC system (*Thermo Scientific*). Samples were loaded on a desalting column, eluted with an acetonitrile gradient, and transferred to the MS unit. Protein spectra were deconvoluted using the Thermo Xcalibur software (*Thermo Scientific*).

3.2.3 Proteomics methods

3.2.3.1 Preparative scale labelling in Hek293 cells

Hek293 cells were cultured in Dulbecco´s Modified Eagle´s Medium (DMEM high glucose, *Sigma*) supplemented with 2 mM L-glutamine and 10% (v/v) heat-inactivated FCS. For labelling, 10 x 10^6 cells were seeded to achieve 60–80% confluence on the following day. Competitors were added to 450–1500 µM (**DA**) or 150 µM (all other catechols) and 0.5% (v/v) DMSO in 10 mL FCS-free growth medium, swirled gently, and incubated 1 h, 37 °C, 5% CO_2. The probe was added to 15 µM and 0.1% (v/v) DMSO, dishes were swirled, and the cells were incubated 1 h, 37 °C, 5% CO_2. After cell treatment, the medium was aspirated and cells were scraped off in 10 mL PBS (on ice), transferred to tubes, washed 1–2 x with 1 mL cold PBS (500 x g, 5 min, 4 °C), flash-frozen, and stored at -80 °C until lysis. Frozen cell pellets were resuspended in 1 mL lysis buffer (1% [v/v] NP-40, 1% [w/v] deoxycholic acid in PBS) + EDTA-free protease inhibitor cocktail (*Roche*) and SDS was added to 0.2% (w/v) (20 µL 10% [w/v] SDS/PBS). Cells were sonicated (2 x 15 s, 60% intensity) to shear nucleic acids, insoluble debris was pelleted (21,000 x g, 15 min, 4 °C), and the supernatant transferred to a new tube. For competition experiments (except **DA**), proteins were precipitated in acetone (≥ 4 x volumes) at -20 °C, washed twice with ice-cold methanol, air-dried, and resuspended in 0.8% (w/v) SDS/PBS as some catechols interfered with the protein concentration determination. Protein concentration was adjusted to 450 µg in 1 mL lysis buffer + 0.2% (w/v) SDS or to 500 µg in 500 µL 0.8% (w/v) SDS/PBS.

3.2.3.2 Analytical scale labelling in Hek293

Analytical gel-based labelling was performed as MS-based labelling seeding 0.5–0.75 x 10^6 cells in 3 mL medium in 6-well dishes. Competitors and probes were added from 200-fold concentrated stocks as indicated and labelling was performed in 1 mL medium. Cells were harvested in 1 mL PBS and lysed in 100 µL lysis buffer + protease inhibitor.

3.2.3.3 Preparative and analytical scale labelling in primary mouse neurons

The growth medium was removed and replaced with 2.5 mL fresh medium containing no antibiotics. **DA** was added to 1500 µM and 0.5% (v/v) DMSO and incubated for 1 h at 37 °C, 5% CO_2. The probe **DA-P3** was added to 15 µM and 0.1% (v/v) DMSO and incubated for 1 h at 37 °C, 5% CO_2. The medium was aspirated, cells were washed with 4 mL PBS and harvested by scraping in 300 µL lysis buffer (1% [v/v] NP-40, 1% [w/v] deoxycholic acid) + protease inhibitor. The cell suspension was transferred to LoBind tubes, SDS was added to 0.2% (w/v) (6 µL 10% [w/v] SDS/PBS) and frozen at -80 °C until lysis. Protein concentration was adjusted to 200 µg in 326 µL lysis buffer + 1% (w/v) SDS.

3.2.3.4 Labelling in heat-denatured lysate

Hek293 cells were grown to 95% confluence in a 15 cm dish, the medium was replaced by cold PBS (10 mL), and cells were scraped off the dish (on ice). Next, cells were pelleted (500 x *g*, 5 min, 4 °C), transferred into a microcentrifuge tube, and washed 2 x with PBS (1 mL). The cell pellet was shock-frozen and stored at -80 °C. Cells were resuspended in cold PBS + protease inhibitor (1 mL) and lysed by sonication (6 x 10 s, 75% intensity, Sonopuls HD 2070 ultrasonic rod, *Bandelin electronic GmbH*) on ice with cooling breaks. The lysate was clarified (20,000 x *g*, 45 min, 4 °C), the protein concentration adjusted to 0.675 mg/mL, and detergents added to 0.5% NP-40 (v/v) and 0.5% (w/v) deoxycholic acid. Lysate (500 µL) was heat-inactivated at 95 °C for 10 min with mild shaking. **DA-P3** was added to 100 µL lysate to 15 µM (1% [v/v] DMSO) and incubated 1 h, r.t., 400 rpm.

3.2.3.5 CuAAC

CuAAC was performed as in the **EPI** project (see section II-3.2.3.4 and II-3.2.3.5) except with biotin-PEG_3-azide (10 mM stock in DMSO, *Jena Bioscience*) for preparative scale. For analytical scale, samples were boiled (90 °C, 3 min, 400 rpm) and centrifuged (16,249 x *g*, 3 min) before SDS-PAGE.

3.2.3.6 SDS-PAGE

See section II-3.2.3.8.

3.2.3.7 Enrichment, alkylation, and digest for target identification

Protein LoBind microcentrifuge tubes and MS-grade reagents were used throughout MS sample preparation. Protein samples were centrifuged to remove particulates, added to 50 µL avidin slurry (*Sigma*) (pre-washed 3 x with 0.4% (w/v) SDS/PBS [400 x *g*, 3 min]), and incubated 1 h at room temperature under constant rotation. Samples were centrifuged, the supernatant discarded, and the beads were washed 3 x with 1 mL 0.4% (w/v) SDS/PBS, 2 x with 1 mL 6 M urea/ddH_2O, and 3 x with 1 mL PBS. Beads were resuspended in 200 µL MS denaturation buffer (7 M urea, 2 M thiourea, 20 mM HEPES, pH 7.5) and reduced with 5 mM TCEP for 1 h at 37 °C with shaking. Next, thiols were alkylated with 10 mM iodoacetamide for 30 min at 25 °C with shaking and alkylation was quenched with 10 mM DTT for 30 min at 25 °C with shaking. Proteins were digested with 0.5 µg LysC (from 0.5 µg/µL, MS-grade, *Wako*) for 2 h at 25 °C with shaking. Samples were diluted by addition of 800 µL 50 mM TEAB and proteins were digested with 0.75 µg trypsin (from 0.5 µg/µL in 50 mM acetic acid, *Promega*) for 16 h at 37 °C with vigorous shaking. The digest was stopped by addition of formic acid to 3% (v/v) (pH 2–3), the beads pelleted (16,249 x *g*, 3 min, r.t.), and the supernatant desalted. For desalting, 50 mg SepPak C18 columns (*Waters*) were washed with 1 x 1 mL acetonitrile and 1 x 1 mL elution buffer (80% [v/v] acetonitrile, 0.5% [v/v] formic acid/water) and then equilibrated with 3 x 1 mL 0.1% (v/v) TFA. Samples were loaded onto the columns and desalted with 3 x 1 mL 0.1% (v/v) TFA and 1 x 0.5 mL 0.5% (v/v) formic acid. Peptides were eluted into 2 mL LoBind tubes with 3 x 250 µL elution buffer and dried in a speed vac. Dried peptides were stored at -80 °C until LC-MS/MS analysis.

3.2.3.8 Chemoproteomics experiments with isoDTB tags

Hek293 cells were treated with **DA-P3** (15 µM) *in situ* and lysed as for target identification experiments. Protein concentration was adjusted to 1 µg/µL in 1400 µL lysis buffer (1% [v/v] NP-40, 1% [w/v] deoxycholic acid/PBS) + 0.8% (w/v) SDS. CuAAC to isoDTB tags[32] and MS sample preparation was carried out as in the **EPI** project (see section II-3.2.3.10).

3.2.3.9 Peptide reconstitution (all proteomics experiments)

See section II-3.2.3.13.

3.2.3.10 LC-MS/MS measurements

Samples were measured on a Q Exactive Plus (see section II-3.2.3.14).

3.2.3.11 Analysis of MS data from target identification experiments

MS data were analysed using MaxQuant[166-167] version 1.6.5.0 and peptides were searched against the UniProt database for *Homo sapiens* (taxon identifier 9606, downloaded on 29.01.2019) where Titin and all proteins containing U, O, or X were removed or the UniProt database for *Mus musculus* (taxon identifier 10090, downloaded on 24.06.2022). Cysteine carbamidomethylation was set as fixed modification and methionine oxidation and N-terminal acetylation as variable modifications. Trypsin/P was set as proteolytic enzyme with a maximum of two allowed missed cleavages. LFQ mode[96] was performed with a minimum ratio count of 1. Protein quantification was performed with the minimal ratio count set to 1 and the match between runs (0.7 min match and 20 min alignment time window) and second peptide identification options were activated. All other parameters were used as pre-set in the software. LFQ intensities were further processed with Perseus[168] version 1.6.1.1. Peptides of the categories “only identified by site”, “reverse”, or “potential contaminant” were removed and LFQ intensities were $\log_2$-transformed. Data were filtered to retain only protein groups identified in at least 3/3 valid values in human cell experiments and 3/4 valid values (mouse cells) in at least one group. A two-sided two-sample Student´s *t*-test with permutation-based FDR (FDR 0.05) was performed and the significance cut-off was set at *p*-value = 0.01 ($-\log_{10}$(*p*-value) = 2) and an enrichment factor of 4 ($\log_2(x) = 2$).

3.2.3.12 Analysis of isoDTB data

IsoDTB data were analysed as in the **EPI** project (see section II-3.2.3.16). In the FASTA file (*Homo sapiens*, taxon identifier 9606, downloaded on 29.01.2019 Titin and all proteins containing U, O, or X were removed and the reverse sequences were added manually. Mass offsets were set as 754.4120 or 760.4206; Labelling based quant masses were set as 754.4120 or 760.4206; Closed Search in MSFragger was performed with variable modifications set as 754.4120 or 760.4206 on Cys; Labelling based quant masses were set as 754.4120 or 760.4206.

3.2.3.13 GO term enrichment analyses

GO term enrichment analysis was performed using the GOrilla tool.[223-224] Gene names of proteins enriched above the cut offs ($-\log_{10}(p\text{-value}) \geq 2$; $\log_2(\text{enrichment}) \geq 2$) were used as target set (unranked) and compared against all proteins detected (after filtering). The *p*-value threshold was set to 10^{-3}–10^{-5} as indicated.

3.2.3.14 Heat maps

Heat maps were generated with Origin 2021 (*OriginLab*) with hierarchical clustering using group average as cluster method and Euclidian distance.

IV References

1. Fonović, M.; Bogyo, M., Activity-based probes as a tool for functional proteomic analysis of proteases. *Expert Rev Proteomics* **2008,** *5* (5), 721-730.

2. Niphakis, M. J.; Cravatt, B. F., Enzyme inhibitor discovery by activity-based protein profiling. *Annu Rev Biochem* **2014,** *83*, 341-377.

3. Cravatt, B. F.; Wright, A. T.; Kozarich, J. W., Activity-based protein profiling: from enzyme chemistry to proteomic chemistry. *Annu Rev Biochem* **2008,** *77*, 383-414.

4. Wright, M. H.; Sieber, S. A., Chemical proteomics approaches for identifying the cellular targets of natural products. *Nat Prod Rep* **2016,** *33* (5), 681-708.

5. Conway, L. P.; Li, W.; Parker, C. G., Chemoproteomic-enabled phenotypic screening. *Cell Chem Biol* **2021,** *28* (3), 371-393.

6. Fux, A.; Pfanzelt, M.; Kirsch, V. C.; Hoegl, A.; Sieber, S. A., Customizing functionalized cofactor mimics to study the human pyridoxal 5'-phosphate-binding proteome. *Cell Chem Biol* **2019,** *26* (10), 1461-1468.

7. Hoegl, A.; Nodwell, M. B.; Kirsch, V. C.; Bach, N. C.; Pfanzelt, M.; Stahl, M.; Schneider, S.; Sieber, S. A., Mining the cellular inventory of pyridoxal phosphate-dependent enzymes with functionalized cofactor mimics. *Nat Chem* **2018,** *10* (12), 1234-1245.

8. Pfanzelt, M.; Maher, T. E.; Absmeier, R. M.; Schwarz, M.; Sieber, S. A., Tailored pyridoxal probes unravel novel cofactor-dependent targets and antibiotic hits in critical bacterial pathogens. *Angew Chem Int Ed* **2022,** *61* (24), e202117724.

9. Wilkinson, I. V. L.; Pfanzelt, M.; Sieber, S. A., Functionalised cofactor mimics for interactome discovery and beyond. *Angew Chem Int Ed* **2022,** *61* (29), e202201136.

10. Thinon, E.; Serwa, R. A.; Broncel, M.; Brannigan, J. A.; Brassat, U.; Wright, M. H.; Heal, W. P.; Wilkinson, A. J.; Mann, D. J.; Tate, E. W., Global profiling of co- and post-translationally *N*-myristoylated proteomes in human cells. *Nat Commun* **2014,** *5* (1), 4919.

11. Wright, M. H.; Fetzer, C.; Sieber, S. A., Chemical Probes Unravel an Antimicrobial Defense Response Triggered by Binding of the Human Opioid Dynorphin to a Bacterial Sensor Kinase. *Journal of the American Chemical Society* **2017,** *139* (17), 6152-6159.

12. Kielkowski, P.; Buchsbaum, I. Y.; Becker, T.; Bach, K.; Cappello, S.; Sieber, S. A., A pronucleotide probe for live-cell Imaging of protein AMPylation. *ChemBioChem* **2020,** *21* (9), 1285-1287.

13. Kielkowski, P.; Buchsbaum, I. Y.; Kirsch, V. C.; Bach, N. C.; Drukker, M.; Cappello, S.; Sieber, S. A., FICD activity and AMPylation remodelling modulate human neurogenesis. *Nat Commun* **2020,** *11* (1), 517.

14. Rauh, T.; Brameyer, S.; Kielkowski, P.; Jung, K.; Sieber, S. A., MS-based *in situ* proteomics reveals AMPylation of host proteins during bacterial infection. *ACS Infect Dis* **2020,** *6* (12), 3277-3289.

15. Allihn, P. W. A.; Hackl, M. W.; Ludwig, C.; Hacker, S. M.; Sieber, S. A., A tailored phosphoaspartate probe unravels CprR as a response regulator in *Pseudomonas aeruginosa* interkingdom signaling. *Chem Sci* **2021,** *12* (13), 4763-4770.

16. Weigert Muñoz, A.; Hoyer, E.; Schumacher, K.; Grognot, M.; Taute, K. M.; Hacker, S. M.; Sieber, S. A.; Jung, K., Eukaryotic catecholamine hormones influence the chemotactic control of *Vibrio campbellii* by binding to the coupling protein CheW. *Proc Natl Acad Sci USA* **2022,** *119* (10), e2118227119.

17. Wright, M. H.; Tao, Y.; Drechsel, J.; Krysiak, J.; Chamni, S.; Weigert-Munoz, A.; Harvey, N. L.; Romo, D.; Sieber, S. A., Quantitative chemoproteomic profiling reveals multiple target interactions of spongiolactone derivatives in leukemia cells. *ChemComm* **2017,** *53* (95), 12818-12821.

18. Zhao, W.; Cross, A. R.; Crowe-McAuliffe, C.; Weigert-Munoz, A.; Csatary, E. E.; Solinski, A. E.; Krysiak, J.; Goldberg, J. B.; Wilson, D. N.; Medina, E.; Wuest, W. M.; Sieber, S. A., The natural product elegaphenone potentiates antibiotic effects against *Pseudomonas aeruginosa*. *Angew Chem Int Ed* **2019,** *58* (25), 8581-8584.

19. Lakemeyer, M.; Zhao, W.; Mandl, F. A.; Hammann, P.; Sieber, S. A., Thinking outside the box–novel antibacterials to tackle the resistance crisis. *Angew Chem Int Ed* **2018,** *57* (44), 14440-14475.

20. Gleissner, C. M. L.; Pyka, C. L.; Heydenreuter, W.; Gronauer, T. F.; Atzberger, C.; Korotkov, V. S.; Cheng, W.; Hacker, S. M.; Vollmar, A. M.; Braig, S.; Sieber, S. A., Neocarzilin A is a potent inhibitor of cancer cell motility targeting VAT-1 controlled pathways. *ACS Cent Sci* **2019,** *5* (7), 1170-1178.

21. Le, P.; Kunold, E.; Macsics, R.; Rox, K.; Jennings, M. C.; Ugur, I.; Reinecke, M.; Chaves-Moreno, D.; Hackl, M. W.; Fetzer, C.; Mandl, F. A. M.; Lehmann, J.; Korotkov, V. S.; Hacker, S. M.; Kuster, B.; Antes, I.; Pieper, D. H.; Rohde, M.; Wuest, W. M.; Medina, E.; Sieber, S. A., Repurposing human kinase inhibitors to create an antibiotic active against drug-resistant *Staphylococcus aureus*, persisters and biofilms. *Nat Chem* **2020,** *12* (2), 145-158.

22. Murale, D. P.; Hong, S. C.; Haque, M. M.; Lee, J.-S., Photo-affinity labeling (PAL) in chemical proteomics: a handy tool to investigate protein-protein interactions (PPIs). *Proteome Sci* **2017,** *15* (1), 14.

23. Kleiner, P.; Heydenreuter, W.; Stahl, M.; Korotkov, V. S.; Sieber, S. A., A whole proteome inventory of background photocrosslinker binding. *Angew Chem Int Ed* **2017,** *56* (5), 1396-1401.

24. Kolb, H. C.; Finn, M. G.; Sharpless, K. B., Click chemistry: diverse chemical function from a few good reactions. *Angew Chem Int Ed* **2001,** *40* (11), 2004-2021.

25. Huisgen, R.; Szeimies, G.; Möbius, L., 1,.3-Dipolare Cycloadditionen, XXXII. Kinetik der Additionen organischer Azide an CC-Mehrfachbindungen. *Chem Ber* **1967,** *100* (8), 2494-2507.

26. Rostovtsev, V. V.; Green, L. G.; Fokin, V. V.; Sharpless, K. B., A stepwise Huisgen cycloaddition process: copper(I)-catalyzed regioselective "ligation" of azides and terminal alkynes. *Angew Chem Int Ed* **2002,** *41* (14), 2596-2599.

27. Tornøe, C. W.; Christensen, C.; Meldal, M., Peptidotriazoles on solid phase: [1,2,3]-triazoles by regiospecific copper(I)-catalyzed 1,3-dipolar cycloadditions of terminal alkynes to azides. *J Org Chem* **2002,** *67* (9), 3057-3064.

28. Sletten, E. M.; Bertozzi, C. R., From mechanism to mouse: a tale of two bioorthogonal reactions. *Acc Chem Res* **2011,** *44* (9), 666-676.

29. Li, Z.; Hao, P.; Li, L.; Tan, C. Y.; Cheng, X.; Chen, G. Y.; Sze, S. K.; Shen, H. M.; Yao, S. Q., Design and synthesis of minimalist terminal alkyne-containing diazirine photo-crosslinkers and their incorporation into kinase inhibitors for cell- and tissue-based proteome profiling. *Angew Chem Int Ed* **2013,** *52* (33), 8551-8556.

30. Dubinsky, L.; Krom, B. P.; Meijler, M. M., Diazirine based photoaffinity labeling. *Bioorg Med Chem* **2012,** *20* (2), 554-570.

31. Zanon, P. R. A.; Yu, F.; Musacchio, P.; Lewald, L.; Zollo, M.; Krauskopf, K.; Mrdović, D.; Raunft, P.; Maher, T. E.; Cigler, M.; Chang, C.; Lang, K.; Toste, F. D.; Nesvizhskii, A. I.; Hacker, S. M., Profiling the proteome-wide selectivity of diverse electrophiles. *ChemRxiv. Cambridge: Cambridge Open Engage; This content is a preprint and has not been peer-reviewed.* **2021**.

32. Zanon, P. R. A.; Lewald, L.; Hacker, S. M., Isotopically labeled desthiobiotin azide (isoDTB) tags enable global profiling of the bacterial cysteinome. *Angew Chem Int Ed* **2020,** *59* (7), 2829-2836.

33. Weerapana, E.; Wang, C.; Simon, G. M.; Richter, F.; Khare, S.; Dillon, M. B.; Bachovchin, D. A.; Mowen, K.; Baker, D.; Cravatt, B. F., Quantitative reactivity profiling predicts functional cysteines in proteomes. *Nature* **2010,** *468* (7325), 790-795.

34. Altenbach, C.; Kusnetzow, A. K.; Ernst, O. P.; Hofmann, K. P.; Hubbell, W. L., High-resolution distance mapping in rhodopsin reveals the pattern of helix movement due to activation. *Proc Natl Acad Sci USA* **2008,** *105* (21), 7439-7444.

35. Vardanyan, R.; Hruby, V., Chapter 12 - Adrenoblockers. In *Synthesis of Best-Seller Drugs*, Vardanyan, R.; Hruby, V., Eds. Academic Press: Boston, 2016; pp 201-214.

36. Purves, D.; Augustine, G. J.; Fitzpatrick, D.; Hall, W. C.; Lamantia, A.-S.; McNamara, J. O.; Williams, S. M., *Neuroscience*. 3 ed.; Sinauer Associates, Inc.: Sunderland, MA 01375 U.S.A., 2004.

37. Kleinau, G.; Pratzka, J.; Nürnberg, D.; Grüters, A.; Führer-Sakel, D.; Krude, H.; Köhrle, J.; Schöneberg, T.; Biebermann, H., Differential modulation of beta-adrenergic receptor signaling by trace amine-associated receptor 1 agonists. *PloS One* **2011,** *6* (10), e27073.

38. Koh, A. H. W.; Chess-Williams, R.; Lohning, A. E., Differential mechanisms of action of the trace amines octopamine, synephrine and tyramine on the porcine coronary and mesenteric artery. *Sci Rep* **2019,** *9* (1), 10925.

39. Khan, A.; Singh, P.; Srivastava, A., Synthesis, nature and utility of universal iron chelator – Siderophore: A review. *Microbiol Res* **2018,** *212-213*, 103-111.

40. O'Brien, I. G.; Gibson, F., The structure of enterochelin and related 2,3-dihydroxy-*N*-benzoyne conjugates from *Eschericha coli*. *Biochim Biophys Acta Gen Subj* **1970,** *215* (2), 393-402.

41. Pollack, J. R.; Neilands, J. B., Enterobactin, an iron transport compound from *Salmonella* Typhimurium. *Biochem Biophys Res Commun* **1970,** *38* (5), 989-992.

42. Müller, S. I.; Valdebenito, M.; Hantke, K., Salmochelin, the long-overlooked catecholate siderophore of *Salmonella*. *Biometals* **2009,** *22* (4), 691-695.

43. Bluhm, M. E.; Kim, S. S.; Dertz, E. A.; Raymond, K. N., Corynebactin and enterobactin: related siderophores of opposite chirality. *J Am Chem Soc* **2002,** *124* (11), 2436-2437.

44. May, J. J.; Wendrich, T. M.; Marahiel, M. A., The dhb operon of *Bacillus subtilis* encodes the biosynthetic template for the catecholic siderophore 2,3-dihydroxybenzoate-glycine-threonine trimeric ester bacillibactin. *J Biol Chem* **2001,** *276* (10), 7209-7217.

45. Griffiths, G. L.; Sigel, S. P.; Payne, S. M.; Neilands, J. B., Vibriobactin, a siderophore from *Vibrio cholerae*. *J Biol Chem* **1984,** *259* (1), 383-385.

46. Duhme, A.-K.; Hider, R. C.; Khodr, H., Spectrophotometric competition study between molybdate and Fe(III) hydroxide on *N*,*N*′-bis(2,3-dihydroxybenzoyl)-l-lysine, a naturally occurring siderophore synthesized by *Azotobacter vinelandii*. *Biometals* **1996,** *9* (3), 245-248.

47. Taraz, K.; Ehlert, G.; Geisen, K.; Budzikiewicz, H.; Korth, H.; Pulverer, G., Protochelin, ein Catecholat-Siderophor aus einem Bakterium (DMS Nr. 5746) [1] / Protocheline — a catecholate siderophore from a bacterium (DMS No. 5746) [1]. *Z Naturforsch B* **1990,** *45* (9), 1327-1332.

48. Page, W. J.; Tigerstrom, M. V., Aminochelin, a catecholamine siderophore produced by *Azotobacter vinelandii*. *Microbiology* **1988,** *134* (2), 453-460.

49. Ito, T.; Neilands, J. B., Products of "low-iron fermentation" with *Bacillus subilis*: isolation, characterization and synthesis of 2,3-dihydroxybenzoylglycine. *J Am Chem Soc* **1958,** *80* (17), 4645-4647.

50. Abdul-Mutakabbir, J. C.; Alosaimy, S.; Morrisette, T.; Kebriaei, R.; Rybak, M. J., Cefiderocol: a novel siderophore cephalosporin against multidrug-resistant Gram-negative pathogens. *Pharmacotherapy* **2020,** *40* (12), 1228-1247.

51. Zhu, W.; Winter, M. G.; Spiga, L.; Hughes, E. R.; Chanin, R.; Mulgaonkar, A.; Pennington, J.; Maas, M.; Behrendt, C. L.; Kim, J.; Sun, X.; Beiting, D. P.; Hooper, L. V.; Winter, S. E., Xenosiderophore utilization promotes *Bacteroides thetaiotaomicron* resilience during colitis. *Cell Host Microbe* **2020,** *27* (3), 376-388.

52. Luscher, A.; Gasser, V.; Bumann, D.; Mislin, G. L. A.; Schalk, I. J.; Köhler, T., Plant-derived catechols are substrates of TonB-dependent transporters and sensitize *Pseudomonas aeruginosa* to siderophore-drug conjugates. *mBio* **2022,** *13* (4), e01498-22.

53. Sandrini, S. M.; Shergill, R.; Woodward, J.; Muralikuttan, R.; Haigh, R. D.; Lyte, M.; Freestone, P. P., Elucidation of the mechanism by which catecholamine stress hormones liberate iron from the innate immune defense proteins transferrin and lactoferrin. *J Bacteriol* **2010,** *192* (2), 587-594.

54. Perraud, Q.; Kuhn, L.; Fritsch, S.; Graulier, G.; Gasser, V.; Normant, V.; Hammann, P.; Schalk, I. J., Opportunistic use of catecholamine neurotransmitters as siderophores to access iron by *Pseudomonas aeruginosa*. *Environ Microbiol* **2022,** *24* (2), 878-893.

55. Marchetti, M.; De Bei, O.; Bettati, S.; Campanini, B.; Kovachka, S.; Gianquinto, E.; Spyrakis, F.; Ronda, L., Iron metabolism at the interface between host and pathogen: from nutritional immunity to antibacterial development. *Int J Mol Sci* **2020,** *21* (6), 2145-2188.

56. Carrano, C. J.; Raymond, K. N., Ferric ion sequestering agents. 2. Kinetics and mechanism of iron removal from transferrin by enterobactin and synthetic tricatechols. *J Am Chem Soc* **1979,** *101* (18), 5401-5404.

57. Sandrini, S.; Aldriwesh, M.; Alruways, M.; Freestone, P., Microbial endocrinology: host-bacteria communication within the gut microbiome. *J Endocrinol* **2015,** *225* (2), R21-R34.

58. Kendall, M. M.; Sperandio, V., What a dinner party! Mechanisms and functions of interkingdom signaling in host-pathogen associations. *mBio* **2016,** *7* (2), e01748-15.

59. Wu, L. R.; Zaborina, O.; Zaborin, A.; Chang, E. B.; Musch, M.; Holbrook, C.; Turner, J. R.; Alverdy, J. C., Surgical injury and metabolic stress enhance the virulence of the human opportunistic pathogen *Pseudomonas aeruginosa*. *Surg Infect (Larchmt)* **2005,** *6* (2), 185-195.

60. Clarke, M. B.; Hughes, D. T.; Zhu, C.; Boedeker, E. C.; Sperandio, V., The QseC sensor kinase: A bacterial adrenergic receptor. *Proc Natl Acad Sci USA* **2006,** *103* (27), 10420-10425.

61. Reading, N. C.; Rasko, D. A.; Torres, A. G.; Sperandio, V., The two-component system QseEF and the membrane protein QseG link adrenergic and stress sensing to bacterial pathogenesis. *Proc Natl Acad Sci USA* **2009,** *106* (14), 5889-5894.

62. Karavolos, M. H.; Winzer, K.; Williams, P.; Khan, C. M. A., Pathogen espionage: multiple bacterial adrenergic sensors eavesdrop on host communication systems. *Mol Microbiol* **2013,** *87* (3), 455-465.

63. Freestone, P. P.; Sandrini, S. M.; Haigh, R. D.; Lyte, M., Microbial endocrinology: how stress influences susceptibility to infection. *Trends Microbiol* **2008,** *16* (2), 55-64.

64. Lyte, M.; Vulchanova, L.; Brown, D. R., Stress at the intestinal surface: catecholamines and mucosa-bacteria interactions. *Cell Tissue Res* **2011,** *343* (1), 23-32.

65. Jacob-Dubuisson, F.; Mechaly, A.; Betton, J.-M.; Antoine, R., Structural insights into the signalling mechanisms of two-component systems. *Nat Rev Microbiol* **2018,** *16* (10), 585-593.

66. Capra, E. J.; Laub, M. T., Evolution of two-component signal transduction systems. *Annu Rev Microbiol* **2012,** *66*, 325-347.

67. Rasko, D. A.; Moreira, C. G.; Li, D. R.; Reading, N. C.; Ritchie, J. M.; Waldor, M. K.; Williams, N.; Taussig, R.; Wei, S.; Roth, M.; Hughes, D. T.; Huntley, J. F.; Fina, M. W.; Falck, J. R.; Sperandio, V., Targeting QseC signaling and virulence for antibiotic development. *Science* **2008,** *321* (5892), 1078-1080.

68. Sperandio, V.; Torres, A. G.; Jarvis, B.; Nataro, J. P.; Kaper, J. B., Bacteria–host communication: The language of hormones. *Proc Natl Acad Sci USA* **2003,** *100* (15), 8951-8956.

69. Kim, C. S.; Gatsios, A.; Cuesta, S.; Lam, Y. C.; Wei, Z.; Chen, H.; Russell, R. M.; Shine, E. E.; Wang, R.; Wyche, T. P.; Piizzi, G.; Flavell, R. A.; Palm, N. W.; Sperandio, V.; Crawford, J. M., Characterization of autoinducer-3 structure and biosynthesis in *E. coli*. *ACS Cent Sci* **2020,** *6* (2), 197-206.

70. Halang, P.; Toulouse, C.; Geißel, B.; Michel, B.; Flauger, B.; Müller, M.; Voegele, R. T.; Stefanski, V.; Steuber, J., Response of *Vibrio cholerae* to the catecholamine hormones epinephrine and norepinephrine. *J Bacteriol* **2015,** *197* (24), 3769-3778.

71. Yang, Q.; Anh, N. D. Q.; Bossier, P.; Defoirdt, T., Norepinephrine and dopamine increase motility, biofilm formation, and virulence of *Vibrio harveyi*. *Front Microbiol* **2014,** *5* (584).

72. Moreira, C. G.; Weinshenker, D.; Sperandio, V., QseC mediates *Salmonella enterica* serovar typhimurium virulence *in vitro* and *in vivo*. *Infect Immun* **2010,** *78* (3), 914-926.

73. Bearson, B. L.; Bearson, S. M., The role of the QseC quorum-sensing sensor kinase in colonization and norepinephrine-enhanced motility of *Salmonella enterica* serovar Typhimurium. *Microb Pathog* **2008,** *44* (4), 271-278.

74. Bearson, B. L.; Bearson, S. M.; Lee, I. S.; Brunelle, B. W., The *Salmonella enterica* serovar Typhimurium QseB response regulator negatively regulates bacterial motility and swine colonization in the absence of the QseC sensor kinase. *Microb Pathog* **2010,** *48* (6), 214-219.

75. Hamed, A.; Pullinger, G.; Stevens, M.; Farveen, F.; Freestone, P., Characterisation of the *E. coli* and *Salmonella* qseC and qseE mutants reveals a metabolic rather than adrenergic receptor role. *FEMS Microbiol Lett* **2022,** *369* (1), 1-12.

76. Merighi, M.; Septer, A. N.; Carroll-Portillo, A.; Bhatiya, A.; Porwollik, S.; McClelland, M.; Gunn, J. S., Genome-wide analysis of the PreA/PreB (QseB/QseC) regulon of *Salmonella enterica* serovar Typhimurium. *BMC Microbiol* **2009,** *9*, 42.

77. Pullinger, G. D.; Carnell, S. C.; Sharaff, F. F.; van Diemen, P. M.; Dziva, F.; Morgan, E.; Lyte, M.; Freestone, P. P. E.; Stevens, M. P., Norepinephrine augments *Salmonella enterica*-induced enteritis in a manner associated with increased net replication but independent of the putative adrenergic sensor kinases QseC and QseE. *Infect Immun* **2010,** *78* (1), 372-380.

78. Bansal, T.; Englert, D.; Lee, J.; Hegde, M.; Wood, T. K.; Jayaraman, A., Differential effects of epinephrine, norepinephrine, and indole on *Escherichia coli* O157:H7 chemotaxis, colonization, and gene expression. *Infect Immun* **2007,** *75* (9), 4597-4607.

79. Sule, N.; Pasupuleti, S.; Kohli, N.; Menon, R.; Dangott, L. J.; Manson, M. D.; Jayaraman, A., The norepinephrine metabolite 3,4-dihydroxymandelic acid is produced by the commensal microbiota and promotes chemotaxis and virulence gene expression in enterohemorrhagic *Escherichia coli*. *Infect Immun* **2017,** *85* (10), e00431-48.

80. Pasupuleti, S.; Sule, N.; Cohn, W. B.; MacKenzie, D. S.; Jayaraman, A.; Manson, M. D., Chemotaxis of *Escherichia coli* to norepinephrine (NE) requires conversion of NE to 3,4-dihydroxymandelic acid. *J Bacteriol* **2014,** *196* (23), 3992-4000.

81. Rivera-Chávez, F.; Lopez, C. A.; Zhang, L. F.; García-Pastor, L.; Chávez-Arroyo, A.; Lokken, K. L.; Tsolis, R. M.; Winter, S. E.; Bäumler, A. J., Energy taxis toward host-derived nitrate supports a *Salmonella* pathogenicity island 1-independent mechanism of invasion. *mBio* **2016,** *7* (4), e00960-16.

82. Stecher, B.; Hapfelmeier, S.; Müller, C.; Kremer, M.; Stallmach, T.; Hardt, W. D., Flagella and chemotaxis are required for efficient induction of *Salmonella enterica* serovar Typhimurium colitis in streptomycin-pretreated mice. *Infect Immun* **2004,** *72* (7), 4138-4150.

83. Butler, S. M.; Camilli, A., Both chemotaxis and net motility greatly influence the infectivity of *Vibrio cholerae*. *Proc Natl Acad Sci USA* **2004,** *101* (14), 5018-5023.

84. Bi, S.; Sourjik, V., Stimulus sensing and signal processing in bacterial chemotaxis. *Curr Opin Microbiol* **2018,** *45*, 22-29.

85. Lopes, J. G.; Sourjik, V., Chemotaxis of *Escherichia coli* to major hormones and polyamines present in human gut. *ISME J* **2018,** *12* (11), 2736-2747.

86. Takase, H.; Nitanai, H.; Hoshino, K.; Otani, T., Requirement of the *Pseudomonas aeruginosa* tonB gene for high-affinity iron acquisition and infection. *Infect Immun* **2000,** *68* (8), 4498-4504.

87. Sandrini, S.; Masania, R.; Zia, F.; Haigh, R.; Freestone, P., Role of porin proteins in acquisition of transferrin iron by enteropathogens. *Microbiology* **2013,** *159* (Pt 12), 2639-2650.

88. Jimenez, P. N.; Koch, G.; Papaioannou, E.; Wahjudi, M.; Krzeslak, J.; Coenye, T.; Cool, R. H.; Quax, W. J., Role of PvdQ in *Pseudomonas aeruginosa* virulence under iron-limiting conditions. *Microbiology* **2010,** *156* (1), 49-59.

89. Lin, B.; Wang, Z.; Malanoski, A. P.; O'Grady, E. A.; Wimpee, C. F.; Vuddhakul, V.; Alves Jr, N.; Thompson, F. L.; Gomez-Gil, B.; Vora, G. J., Comparative genomic analyses identify the *Vibrio harveyi* genome sequenced strains BAA-1116 and HY01 as *Vibrio campbellii*. *Environ Microbiol Rep* **2010,** *2* (1), 81-89.

90. Austin, B.; Zhang, X.-H., *Vibrio harveyi*: a significant pathogen of marine vertebrates and invertebrates. *Lett Appl Microbiol* **2006,** *43* (2), 119-124.

91. Ottemann, K. M.; Miller, J. F., Roles for motility in bacterial-host interactions. *Mol Microbiol* **1997,** *24* (6), 1109-1117.

92. Bassler, B. L.; Wright, M.; Showalter, R. E.; Silverman, M. R., Intercellular signalling in *Vibrio harveyi*: sequence and function of genes regulating expression of luminescence. *Mol Microbiol* **1993,** *9* (4), 773-786.

93. Papenfort, K.; Bassler, B. L., Quorum sensing signal–response systems in Gram-negative bacteria. *Nat Rev Microbiol* **2016,** *14* (9), 576-588.

94. Anetzberger, C.; Reiger, M.; Fekete, A.; Schell, U.; Stambrau, N.; Plener, L.; Kopka, J.; Schmitt-Kopplin, P.; Hilbi, H.; Jung, K., Autoinducers act as biological timers in *Vibrio harveyi*. *PloS One* **2012,** *7* (10), e48310.

95. Weigert Muñoz, A.-M. Synthesis and evaluation of an epinephrine photoprobe for the identification of bacterial adrenergic targets. Master´s thesis, Technical University of Munich, München, 2018.

96. Cox, J.; Hein, M. Y.; Luber, C. A.; Paron, I.; Nagaraj, N.; Mann, M., Accurate proteome-wide label-free quantification by delayed normalization and maximal peptide ratio extraction, termed MaxLFQ. *Molecular & Cellular Proteomics* **2014,** *13* (9), 2513-2526.

97. A7MSY4. https://www.uniprot.org/uniprotkb/A7MSY4/entry (accessed 11.11.22).

98. A7MZS4. https://www.uniprot.org/uniprotkb/A7MZS4/entry (accessed 11.11.22).

99. VIBHAR_01404 https://www.genome.jp/dbget-bin/www_bget?vha:VIBHAR_01404 (accessed 11.11.22).

100. Kanehisa, M., Toward understanding the origin and evolution of cellular organisms. *Protein Science: a Publication of the Protein Society* **2019,** *28* (11), 1947-1951.

101. Kanehisa, M.; Furumichi, M.; Sato, Y.; Ishiguro-Watanabe, M.; Tanabe, M., KEGG: integrating viruses and cellular organisms. *Nucleic Acids Res* **2021,** *49* (D1), 545-551.

102. Kanehisa, M.; Goto, S., KEGG: kyoto encyclopedia of genes and genomes. *Nucleic Acids Res* **2000,** *28* (1), 27-30.

103. Hantke, K., Dihydroxybenzoylserine – a siderophore for *E. coli*. *FEMS Microbiol Lett* **1990,** *55* (1-2), 5-8.

104. Nikaido, H.; Rosenberg, E. Y., Cir and Fiu proteins in the outer membrane of *Escherichia coli* catalyze transport of monomeric catechols: study with beta-lactam antibiotics containing catechol and analogous groups. *J Bacteriol* **1990,** *172* (3), 1361-1367.

105. Altschul, S. F.; Madden, T. L.; Schäffer, A. A.; Zhang, J.; Zhang, Z.; Miller, W.; Lipman, D. J., Gapped BLAST and PSI-BLAST: a new generation of protein database search programs. *Nucleic Acids Res* **1997,** *25* (17), 3389-3402.

106. McRose, D. L.; Baars, O.; Seyedsayamdost, M. R.; Morel, F. M. M., Quorum sensing and iron regulate a two-for-one siderophore gene cluster in *Vibrio harveyi*. *Proc Natl Acad Sci USA* **2018,** *115* (29), 7581-7586.

107. A7MY64. https://www.uniprot.org/uniprotkb/A7MY64/entry (accessed 11.11.22).

108. UniProt: the universal protein knowledgebase in 2021. *Nucleic Acids Res* **2020,** *49* (D1), 480-489.

109. A7N6I6. https://www.uniprot.org/uniprotkb/A7N6I6/entry (accessed 11.11.22).

110. A7MY66. https://www.uniprot.org/uniprotkb/A7MY66/entry (accessed 11.11.22).

111. A7N1M5. https://www.uniprot.org/uniprotkb/A7N1M5/entry (accessed 11.11.22).

112. A7N283. https://www.uniprot.org/uniprotkb/A7N283/entry (accessed 11.11.22).

113. A7MS42. https://www.uniprot.org/uniprotkb/A7MS42/entry (accessed 11.11.22).

114. Huang, Z.; Pan, X.; Xu, N.; Guo, M., Bacterial chemotaxis coupling protein: Structure, function and diversity. *Microbiol Res* **2019,** *219*, 40-48.

115. A7MTV7. https://www.uniprot.org/uniprotkb/A7MTV7/entry (accessed 11.11.22).

116. A7MZ63. https://www.uniprot.org/uniprotkb/A7MZ63/entry (accessed 11.11.22).

117. A7N1L7. https://www.uniprot.org/uniprotkb/A7N1L7/entry (accessed 11.11.22).

118. A7MYT1. https://www.uniprot.org/uniprotkb/A7MYT1/entry (accessed 11.11.22).

119. A7MUD0. https://www.uniprot.org/uniprotkb/A7MUD0/entry (accessed 11.11.22).

120. A7MXS1. https://www.uniprot.org/uniprotkb/A7MXS1/entry (accessed 11.11.22).

121. A7N8F2. https://www.uniprot.org/uniprotkb/A7N8F2/entry (accessed 11.11.22).

122. A7N2H7. https://www.uniprot.org/uniprotkb/A7N2H7/entry (accessed 11.11.22).

123. Rhee, H. W.; Zou, P.; Udeshi, N. D.; Martell, J. D.; Mootha, V. K.; Carr, S. A.; Ting, A. Y., Proteomic mapping of mitochondria in living cells via spatially restricted enzymatic tagging. *Science* **2013,** *339* (6125), 1328-1331.

124. Minamihata, K.; Goto, M.; Kamiya, N., Protein heteroconjugation by the peroxidase-catalyzed tyrosine coupling reaction. *Bioconjug Chem* **2011,** *22* (11), 2332-2338.

125. Rogers, M. S.; Hurtado-Guerrero, R.; Firbank, S. J.; Halcrow, M. A.; Dooley, D. M.; Phillips, S. E.; Knowles, P. F.; McPherson, M. J., Cross-link formation of the cysteine 228-tyrosine 272 catalytic cofactor of galactose oxidase does not require dioxygen. *Biochemistry* **2008,** *47* (39), 10428-10439.

126. Bhaskar, B.; Immoos, C. E.; Shimizu, H.; Sulc, F.; Farmer, P. J.; Poulos, T. L., A novel heme and peroxide-dependent tryptophan-tyrosine cross-link in a mutant of cytochrome *c* peroxidase. *J Mol Biol* **2003,** *328* (1), 157-166.

127. Amini, F.; Kodadek, T.; Brown, K. C., Protein affinity labeling mediated by genetically encoded peptide tags. *Angew Chem Int Ed* **2002,** *41* (2), 356-359.

128. Xu, Y.; Fan, X.; Hu, Y., *In vivo* interactome profiling by enzyme-catalyzed proximity labeling. *Cell Biosci* **2021,** *11* (1), 27.

129. Jumper, J.; Evans, R.; Pritzel, A.; Green, T.; Figurnov, M.; Ronneberger, O.; Tunyasuvunakool, K.; Bates, R.; Žídek, A.; Potapenko, A.; Bridgland, A.; Meyer, C.; Kohl, S. A. A.; Ballard, A. J.; Cowie, A.; Romera-Paredes, B.; Nikolov, S.; Jain, R.; Adler, J.; Back, T.; Petersen, S.; Reiman, D.; Clancy, E.; Zielinski, M.; Steinegger, M.; Pacholska, M.; Berghammer, T.; Bodenstein, S.; Silver, D.; Vinyals, O.; Senior, A. W.; Kavukcuoglu, K.; Kohli, P.; Hassabis, D., Highly accurate protein structure prediction with AlphaFold. *Nature* **2021,** *596* (7873), 583-589.

130. Alexander, R. P.; Lowenthal, A. C.; Harshey, R. M.; Ottemann, K. M., CheV: CheW-like coupling proteins at the core of the chemotaxis signaling network. *Trends Microbiol* **2010,** *18* (11), 494-503.

131. Schrödinger, L.; DeLano, W. PyMOL. http://www.pymol.org/pymol.

132. Jin, C., Li, Y. Solution structure of chemotaxis protein CheW from *Escherichia coli*. (accessed 11.11.22).

133. Fux, A.; Korotkov, V. S.; Schneider, M.; Antes, I.; Sieber, S. A., Chemical cross-linking enables drafting ClpXP proximity maps and taking snapshots of *in situ* interaction networks. *Cell Chem Biol* **2019,** *26* (1), 48-59.

134. Kanehisa, M.; Furumichi, M.; Sato, Y.; Kawashima, M.; Ishiguro-Watanabe, M., KEGG for taxonomy-based analysis of pathways and genomes. *Nucleic Acids Res* **2022**.

135. Ashburner, M.; Ball, C. A.; Blake, J. A.; Botstein, D.; Butler, H.; Cherry, J. M.; Davis, A. P.; Dolinski, K.; Dwight, S. S.; Eppig, J. T.; Harris, M. A.; Hill, D. P.; Issel-Tarver, L.; Kasarskis, A.; Lewis, S.; Matese, J. C.; Richardson, J. E.; Ringwald, M.; Rubin, G. M.; Sherlock, G., Gene ontology: tool for the unification of biology. The Gene Ontology Consortium. *Nat Genet* **2000,** *25* (1), 25-29.

136. The Gene Ontology resource: enriching a GOld mine. *Nucleic Acids Res* **2021,** *49* (D1), 325-334.

137. Briegel, A.; Beeby, M.; Thanbichler, M.; Jensen, G. J., Activated chemoreceptor arrays remain intact and hexagonally packed. *Mol Microbiol* **2011,** *82* (3), 748-257.

138. A7N237. https://www.uniprot.org/uniprotkb/A7N237/entry (accessed 11.11.22).

139. A7N8H5. https://www.uniprot.org/uniprotkb/A7N8H5/entry (accessed 11.11.22).

140. A7N0E3. https://www.uniprot.org/uniprotkb/A7N0E3/entry (accessed 11.11.22).

141. A7MS66. https://www.uniprot.org/uniprotkb/A7MS66/entry (accessed 11.11.22).

142. A7MZS8. https://www.uniprot.org/uniprotkb/A7MZS8/entry (accessed 11.11.22).

143. A7N8L7. https://www.uniprot.org/uniprotkb/A7N8L7/entry (accessed 11.11.22).

144. Colin, R.; Ni, B.; Laganenka, L.; Sourjik, V., Multiple functions of flagellar motility and chemotaxis in bacterial physiology. *FEMS Microbiol Lett* **2021,** *45* (6), 1–19.

145. Narla, A. V.; Cremer, J.; Hwa, T., A traveling-wave solution for bacterial chemotaxis with growth. *Proc Natl Acad Sci USA* **2021,** *118* (48), 2105138118-2105138130.

146. Ringgaard, S.; Zepeda-Rivera, M.; Wu, X.; Schirner, K.; Davis, B. M.; Waldor, M. K., ParP prevents dissociation of CheA from chemotactic signaling arrays and tethers them to a polar anchor. *Proc Natl Acad Sci USA* **2014,** *111* (2), E255-E264.

147. Adler, J., A method for measuring chemotaxis and use of the method to determine optimum conditions for chemotaxis by *Escherichia coli*. *J Gen Microbiol* **1973,** *74* (1), 77-91.

148. Matilla, M. A.; Velando, F.; Tajuelo, A.; Martín-Mora, D.; Xu, W.; Sourjik, V.; Gavira, J. A.; Krell, T., Chemotaxis of the human pathogen *Pseudomonas aeruginosa* to the neurotransmitter acetylcholine. *mBio* **2022,** *13* (2), e03458-21.

149. Matilla, M. A.; Krell, T., The effect of bacterial chemotaxis on host infection and pathogenicity. *FEMS Microbiol Lett* **2018,** *42* (1), 40–67.

150. Merrell, D. S.; Butler, S. M.; Qadri, F.; Dolganov, N. A.; Alam, A.; Cohen, M. B.; Calderwood, S. B.; Schoolnik, G. K.; Camilli, A., Host-induced epidemic spread of the cholera bacterium. *Nature* **2002,** *417* (6889), 642-645.

151. Butler, S. M.; Nelson, E. J.; Chowdhury, N.; Faruque, S. M.; Calderwood, S. B.; Camilli, A., Cholera stool bacteria repress chemotaxis to increase infectivity. *Mol Microbiol* **2006,** *60* (2), 417-426.

152. Macinga, D. R.; Parojcic, M. M.; Rather, P. N., Identification and analysis of aarP, a transcriptional activator of the 2'-*N*-acetyltransferase in *Providencia stuartii*. *J Bacteriol* **1995,** *177* (12), 3407-3413.

153. Studier, F. W.; Moffatt, B. A., Use of bacteriophage T7 RNA polymerase to direct selective high-level expression of cloned genes. *J Mol Biol* **1986,** *189* (1), 113-130.

154. Farmer, J. J., 3rd; Jorgensen, J. H.; Grimont, P. A.; Akhurst, R. J.; Poinar, G. O., Jr.; Ageron, E.; Pierce, G. V.; Smith, J. A.; Carter, G. P.; Wilson, K. L.; et al., *Xenorhabdus luminescens* (DNA hybridization group 5) from human clinical specimens. *J Clin Microbiol* **1989,** *27* (7), 1594-600.

155. Fischer-Le Saux, M.; Viallard, V.; Brunel, B.; Normand, P.; Boemare, N. E., Polyphasic classification of the genus *Photorhabdus* and proposal of new taxa: *P. luminescens* subsp. *luminescens* subsp. nov., *P. luminescens* subsp. *akhurstii* subsp. nov., *P. luminescens* subsp. *laumondii* subsp. nov., *P. temperata* sp. nov., *P. temperata* subsp. *temperata* subsp. nov. and *P. asymbiotica* sp. nov. *Int J Syst Bacteriol* **1999,** *49 Pt 4*, 1645-1656.

156. Urbanczyk, H.; Ast, J. C.; Higgins, M. J.; Carson, J.; Dunlap, P. V., Reclassification of *Vibrio fischeri*, *Vibrio logei*, *Vibrio salmonicida* and *Vibrio wodanis* as *Aliivibrio fischeri* gen. nov., comb. nov., *Aliivibrio logei* comb. nov., *Aliivibrio salmonicida* comb. nov. and *Aliivibrio wodanis* comb. nov. *Int J Syst Evol Microbiol* **2007,** *57* (Pt 12), 2823-2829.

157. McClelland, M.; Sanderson, K. E.; Spieth, J.; Clifton, S. W.; Latreille, P.; Courtney, L.; Porwollik, S.; Ali, J.; Dante, M.; Du, F.; Hou, S.; Layman, D.; Leonard, S.; Nguyen, C.; Scott, K.; Holmes, A.; Grewal, N.; Mulvaney, E.; Ryan, E.; Sun, H.; Florea, L.; Miller, W.; Stoneking, T.; Nhan, M.; Waterston, R.; Wilson, R. K., Complete genome sequence of *Salmonella enterica* serovar Typhimurium LT2. *Nature* **2001,** *413* (6858), 852-856.

158. Lassak, J.; Henche, A. L.; Binnenkade, L.; Thormann, K. M., ArcS, the cognate sensor kinase in an atypical Arc system of *Shewanella oneidensis* MR-1. *Appl Environ Microbiol* **2010,** *76* (10), 3263-3274.

159. Grognot, M.; Taute, K. M., A multiscale 3D chemotaxis assay reveals bacterial navigation mechanisms. *Commun Biol* **2021,** *4* (1), 669.

160. Taute, K. M.; Gude, S.; Tans, S. J.; Shimizu, T. S., High-throughput 3D tracking of bacteria on a standard phase contrast microscope. *Nat Commun* **2015,** *6*, 8776.

161. Brennan, C. A.; Mandel, M. J.; Gyllborg, M. C.; Thomasgard, K. A.; Ruby, E. G., Genetic determinants of swimming motility in the squid light-organ symbiont *Vibrio fischeri*. *MicrobiologyOpen* **2013,** *2* (4), 576-594.

162. Sar, N.; McCarter, L.; Simon, M.; Silverman, M., Chemotactic control of the two flagellar systems of *Vibrio parahaemolyticus*. *J Bacteriol* **1990,** *172* (1), 334-341.

163. Ruby, E. G.; Nealson, K. H., Symbiotic association of *Photobacterium fischeri* with the marine luminous fish *Monocentris japonica*; a model of symbiosis based on bacterial studies. *Biol Bull* **1976,** *151* (3), 574-586.

164. Eirich, J.; Burkhart, J. L.; Ullrich, A.; Rudolf, G. C.; Vollmar, A.; Zahler, S.; Kazmaier, U.; Sieber, S. A., Pretubulysin derived probes as novel tools for monitoring the microtubule network via activity-based protein profiling and fluorescence microscopy. *Mol Biosyst* **2012,** *8* (8), 2067-2075.

165. Laganenka, L.; López, M. E.; Colin, R.; Sourjik, V., Flagellum-mediated mechanosensing and RflP control motility state of pathogenic *Escherichia coli*. *mBio* **2020,** *11* (2), e02269-19

166. Cox, J.; Mann, M., MaxQuant enables high peptide identification rates, individualized p.p.b.-range mass accuracies and proteome-wide protein quantification. *Nat Biotechnol* **2008,** *26* (12), 1367-1372.

167. Tyanova, S.; Temu, T.; Cox, J., The MaxQuant computational platform for mass spectrometry-based shotgun proteomics. *Nat Protoc* **2016,** *11* (12), 2301-2319.

168. Tyanova, S.; Temu, T.; Sinitcyn, P.; Carlson, A.; Hein, M. Y.; Geiger, T.; Mann, M.; Cox, J., The Perseus computational platform for comprehensive analysis of (prote)omics data. *Nat Methods* **2016,** *13* (9), 731-740.

169. Benson, D. A.; Cavanaugh, M.; Clark, K.; Karsch-Mizrachi, I.; Lipman, D. J.; Ostell, J.; Sayers, E. W., GenBank. *Nucleic Acids Res* **2013,** *41* (Database issue), 36-42.

170. Kessner, D.; Chambers, M.; Burke, R.; Agus, D.; Mallick, P., ProteoWizard: open source software for rapid proteomics tools development. *Bioinformatics* **2008,** *24* (21), 2534-2536.

171. Kong, A. T.; Leprevost, F. V.; Avtonomov, D. M.; Mellacheruvu, D.; Nesvizhskii, A. I., MSFragger: ultrafast and comprehensive peptide identification in mass spectrometry-based proteomics. *Nat Methods* **2017,** *14* (5), 513-520.

172. Yu, F.; Teo, G. C.; Kong, A. T.; Haynes, S. E.; Avtonomov, D. M.; Geiszler, D. J.; Nesvizhskii, A. I., Identification of modified peptides using localization-aware open search. *Nat Commun* **2020,** *11* (1), 4065.

173. da Veiga Leprevost, F.; Haynes, S. E.; Avtonomov, D. M.; Chang, H. Y.; Shanmugam, A. K.; Mellacheruvu, D.; Kong, A. T.; Nesvizhskii, A. I., Philosopher: a versatile toolkit for shotgun proteomics data analysis. *Nat Methods* **2020,** *17* (9), 869-870.

174. Yu, F.; Haynes, S. E.; Teo, G. C.; Avtonomov, D. M.; Polasky, D. A.; Nesvizhskii, A. I., Fast Quantitative Analysis of timsTOF PASEF Data with MSFragger and IonQuant. *Molecular & Cellular Proteomics* **2020,** *19* (9), 1575-1585.

175. Brameyer, S.; Hoyer, E.; Bibinger, S.; Burdack, K.; Lassak, J.; Jung, K., Molecular design of a signaling system influences noise in protein abundance under acid stress in different γ-Proteobacteria. *J Bacteriol* **2020,** *202* (16), e00121-20.

176. Monzani, E.; Nicolis, S.; Dell'Acqua, S.; Capucciati, A.; Bacchella, C.; Zucca, F. A.; Mosharov, E. V.; Sulzer, D.; Zecca, L.; Casella, L., Dopamine, oxidative stress and protein–quinone modifications in Parkinson's and other neurodegenerative diseases. *Angew Chem Int Ed* **2019,** *58* (20), 6512-6527.

177. Bruning, J. M.; Wang, Y.; Oltrabella, F.; Tian, B.; Kholodar, S. A.; Liu, H.; Bhattacharya, P.; Guo, S.; Holton, J. M.; Fletterick, R. J.; Jacobson, M. P.; England, P. M., Covalent modification and regulation of the nuclear receptor Nurr1 by a dopamine metabolite. *Cell Chem Biol* **2019,** *26* (5), 674–685.

178. Umek, N.; Geršak, B.; Vintar, N.; Šoštarič, M.; Mavri, J., Dopamine autoxidation is controlled by acidic pH. *Front Mol Neurosci* **2018,** *11*, 467.

179. Sulzer, D.; Bogulavsky, J.; Larsen, K. E.; Behr, G.; Karatekin, E.; Kleinman, M. H.; Turro, N.; Krantz, D.; Edwards, R. H.; Greene, L. A.; Zecca, L., Neuromelanin biosynthesis is driven by excess cytosolic catecholamines not accumulated by synaptic vesicles. *Proc Natl Acad Sci USA* **2000,** *97* (22), 11869-11874.

180. Sabens, E. A.; Distler, A. M.; Mieyal, J. J., Levodopa deactivates enzymes that regulate thiol-disulfide homeostasis and promotes neuronal cell death: implications for therapy of Parkinson's disease. *Biochemistry* **2010,** *49* (12), 2715-2724.

181. Burbulla, L. F.; Song, P.; Mazzulli, J. R.; Zampese, E.; Wong, Y. C.; Jeon, S.; Santos, D. P.; Blanz, J.; Obermaier, C. D.; Strojny, C.; Savas, J. N.; Kiskinis, E.; Zhuang, X.; Krüger, R.; Surmeier, D. J.; Krainc, D., Dopamine oxidation mediates mitochondrial and lysosomal dysfunction in Parkinson's disease. *Science* **2017,** *357* (6357), 1255-1261.

182. LaVoie, M. J.; Ostaszewski, B. L.; Weihofen, A.; Schlossmacher, M. G.; Selkoe, D. J., Dopamine covalently modifies and functionally inactivates parkin. *Nat Med* **2005,** *11* (11), 1214-1221.

183. Bisaglia, M.; Tosatto, L.; Munari, F.; Tessari, I.; de Laureto, P. P.; Mammi, S.; Bubacco, L., Dopamine quinones interact with alpha-synuclein to form unstructured adducts. *Biochem Biophys Res Commun* **2010,** *394* (2), 424-428.

184. Conway, K. A.; Rochet, J.-C.; Bieganski, R. M.; Lansbury, P. T., Kinetic stabilization of the alpha-synuclein protofibril by a dopamine-alpha-synuclein adduct. *Science* **2001,** *294* (5545), 1346-1349.

185. Lev, N.; Barhum, Y.; Pilosof, N. S.; Ickowicz, D.; Cohen, H. Y.; Melamed, E.; Offen, D., DJ-1 protects against dopamine toxicity: implications for Parkinson's disease and aging. *J Gerontol A Biol Sci Med Sci* **2013,** *68* (3), 215-225.

186. Bonifati, V.; Oostra, B. A.; Heutink, P., Linking DJ-1 to neurodegeneration offers novel insights for understanding the pathogenesis of Parkinson's disease. *Journal of Molecular Medicine* **2004,** *82* (3), 163-174.

187. Blesa, J.; Phani, S.; Jackson-Lewis, V.; Przedborski, S., Classic and new animal models of Parkinson's disease. *J Biomed Biotechnol* **2012,** *2012*, 845618.

188. Van Laar, V. S.; Mishizen, A. J.; Cascio, M.; Hastings, T. G., Proteomic identification of dopamine-conjugated proteins from isolated rat brain mitochondria and SH-SY5Y cells. *Neurobiol Dis* **2009,** *34* (3), 487-500.

189. Hurben, A. K.; Erber, L. N.; Tretyakova, N. Y.; Doran, T. M., Proteome-wide profiling of cellular targets modified by dopamine metabolites using a bio-orthogonally functionalized catecholamine. *ACS Chem Biol* **2021,** *16* (11), 2581-2594.

190. Kaplan, A.; Stockwell, B. R., Structural elucidation of a small molecule inhibitor of protein disulfide isomerase. *ACS Med Chem Lett* **2015,** *6* (9), 966-971.

191. Teoh, E. S., *Secondary metabolites of plants*.

192. Bhagwat, S.; Haytowitz, D. B.; Holden, J. M. USDA database for the flavonoid content of selected foods, release 3.0. http://www.ars.usda.gov/nutrientdata/flav (accessed September 2022).

193. Yang, C. S.; Landau, J. M.; Huang, M. T.; Newmark, H. L., Inhibition of carcinogenesis by dietary polyphenolic compounds. *Annu Rev Nutr* **2001,** *21*, 381-406.

194. Ramassamy, C., Emerging role of polyphenolic compounds in the treatment of neurodegenerative diseases: a review of their intracellular targets. *Eur J Pharmacol* **2006,** *545* (1), 51-64.

195. Liu, H.; He, S.; Wang, T.; Orang-Ojong, B.; Lu, Q.; Zhang, Z.; Pan, L.; Chai, X.; Wu, H.; Fan, G.; Zhang, P.; Feng, Y.; Song, Y. S.; Gao, X.; Karas, R. H.; Zhu, Y., Selected phytoestrogens distinguish roles of ERα transactivation and ligand binding for anti-inflammatory activity. *Endocrinology* **2018,** *159* (9), 3351-3364.

196. Cho, S. Y.; Park, S. J.; Kwon, M. J.; Jeong, T. S.; Bok, S. H.; Choi, W. Y.; Jeong, W. I.; Ryu, S. Y.; Do, S. H.; Lee, C. S.; Song, J. C.; Jeong, K. S., Quercetin suppresses proinflammatory cytokines production through MAP kinases and NF-kappaB pathway in lipopolysaccharide-stimulated macrophage. *Mol Cell Biochem* **2003,** *243* (1-2), 153-160.

197. Cao, Y.; Cao, R., Angiogenesis inhibited by drinking tea. *Nature* **1999,** *398* (6726), 381.

198. Fattori, V.; Hohmann, M. S.; Rossaneis, A. C.; Pinho-Ribeiro, F. A.; Verri, W. A., Capsaicin: current understanding of its mechanisms and therapy of pain and other pre-clinical and clinical uses. *Molecules* **2016,** *21* (7).

199. Zwicker, J. I.; Schlechter, B. L.; Stopa, J. D.; Liebman, H. A.; Aggarwal, A.; Puligandla, M.; Caughey, T.; Bauer, K. A.; Kuemmerle, N.; Wong, E.; Wun, T.; McLaughlin, M.; Hidalgo, M.; Neuberg, D.; Furie, B.; Flaumenhaft, R., Targeting protein disulfide isomerase with the flavonoid isoquercetin to improve hypercoagulability in advanced cancer. *JCI Insight* **2019,** *4* (4), e125851.

200. Tachibana, H.; Koga, K.; Fujimura, Y.; Yamada, K., A receptor for green tea polyphenol EGCG. *Nat Struct Mol Biol* **2004,** *11* (4), 380-381.

201. Jankun, J.; Selman, S. H.; Swiercz, R.; Skrzypczak-Jankun, E., Why drinking green tea could prevent cancer. *Nature* **1997,** *387* (6633), 561.

202. Garbisa, S.; Biggin, S.; Cavallarin, N.; Sartor, L.; Benelli, R.; Albini, A., Tumor invasion: molecular shears blunted by green tea. *Nat Med* **1999,** *5* (11), 1216.

203. Brusselmans, K.; Vrolix, R.; Verhoeven, G.; Swinnen, J. V., Induction of cancer cell apoptosis by flavonoids is associated with their ability to inhibit fatty acid synthase activity. *J Biol Chem* **2005,** *280* (7), 5636-5645.

204. Seo, H. S.; Choi, H. S.; Choi, H. S.; Choi, Y. K.; Um, J. Y.; Choi, I.; Shin, Y. C.; Ko, S. G., Phytoestrogens induce apoptosis via extrinsic pathway, inhibiting nuclear factor-kappaB signaling in HER2-overexpressing breast cancer cells. *Anticancer Res* **2011,** *31* (10), 3301-3313.

205. Carpi, S.; Scoditti, E.; Massaro, M.; Polini, B.; Manera, C.; Digiacomo, M.; Esposito Salsano, J.; Poli, G.; Tuccinardi, T.; Doccini, S.; Santorelli, F. M.; Carluccio, M. A.; Macchia, M.; Wabitsch, M.; De Caterina, R.; Nieri, P., The extra-virgin olive oil polyphenols oleocanthal and oleacein counteract inflammation-related gene and miRNA expression in adipocytes by attenuating NF-κB activation. *Nutrients* **2019,** *11* (12), 2855.

206. Boly, R.; Gras, T.; Lamkami, T.; Guissou, P.; Serteyn, D.; Kiss, R.; Dubois, J., Quercetin inhibits a large panel of kinases implicated in cancer cell biology. *Int J Oncol* **2011,** *38* (3), 833-842.

207. Murakami, A.; Ashida, H.; Terao, J., Multitargeted cancer prevention by quercetin. *Cancer Lett* **2008,** *269* (2), 315-325.

208. Puranik, N. V.; Srivastava, P.; Bhatt, G.; John Mary, D. J. S.; Limaye, A. M.; Sivaraman, J., Determination and analysis of agonist and antagonist potential of naturally occurring flavonoids for estrogen receptor (ERα) by various parameters and molecular modelling approach. *Sci Rep* **2019,** *9* (1), 7450

209. Jeong, S. H.; Kim, H. H.; Ha, S. E.; Park, M. Y.; Bhosale, P. B.; Abusaliya, A.; Park, K. I.; Heo, J. D.; Kim, H. W.; Kim, G. S., Flavones: six selected flavones and their related signaling pathways that induce apoptosis in cancer. *Int J Mol Sci* **2022,** *23* (18), 10965.

210. Khan, N.; Afaq, F.; Saleem, M.; Ahmad, N.; Mukhtar, H., Targeting multiple signaling pathways by green tea polyphenol (-)-epigallocatechin-3-gallate. *Cancer Resarch* **2006,** *66* (5), 2500-2505.

211. Chapa-Oliver, A. M.; Mejía-Teniente, L., Capsaicin: from plants to a cancer-suppressing agent. *Molecules* **2016,** *21* (8), 931.

212. Soeda, Y.; Yoshikawa, M.; Almeida, O. F.; Sumioka, A.; Maeda, S.; Osada, H.; Kondoh, Y.; Saito, A.; Miyasaka, T.; Kimura, T.; Suzuki, M.; Koyama, H.; Yoshiike, Y.; Sugimoto, H.; Ihara, Y.; Takashima, A., Toxic tau oligomer formation blocked by capping of cysteine residues with 1,2-dihydroxybenzene groups. *Nat Commun* **2015,** *6*, 10216.

213. Velander, P.; Wu, L.; Hildreth, S. B.; Vogelaar, N. J.; Mukhopadhyay, B.; Helm, R. F.; Zhang, S.; Xu, B., Catechol-containing compounds are a broad class of protein aggregation inhibitors: Redox state is a key determinant of the inhibitory activities. *Pharmacol Research* **2022,** *184*, 106409.

214. Robinson, R. M.; Reyes, L.; Duncan, R. M.; Bian, H.; Reitz, A. B.; Manevich, Y.; McClure, J. J.; Champion, M. M.; Chou, C. J.; Sharik, M. E.; Chesi, M.; Bergsagel, P. L.; Dolloff, N. G., Inhibitors of the protein disulfide isomerase family for the treatment of multiple myeloma. *Leukemia* **2019,** *33* (4), 1011-1022.

215. Zhang, Q.; Luo, P.; Xia, F.; Tang, H.; Chen, J.; Zhang, J.; Liu, D.; Zhu, Y.; Liu, Y.; Gu, L.; Zheng, L.; Li, Z.; Yang, F.; Dai, L.; Liao, F.; Xu, C.; Wang, J., Capsaicin ameliorates inflammation in a TRPV1-independent mechanism by inhibiting PKM2-LDHA-mediated Warburg effect in sepsis. *Cell Chem Biol* **2022,** *29* (8), 1248-1259.

216. Farzam, A.; Chohan, K.; Strmiskova, M.; Hewitt, S. J.; Park, D. S.; Pezacki, J. P.; Özcelik, D., A functionalized hydroxydopamine quinone links thiol modification to neuronal cell death. *Redox Biol* **2020,** *28*, 101377.

217. Hurben, A. K.; Tretyakova, N. Y., Role of protein damage inflicted by dopamine metabolites in Parkinson's disease: evidence, tools, and outlook. *Chem Res Toxicol* **2022**, 1789-1804.

218. Nawaratne, V.; McLaughlin, S. P.; Mayer, F. P.; Gichi, Z.; Mastriano, A.; Carvelli, L., Prolonged amphetamine exposures increase the endogenous human dopamine receptors 2 at the cellular membrane in cells lacking the dopamine transporter. *Front Cell Neurosci* **2021,** *15*, 681539.

219. Boxberger, K. H.; Hagenbuch, B.; Lampe, J. N., Common drugs inhibit human organic cation transporter 1 (OCT1)-mediated neurotransmitter uptake. *Drug Metab Dispos* **2014,** *42* (6), 990-995.

220. Pontén, F.; Jirström, K.; Uhlen, M., The Human Protein Atlas—a tool for pathology. *J Pathol* **2008,** *216* (4), 387-393.

221. Human Protein Atlas. https://www.proteinatlas.org/ENSG00000175003-SLC22A1/cell+line (accessed 11.11.22).

222. Morstein, J.; Capecchi, A.; Hinnah, K.; Park, B.; Petit-Jacques, J.; Van Lehn, R. C.; Reymond, J. L.; Trauner, D., Medium-chain lipid conjugation facilitates cell-permeability and bioactivity. *J Am Chem Soc* **2022,** *144* (40), 18532-18544.

223. Eden, E.; Lipson, D.; Yogev, S.; Yakhini, Z., Discovering motifs in ranked lists of DNA sequences. *PLoS Comput Biol* **2007,** *3* (3), e39.

224. Eden, E.; Navon, R.; Steinfeld, I.; Lipson, D.; Yakhini, Z., GOrilla: a tool for discovery and visualization of enriched GO terms in ranked gene lists. *BMC Bioinform* **2009,** *10*, 48.

225. Zhu, B. T., Catechol-*O*-Methyltransferase (COMT)-mediated methylation metabolism of endogenous bioactive catechols and modulation by endobiotics and xenobiotics: importance in pathophysiology and pathogenesis. *Curr Drug Metab* **2002,** *3* (3), 321-349.

226. Bley, K.; Boorman, G.; Mohammad, B.; McKenzie, D.; Babbar, S., A comprehensive review of the carcinogenic and anticarcinogenic potential of capsaicin. *Toxicol Pathol* **2012,** *40* (6), 847-873.

227. Zhang, S.; Wang, R.; Wang, G., Impact of dopamine oxidation on dopaminergic neurodegeneration. *ACS Chem Neurosci* **2019,** *10* (2), 945-953.

228. Akopian, D.; Shen, K.; Zhang, X.; Shan, S. O., Signal recognition particle: an essential protein-targeting machine. *Annu Rev Biochem* **2013,** *82*, 693-721.

229. Faoro, C.; Ataide, S. F., Noncanonical functions and cellular dynamics of the mammalian signal recognition particle components. *Front Mol Biosci* **2021,** *8*, 679584.

230. San Francisco, B.; Bretsnyder, E. C.; Kranz, R. G., Human mitochondrial holocytochrome *c* synthase´s heme binding, maturation determinants, and complex formation with cytochrome *c*. *Proc Natl Acad Sci USA* **2013,** *110* (9), E788-E797.

231. Babbitt, S. E.; San Francisco, B.; Mendez, D. L.; Lukat-Rodgers, G. S.; Rodgers, K. R.; Bretsnyder, E. C.; Kranz, R. G., Mechanisms of mitochondrial holocytochrome *c* synthase and the key roles played by cysteines and histidine of the heme attachment site, Cys-XX-Cys-His. *J Biol Chem* **2014,** *289* (42), 28795-28807.

232. Prakash, S. K.; Cormier, T. A.; McCall, A. E.; Garcia, J. J.; Sierra, R.; Haupt, B.; Zoghbi, H. Y.; Van Den Veyver, I. B., Loss of holocytochrome *c*-type synthetase causes the male lethality of X-linked dominant microphthalmia with linear skin defects (MLS) syndrome. *Hum Mol Genet* **2002,** *11* (25), 3237-3248.

233. Giordano, F.; Saheki, Y.; Idevall-Hagren, O.; Colombo, S. F.; Pirruccello, M.; Milosevic, I.; Gracheva, E. O.; Bagriantsev, S. N.; Borgese, N.; De Camilli, P., PI(4,5)P(2)-dependent and Ca(2+)-regulated ER-PM interactions mediated by the extended synaptotagmins. *Cell* **2013,** *153* (7), 1494-1509.

234. Chang, C. L.; Hsieh, T. S.; Yang, T. T.; Rothberg, K. G.; Azizoglu, D. B.; Volk, E.; Liao, J. C.; Liou, J., Feedback regulation of receptor-induced Ca2+ signaling mediated by E-Syt1 and Nir2 at endoplasmic reticulum-plasma membrane junctions. *Cell Rep* **2013,** *5* (3), 813-825.

235. Liaci, A. M.; Steigenberger, B.; Telles de Souza, P. C.; Tamara, S.; Gröllers-Mulderij, M.; Ogrissek, P.; Marrink, S. J.; Scheltema, R. A.; Förster, F., Structure of the human signal peptidase complex reveals the determinants for signal peptide cleavage. *Mol Cell* **2021,** *81* (19), 3934-3948.

236. Takei, D.; Ishihara, H.; Yamaguchi, S.; Yamada, T.; Tamura, A.; Katagiri, H.; Maruyama, Y.; Oka, Y., WFS1 protein modulates the free Ca(2+) concentration in the endoplasmic reticulum. *FEBS Lett* **2006,** *580* (24), 5635-5640.

237. Istvan, E. S.; Deisenhofer, J., Structural mechanism for statin inhibition of HMG-CoA reductase. *Science* **2001,** *292* (5519), 1160-1164.

238. Luskey, K. L.; Stevens, B., Human 3-hydroxy-3-methylglutaryl coenzyme A reductase. Conserved domains responsible for catalytic activity and sterol-regulated degradation. *J Biol Chem* **1985,** *260* (18), 10271-10277.

239. Cuccioloni, M.; Mozzicafreddo, M.; Spina, M.; Tran, C. N.; Falconi, M.; Eleuteri, A. M.; Angeletti, M., Epigallocatechin-3-gallate potently inhibits the *in vitro* activity of hydroxy-3-methyl-glutaryl-CoA reductase. *J Lipid Res* **2011,** *52* (5), 897-907.

240. Nishiyama, A.; Frappier, L.; Méchali, M., MCM-BP regulates unloading of the MCM2-7 helicase in late S phase. *Genes Dev* **2011,** *25* (2), 165-175.

241. Martin, C. A.; Murray, J. E.; Carroll, P.; Leitch, A.; Mackenzie, K. J.; Halachev, M.; Fetit, A. E.; Keith, C.; Bicknell, L. S.; Fluteau, A.; Gautier, P.; Hall, E. A.; Joss, S.; Soares, G.; Silva, J.; Bober, M. B.; Duker, A.; Wise, C. A.; Quigley, A. J.; Phadke, S. R.; Wood, A. J.; Vagnarelli, P.; Jackson, A. P., Mutations in genes encoding condensin complex proteins cause microcephaly through decatenation failure at mitosis. *Genes Dev* **2016,** *30* (19), 2158-2172.

242. Yadav, S.; Verma, P. J.; Panda, D., C-terminal region of MAP7 domain containing protein 3 (MAP7D3) promotes microtubule polymerization by binding at the C-terminal tail of tubulin. *PloS One* **2014,** *9* (6), e99539.

243. Guyot, R.; Vincent, S.; Bertin, J.; Samarut, J.; Ravel-Chapuis, P., The transforming acidic coiled coil (TACC1) protein modulates the transcriptional activity of the nuclear receptors TR and RAR. *BMC Mol Biol* **2010,** *11*, 3.

244. Tan, B. C.; Lee, S. C., Nek9, a novel FACT-associated protein, modulates interphase progression. *J Biol Chem* **2004,** *279* (10), 9321-9330.

245. Yuan, J.; Luo, K.; Zhang, L.; Cheville, J. C.; Lou, Z., USP10 regulates p53 localization and stability by deubiquitinating p53. *Cell* **2010,** *140* (3), 384-396.

246. Lattanzio, R.; Piantelli, M.; Falasca, M., Role of phospholipase C in cell invasion and metastasis. *Adv Biol Regul* **2013,** *53* (3), 309-318.

247. Takayama, S.; Xie, Z.; Reed, J. C., An evolutionarily conserved family of Hsp70/Hsc70 molecular chaperone regulators. *J Biol Chem* **1999,** *274* (2), 781-786.

248. Stehling, O.; Netz, D. J.; Niggemeyer, B.; Rösser, R.; Eisenstein, R. S.; Puccio, H.; Pierik, A. J.; Lill, R., Human Nbp35 is essential for both cytosolic iron-sulfur protein assembly and iron homeostasis. *Mol Cell Biol* **2008,** *28* (17), 5517-5528.

249. Kleylein-Sohn, J.; Westendorf, J.; Le Clech, M.; Habedanck, R.; Stierhof, Y. D.; Nigg, E. A., Plk4-induced centriole biogenesis in human cells. *Dev Cell* **2007,** *13* (2), 190-202.

250. Spektor, A.; Tsang, W. Y.; Khoo, D.; Dynlacht, B. D., Cep97 and CP110 suppress a cilia assembly program. *Cell* **2007,** *130* (4), 678-690.

251. Uematsu, S.; Sato, S.; Yamamoto, M.; Hirotani, T.; Kato, H.; Takeshita, F.; Matsuda, M.; Coban, C.; Ishii, K. J.; Kawai, T.; Takeuchi, O.; Akira, S., Interleukin-1 receptor-associated kinase-1 plays an essential role for Toll-like receptor (TLR)7- and TLR9-mediated interferon-α induction. *J Exp Med* **2005,** *201* (6), 915-923.

252. Dunne, A.; Carpenter, S.; Brikos, C.; Gray, P.; Strelow, A.; Wesche, H.; Morrice, N.; O'Neill, L. A., IRAK1 and IRAK4 promote phosphorylation, ubiquitination, and degradation of MyD88 adaptor-like (Mal). *J Biol Chem* **2010,** *285* (24), 18276-18282.

253. Tanida, I.; Tanida-Miyake, E.; Komatsu, M.; Ueno, T.; Kominami, E., Human Apg3p/Aut1p homologue is an authentic E2 enzyme for multiple substrates, GATE-16, GABARAP, and MAP-LC3, and facilitates the conjugation of hApg12p to hApg5p. *J Biol Chem* **2002,** *277* (16), 13739-13744.

254. Xu, S.; Sankar, S.; Neamati, N., Protein disulfide isomerase: a promising target for cancer therapy. *Drug Discov Today* **2014,** *19* (3), 222-240.

255. Özcelik, D.; Pezacki, J. P., Small molecule inhibition of protein disulfide isomerase in neuroblastoma cells induces an oxidative stress response and apoptosis pathways. *ACS Chem Neurosci* **2019,** *10* (9), 4068-4075.

256. Liang, Y. C.; Lin-Shiau, S. Y.; Chen, C. F.; Lin, J. K., Inhibition of cyclin-dependent kinases 2 and 4 activities as well as induction of Cdk inhibitors p21 and p27 during growth arrest of human breast carcinoma cells by (-)-epigallocatechin-3-gallate. *J Cell Biochem* **1999,** *75* (1), 1-12.

257. Palhano, F. L.; Lee, J.; Grimster, N. P.; Kelly, J. W., Toward the molecular mechanism(s) by which EGCG treatment remodels mature amyloid fibrils. *J Am Chem Soc* **2013,** *135* (20), 7503-7510.

258. Bieschke, J.; Russ, J.; Friedrich, R. P.; Ehrnhoefer, D. E.; Wobst, H.; Neugebauer, K.; Wanker, E. E., EGCG remodels mature alpha-synuclein and amyloid-beta fibrils and reduces cellular toxicity. *Proc Natl Acad Sci USA* **2010,** *107* (17), 7710-7715.

259. Li, J.; Zhu, M.; Manning-Bog, A. B.; Di Monte, D. A.; Fink, A. L., Dopamine and L-dopa disaggregate amyloid fibrils: implications for Parkinson's and Alzheimer's disease. *FASEB Journal* **2004,** *18* (9), 962-964.

260. Ehrnhoefer, D. E.; Bieschke, J.; Boeddrich, A.; Herbst, M.; Masino, L.; Lurz, R.; Engemann, S.; Pastore, A.; Wanker, E. E., EGCG redirects amyloidogenic polypeptides into unstructured, off-pathway oligomers. *Nat Struct Mol Biol* **2008,** *15* (6), 558-566.

261. Mitsiades, C. S.; Mitsiades, N. S.; McMullan, C. J.; Poulaki, V.; Kung, A. L.; Davies, F. E.; Morgan, G.; Akiyama, M.; Shringarpure, R.; Munshi, N. C.; Richardson, P. G.; Hideshima, T.; Chauhan, D.; Gu, X.; Bailey, C.; Joseph, M.; Libermann, T. A.; Rosen,

N. S.; Anderson, K. C., Antimyeloma activity of heat shock protein-90 inhibition. *Blood* **2006,** *107* (3), 1092-1100.

262. Richardson, P. G.; Mitsiades, C.; Hideshima, T.; Anderson, K. C., Bortezomib: proteasome inhibition as an effective anticancer therapy. *Annu Rev Med* **2006,** *57*, 33-47.

263. Vatolin, S.; Phillips, J. G.; Jha, B. K.; Govindgari, S.; Hu, J.; Grabowski, D.; Parker, Y.; Lindner, D. J.; Zhong, F.; Distelhorst, C. W.; Smith, M. R.; Cotta, C.; Xu, Y.; Chilakala, S.; Kuang, R. R.; Tall, S.; Reu, F. J., Novel protein disulfide isomerase inhibitor with anticancer activity in multiple myeloma. *Cancer Resarch* **2016,** *76* (11), 3340-3350.

264. Xu, S.; Butkevich, A. N.; Yamada, R.; Zhou, Y.; Debnath, B.; Duncan, R.; Zandi, E.; Petasis, N. A.; Neamati, N., Discovery of an orally active small-molecule irreversible inhibitor of protein disulfide isomerase for ovarian cancer treatment. *Proc Natl Acad Sci USA* **2012,** *109* (40), 16348-16353.

265. Ge, J.; Zhang, C. J.; Li, L.; Chong, L. M.; Wu, X.; Hao, P.; Sze, S. K.; Yao, S. Q., Small molecule probe suitable for *in situ* profiling and inhibition of protein disulfide isomerase. *ACS Chem Biol* **2013,** *8* (11), 2577-2585.

266. Khan, M. M.; Simizu, S.; Kawatani, M.; Osada, H., The potential of protein disulfide isomerase as a therapeutic drug target. *Oncol Res* **2011,** *19* (10-11), 445-453.

267. Benham, A. M., The protein disulfide isomerase family: key players in health and disease. *Antioxid Redox Signal* **2012,** *16* (8), 781-789.

268. Hoffstrom, B. G.; Kaplan, A.; Letso, R.; Schmid, R. S.; Turmel, G. J.; Lo, D. C.; Stockwell, B. R., Inhibitors of protein disulfide isomerase suppress apoptosis induced by misfolded proteins. *Nat Chem Biol* **2010,** *6* (12), 900-906.

269. Elumalai, N.; Berg, A.; Natarajan, K.; Scharow, A.; Berg, T., Nanomolar inhibitors of the transcription factor STAT5b with high selectivity over STAT5a. *Angew Chem Int Ed Engl* **2015,** *54* (16), 4758-4763.

270. Pham, T. T.; Giesert, F.; Röthig, A.; Floss, T.; Kallnik, M.; Weindl, K.; Hölter, S. M.; Ahting, U.; Prokisch, H.; Becker, L.; Klopstock, T.; Hrabé de Angelis, M.; Beyer, K.; Görner, K.; Kahle, P. J.; Vogt Weisenhorn, D. M.; Wurst, W., DJ-1-deficient mice show less TH-positive neurons in the ventral tegmental area and exhibit non-motoric behavioural impairments. *Genes Brain Behav* **2010,** *9* (3), 305-317.

271. Drechsel, J.; Mandl, F. A.; Sieber, S. A., Chemical Probe To Monitor the Parkinsonism-Associated Protein DJ-1 in Live Cells. *ACS Chem Biol* **2018,** *13* (8), 2016-2019.

V Abbreviations

ABC	adenosine triphosphate-binding cassette
AcOD	deuterated acetic acid
AcOH	acetic acid
ANOVA	analysis of variance
APEX	engineered ascorbate peroxidase
BLAST	basic local alignment search tool
$CDCl_3$	deuterated chloroform
Co-IP	co-immunprecipitation
COMT	catechol-*O*-methyltransferase
CuAAC	copper-catalysed azide-alkyne cycloaddition
CV	cyclic voltammetry
D_2O	deuterated water
DAP	2,6-diaminopimelic acid
DMEM	Dulbecco's Modified Eagle Medium
DMF	*N*,*N*-dimethylformamide
DMSO	dimethyl sulfoxide
DMSO-d_6	deuterated dimethyl sulfoxide
DNA	deoxyribonucleic acid
DSSO	disuccinimidyl sulfoxide
DTT	dithiothreitol
DUF	domain of unknown function
EDC·HCl	1-(3-dimethylaminopropyl)-3-ethylcarbodiimide hydrochloride
EHEC	enterohaemorrhagic *E. coli*
eq.	equivalents
ER	endoplasmic reticulum
ESI	electrospray ionisation
EtOAc	ethyl acetate
EtOH	ethanol
Fc	ferrocene
FCS	foetal calf serum
FDR	false discovery rate
FMN	flavin mononucleotide
GO	gene ontology
GOBP	gene ontology biological process
GOCC	gene ontology cellular compartment
GOMF	gene ontology molecular function
GPCR	G protein-coupled receptor
GST	glutathione *S*-transferase
H-ASW	HEPES-buffered artificial seawater
HBBS	Hanks' balanced salt solution
Hccs	holocytochrome *c*-type synthase
HEPES	2-(4-(2-hydroxyethyl)piperazin-1-yl)ethane-1-sulfonic acid
HOBt	hydroxybenzotriazole
HPLC	high-performance liquid chromatography
HRMS	high-resolution mass spectrometry
Hsc70/Hsp70	70-kDa heat shock cognate protein/70 kilodalton heat shock proteins
IgG	immunoglobulin G
IPTG	β-D-1-thiogalactopyranoside
isoDTB	isotopically labelled desthiobiotin azide
KEGG	Kyoto Encyclopedia of Genes and Genomes
LB	lysogeny broth

LC-MS	liquid chromatography with mass spectrometry
LFQ	label-free quantification
LMU	Ludwig Maximilian University of Munich
m/z	mass-to-charge ratio
MCP	methyl-accepting chemotaxis protein
MeOH	methanol
MS	mass spectrometry
MS/MS	tandem mass spectrometry
MST	microscale thermophoresis
NADH	nicotinamide adenine dinucleotide
NMR	nuclear magnetic resonance
NP-40	Nonidet P-40
NTA	nitrilotriacetic acid
OD_{600}	optical density measured at 600 nm
OmpA	outer membrane protein A
PAGE	polyacrylamide gel electrophoresis
PAL	photoaffinity labelling
PBS	phosphate-buffered saline
PCL	photocrosslinker
PCR	polymerase chain reaction
PD	Parkinson´s disease
PDB	protein data bank
PMSF	phenazine methosulfate
PPh_3	triphenylphosphine
ppm	parts per million
PSM	peptide spectrum match
PTM	post-translational protein modification
PTS	phosphotransferase system
PVDF	polyvinylidenfluoride
r.t.	room temperature
R_f	retention factor
RMSD	root-mean-square deviation
RNA	ribonucleic acid
SDS	sodium dodecyl sulphate
SPAAC	strain-promoted azide-alkyne cycloaddition
Srp19	signal recognition particle 19 kDa protein
$TBAPF_6$	tetrabutylammonium hexafluorophosphate
TBTA	tris((1-benzyl-4-triazolyl)methyl)amine
t-BuOH	*tert*-butanol
TCEP	tris(2-carboxyethyl)phosphine hydrochloride
TEA	triethylamine
TEAB	triethylammonium bicarbonate buffer
TEV	Tobacco Etch Virus nuclear-inclusion-a endopeptidase
TFA	trifluoroacetic acid
TLC	thin-layer chromatography
Tris	tris(hydroxymethyl)aminomethane
TUM	Technical University of Munich
TX100	triton X-100; 2-[4-(2,4,4-trimethylpentan-2-yl)phenoxy]ethanol
UPR	unfolded protein response
UV	ultraviolet
VC	*Vibrio campbellii*

VI Appendix

1 NMR spectra

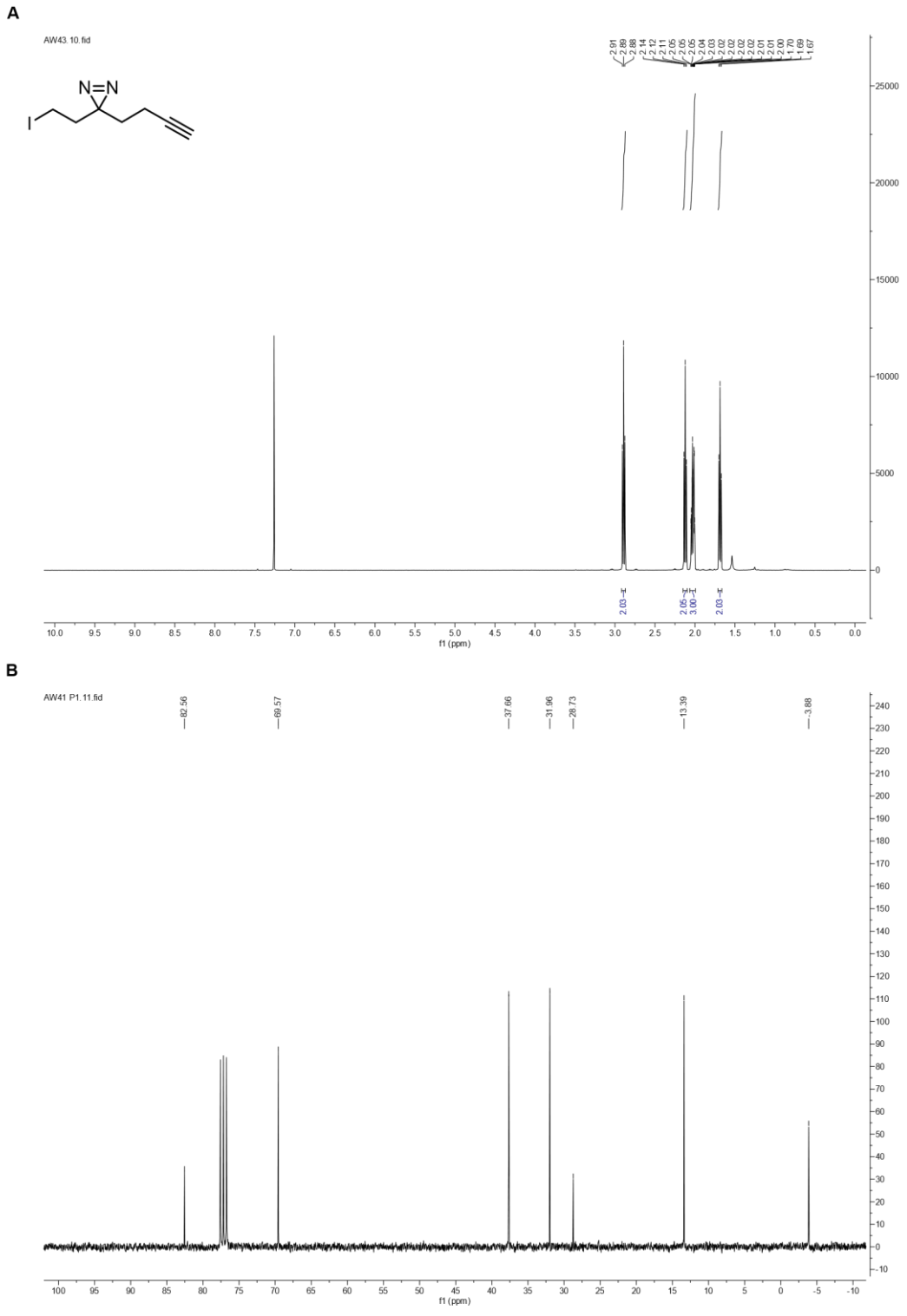

Figure VI-1. NMR spectra of 3-(but-3-yn-1-yl)-3-(2-iodoethyl)-3*H*-diazirine (**PCL-I**) in $CDCl_3$. (A) ^{1}H-NMR (500 MHz). (B) ^{13}C-NMR (75 MHz).

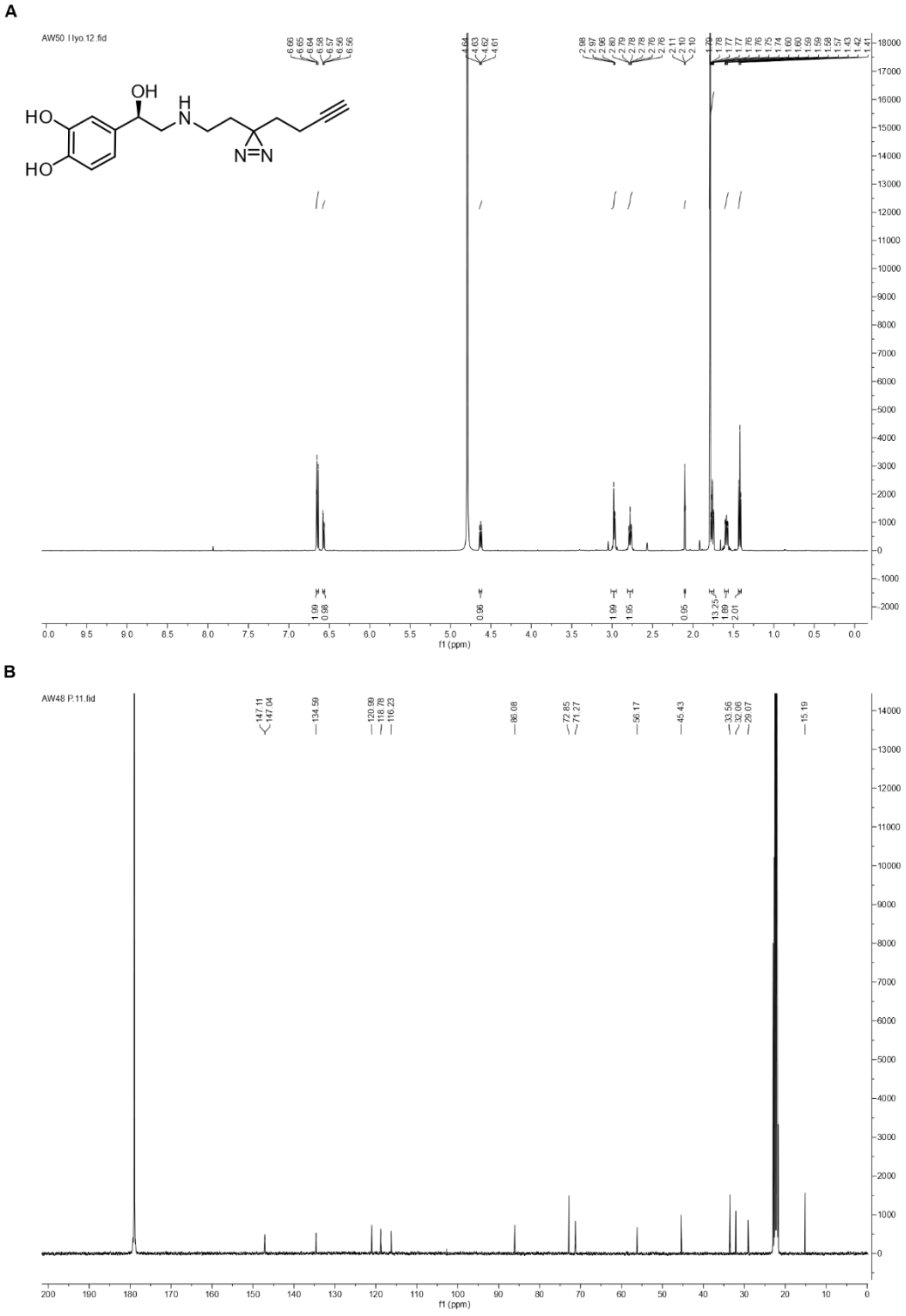

Figure VI-2. NMR spectra of (*R*)-4-(2-((2-(3-(but-3-yn-1-yl)-3*H*-diazirin-3-yl)ethyl)amino)-1-hydroxyethyl)-benzene-1,2-diol (**EPI-P1**) as a 1:3.5 mixture with acetic acid. (A) ^{1}H-NMR (500 MHz, DCl:D_2O 38:962). (B) ^{13}C-NMR (101 MHz, AcOD/D_2O 1:1).

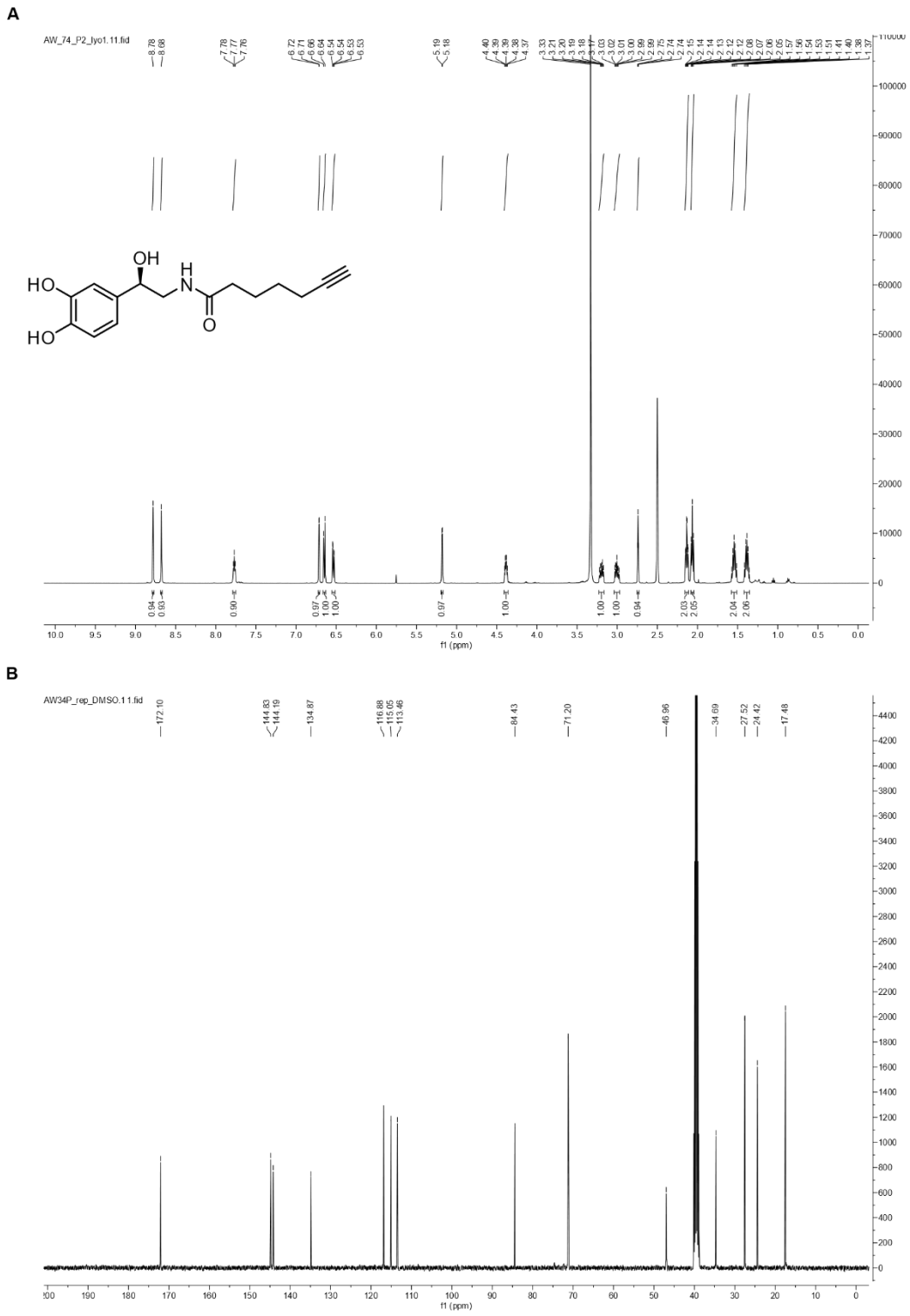

Figure VI-3. NMR spectra of (*R*)-*N*-(2-(3,4-dihydroxyphenyl)-2-hydroxyethyl)hept-6-ynamide (**EPI-P2**) in DMSO-d_6. (A) ^{1}H-NMR (500 MHz). (B) ^{13}C-NMR (101 MHz).

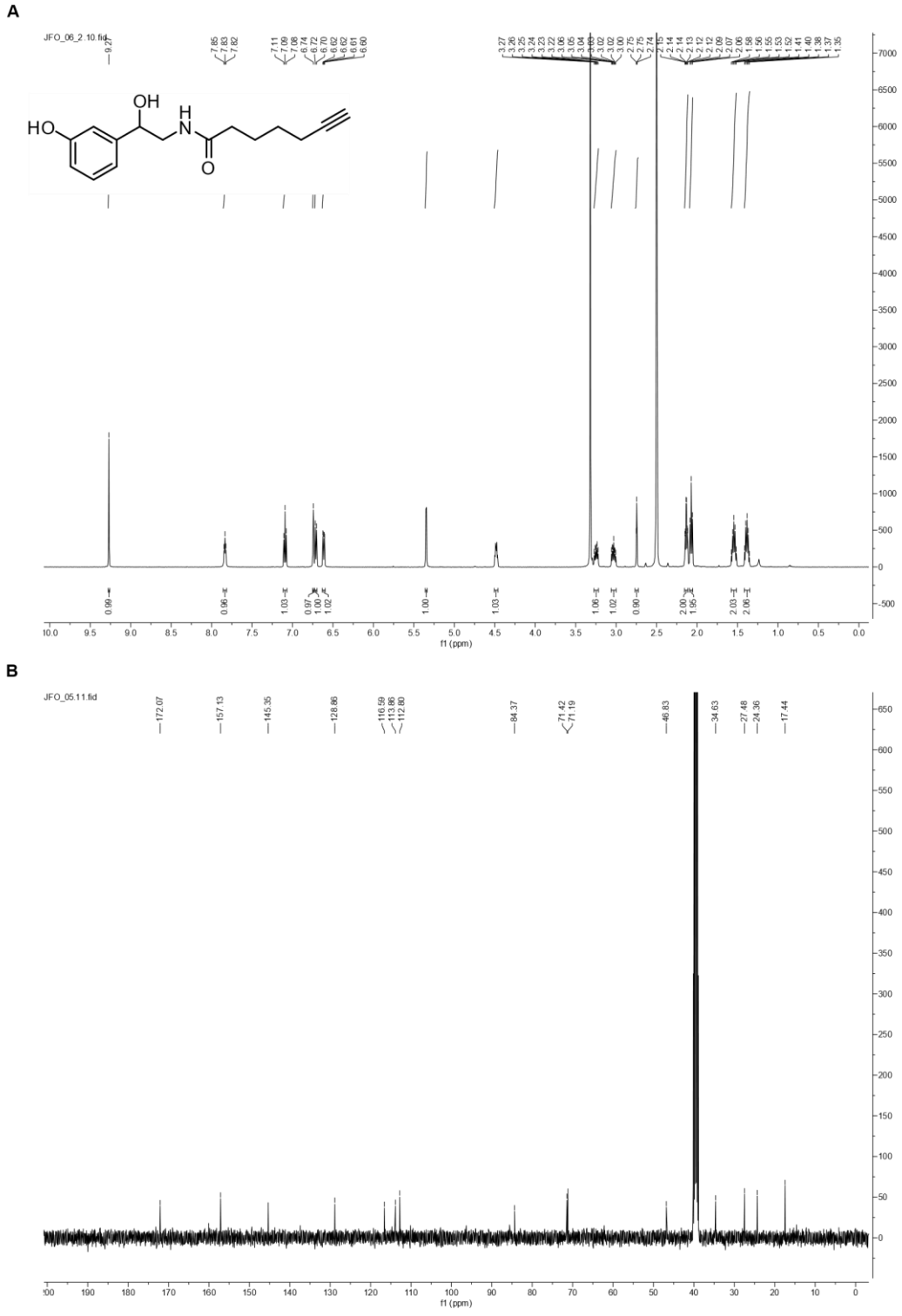

Figure VI-4. NMR spectra of *N*-(2-hydroxy-2-(3-hydroxyphenyl)ethyl)hept-6-ynamide (**PE-P**) in DMSO-d_6. (A) ^{1}H-NMR (500 MHz). (B) ^{13}C-NMR (101 MHz).

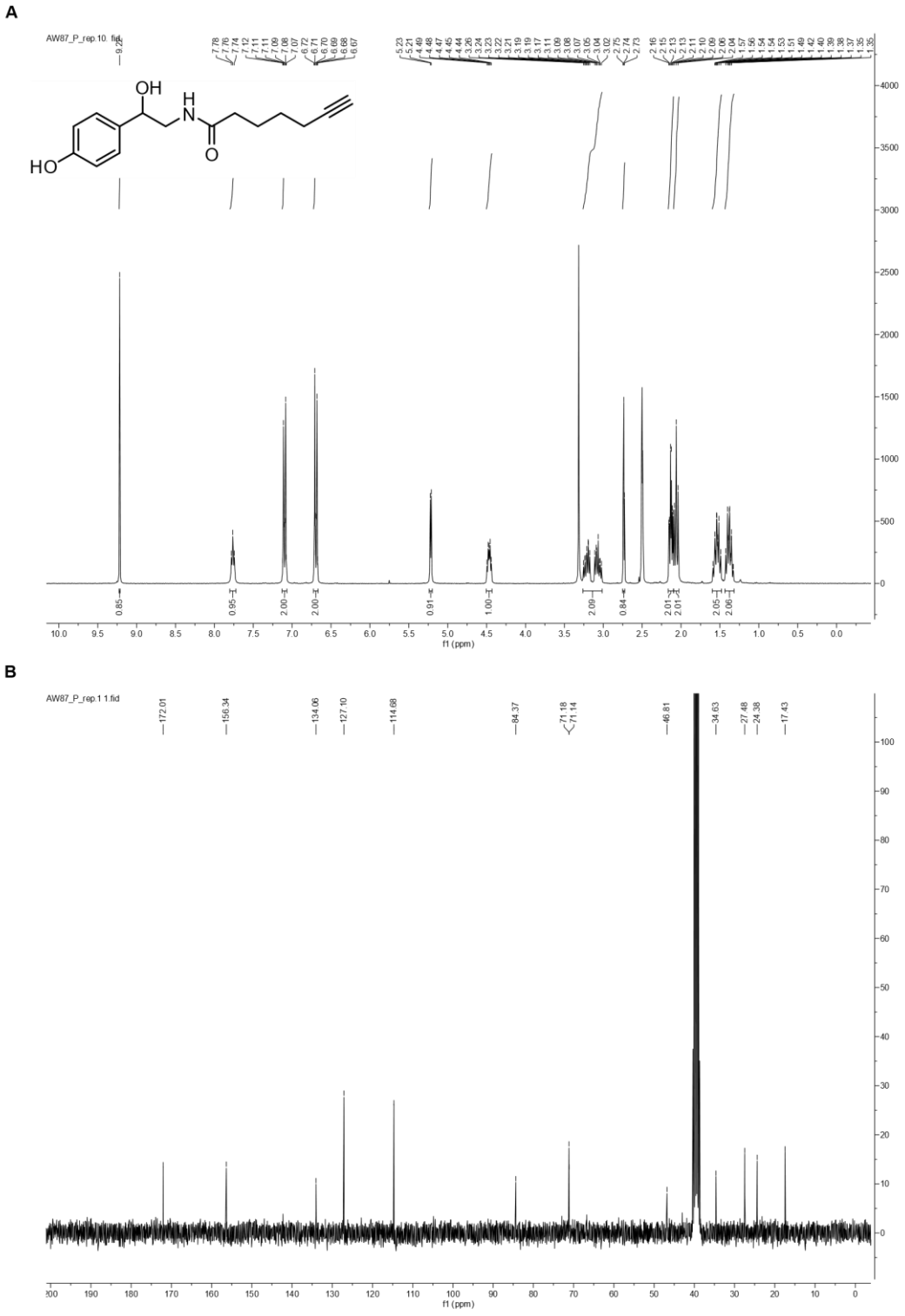

Figure VI-5. NMR spectra of *N*-(2-hydroxy-2-(4-hydroxyphenyl)ethyl)hept-6-ynamide (**OA-P**) in DMSO-d_6. (A) ^{1}H-NMR (300 MHz). (B) ^{13}C-NMR (75 MHz).

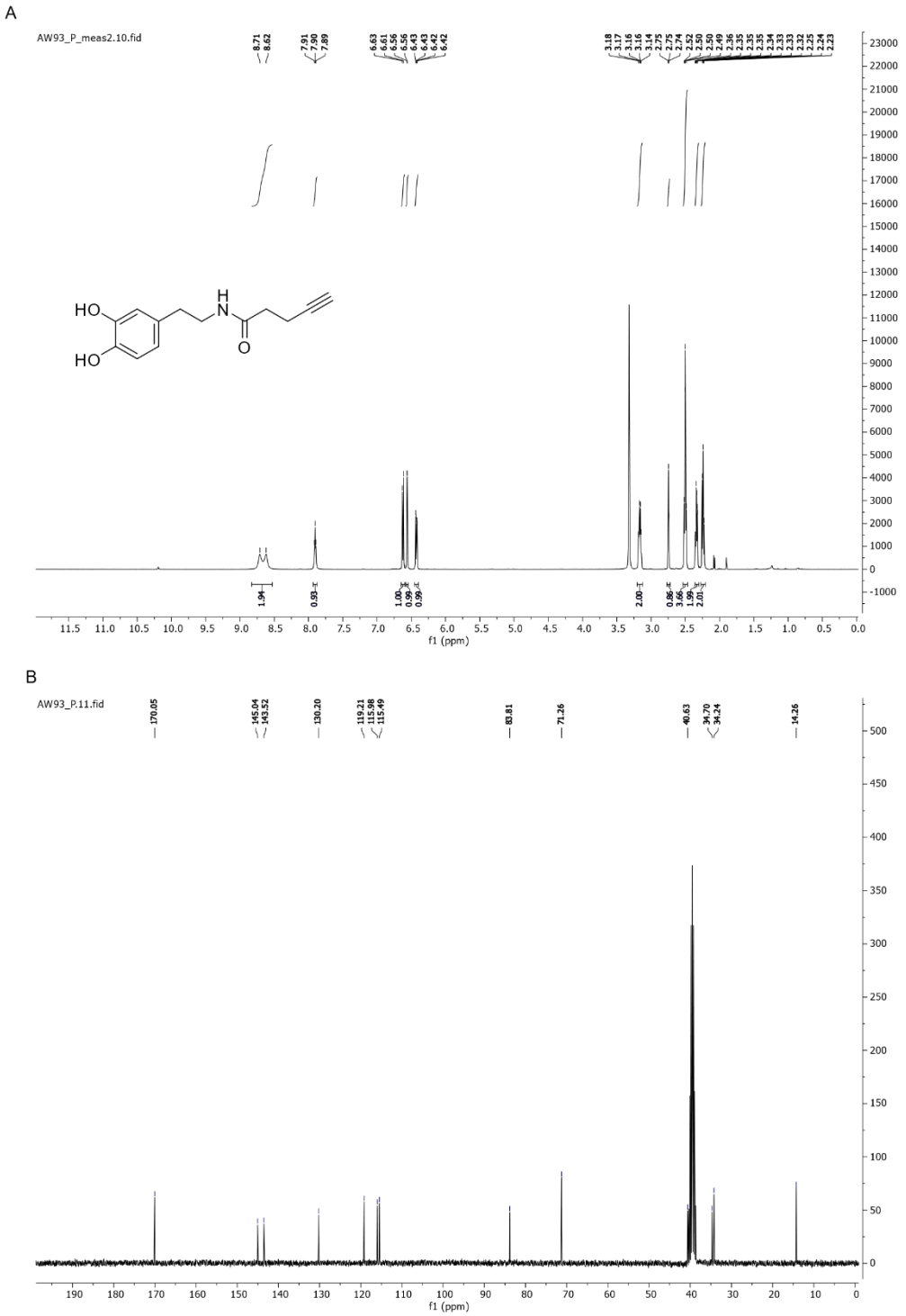

Figure VI-6. NMR spectra of *N*-(3,4-dihydroxyphenethyl)pent-4-ynamide (**DA-P1**) in DMSO-d_6. (A) ^{1}H-NMR (500 MHz). (B) ^{13}C-NMR (75 MHz).

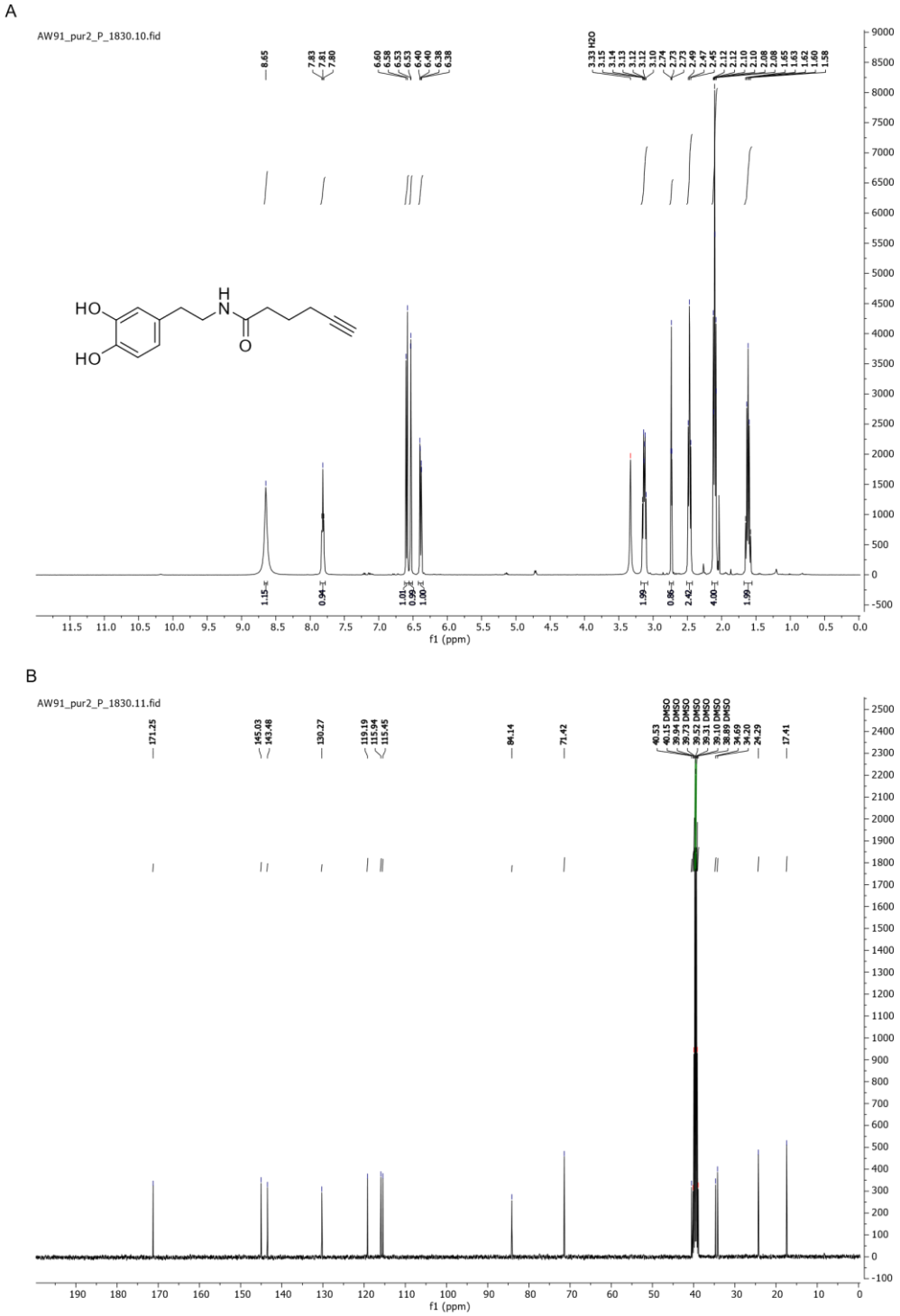

Figure VI-7. NMR spectra of *N*-(3,4-dihydroxyphenethyl)hex-5-ynamide (**DA-P2**) in DMSO-d_6. (A) ^{1}H-NMR (400 MHz). (B) ^{13}C-NMR (101 MHz).

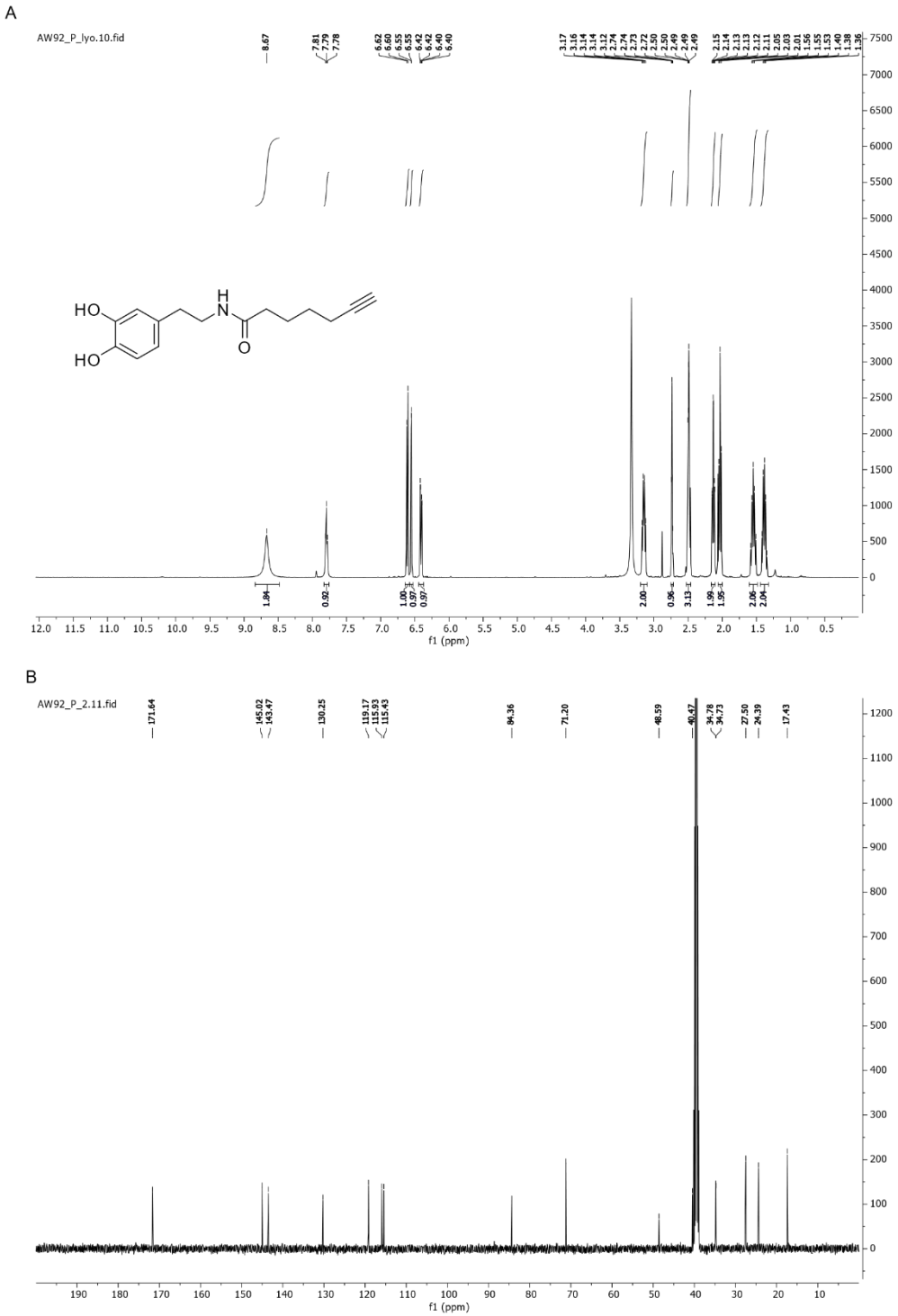

Figure VI-8. NMR spectra of *N*-(3,4-dihydroxyphenethyl)hept-6-ynamide (**DA-P3**) in DMSO-d_6. (A) ^{1}H-NMR (400 MHz). (B) ^{13}C-NMR (101 MHz).

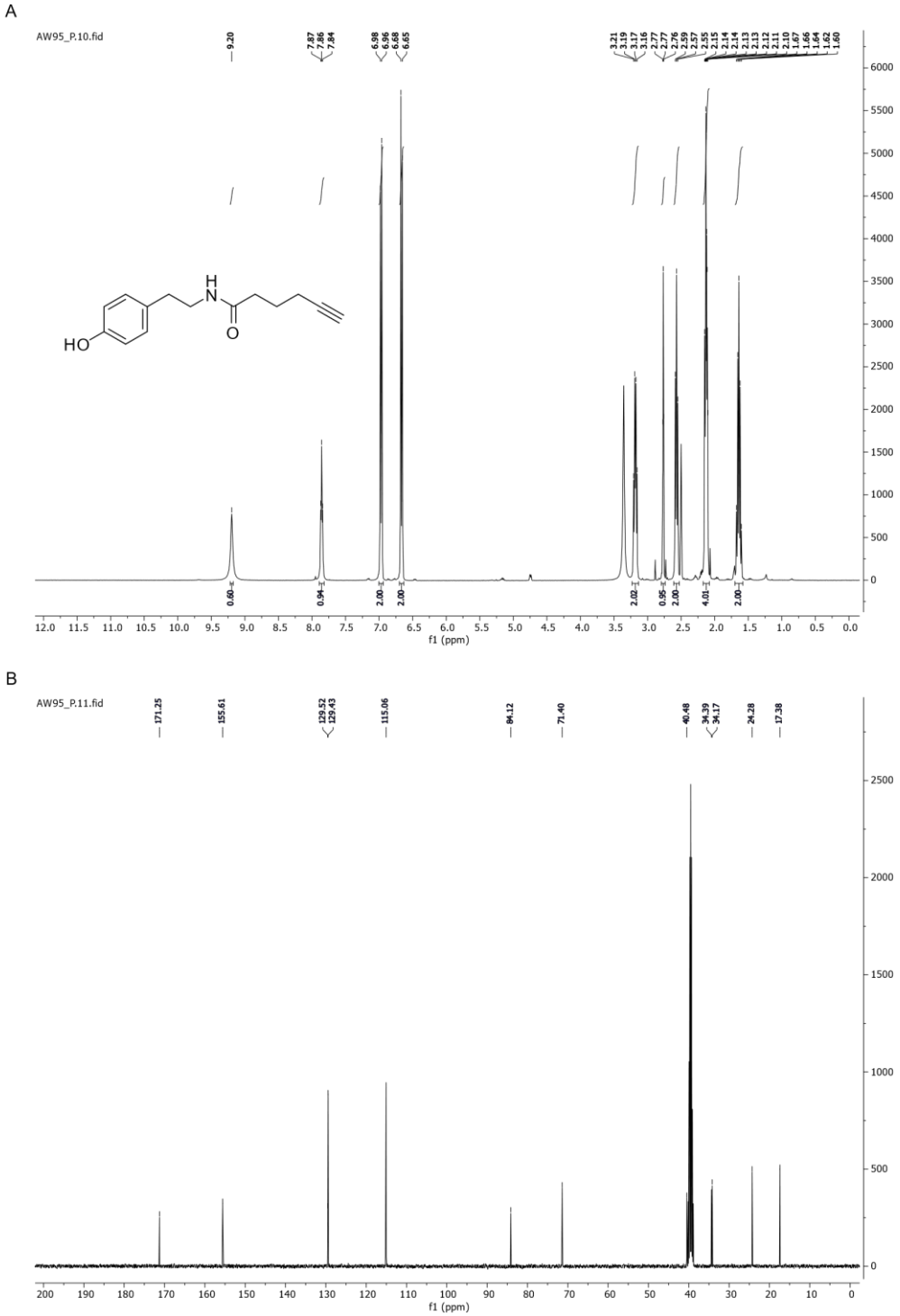

Figure VI-9. NMR spectra of *N*-(4-hydroxyphenethyl)hex-5-ynamide (**DA-P4**) in DMSO-d_6. (A) ^{1}H-NMR (400 MHz). (B) ^{13}C-NMR (101 MHz).

2 Protein tables

Table VI-1: Proteins significantly enriched by **DA-P3** (15 µM) compared to a DMSO control in Hek293 cells.

Protein IDs	Gene names	Protein names	-log$_{10}$(*p*-value)	log$_2$(enrichment)
O75410	*TACC1*	Transforming acidic coiled-coil-containing protein 1	2.36	8.44
Q92575	*UBXN4*	UBX domain-containing protein 4	3.33	8.21
Q6NUQ1	*RINT1*	RAD50-interacting protein 1	6.43	7.64
Q9Y6A5	*TACC3*	Transforming acidic coiled-coil-containing protein 3	3.01	6.43
Q8N2G8	*GHDC*	GH3 domain-containing protein	2.23	6.35
P33981	*TTK*	Dual specificity protein kinase TTK	3.79	6.28
P46821	*MAP1B*	Microtubule-associated protein 1B	3.43	6.20
O75330	*HMMR*	Hyaluronan mediated motility receptor	2.76	6.20
Q86XL3	*ANKLE2*	Ankyrin repeat and LEM domain-containing protein 2	4.02	6.18
P18031	*PTPN1*	Tyrosine-protein phosphatase non-receptor type 1	2.56	6.17
Q969V6	*MKL1*	MKL/myocardin-like protein 1	3.45	6.14
Q14318	*FKBP8*	Peptidyl-prolyl cis-trans isomerase FKBP8	4.60	6.04
Q8IX90	*SKA3*	Spindle and kinetochore-associated protein 3	3.26	6.04
Q69YH5	*CDCA2*	Cell division cycle-associated protein 2	4.33	6.00
Q9UJY4	*GGA2*	ADP-ribosylation factor-binding protein GGA2	3.46	5.99
Q96PC5	*MIA2*	Melanoma inhibitory activity protein 2	3.13	5.98
Q32MZ4	*LRRFIP1*	Leucine-rich repeat flightless-interacting protein 1	5.83	5.98
O95817	*BAG3*	BAG family molecular chaperone regulator 3	4.61	5.91
Q8ND24	*RNF214*	RING finger protein 214	3.99	5.81
P18850	*ATF6*	Cyclic AMP-dependent transcription factor ATF-6 alpha	4.44	5.69
O95197	*RTN3*	Reticulon-3	4.00	5.66
O95881	*TXNDC12*	Thioredoxin domain-containing protein 12	3.77	5.59
P20810	*CAST*	Calpastatin	3.15	5.58
Q2NKX8	*ERCC6L*	DNA excision repair protein ERCC-6-like	2.60	5.53
O60566	*BUB1B*	Mitotic checkpoint serine/threonine-protein kinase BUB1 beta	4.09	5.51
Q8N6T3	*ARFGAP1*	ADP-ribosylation factor GTPase-activating protein 1	5.00	5.51
Q8TEY7	*USP33*	Ubiquitin carboxyl-terminal hydrolase 33	4.70	5.39
Q9Y371	*SH3GLB1*	Endophilin-B1	3.00	5.34
Q5VV42	*CDKAL1*	Threonylcarbamoyladenosine tRNA methylthiotransferase	5.43	5.32
P30519	*HMOX2*	Heme oxygenase 2	5.41	5.31
Q96A49	*SYAP1*	Synapse-associated protein 1	4.61	5.25
Q9UJW0	*DCTN4*	Dynactin subunit 4	3.04	5.15
P05556	*ITGB1*	Integrin beta-1	3.62	5.11
Q9HC62	*SENP2*	Sentrin-specific protease 2	4.15	5.09
P29372	*MPG*	DNA-3-methyladenine glycosylase	3.52	5.05
Q9UGP4	*LIMD1*	LIM domain-containing protein 1	6.07	4.95
P82094	*TMF1*	TATA element modulatory factor	3.66	4.65
O15121	*DEGS1*	Sphingolipid delta(4)-desaturase DES1	2.20	4.65
Q8N2K0	*ABHD12*	Monoacylglycerol lipase ABHD12	3.59	4.65
Q8NG31	*CASC5*	Protein CASC5	2.87	4.65
Q08379	*GOLGA2*	Golgin subfamily A member 2	2.13	4.63
Q8NF37	*LPCAT1*	Lysophosphatidylcholine acyltransferase 1	5.37	4.59
P07942	*LAMB1*	Laminin subunit beta-1	2.95	4.56
Q31612	*HLA-B*	HLA class I histocompatibility antigen, B-73 alpha chain	2.95	4.56
Q9Y2W6	*TDRKH*	Tudor and KH domain-containing protein	4.86	4.52
P37198	*NUP62*	Nuclear pore glycoprotein p62	4.79	4.50
P51617	*IRAK1*	Interleukin-1 receptor-associated kinase 1	3.59	4.46
Q9Y4P3	*TBL2*	Transducin beta-like protein 2	2.68	4.43
Q5W0B1	*RNF219*	RING finger protein 219	2.89	4.43
Q92667	*AKAP1*	A-kinase anchor protein 1, mitochondrial	5.54	4.40
Q8NFH5	*NUP35*	Nucleoporin NUP53	6.41	4.38
Q9C0E8	*LNP*	Protein lunapark	3.05	4.37
Q15005	*SPCS2*	Signal peptidase complex subunit 2	5.46	4.32
Q9C0C9	*UBE2O*	E2/E3 hybrid ubiquitin-protein ligase UBE2O	3.97	4.29
O15270	*SPTLC2*	Serine palmitoyltransferase 2	3.72	4.28
P04035	*HMGCR*	3-hydroxy-3-methylglutaryl-coenzyme A reductase	2.42	4.22
Q99640	*PKMYT1*	Membrane-associated tyrosine- and threonine-specific cdc2-inhibitory kinase	2.36	4.21
Q6WKZ4	*RAB11FIP1*	Rab11 family-interacting protein 1	3.11	4.20
Q12802	*AKAP13*	A-kinase anchor protein 13	2.67	4.19
Q95604	*HLA-C*	HLA class I histocompatibility antigen, Cw-17 alpha chain	3.28	4.18
Q53GS7	*GLE1*	Nucleoporin GLE1	3.53	4.18
O14967	*CLGN*	Calmegin	2.41	4.16
Q8N511	*TMEM199*	Transmembrane protein 199	4.59	4.13
Q9NSV4	*DIAPH3*	Protein diaphanous homolog 3	3.72	4.12
O14976	*GAK*	Cyclin-G-associated kinase	4.44	4.12

Q99661	*KIF2C*	Kinesin-like protein KIF2C	2.08	4.06
Q5JRA6	*MIA3*	Melanoma inhibitory activity protein 3	4.22	4.05
P01891	*HLA-A*	HLA class I histocompatibility antigen, A-68 alpha chain	2.86	4.05
O95613	*PCNT*	Pericentrin	2.19	4.01
Q92551	*IP6K1*	Inositol hexakisphosphate kinase 1	4.10	4.01
Q66K74	*MAP1S*	Microtubule-associated protein 1S	2.74	4.00
Q7Z434	*MAVS*	Mitochondrial antiviral-signaling protein	5.30	3.90
O60664	*PLIN3*	Perilipin-3	2.25	3.87
Q3KQU3	*MAP7D1*	MAP7 domain-containing protein 1	2.74	3.87
Q9BSJ8	*ESYT1*	Extended synaptotagmin-1	5.29	3.86
Q8N0X7	*SPG20*	Spartin	4.36	3.84
Q9Y679	*AUP1*	Ancient ubiquitous protein 1	3.36	3.81
Q92615	*LARP4B*	La-related protein 4B	2.76	3.78
Q9Y6I9	*TEX264*	Testis-expressed sequence 264 protein	3.48	3.77
Q9NUQ3	*TXLNG*	Gamma-taxilin	2.98	3.75
O75179	*ANKRD17*	Ankyrin repeat domain-containing protein 17	2.81	3.74
Q8WZA9	*IRGQ*	Immunity-related GTPase family Q protein	4.08	3.69
O60343	*TBC1D4*	TBC1 domain family member 4	4.47	3.66
P49790	*NUP153*	Nuclear pore complex protein Nup153	6.05	3.63
P15170	*GSPT1*	Eukaryotic peptide chain release factor GTP-binding subunit ERF3A	4.67	3.54
Q9P246	*STIM2*	Stromal interaction molecule 2	4.13	3.53
O14910	*LIN7A*	Protein lin-7 homolog A	2.72	3.51
Q96TC7	*RMDN3*	Regulator of microtubule dynamics protein 3	4.06	3.51
O95861	*BPNT1*	3(2),5-bisphosphate nucleotidase 1	2.37	3.50
Q86Y07	*VRK2*	Serine/threonine-protein kinase VRK2	2.32	3.47
Q9UKX7	*NUP50*	Nuclear pore complex protein Nup50	4.36	3.44
P14314	*PRKCSH*	Glucosidase 2 subunit beta	2.69	3.42
P08240	*SRPR*	Signal recognition particle receptor subunit alpha	4.49	3.42
Q96T51	*RUFY1*	RUN and FYVE domain-containing protein 1	2.20	3.38
Q5T5U3	*ARHGAP21*	Rho GTPase-activating protein 21	2.95	3.36
Q9HD26	*GOPC*	Golgi-associated PDZ and coiled-coil motif-containing protein	2.79	3.36
Q5SNT2	*TMEM201*	Transmembrane protein 201	3.27	3.33
P60468	*SEC61B*	Protein transport protein Sec61 subunit beta	4.38	3.31
P27816	*MAP4*	Microtubule-associated protein 4	5.75	3.30
Q9Y2U8	*LEMD3*	Inner nuclear membrane protein Man1	4.38	3.29
Q6PJG6	*BRAT1*	BRCA1-associated ATM activator 1	2.26	3.29
Q96EA4	*SPDL1*	Protein Spindly	3.09	3.27
Q14554	*PDIA5*	Protein disulfide-isomerase A5	4.55	3.26
O43683	*BUB1*	Mitotic checkpoint serine/threonine-protein kinase BUB1	2.11	3.25
A0MZ66	*KIAA1598*	Shootin-1	4.16	3.23
Q99961	*SH3GL1*	Endophilin-A2	4.14	3.23
Q9UI30	*TRMT112*	Multifunctional methyltransferase subunit TRM112-like protein	3.41	3.21
Q99614	*TTC1*	Tetratricopeptide repeat protein 1	4.46	3.21
Q96R06	*SPAG5*	Sperm-associated antigen 5	3.38	3.20
Q15084	*PDIA6*	Protein disulfide-isomerase A6	3.51	3.19
Q8IWC1	*MAP7D3*	MAP7 domain-containing protein 3	4.25	3.18
Q16204	*CCDC6*	Coiled-coil domain-containing protein 6	2.97	3.17
Q86VQ1	*GLCCI1*	Glucocorticoid-induced transcript 1 protein	3.44	3.14
O95292	*VAPB*	Vesicle-associated membrane protein-associated protein B/C	3.47	3.14
Q8IYA6	*CKAP2L*	Cytoskeleton-associated protein 2-like	2.90	3.13
P49585	*PCYT1A*	Choline-phosphate cytidylyltransferase A	3.43	3.07
Q8ND83	*SLAIN1*	SLAIN motif-containing protein 1	3.93	3.06
Q9HDC5	*JPH1*	Junctophilin-1	3.53	3.05
P46109	*CRKL*	Crk-like protein	3.23	3.03
O94966	*USP19*	Ubiquitin carboxyl-terminal hydrolase 19	3.03	3.02
Q15027	*ACAP1*	Arf-GAP with coiled-coil, ANK repeat and PH domain-containing protein 1	3.53	3.02
O43303	*CCP110*	Centriolar coiled-coil protein of 110 kDa	3.78	2.92
Q5SQN1	*SNAP47*	Synaptosomal-associated protein 47	5.24	2.89
Q15398	*DLGAP5*	Disks large-associated protein 5	3.34	2.87
P50402	*EMD*	Emerin	4.38	2.87
Q9Y4K4	*MAP4K5*	Mitogen-activated protein kinase kinase kinase kinase 5	2.86	2.86
P22681	*CBL*	E3 ubiquitin-protein ligase CBL	2.19	2.85
Q92545	*TMEM131*	Transmembrane protein 131	3.06	2.84
Q9H7E9	*C8orf33*	UPF0488 protein C8orf33	3.46	2.84
O75113	*N4BP1*	NEDD4-binding protein 1	2.47	2.84
Q9BXB4	*OSBPL11*	Oxysterol-binding protein-related protein 11	3.63	2.81
Q9UL46	*PSME2*	Proteasome activator complex subunit 2	2.51	2.81
Q8IV63	*VRK3*	Inactive serine/threonine-protein kinase VRK3	2.04	2.80
Q96HE7	*ERO1L*	ERO1-like protein alpha	2.85	2.79
P04080	*CSTB*	Cystatin-B	2.96	2.78
O15027	*SEC16A*	Protein transport protein Sec16A	3.65	2.78

Q96SK2	*TMEM209*	Transmembrane protein 209	3.09	2.75
Q9NYZ3	*GTSE1*	G2 and S phase-expressed protein 1	2.59	2.74
Q9H3P7	*ACBD3*	Golgi resident protein GCP60	2.35	2.74
O75475	*PSIP1*	PC4 and SFRS1-interacting protein	2.34	2.73
Q96HA1	*POM121*	Nuclear envelope pore membrane protein POM 121	2.94	2.73
Q8NB90	*SPATA5*	Spermatogenesis-associated protein 5	2.18	2.72
P02545	*LMNA*	Prelamin-A/C	6.73	2.71
Q9NQW6	*ANLN*	Actin-binding protein anillin	3.06	2.71
Q14BN4	*SLMAP*	Sarcolemmal membrane-associated protein	2.12	2.71
Q9BSD7	*NTPCR*	Cancer-related nucleoside-triphosphatase	2.39	2.69
P11047	*LAMC1*	Laminin subunit gamma-1	2.01	2.68
P35670	*ATP7B*	Copper-transporting ATPase 2	2.74	2.68
P40855	*PEX19*	Peroxisomal biogenesis factor 19	3.54	2.66
Q6P2H3	*CEP85*	Centrosomal protein of 85 kDa	3.41	2.66
Q14145	*KEAP1*	Kelch-like ECH-associated protein 1	2.63	2.65
O60427	*FADS1*	Fatty acid desaturase 1	4.92	2.64
O60678	*PRMT3*	Protein arginine N-methyltransferase 3	2.04	2.63
Q92542	*NCSTN*	Nicastrin	2.04	2.62
Q9NXV2	*KCTD5*	BTB/POZ domain-containing protein KCTD5	4.32	2.62
Q9NRY5	*FAM114A2*	Protein FAM114A2	3.04	2.60
Q16643	*DBN1*	Drebrin	4.39	2.59
Q8TCT9	*HM13*	Minor histocompatibility antigen H13	2.38	2.56
Q9H0U3	*MAGT1*	Magnesium transporter protein 1	2.13	2.56
Q9H910	*HN1L*	Hematological and neurological expressed 1-like protein	3.94	2.55
O75131	*CPNE3*	Copine-3	4.14	2.53
Q8WU90	*ZC3H15*	Zinc finger CCCH domain-containing protein 15	3.04	2.52
E7EVH7	*KLC1*	Kinesin light chain 1	2.84	2.51
Q9UBP0	*SPAST*	Spastin	2.23	2.51
Q9HC38	*GLOD4*	Glyoxalase domain-containing protein 4	3.96	2.50
Q9Y4E8	*USP15*	Ubiquitin carboxyl-terminal hydrolase 15	2.13	2.50
O94901	*SUN1*	SUN domain-containing protein 1	3.57	2.49
Q9Y3C8	*UFC1*	Ubiquitin-fold modifier-conjugating enzyme 1	2.82	2.48
Q9Y277	*VDAC3*	Voltage-dependent anion-selective channel protein 3	4.11	2.48
Q6PL18	*ATAD2*	ATPase family AAA domain-containing protein 2	2.51	2.47
P30101	*PDIA3*	Protein disulfide-isomerase A3	5.01	2.47
P40763	*STAT3*	Signal transducer and activator of transcription 3	2.85	2.46
Q8IYL3	*C1orf174*	UPF0688 protein C1orf174	3.69	2.46
Q5TAX3	*ZCCHC11*	Terminal uridylyltransferase 4	2.25	2.43
Q9BZI7	*UPF3B*	Regulator of nonsense transcripts 3B	2.09	2.42
Q5UIP0	*RIF1*	Telomere-associated protein RIF1	3.99	2.42
Q15003	*NCAPH*	Condensin complex subunit 2	4.03	2.41
A1X283	*SH3PXD2B*	SH3 and PX domain-containing protein 2B	2.60	2.41
P14635	*CCNB1*	G2/mitotic-specific cyclin-B1	3.24	2.41
Q9NT62	*ATG3*	Ubiquitin-like-conjugating enzyme ATG3	3.38	2.41
P48506	*GCLC*	Glutamate--cysteine ligase catalytic subunit	3.42	2.41
Q6P1L5	*FAM117B*	Protein FAM117B	2.68	2.40
O15269	*SPTLC1*	Serine palmitoyltransferase 1	3.37	2.38
P07237	*P4HB*	Protein disulfide-isomerase	4.05	2.37
Q16352	*INA*	Alpha-internexin	2.90	2.37
Q13111	*CHAF1A*	Chromatin assembly factor 1 subunit A	2.34	2.35
Q8WXH0	*SYNE2*	Nesprin-2	3.40	2.34
O60547	*GMDS*	GDP-mannose 4,6 dehydratase	2.68	2.34
Q9Y2I1	*NISCH*	Nischarin	3.54	2.33
O43847	*NRD1*	Nardilysin	2.71	2.33
P22059	*OSBP*	Oxysterol-binding protein 1	3.36	2.33
Q9Y2Z0	*SUGT1*	Suppressor of G2 allele of SKP1 homolog	3.38	2.30
O95336	*PGLS*	6-phosphogluconolactonase	2.27	2.27
Q15417	*CNN3*	Calponin-3	2.82	2.25
Q9Y2H6	*FNDC3A*	Fibronectin type-III domain-containing protein 3A	3.20	2.25
Q8NDC0	*MAPK1IP1L*	MAPK-interacting and spindle-stabilizing protein-like	2.70	2.24
P10599	*TXN*	Thioredoxin	2.00	2.24
Q96JN0	*LCOR*	Ligand-dependent corepressor	2.32	2.22
Q04864	*REL*	Proto-oncogene c-Rel	2.47	2.22
Q00577	*PURA*	Transcriptional activator protein Pur-alpha	2.89	2.21
Q9NRL3	*STRN4*	Striatin-4	3.43	2.21
O60271	*SPAG9*	C-Jun-amino-terminal kinase-interacting protein 4	2.03	2.21
Q8N8S7	*ENAH*	Protein enabled homolog	3.63	2.20
Q9Y5K6	*CD2AP*	CD2-associated protein	2.35	2.20
P13861	*PRKAR2A*	cAMP-dependent protein kinase type II-alpha regulatory subunit	3.32	2.20
Q9H6S0	*YTHDC2*	Probable ATP-dependent RNA helicase YTHDC2	3.33	2.20
Q5JSH3	*WDR44*	WD repeat-containing protein 44	2.21	2.19
P22061	*PCMT1*	Protein-L-isoaspartate(D-aspartate) O-methyltransferase	3.16	2.19
Q9Y3P9	*RABGAP1*	Rab GTPase-activating protein 1	5.03	2.19

O75694	*NUP155*	Nuclear pore complex protein Nup155	2.63	2.17
P49589	*CARS*	Cysteine--tRNA ligase, cytoplasmic	2.73	2.17
P42166	*TMPO*	Lamina-associated polypeptide 2, isoform alpha	4.33	2.17
Q15654	*TRIP6*	Thyroid receptor-interacting protein 6	2.71	2.17
Q13162	*PRDX4*	Peroxiredoxin-4	3.86	2.15
Q9NZT2	*OGFR*	Opioid growth factor receptor	2.73	2.15
Q9BW91	*NUDT9*	ADP-ribose pyrophosphatase, mitochondrial	2.45	2.15
Q9UHR4	*BAIAP2L1*	Brain-specific angiogenesis inhibitor 1-associated protein 2-like protein 1	4.27	2.12
Q6UVJ0	*SASS6*	Spindle assembly abnormal protein 6 homolog	4.50	2.12
Q5H8A4	*PIGG*	GPI ethanolamine phosphate transferase 2	2.94	2.12
O95757	*HSPA4L*	Heat shock 70 kDa protein 4L	3.34	2.10
P40222	*TXLNA*	Alpha-taxilin	3.85	2.10
Q9Y2G8	*DNAJC16*	DnaJ homolog subfamily C member 16	3.20	2.10
Q9Y266	*NUDC*	Nuclear migration protein nudC	2.95	2.10
P49792	*RANBP2*	E3 SUMO-protein ligase RanBP2	5.46	2.09
Q9HCU5	*PREB*	Prolactin regulatory element-binding protein	2.35	2.08
P27348	*YWHAQ*	14-3-3 protein theta	3.70	2.08
Q8NHH9	*ATL2*	Atlastin-2	3.02	2.08
O75044	*SRGAP2*	SLIT-ROBO Rho GTPase-activating protein 2	4.15	2.07
Q6P1N0	*CC2D1A*	Coiled-coil and C2 domain-containing protein 1A	2.87	2.07
Q5VZ89	*DENND4C*	DENN domain-containing protein 4C	3.23	2.07
P61586	*RHOA*	Transforming protein RhoA	2.93	2.05
P0DN79	*CBS*	Cystathionine beta-synthase	3.50	2.04
Q8WX93	*PALLD*	Palladin	2.44	2.04
Q9NPH2	*ISYNA1*	Inositol-3-phosphate synthase 1	3.85	2.02
Q86WB0	*ZC3HC1*	Nuclear-interacting partner of ALK	3.60	2.01
Q9BZE9	*ASPSCR1*	Tether containing UBX domain for GLUT4	2.02	2.01

Table VI-2: Proteins significantly outcompeted by a 30-fold excess of **DA** vs. 15 µM **DA-P3** in Hek293 cells.

Protein IDs	**Gene names**	**Protein names**	**$-\log_{10}$(*p*-value)**	**$\log_2$(enrichment)**
Q969V6	*MKL1*	MKL/myocardin-like protein 1	4.22	6.80
O75410	*TACC1*	Transforming acidic coiled-coil-containing protein 1	2.68	6.53
Q7Z3T8	*ZFYVE16*	Zinc finger FYVE domain-containing protein 16	2.22	5.82
Q6NUQ1	*RINT1*	RAD50-interacting protein 1	2.87	5.71
Q9Y371	*SH3GLB1*	Endophilin-B1	2.83	5.50
Q96A49	*SYAP1*	Synapse-associated protein 1	5.49	5.23
Q9NQC3	*RTN4*	Reticulon-4	2.76	5.19
Q8ND24	*RNF214*	RING finger protein 214	2.43	5.02
Q8N2G8	*GHDC*	GH3 domain-containing protein	2.08	4.98
P20810	*CAST*	Calpastatin	3.14	4.96
Q12802	*AKAP13*	A-kinase anchor protein 13	3.63	4.84
Q9HC62	*SENP2*	Sentrin-specific protease 2	2.90	4.70
Q32MZ4	*LRRFIP1*	Leucine-rich repeat flightless-interacting protein 1	2.32	4.69
Q8N6T3	*ARFGAP1*	ADP-ribosylation factor GTPase-activating protein 1	4.94	4.69
Q9HBM0	*VEZT*	Vezatin	2.24	4.51
Q9UJW0	*DCTN4*	Dynactin subunit 4	2.05	4.49
Q8IX90	*SKA3*	Spindle and kinetochore-associated protein 3	2.35	4.49
O75330	*HMMR*	Hyaluronan mediated motility receptor	2.32	4.40
P33981	*TTK*	Dual specificity protein kinase TTK	2.81	4.39
Q5W0B1	*RNF219*	RING finger protein 219	2.78	4.37
Q99640	*PKMYT1*	Membrane-associated tyrosine- and threonine-specific cdc2-inhibitory kinase	2.16	4.37
Q2NKX8	*ERCC6L*	DNA excision repair protein ERCC-6-like	3.52	4.37
O95817	*BAG3*	BAG family molecular chaperone regulator 3	4.00	4.33
Q9NW68	*BSDC1*	BSD domain-containing protein 1	2.72	4.30
Q9UGP4	*LIMD1*	LIM domain-containing protein 1	3.43	4.28
Q9NSV4	*DIAPH3*	Protein diaphanous homolog 3	2.87	4.16
Q5UCC4	*EMC10*	ER membrane protein complex subunit 10	2.53	4.14
O60566	*BUB1B*	Mitotic checkpoint serine/threonine-protein kinase BUB1 beta	2.17	4.00
O95197	*RTN3*	Reticulon-3	2.62	3.93
Q9UJY4	*GGA2*	ADP-ribosylation factor-binding protein GGA2	3.43	3.93
Q69YH5	*CDCA2*	Cell division cycle-associated protein 2	2.31	3.90
P49069	*CAMLG*	Calcium signal-modulating cyclophilin ligand	2.10	3.88
Q92551	*IP6K1*	Inositol hexakisphosphate kinase 1	2.69	3.87
O95613	*PCNT*	Pericentrin	2.77	3.85
P46821	*MAP1B*	Microtubule-associated protein 1B	3.60	3.85
Q6ZWJ1	*STXBP4*	Syntaxin-binding protein 4	2.23	3.84
Q8NG31	*CASC5*	Protein CASC5	2.33	3.82
O60427	*FADS1*	Fatty acid desaturase 1	4.16	3.82
Q9Y2W6	*TDRKH*	Tudor and KH domain-containing protein	3.27	3.80
O75223	*GGCT*	Gamma-glutamylcyclotransferase	2.26	3.79

P20290	*BTF3*	Transcription factor BTF3	2.88	3.77
P98194	*ATP2C1*	Calcium-transporting ATPase type 2C member 1	2.57	3.75
Q92615	*LARP4B*	La-related protein 4B	2.57	3.74
Q96R06	*SPAG5*	Sperm-associated antigen 5	2.48	3.67
Q9C0E8	*LNP*	Protein lunapark	2.95	3.67
P51617	*IRAK1*	Interleukin-1 receptor-associated kinase 1	2.55	3.66
Q92575	*UBXN4*	UBX domain-containing protein 4	2.00	3.64
Q8NFQ8	*TOR1AIP2*	Torsin-1A-interacting protein 2	2.07	3.62
Q6PJG6	*BRAT1*	BRCA1-associated ATM activator 1	2.87	3.62
P28290	*SSFA2*	Sperm-specific antigen 2	2.42	3.61
Q5T8D3	*ACBD5*	Acyl-CoA-binding domain-containing protein 5	2.44	3.57
Q14318	*FKBP8*	Peptidyl-prolyl cis-trans isomerase FKBP8	2.35	3.57
P01891	*HLA-A*	HLA class I histocompatibility antigen, A-68 alpha chain	2.95	3.57
Q08379	*GOLGA2*	Golgin subfamily A member 2	2.22	3.56
P29372	*MPG*	DNA-3-methyladenine glycosylase	2.58	3.49
Q53GS7	*GLE1*	Nucleoporin GLE1	2.63	3.48
O95816	*BAG2*	BAG family molecular chaperone regulator 2	2.13	3.48
Q9Y6A5	*TACC3*	Transforming acidic coiled-coil-containing protein 3	2.47	3.47
Q9Y4P1	*ATG4B*	Cysteine protease ATG4B	3.23	3.47
O14967	*CLGN*	Calmegin	2.80	3.41
P04035	*HMGCR*	3-hydroxy-3-methylglutaryl-coenzyme A reductase	2.31	3.41
Q8WZA9	*IRGQ*	Immunity-related GTPase family Q protein	3.56	3.38
Q3KQU3	*MAP7D1*	MAP7 domain-containing protein 1	2.06	3.37
Q9NZZ3	*CHMP5*	Charged multivesicular body protein 5	2.43	3.36
Q9NP61	*ARFGAP3*	ADP-ribosylation factor GTPase-activating protein 3	2.32	3.35
Q5VV42	*CDKAL1*	Threonylcarbamoyladenosine tRNA methylthiotransferase	2.80	3.32
O60664	*PLIN3*	Perilipin-3	2.22	3.32
O75113	*N4BP1*	NEDD4-binding protein 1	2.97	3.29
Q96PC5	*MIA2*	Melanoma inhibitory activity protein 2	2.45	3.27
P49585	*PCYT1A*	Choline-phosphate cytidylyltransferase A	3.45	3.25
Q8TEY7	*USP33*	Ubiquitin carboxyl-terminal hydrolase 33	2.05	3.24
Q9C0C2	*TNKS1BP1*	182 kDa tankyrase-1-binding protein	2.61	3.24
Q9Y6I9	*TEX264*	Testis-expressed sequence 264 protein	2.94	3.20
O43169	*CYB5B*	Cytochrome b5 type B	2.52	3.14
O60343	*TBC1D4*	TBC1 domain family member 4	2.60	3.13
Q9Y4P3	*TBL2*	Transducin beta-like protein 2	2.46	3.12
Q9HD20	*ATP13A1*	Manganese-transporting ATPase 13A1	3.00	3.10
Q9H3P7	*ACBD3*	Golgi resident protein GCP60	2.21	3.09
O95861	*BPNT1*	3(2),5-bisphosphate nucleotidase 1	2.00	3.09
Q8NF37	*LPCAT1*	Lysophosphatidylcholine acyltransferase 1	2.73	3.07
A6NDG6	*PGP*	Phosphoglycolate phosphatase	3.15	3.06
O00244	*ATOX1*	Copper transport protein ATOX1	2.24	3.04
Q6P1L5	*FAM117B*	Protein FAM117B	3.62	3.04
O75179	*ANKRD17*	Ankyrin repeat domain-containing protein 17	2.54	3.03
Q66K74	*MAP1S*	Microtubule-associated protein 1S	2.76	3.03
Q8N511	*TMEM199*	Transmembrane protein 199	2.05	3.00
O14618	*CCS*	Copper chaperone for superoxide dismutase	2.22	2.93
Q9UKA4	*AKAP11*	A-kinase anchor protein 11	2.02	2.93
P37198	*NUP62*	Nuclear pore glycoprotein p62	3.46	2.92
P30519	*HMOX2*	Heme oxygenase 2	2.64	2.92
O14910	*LIN7A*	Protein lin-7 homolog A	2.38	2.91
O14976	*GAK*	Cyclin-G-associated kinase	2.58	2.91
Q8N0X7	*SPG20*	Spartin	2.87	2.91
O00161	*SNAP23*	Synaptosomal-associated protein 23	2.01	2.89
Q6WKZ4	*RAB11FIP1*	Rab11 family-interacting protein 1	2.85	2.88
Q8N5S9	*CAMKK1*	Calcium/calmodulin-dependent protein kinase kinase 1	3.56	2.88
Q86VQ1	*GLCCI1*	Glucocorticoid-induced transcript 1 protein	2.72	2.85
O43164	*PJA2*	E3 ubiquitin-protein ligase Praja-2	2.75	2.85
Q8IYA6	*CKAP2L*	Cytoskeleton-associated protein 2-like	3.45	2.84
Q9BSJ8	*ESYT1*	Extended synaptotagmin-1	2.96	2.84
Q8NFH5	*NUP35*	Nucleoporin NUP53	2.99	2.82
Q15005	*SPCS2*	Signal peptidase complex subunit 2	2.57	2.78
Q96GA3	*LTV1*	Protein LTV1 homolog	2.06	2.78
P08240	*SRPR*	Signal recognition particle receptor subunit alpha	3.29	2.73
Q5T5U3	*ARHGAP21*	Rho GTPase-activating protein 21	2.05	2.72
Q6P2H3	*CEP85*	Centrosomal protein of 85 kDa	3.18	2.71
Q8NB90	*SPATA5*	Spermatogenesis-associated protein 5	2.19	2.71
Q9HD26	*GOPC*	Golgi-associated PDZ and coiled-coil motif-containing protein	3.48	2.70
Q9HC38	*GLOD4*	Glyoxalase domain-containing protein 4	3.98	2.69
Q7Z434	*MAVS*	Mitochondrial antiviral-signaling protein	2.38	2.69
Q86Y07	*VRK2*	Serine/threonine-protein kinase VRK2	3.04	2.68
Q16204	*CCDC6*	Coiled-coil domain-containing protein 6	2.55	2.67
Q6PGQ7	*BORA*	Protein aurora borealis	2.27	2.66

Q5SQN1	*SNAP47*	Synaptosomal-associated protein 47	4.58	2.66
A0MZ66	*KIAA1598*	Shootin-1	2.89	2.64
Q96IZ6	*METTL2A*	Methyltransferase-like protein 2A	2.37	2.62
Q9NQW6	*ANLN*	Actin-binding protein anillin	3.22	2.62
Q9BWU0	*SLC4A1AP*	Kanadaptin	2.56	2.62
O43683	*BUB1*	Mitotic checkpoint serine/threonine-protein kinase BUB1	3.51	2.61
O43303	*CCP110*	Centriolar coiled-coil protein of 110 kDa	4.00	2.61
Q92667	*AKAP1*	A-kinase anchor protein 1, mitochondrial	2.52	2.60
P01893	*HLA-H*	Putative HLA class I histocompatibility antigen, alpha chain H	2.05	2.58
Q9Y679	*AUP1*	Ancient ubiquitous protein 1	2.63	2.57
Q9C0C9	*UBE2O*	E2/E3 hybrid ubiquitin-protein ligase UBE2O	2.19	2.56
Q96TC7	*RMDN3*	Regulator of microtubule dynamics protein 3	3.05	2.56
Q9GZP4	*PITHD1*	PITH domain-containing protein 1	2.08	2.55
Q6UVJ0	*SASS6*	Spindle assembly abnormal protein 6 homolog	3.17	2.54
Q9NXV2	*KCTD5*	BTB/POZ domain-containing protein KCTD5	3.86	2.54
Q99614	*TTC1*	Tetratricopeptide repeat protein 1	2.28	2.53
P22681	*CBL*	E3 ubiquitin-protein ligase CBL	2.47	2.52
P27816	*MAP4*	Microtubule-associated protein 4	3.09	2.51
Q96HA1	*POM121*	Nuclear envelope pore membrane protein POM 121	3.29	2.49
P07942	*LAMB1*	Laminin subunit beta-1	2.08	2.49
P49247	*RPIA*	Ribose-5-phosphate isomerase	2.46	2.48
Q9NUQ3	*TXLNG*	Gamma-taxilin	2.98	2.48
Q5JRA6	*MIA3*	Melanoma inhibitory activity protein 3	2.03	2.46
O76024	*WFS1*	Wolframin	2.69	2.43
Q9Y2U8	*LEMD3*	Inner nuclear membrane protein Man1	2.65	2.43
Q9NP72	*RAB18*	Ras-related protein Rab-18	2.54	2.41
Q9UI30	*TRMT112*	Multifunctional methyltransferase subunit TRM112-like protein	2.49	2.41
P15170	*GSPT1*	Eukaryotic peptide chain release factor GTP-binding subunit ERF3A	3.93	2.40
Q8IWC1	*MAP7D3*	MAP7 domain-containing protein 3	2.67	2.40
Q9NZT2	*OGFR*	Opioid growth factor receptor	2.71	2.39
P12109	*COL6A1*	Collagen alpha-1(VI) chain	2.27	2.39
Q99661	*KIF2C*	Kinesin-like protein KIF2C	3.29	2.38
Q99961	*SH3GL1*	Endophilin-A2	2.54	2.37
Q9Y4E8	*USP15*	Ubiquitin carboxyl-terminal hydrolase 15	2.45	2.34
Q96T51	*RUFY1*	RUN and FYVE domain-containing protein 1	2.02	2.33
P60468	*SEC61B*	Protein transport protein Sec61 subunit beta	2.45	2.33
Q9H7E9	*C8orf33*	UPF0488 protein C8orf33	3.14	2.31
P40763	*STAT3*	Signal transducer and activator of transcription 3	2.87	2.31
E7EVH7	*KLC1*	Kinesin light chain 1	3.49	2.31
P46109	*CRKL*	Crk-like protein	2.23	2.31
P49790	*NUP153*	Nuclear pore complex protein Nup153	2.37	2.30
Q9UKX7	*NUP50*	Nuclear pore complex protein Nup50	2.97	2.29
Q96KC8	*DNAJC1*	DnaJ homolog subfamily C member 1	4.40	2.28
Q8NDI1	*EHBP1*	EH domain-binding protein 1	2.05	2.26
O60784	*TOM1*	Target of Myb protein 1	3.44	2.25
Q9HDC5	*JPH1*	Junctophilin-1	3.23	2.25
Q14BN4	*SLMAP*	Sarcolemmal membrane-associated protein	2.16	2.24
Q9Y4K4	*MAP4K5*	Mitogen-activated protein kinase kinase kinase kinase 5	2.64	2.24
O60547	*GMDS*	GDP-mannose 4,6 dehydratase	2.65	2.24
Q9UHD1	*CHORDC1*	Cysteine and histidine-rich domain-containing protein 1	2.52	2.23
Q16512	*PKN1*	Serine/threonine-protein kinase N1	2.08	2.23
Q8NBK3	*SUMF1*	Sulfatase-modifying factor 1	2.80	2.22
Q9NRY5	*FAM114A2*	Protein FAM114A2	3.04	2.21
Q9Y3C8	*UFC1*	Ubiquitin-fold modifier-conjugating enzyme 1	2.48	2.21
O60232	*SSSCA1*	Sjoegren syndrome/scleroderma autoantigen 1	3.11	2.20
O75131	*CPNE3*	Copine-3	3.11	2.20
Q8ND83	*SLAIN1*	SLAIN motif-containing protein 1	2.68	2.20
P48506	*GCLC*	Glutamate--cysteine ligase catalytic subunit	4.03	2.19
Q9NT62	*ATG3*	Ubiquitin-like-conjugating enzyme ATG3	3.19	2.18
P04080	*CSTB*	Cystatin-B	2.59	2.16
Q8IV63	*VRK3*	Inactive serine/threonine-protein kinase VRK3	2.11	2.15
Q2M3G4	*SHROOM1*	Protein Shroom1	2.67	2.15
O60678	*PRMT3*	Protein arginine N-methyltransferase 3	3.63	2.15
Q9H0U3	*MAGT1*	Magnesium transporter protein 1	2.20	2.14
Q9P246	*STIM2*	Stromal interaction molecule 2	2.97	2.13
P54646	*PRKAA2*	5-AMP-activated protein kinase catalytic subunit alpha-2	2.54	2.13
Q14554	*PDIA5*	Protein disulfide-isomerase A5	2.50	2.12
Q14145	*KEAP1*	Kelch-like ECH-associated protein 1	2.78	2.11
Q15398	*DLGAP5*	Disks large-associated protein 5	2.03	2.11
Q04864	*REL*	Proto-oncogene c-Rel	2.45	2.10
Q9Y478	*PRKAB1*	5-AMP-activated protein kinase subunit beta-1	2.16	2.10
Q13190	*STX5*	Syntaxin-5	2.56	2.10

Q8TC07	*TBC1D15*	TBC1 domain family member 15	2.42	2.10
P40855	*PEX19*	Peroxisomal biogenesis factor 19	2.38	2.09
O15027	*SEC16A*	Protein transport protein Sec16A	2.37	2.09
Q9UL46	*PSME2*	Proteasome activator complex subunit 2	2.60	2.09
P22059	*OSBP*	Oxysterol-binding protein 1	3.20	2.07
Q9BZI7	*UPF3B*	Regulator of nonsense transcripts 3B	2.51	2.06
Q96C19	*EFHD2*	EF-hand domain-containing protein D2	2.26	2.05
Q96I15	*SCLY*	Selenocysteine lyase	2.50	2.05
Q8IYL3	*C1orf174*	UPF0688 protein C1orf174	2.59	2.05
Q7Z4H7	*HAUS6*	HAUS augmin-like complex subunit 6	3.67	2.04
Q15003	*NCAPH*	Condensin complex subunit 2	3.66	2.04
Q96EA4	*SPDL1*	Protein Spindly	2.52	2.03
Q9Y5A7	*NUB1*	NEDD8 ultimate buster 1	2.03	2.02
Q12968	*NFATC3*	Nuclear factor of activated T-cells, cytoplasmic 3	2.06	2.02
Q96BW5	*PTER*	Phosphotriesterase-related protein	2.56	2.02
Q5H8A4	*PIGG*	GPI ethanolamine phosphate transferase 2	3.02	2.01
Q7Z569	*BRAP*	BRCA1-associated protein	2.61	2.01
Q9Y2H6	*FNDC3A*	Fibronectin type-III domain-containing protein 3A	2.74	2.01
Q8WU90	*ZC3H15*	Zinc finger CCCH domain-containing protein 15	2.41	2.00
Q9H6S0	*YTHDC2*	Probable ATP-dependent RNA helicase YTHDC2	2.82	2.00

Table VI-3: Proteins significantly enriched by **DA-P3** (15 µM) in *DJ-1*$^{+/+}$ mouse neurons.

Protein IDs	**Gene names**	**Protein names**	**-log$_{10}$(*p*-value)**	**log$_2$(enrichment)**
Q9CQU0	*Txndc12*	Thioredoxin domain-containing protein 12	4.75	8.67
Q9JLV1	*Bag3*	BAG family molecular chaperone regulator 3	4.94	7.82
Q6GU23	*Stat3*	Signal transducer and activator of transcription	6.72	7.57
Q80YN3	*Bcas1*	Breast carcinoma-amplified sequence 1 homolog	5.34	7.52
Z4YM84	*Acbd5*		6.74	7.26
F8VQ95	*Tacc1*	Transforming acidic coiled-coil-containing protein 1	5.64	7.07
Q9CWE0	*Mtfr1l*	Mitochondrial fission regulator 1-like	3.53	6.84
Q6P9S0	*Mtss1l*	MTSS1-like protein	7.04	6.56
Q99KC8	*Vwa5a*	von Willebrand factor A domain-containing protein 5A	3.99	5.84
Q9ESW8	*Pgpep1*	Pyroglutamyl-peptidase 1	4.53	5.73
Q5DTJ4	*Prrc2a*	Protein PRRC2A	6.47	5.68
Q8WTY4	*Ciapin1*	Anamorsin	6.78	5.56
A2RS58	*Crkl*	Crk-like protein	4.31	5.29
P52479	*Usp10*	Ubiquitin carboxyl-terminal hydrolase 10	4.94	5.23
E9QAT4	*Sec16a*		4.04	5.21
A0A0R4J078	*Ubxn4*	UBX domain-containing protein 4	3.58	5.19
Q8C078	*Camkk2*	Calcium/calmodulin-dependent protein kinase kinase 2	5.43	5.10
Q5SWP3	*Nacad*	NAC-alpha domain-containing protein 1	3.75	5.06
Q544R7	*Hmox2*	Heme oxygenase 2	5.34	5.06
Q8K354	*Cbr3*	Carbonyl reductase [NADPH] 3	4.11	4.98
Q80WR0	*Nup153*		4.39	4.96
E9QKG6	*Ankrd17*	Ankyrin repeat domain-containing protein 17	3.08	4.91
Q6P5H2	*Nes*	Nestin	3.22	4.91
P70271	*Pdlim4*	PDZ and LIM domain protein 4	3.43	4.74
S4R2J9	*Prrc2c*	Protein PRRC2C	3.47	4.66
F7AA26	*Pakap*	A-kinase anchor protein 2	4.78	4.64
Q9DAW9	*Cnn3*	Calponin-3	3.60	4.60
Q9QYG0	*Ndrg2*	Protein NDRG2	4.16	4.60
Q9ES97	*Rtn3*	Reticulon-3	6.56	4.54
Q8C0M9	*Asrgl1*	Isoaspartyl peptidase/L-asparaginase	6.73	4.52
Q80WJ7	*Mtdh*	Protein LYRIC	6.05	4.51
Q9CY49	*Tbl2*	Transducin beta-like protein 2	4.45	4.47
Q9CQ65	*Mtap*	S-methyl-5-thioadenosine phosphorylase	4.79	4.45
A0A1W2P872			3.66	4.40
E9QP59	*Lemd3*	Inner nuclear membrane protein Man1	3.83	4.38
Q9D7S9	*Chmp5*	Charged multivesicular body protein 5	6.30	4.36
A0A0A6YW06	*Enah*	Protein enabled homolog	6.56	4.34
P48774	*Gstm5*	Glutathione S-transferase Mu 5	3.00	4.33
Q8BI84	*Mia3*	Melanoma inhibitory activity protein 3	4.97	4.33
Q8BGR3	*Camk4*	Calcium/calmodulin-dependent protein kinase type IV	4.47	4.32
Q921M8	*Usp4*	Ubiquitin carboxyl-terminal hydrolase	4.16	4.27
A2AMY5	*Ubap2*	Ubiquitin-associated protein 2	2.20	4.15
Q60865	*Caprin1*	Caprin-1	3.87	4.12
A2AG50	*Map7d2*	MAP7 domain-containing protein 2	2.45	4.11
Q3TDD8	*Eif4b*	Eukaryotic translation initiation factor 4B	7.21	4.09
Q8VBT0	*Tmx1*	Thioredoxin-related transmembrane protein 1	3.96	4.07
E9PUC4	*Sphkap*	A-kinase anchor protein SPHKAP	2.61	4.06
Q8BFU3	*Rnf214*	RING finger protein 214	3.06	4.05
Q3U7E0	*Atp6v1g1*	V-type proton ATPase subunit G 1	5.06	4.01

Q80UU9	*Pgrmc2*	Membrane-associated progesterone receptor component 2	4.16	4.01
Q5SSZ5	*Tns3*	Tensin-3	3.72	4.00
P31230	*Aimp1*	Aminoacyl tRNA synthase complex-interacting multifunctional protein 1	5.94	4.00
P49586	*Pcyt1a*	Choline-phosphate cytidylyltransferase A	3.22	4.00
Q5NCM6	*Epn2*	Epsin-2	5.18	3.98
O35465	*Fkbp8*	Peptidyl-prolyl cis-trans isomerase FKBP8	5.82	3.95
Q9DBG7	*Srpr*	Signal recognition particle receptor subunit alpha	4.44	3.93
Q8BIW1	*Prune*	Protein prune homolog	4.31	3.93
Q3TNH0	*Tmpo*	Lamina-associated polypeptide 2, isoforms beta/delta/epsilon/gamma	4.37	3.92
Q3TA75	*Fxr2*	Fragile X mental retardation syndrome-related protein 2	7.43	3.84
Q9ERR1	*Ndel1*	Nuclear distribution protein nudE-like 1	2.72	3.83
Q8CHP8	*Pgp*	Phosphoglycolate phosphatase	6.50	3.83
Q64337	*Sqstm1*	Sequestosome-1	3.74	3.79
Q921L9	*Prkar1b*	cAMP-dependent protein kinase type I-beta regulatory subunit	5.51	3.79
A0A0J9YUR2	*Specc1*	Cytospin-B	2.88	3.78
A0A5F8MPP7	*Sh3pxd2b*	SH3 and PX domain-containing protein 2B	3.53	3.77
Q8VIM9	*Irgq*	Immunity-related GTPase family Q protein	3.92	3.68
D3YU22	*Limch1*	LIM and calponin homology domains-containing protein 1	4.78	3.66
Q99P72	*Rtn4*	Reticulon-4	5.22	3.64
Q9EPJ9	*Arfgap1*	ADP-ribosylation factor GTPase-activating protein 1	4.01	3.64
Q8BZ07	*Srp19*	Signal recognition particle 19 kDa protein	5.04	3.64
Q9JJU8	*Sh3bgrl*	SH3 domain-binding glutamic acid-rich-like protein	5.62	3.63
O08997	*Atox1*	Copper transport protein ATOX1	4.57	3.63
P63040	*Cplx1*	Complexin-1	3.94	3.62
Q91YQ3	*Csdc2*	Cold shock domain-containing protein C2	3.40	3.59
E9QMB7	*Naa30*	N-alpha-acetyltransferase 30	4.77	3.59
Q9CQU5	*Zwint*	ZW10 interactor	2.31	3.54
E9Q3M9	*2010300C02Rik*		3.11	3.54
A0A3B2WBC6			4.92	3.53
E9PVQ3	*Spats2l*	SPATS2-like protein	3.25	3.52
Q922Q1	*Marc2*	Mitochondrial amidoxime reducing component 2	5.69	3.49
Q3UCZ5	*Ptpn1*	Tyrosine-protein phosphatase non-receptor type	5.71	3.46
Q8CCJ4	*Amer2*	APC membrane recruitment protein 2	5.27	3.45
Z4YJU8	*Golga2*	Golgin subfamily A member 2	4.11	3.45
A0A0G2JDN7			3.74	3.43
Q9CPV4	*Glod4*	Glyoxalase domain-containing protein 4	3.71	3.40
P62774	*Mtpn*	Myotrophin	3.32	3.40
Q9CTE8	*Alg5*	Dolichyl-phosphate beta-glucosyltransferase	4.96	3.40
B7ZNS2	*Dlgap4*	Disks large-associated protein 4	4.15	3.38
Q61584	*Fxr1*	Fragile X mental retardation syndrome-related protein 1	6.22	3.36
A0A1D5RLY6	*Map1s*	Microtubule-associated protein 1S	4.81	3.36
E9PZ43	*Map4*	Microtubule-associated protein	5.40	3.35
A0A668KL65			3.87	3.34
P42669	*Pura*	Transcriptional activator protein Pur-alpha	7.04	3.34
O55091	*Impact*	Protein IMPACT	5.42	3.33
Q99PU5	*Acsbg1*	Long-chain-fatty-acid--CoA ligase ACSBG1	6.76	3.32
A0A140LJG6	*Spcs2*	Signal peptidase complex subunit 2	5.53	3.31
P10639	*Txn*	Thioredoxin	6.44	3.25
A0A0A6YX71	*Dclk2*	Serine/threonine-protein kinase DCLK2	4.07	3.24
A8Y5P4	*Map7d1*	MAP7 domain-containing protein 1	6.26	3.19
Q6P1H6	*Ankle2*	Ankyrin repeat and LEM domain-containing protein 2	3.56	3.17
Q6NZD2	*Snx1*	Sorting nexin-1	4.84	3.16
V9GWW6	*Mlip*		3.65	3.15
Q9D898	*Arpc5l*	Actin-related protein 2/3 complex subunit 5-like protein	4.61	3.13
P27546	*Map4*	Microtubule-associated protein 4	9.04	3.13
D3YXP6	*Pmvk*	Phosphomevalonate kinase	2.01	3.12
Q9CQS8	*Sec61b*	Protein transport protein Sec61 subunit beta	5.20	3.10
Q91WT9	*Cbs*	Cystathionine beta-synthase	4.05	3.09
Q4FJL2	*Rtn1*	Reticulon	6.44	3.09
D3Z4S3	*Ptrhd1*	Putative peptidyl-tRNA hydrolase PTRHD1	5.61	3.07
Q8C0L0	*Tmx4*	Thioredoxin-related transmembrane protein 4	4.99	3.07
P17751	*Tpi1*	Triosephosphate isomerase	6.04	3.04
Q99LR1	*Abhd12*	Monoacylglycerol lipase ABHD12	3.52	3.03
P60761	*Nrgn*	Neurogranin	6.26	3.03
Q80Z38	*Shank2*	SH3 and multiple ankyrin repeat domains protein 2	3.21	3.03
O35551	*Rabep1*	Rab GTPase-binding effector protein 1	3.15	3.03
Q3U8S5	*Capn2*	Calpain-2 catalytic subunit	4.65	3.02
A0A1W2P7V0	*Gopc*	Golgi-associated PDZ and coiled-coil motif-containing protein	3.45	3.01

V9GXD9	*Synrg*	Synergin gamma	5.57	3.00
Q99JZ9	*Srp54c*		3.02	2.99
B9EJA2	*Cttnbp2*	Cortactin-binding protein 2	2.91	2.96
Q3TDF3	*Ttc1*	Tetratricopeptide repeat protein 1	5.78	2.95
Q78JW9	*Ubfd1*	Ubiquitin domain-containing protein UBFD1	4.14	2.95
Q8CJ67	*Stau2*	Double-stranded RNA-binding protein Staufen homolog 2	3.18	2.93
Q91YS2	*Rangap1*	Ran GTPase-activating protein 1	3.26	2.92
Q3URF1	*Synpo*	Synaptopodin	2.35	2.91
Q8BKI2	*Tnrc6b*	Trinucleotide repeat-containing gene 6B protein	3.79	2.91
A2AVJ7	*Rrbp1*	Ribosome-binding protein 1	7.24	2.91
P60335	*Pcbp1*	Poly(rC)-binding protein 1	5.85	2.90
Q80YS6	*Afap1*	Actin filament-associated protein 1	3.32	2.89
Q4FK49	*Ppa1*	Inorganic pyrophosphatase	5.21	2.88
F8WJ74	*Gramd1a*	GRAM domain-containing protein 1A	2.34	2.87
Q9R0Z4	*Ehhadh*	Peroxisomal bifunctional enzyme	4.01	2.87
A0A0R4J260	*Otud4*	OTU domain-containing protein 4	4.06	2.86
A2AEM2	*Clcc1*	Chloride channel CLIC-like protein 1	3.79	2.86
Q80U93	*Nup214*	Nuclear pore complex protein Nup214	3.52	2.86
Q9ER73	*Elp4*	Elongator complex protein 4	5.64	2.85
Q8BP79	*Hccs*	Cytochrome c-type heme lyase	4.02	2.85
Q3TRK3	*Dbn1*	Drebrin	5.60	2.85
Q6PD03	*Ppp2r5a*	Serine/threonine-protein phosphatase 2A 56 kDa regulatory subunit alpha isoform	3.51	2.84
Q6ZQ58	*Larp1*	La-related protein 1	3.33	2.82
Q9D250	*Irak4*	Interleukin-1 receptor-associated kinase 4	2.64	2.81
P35831	*Ptpn12*	Tyrosine-protein phosphatase non-receptor type 12	5.22	2.81
Q99LG2	*Tnpo2*	Transportin-2	2.89	2.80
Q4FJZ6	*Gclm*	Glutamate--cysteine ligase regulatory subunit	4.23	2.80
F7DBQ0	*Pdia6*	Protein disulfide-isomerase A6	6.72	2.80
Q3TJN1	*Bcat1*	Branched-chain-amino-acid aminotransferase	3.83	2.78
Q6EDY6	*Lrrc16a*	Leucine-rich repeat-containing protein 16A	2.35	2.78
A0A0N4SVL0	*Eif4g3*	Eukaryotic translation initiation factor 4 gamma 3	3.26	2.77
Q8R050	*Gspt1*	Eukaryotic peptide chain release factor GTP-binding subunit ERF3A	7.53	2.76
Q61749	*Eif2b4*	Translation initiation factor eIF-2B subunit delta	4.16	2.76
Q3UGJ5	*Rasa3*	Ras GTPase-activating protein 3	5.04	2.75
M0QWS4	*Ufc1*	Ubiquitin-fold modifier-conjugating enzyme 1	5.21	2.74
A2AKD7	*Snta1*	Alpha-1-syntrophin	2.31	2.74
B1AVZ0	*Uprt*	Uracil phosphoribosyltransferase homolog	3.06	2.73
Q3UHD6	*Snx27*	Sorting nexin-27	4.46	2.72
Q9CRD0	*Ociad1*	OCIA domain-containing protein 1	2.65	2.72
A0A0R4J079	*Acbd3*	Golgi resident protein GCP60	4.75	2.70
Q8BR90		UPF0600 protein C5orf51 homolog	3.29	2.70
Q9CQ92	*Fis1*	Mitochondrial fission 1 protein	4.75	2.68
Q62426	*Cstb*	Cystatin-B	5.15	2.67
Q3U2S1	*Dfna5*	Non-syndromic hearing impairment protein 5 homolog	2.54	2.67
Q5DTT2	*Psd*	PH and SEC7 domain-containing protein 1	3.20	2.67
Q3UMP4	*Serbp1*	Plasminogen activator inhibitor 1 RNA-binding protein	4.09	2.66
Q3U1C5	*Tsc22d2*		2.74	2.65
Q921W0	*Chmp1a*	Charged multivesicular body protein 1a	4.35	2.65
Q545E6	*Tsn*	Translin	4.76	2.65
Q8R562	*Trove2*	60 kDa SS-A/Ro ribonucleoprotein	4.47	2.64
Q3TEF1	*Gclc*	Glutamate--cysteine ligase catalytic subunit	3.12	2.64
Q8C0D5	*Eftud1*	Elongation factor Tu GTP-binding domain-containing protein 1	5.82	2.61
B2KGP3	*Ppm1e*	Protein phosphatase 1E	6.23	2.61
Q8R4H2	*Arhgef12*	Rho guanine nucleotide exchange factor 12	4.75	2.60
Q3TFD2	*Lpcat1*	Lysophosphatidylcholine acyltransferase 1	4.17	2.60
P47757	*Capzb*	F-actin-capping protein subunit beta	5.61	2.60
G3X9V0	*Psme2*	Proteasome activator complex subunit 2	3.04	2.59
Q9D066	*Impa1*	Inositol monophosphatase 1	6.71	2.59
Q8BXK8	*Agap1*	Arf-GAP with GTPase, ANK repeat and PH domain-containing protein 1	4.81	2.59
Q3UNH4	*Gprin1*	G protein-regulated inducer of neurite outgrowth 1	5.49	2.58
Q3UB06	*Srpk1*	SRSF protein kinase 1	3.21	2.56
Q9D394	*Rufy3*	Protein RUFY3	4.72	2.54
Q9CPX6	*Atg3*	Ubiquitin-like-conjugating enzyme ATG3	6.81	2.54
Q3TW96	*Uap1l1*	UDP-N-acetylhexosamine pyrophosphorylase-like protein 1	4.13	2.54
E9QQ10	*Akap9*	A-kinase anchor protein 9	2.27	2.54
Q9DBU8	*Ap3m1*	AP-3 complex subunit mu-1	2.67	2.53
P28667	*Marcksl1*	MARCKS-related protein	3.86	2.52
Q3U590	*C2cd2l*	C2 domain-containing protein 2-like	2.57	2.51
P26645	*Marcks*	Myristoylated alanine-rich C-kinase substrate	3.97	2.51

Q8R127	*Sccpdh*	Saccharopine dehydrogenase-like oxidoreductase	5.29	2.51
O08915	*Aip*	AH receptor-interacting protein	6.23	2.51
F6T836	*Arhgap26*	Rho GTPase-activating protein 26	3.61	2.50
Q9JKK7	*Tmod2*	Tropomodulin-2	3.75	2.49
Q8VD37	*Sgip1*	SH3-containing GRB2-like protein 3-interacting protein 1	4.22	2.48
A3KML3	*Ywhaq*	14-3-3 protein theta	6.61	2.48
Q543P6	*Acot11*	Acyl-coenzyme A thioesterase 11	4.48	2.48
A0A0R4J1Q0	*Edc4*	Enhancer of mRNA-decapping protein 4	2.10	2.48
Q9DB60	*Fam213b*	Prostamide/prostaglandin F synthase	2.93	2.46
B2RSC8	*Nedd4*	E3 ubiquitin-protein ligase NEDD4	3.10	2.45
Q8K0C9	*Gmds*	GDP-mannose 4,6 dehydratase	5.30	2.45
Q3URQ4	*C78339*		2.97	2.44
Q8BVU5	*Nudt9*	ADP-ribose pyrophosphatase, mitochondrial	3.31	2.44
P70268	*Pkn1*	Serine/threonine-protein kinase N1	3.14	2.44
Q99J57	*Mat2a*	S-adenosylmethionine synthase	3.88	2.44
Q9WVK8	*Cyp46a1*	Cholesterol 24-hydroxylase	4.62	2.43
P61759	*Vbp1*	Prefoldin subunit 3	3.69	2.43
Q4FJQ6	*Serpinb6a*	Serpin B6	3.33	2.42
Q3UM45	*Ppp1r7*	Protein phosphatase 1 regulatory subunit 7	3.87	2.41
Q0PD38	*Rab18*	Ras-related protein Rab-18	4.01	2.41
Q3TCY0	*Rab33b*	Ras-related protein Rab-33B	2.61	2.40
Q542D6	*Sptlc2*	Serine palmitoyltransferase 2	2.50	2.40
Q6PDL0	*Dync1li2*	Cytoplasmic dynein 1 light intermediate chain 2	3.24	2.40
Q61249	*Igbp1*	Immunoglobulin-binding protein 1	3.47	2.40
Q3UE40	*Gna13*	Guanine nucleotide-binding protein subunit alpha-13	2.59	2.38
Q8BK64	*Ahsa1*	Activator of 90 kDa heat shock protein ATPase homolog 1	4.50	2.36
Q3TEG0	*A830010M20Rik*		4.38	2.34
F8WHT3	*Prrc2b*		4.72	2.33
A2A6U3	*Sept9*	Septin-9	2.76	2.33
Q8BGS2	*Bola2*	BolA-like protein 2	3.62	2.32
A0A668KLC6	*Map2*	Microtubule-associated protein 2	4.97	2.32
D3Z4T6	*Negr1*	Neuronal growth regulator 1	3.99	2.31
A2ALS4	*Rap1gap*	Rap1 GTPase-activating protein 1	2.84	2.31
A0A0A0MQE5	*Camsap1*	Calmodulin-regulated spectrin-associated protein 1	3.55	2.30
Q8VBT9	*Aspscr1*	Tether containing UBX domain for GLUT4	4.45	2.30
Q64433	*Hspe1*	10 kDa heat shock protein, mitochondrial	3.20	2.30
Q8BGT8	*Phyhipl*	Phytanoyl-CoA hydroxylase-interacting protein-like	5.90	2.30
Q8BTG7	*Ndrg4*	Protein NDRG4	3.82	2.29
Q8CIP4	*Mark4*	MAP/microtubule affinity-regulating kinase 4	3.35	2.26
Q3TN35	*Sgta*	Small glutamine-rich tetratricopeptide repeat-containing protein alpha	4.88	2.25
Q2M3X8	*Phactr1*	Phosphatase and actin regulator 1	3.43	2.25
Q5ICG5	*Acsl6*	Long-chain-fatty-acid--CoA ligase 6	4.14	2.24
Q91V47	*DXS254E*	Ubiquitin-like protein 4A	2.20	2.24
Q3U8R9	*Txnl1*	Thioredoxin-like protein 1	4.00	2.24
A0A087WQG4	*Ktn1*		6.08	2.23
F8WJB9	*Evl*	Ena/VASP-like protein	2.06	2.22
Q9Z1E4	*Gys1*	Glycogen [starch] synthase, muscle	3.97	2.22
Q9CQB4	*Uqcrb*	Cytochrome b-c1 complex subunit 7	4.18	2.21
P34022	*Ranbp1*	Ran-specific GTPase-activating protein	5.07	2.21
A0A0G2JG35			5.00	2.19
A0A0R4J2B2	*Kctd12*	BTB/POZ domain-containing protein KCTD12	4.59	2.19
Q3THA0	*Eif3g*	Eukaryotic translation initiation factor 3 subunit G	7.50	2.18
Q3TWZ9	*Cltb*		3.29	2.18
Q547J4	*Mapt*	Microtubule-associated protein	6.68	2.16
P14231	*Atp1b2*	Sodium/potassium-transporting ATPase subunit beta-2	3.95	2.16
Q6ZQJ2	*mKIAA0094*	Methionine aminopeptidase	2.65	2.14
Q3U484	*Ddx3y*	ATP-dependent RNA helicase DDX3Y	2.33	2.14
Q9DBR7	*Ppp1r12a*	Protein phosphatase 1 regulatory subunit 12A	2.62	2.14
A0A1D5RLL0			3.45	2.13
A0A171KXD3	*Prmt1*	Protein arginine N-methyltransferase 1	2.23	2.12
Q60625	*Icam5*	Intercellular adhesion molecule 5	2.69	2.12
Q3TLL4	*Hgs*	Hepatocyte growth factor-regulated tyrosine kinase substrate	3.76	2.12
Q3TWE3	*P4hb*	Protein disulfide-isomerase	6.15	2.12
Q9CQX2	*Cyb5b*	Cytochrome b5 type B	5.76	2.11
A2RTH5	*Lcmt1*		4.93	2.11
Q4FK36	*Dstn*	Destrin	3.26	2.11
P35235	*Ptpn11*	Tyrosine-protein phosphatase non-receptor type 11	7.00	2.11
O55042	*Snca*	Alpha-synuclein	4.32	2.10
Q58E70	*Tpm3*		5.98	2.10
B1APX2	*5031439G07Rik*	Uncharacterized protein KIAA0930 homolog	3.30	2.09
A0A0A6YVU8	*Gm9774*	Proteasomal ubiquitin receptor ADRM1	5.20	2.08

Q3TX38	*Vdac3*	Voltage-dependent anion-selective channel protein 3	5.98	2.08
Q80UK0	*Sestd1*	SEC14 domain and spectrin repeat-containing protein 1	3.80	2.08
Q8BXR9	*Osbpl6*	Oxysterol-binding protein-related protein 6	2.92	2.08
Q7TPU5	*Tbc1d15*	TBC1 domain family member 15	3.58	2.07
A0A0R4J0S4	*Llgl1*	Lethal(2) giant larvae protein homolog 1	2.01	2.07
Q64737	*Gart*	Trifunctional purine biosynthetic protein adenosine-3	3.76	2.07
Q8CHT1	*Ngef*	Ephexin-1	3.36	2.06
Q3UYK6	*Slc1a2*	Amino acid transporter	3.69	2.06
D3YZP9	*Ccdc6*	Coiled-coil domain-containing protein 6	4.24	2.05
Q8CDA1	*Inpp5f*	Phosphatidylinositide phosphatase SAC2	3.84	2.04
P15105	*Glul*	Glutamine synthetase	2.70	2.04
Q8BMS9	*Rassf2*	Ras association domain-containing protein 2	2.95	2.04
P27773	*Pdia3*	Protein disulfide-isomerase A3	7.17	2.03
Q68FM6	*Elfn2*	Protein phosphatase 1 regulatory subunit 29	2.48	2.03
G3UX26	*Vdac2*	Voltage-dependent anion-selective channel protein 2	5.76	2.03
Q3UBU9	*Fkbp3*	Peptidyl-prolyl cis-trans isomerase	4.10	2.03
F8VQE9	*Agap3*	Arf-GAP with GTPase, ANK repeat and PH domain-containing protein 3	3.29	2.02
P06837	*Gap43*	Neuromodulin	8.00	2.02
B2RRE3	*Camsap2*	Calmodulin-regulated spectrin-associated protein 2	4.63	2.02
F8WHP5	*Ddhd1*	Phospholipase DDHD1	4.57	2.02
A2ARP8	*Map1a*	Microtubule-associated protein 1A	4.82	2.01
P08228	*Sod1*	Superoxide dismutase [Cu-Zn]	2.58	2.00

Table VI-4: Proteins significantly enriched by **DA-P3** (15 µM) in *DJ-1*$^{-/-}$ mouse neurons.

Protein IDs	**Gene names**	**Protein names**	**-log$_{10}$(*p*-value)**	**log$_2$(enrichment)**
Q9CWE0	*Mtfr1l*	Mitochondrial fission regulator 1-like	4.27	6.93
Q9CQU0	*Txndc12*	Thioredoxin domain-containing protein 12	4.48	6.58
A2RS58	*Crkl*	Crk-like protein	4.45	6.41
Q544R7	*Hmox2*	Heme oxygenase 2	5.56	5.96
A0A0R4J078	*Ubxn4*	UBX domain-containing protein 4	7.68	5.56
Q6GU23	*Stat3*	Signal transducer and activator of transcription	4.33	5.16
Q9CQ65	*Mtap*	S-methyl-5-thioadenosine phosphorylase	3.72	4.90
Q4FK36	*Dstn*	Destrin	4.58	4.89
Q6P9S0	*Mtss1l*	MTSS1-like protein	3.02	4.85
Q8CHP8	*Pgp*	Phosphoglycolate phosphatase	4.94	4.81
P10639	*Txn*	Thioredoxin	3.37	4.68
B2RXC2	*Itpkb*		3.20	4.60
O35465	*Fkbp8*	Peptidyl-prolyl cis-trans isomerase FKBP8	6.09	4.46
Q8C0M9	*Asrgl1*	Isoaspartyl peptidase/L-asparaginase	5.03	4.44
Q9CPV4	*Glod4*	Glyoxalase domain-containing protein 4	3.54	4.39
Q8C078	*Camkk2*	Calcium/calmodulin-dependent protein kinase kinase 2	4.14	4.39
Z4YKC4	*Eif4g3*		2.79	4.35
Q9D898	*Arpc5l*	Actin-related protein 2/3 complex subunit 5-like protein	4.84	4.27
Q60865	*Caprin1*	Caprin-1	3.91	4.16
Q4FK49	*Ppa1*	Inorganic pyrophosphatase	3.95	4.15
Q9QYG0	*Ndrg2*	Protein NDRG2	4.07	4.14
Q9ER73	*Elp4*	Elongator complex protein 4	3.87	4.10
Q9DAW9	*Cnn3*	Calponin-3	4.79	4.05
Q5DTJ4	*Prrc2a*	Protein PRRC2A	6.48	4.01
P48722	*Hspa4l*	Heat shock 70 kDa protein 4L	3.51	3.99
E9Q3M9	*2010300C02Rik*		3.75	3.96
Q6P5H2	*Nes*	Nestin	4.26	3.88
F7AA26	*Pakap*	A-kinase anchor protein 2	5.75	3.88
Q8BFU3	*Rnf214*	RING finger protein 214	6.16	3.88
P60335	*Pcbp1*	Poly(rC)-binding protein 1	5.43	3.85
Q9DBG7	*Srpr*	Signal recognition particle receptor subunit alpha	5.22	3.84
Q9ERU9	*Ranbp2*	E3 SUMO-protein ligase RanBP2	4.21	3.82
Q8BI84	*Mia3*	Melanoma inhibitory activity protein 3	3.80	3.81
Q9D7S9	*Chmp5*	Charged multivesicular body protein 5	6.03	3.81
Q3TA75	*Fxr2*		6.73	3.77
Q80WR0	*Nup153*		2.70	3.72
Q3TDD8	*Eif4b*	Eukaryotic translation initiation factor 4B	6.16	3.70
P49586	*Pcyt1a*	Choline-phosphate cytidylyltransferase A	2.44	3.68
A0A0A6YX73	*Prkar2a*	cAMP-dependent protein kinase type II-alpha regulatory subunit	4.70	3.67
P08414	*Camk4*	Calcium/calmodulin-dependent protein kinase type IV	4.43	3.65
A0A1D5RL96	*Kiaa1107*	Uncharacterized protein KIAA1107	2.52	3.65
A2RTH5	*Lcmt1*		3.44	3.62
Q921M8	*Usp4*	Ubiquitin carboxyl-terminal hydrolase	5.36	3.61
Q99P72	*Rtn4*	Reticulon-4	6.23	3.61
Q9ES97	*Rtn3*	Reticulon-3	6.36	3.60

P60761	*Nrgn*	Neurogranin	6.58	3.59
E9QAT4	*Sec16a*		4.47	3.55
Q8VIM9	*Irgq*	Immunity-related GTPase family Q protein	3.64	3.52
A0A286YCI8	*Sorbs1*	Sorbin and SH3 domain-containing protein 1	3.21	3.49
Q91XL9	*Osbpl1a*	Oxysterol-binding protein-related protein 1	2.77	3.46
Q9ERR1	*Ndel1*	Nuclear distribution protein nudE-like 1	3.72	3.44
D3YU22	*Limch1*	LIM and calponin homology domains-containing protein 1	3.06	3.43
Q4FJQ6	*Serpinb6a*	Serpin B6	3.21	3.38
A0A654ICD2	*Gja1*	Gap junction alpha-1 protein	5.05	3.36
A0A0R4J0B4	*Cmas*	N-acylneuraminate cytidylyltransferase	3.57	3.35
Q921L9	*Prkar1b*	cAMP-dependent protein kinase type I-beta regulatory subunit	5.84	3.35
Q3TB93	*Ptpn1*	Tyrosine-protein phosphatase non-receptor type	5.33	3.34
P48678	*Lmna*	Prelamin-A/C	3.31	3.33
P84086	*Cplx2*	Complexin-2	6.67	3.30
P0C7L0	*Wipf3*	WAS/WASL-interacting protein family member 3	3.44	3.30
Q8VEF1	*Gramd1a*	GRAM domain-containing protein 1A	2.15	3.29
Q9CQS8	*Sec61b*	Protein transport protein Sec61 subunit beta	5.16	3.27
A2AJK8	*Ttc1*	Tetratricopeptide repeat protein 1	4.42	3.27
A2AAY5	*Sh3pxd2b*	SH3 and PX domain-containing protein 2B	6.00	3.25
Q8BTG7	*Ndrg4*	Protein NDRG4	2.38	3.25
P42669	*Pura*	Transcriptional activator protein Pur-alpha	6.17	3.21
Q8BP79	*Hccs*	Cytochrome c-type heme lyase	3.45	3.20
Q3U8S5	*Capn2*	Calpain-2 catalytic subunit	4.81	3.20
Q99LR1	*Abhd12*	Monoacylglycerol lipase ABHD12	3.30	3.17
Q9CQ92	*Fis1*	Mitochondrial fission 1 protein	3.05	3.15
Q3U7E0	*Atp6v1g1*	V-type proton ATPase subunit G 1	3.59	3.14
Q8WTY4	*Ciapin1*	Anamorsin	3.36	3.12
P28667	*Marcksl1*	MARCKS-related protein	3.94	3.08
A0A5F8MP98	*Tns3*	Tensin-3	3.48	3.05
Q9JJU8	*Sh3bgrl*	SH3 domain-binding glutamic acid-rich-like protein	4.12	3.02
Q3UL43	*Nup155*	Nuclear pore complex protein Nup155	3.73	3.02
P61759	*Vbp1*	Prefoldin subunit 3	3.67	3.02
Q99PU5	*Acsbg1*	Long-chain-fatty-acid--CoA ligase ACSBG1	5.99	3.01
E9PZ43	*Map4*	Microtubule-associated protein	4.39	3.00
Q91YS2	*Rangap1*	Ran GTPase-activating protein 1	4.88	2.98
O55042	*Snca*	Alpha-synuclein	2.66	2.97
P31230	*Aimp1*	Aminoacyl tRNA synthase complex-interacting multifunctional protein 1	5.01	2.97
Q922Q1	*Mtarc2*	Mitochondrial amidoxime reducing component 2	6.57	2.94
Q921W0	*Chmp1a*	Charged multivesicular body protein 1a	3.86	2.94
Q8R4H2	*Arhgef12*	Rho guanine nucleotide exchange factor 12	3.08	2.94
P35235	*Ptpn11*	Tyrosine-protein phosphatase non-receptor type 11	3.71	2.94
Q3TJN1	*Bcat1*	Branched-chain-amino-acid aminotransferase	2.95	2.94
B2KGP3	*Ppm1e*	Protein phosphatase 1E	5.22	2.93
Q9CZZ4	*Psmd9*	26S proteasome non-ATPase regulatory subunit 9	4.27	2.90
P27546	*Map4*	Microtubule-associated protein 4	6.15	2.89
P62774	*Mtpn*	Myotrophin	4.38	2.88
K0BWC3	*Palld*	Palladin	2.50	2.87
Q8R050	*Gspt1*	Eukaryotic peptide chain release factor GTP-binding subunit ERF3A	3.84	2.85
Q6NZD2	*Snx1*	Sorting nexin-1	3.91	2.81
Q3TLH4	*Prrc2c*	Protein PRRC2C	7.58	2.81
P17751	*Tpi1*	Triosephosphate isomerase	7.11	2.80
A0A3B2WBC6			7.67	2.80
A0A140LJG6	*Spcs2*	Signal peptidase complex subunit 2	5.06	2.79
E9Q137	*Tex264*		5.02	2.79
O55091	*Impact*	Protein IMPACT	3.80	2.76
Q0PD38	*Rab18*	Ras-related protein Rab-18	2.43	2.76
F7DBQ0	*Pdia6*	Protein disulfide-isomerase A6	8.06	2.76
E9PVQ3	*Spats2l*	SPATS2-like protein	3.25	2.75
Q61584	*Fxr1*	Fragile X mental retardation syndrome-related protein 1	2.34	2.74
Q3U7A6	*Stau1*	Double-stranded RNA-binding protein Staufen homolog 1	4.58	2.72
A2AVJ7	*Rrbp1*	Ribosome-binding protein 1	4.52	2.71
P26645	*Marcks*	Myristoylated alanine-rich C-kinase substrate	4.23	2.70
E9QP59	*Lemd3*	Inner nuclear membrane protein Man1	4.07	2.70
P70271	*Pdlim4*	PDZ and LIM domain protein 4	3.85	2.68
E9QMB7	*Naa30*	N-alpha-acetyltransferase 30	4.13	2.68
Q3TNH0	*Tmpo*	Lamina-associated polypeptide 2, isoforms beta/delta/epsilon/gamma	4.20	2.67
Q62426	*Cstb*	Cystatin-B	4.51	2.66
Q9EPE9	*Atp13a1*	Manganese-transporting ATPase 13A1	3.65	2.64
Q545B6	*Stmn1*	Stathmin	4.46	2.64

Q6NSW3	*Sphkap*	A-kinase anchor protein SPHKAP	3.14	2.63
Q3TRK3	*Dbn1*	Drebrin	4.53	2.63
G3UX26	*Vdac2*	Voltage-dependent anion-selective channel protein 2	5.35	2.62
Q9CXW3	*Cacybp*	Calcyclin-binding protein	2.71	2.62
Q3TFD2	*Lpcat1*	Lysophosphatidylcholine acyltransferase 1	4.42	2.62
Q4FJL2	*Rtn1*	Reticulon	5.84	2.61
A8Y5P4	*Map7d1*	MAP7 domain-containing protein 1	6.41	2.58
Q3TN35	*Sgta*	Small glutamine-rich tetratricopeptide repeat-containing protein alpha	3.62	2.58
Q91WT9	*Cbs*	Cystathionine beta-synthase	4.25	2.57
Q80WJ7	*Mtdh*	Protein LYRIC	4.95	2.55
Q543P6	*Acot11*	Acyl-coenzyme A thioesterase 11	4.42	2.54
Q2M3X8	*Phactr1*	Phosphatase and actin regulator 1	3.41	2.51
Q8CJ67	*Stau2*	Double-stranded RNA-binding protein Staufen homolog 2	3.69	2.50
B7ZNS2	*Dlgap4*	Disks large-associated protein 4	2.25	2.49
Q9D066	*Impa1*	Inositol monophosphatase 1	5.62	2.44
A0A1D5RLY6	*Map1s*	Microtubule-associated protein 1S	3.56	2.44
Q3TN44	*Cyb5b*	Cytochrome b5 type B	4.65	2.44
B2RSC8	*Nedd4*	E3 ubiquitin-protein ligase NEDD4	3.96	2.44
Q3UNA7	*Gclc*	Glutamate--cysteine ligase catalytic subunit	4.37	2.44
Q80UG5	*Sept9*	Septin-9	3.43	2.42
Q64337	*Sqstm1*	Sequestosome-1	2.25	2.39
A0A087WQG4	*Ktn1*		4.58	2.37
P63040	*Cplx1*	Complexin-1	5.38	2.36
Q8BXK8	*Agap1*	Arf-GAP with GTPase, ANK repeat and PH domain-containing protein 1	4.45	2.36
Q3TL79	*Ahsa1*	Activator of 90 kDa heat shock protein ATPase homolog 1	3.66	2.35
Q3TVI6	*Appl2*	DCC-interacting protein 13-beta	4.40	2.33
Q3THA0	*Eif3g*	Eukaryotic translation initiation factor 3 subunit G	4.51	2.33
Q3UNH4	*Gprin1*	G protein-regulated inducer of neurite outgrowth 1	5.40	2.32
Q9D394	*Rufy3*	Protein RUFY3	4.27	2.30
A0A1Y7VLY5	*Iah1*	Isoamyl acetate-hydrolyzing esterase 1 homolog	4.50	2.30
G3X9V0	*Psme2*	Proteasome activator complex subunit 2	4.73	2.29
O08915	*Aip*	AH receptor-interacting protein	3.89	2.27
Q545E6	*Tsn*	Translin	4.20	2.27
Q9CTE8	*Alg5*	Dolichyl-phosphate beta-glucosyltransferase	2.77	2.25
Q9ERL9	*Gucy1a3*	Guanylate cyclase soluble subunit alpha-3	3.44	2.22
Q9EPJ9	*Arfgap1*	ADP-ribosylation factor GTPase-activating protein 1	3.95	2.22
Q9CPX6	*Atg3*	Ubiquitin-like-conjugating enzyme ATG3	5.11	2.21
J3QPB5	*Ndc1*	Nucleoporin NDC1	2.46	2.20
Q8BZ65	*Pgm3*	Phosphoacetylglucosamine mutase	2.01	2.20
Q6NZL0	*Soga3*	Protein SOGA3	2.23	2.18
O08576	*Rundc3a*	RUN domain-containing protein 3A	2.64	2.18
Q9BCZ4	*Vimp*	Selenoprotein S	2.43	2.18
P47757	*Capzb*	F-actin-capping protein subunit beta	6.04	2.18
O35551	*Rabep1*	Rab GTPase-binding effector protein 1	3.78	2.17
Q3TG12	*Farsb*	Phenylalanine--tRNA ligase beta subunit	5.76	2.14
Q3ULN6	*Sccpdh*	Saccharopine dehydrogenase-like oxidoreductase	5.33	2.13
Q8JZS0	*Lin7a*	Protein lin-7 homolog A	3.09	2.13
A2APL5	*Slc1a2*	Amino acid transporter	3.88	2.13
F6T836	*Arhgap26*	Rho GTPase-activating protein 26	5.03	2.12
Q8BGT8	*Phyhipl*	Phytanoyl-CoA hydroxylase-interacting protein-like	5.67	2.12
Q3UDG2	*Wars*	Tryptophan--tRNA ligase, cytoplasmic	3.25	2.11
Q3TWZ9	*Cltb*		5.57	2.11
Q3UHD6	*Snx27*	Sorting nexin-27	4.03	2.10
A2VCP7	*Psmf1*	Proteasome inhibitor PI31 subunit	2.96	2.10
Q3TX38	*Vdac3*	Voltage-dependent anion-selective channel protein 3	5.57	2.09
A0A0R4J2B2	*Kctd12*	BTB/POZ domain-containing protein KCTD12	2.52	2.08
E9Q9D6	*R3hdm2*	R3H domain-containing protein 2	4.10	2.08
Q8BLN5	*Lss*	Lanosterol synthase	2.24	2.08
Q8BVU5	*Nudt9*	ADP-ribose pyrophosphatase, mitochondrial	5.68	2.07
A0A668KLC6	*Map2*	Microtubule-associated protein 2	6.22	2.07
A3KML3	*Ywhaq*	14-3-3 protein theta	5.49	2.07
Q58E70	*Tpm3*		5.64	2.05
A0A0A6YW88	*Camkv*	CaM kinase-like vesicle-associated protein	5.78	2.05
Q544Y7	*Cfl1*	Cofilin-1	6.03	2.03
A0PJL3	*Sarm1*	Sterile alpha and TIR motif-containing protein 1	2.25	2.03
R7RU63	*Cttnbp2*	Cortactin-binding protein 2	2.70	2.02
B1ATL6	*Map2k4*	Dual specificity mitogen-activated protein kinase kinase 4	4.82	2.02
Q99J57	*Mat2a*	S-adenosylmethionine synthase	4.48	2.02
D3YWL1	*Rab3d*	Ras-related protein Rab-3D	6.09	2.01
Q80UK0	*Sestd1*	SEC14 domain and spectrin repeat-containing protein 1	2.87	2.00
A0A0N4SW14	*Ccdc136*	Coiled-coil domain-containing protein 136	3.68	2.00

Table VI-5: Proteins significantly outcompeted by a 10-fold excess of **DB** vs. 15 µM **DA-P3** in Hek293 cells.

Protein IDs	Gene names	Protein names	-log$_{10}$(*p*-value)	log$_2$(enrichment)
Q8N2K0	*ABHD12*	Monoacylglycerol lipase ABHD12	2.34	5.66
Q9H773	*DCTPP1*	dCTP pyrophosphatase 1	2.39	5.16
Q96TC7	*RMDN3*	Regulator of microtubule dynamics protein 3	2.52	5.11
P33981	*TTK*	Dual specificity protein kinase TTK	3.55	5.10
Q6P2H3	*CEP85*	Centrosomal protein of 85 kDa	2.29	4.96
Q6NUQ1	*RINT1*	RAD50-interacting protein 1	3.34	4.89
Q2NKX8	*ERCC6L*	DNA excision repair protein ERCC-6-like	3.64	4.88
P09132	*SRP19*	Signal recognition particle 19 kDa protein	2.80	4.63
Q96KC8	*DNAJC1*	DnaJ homolog subfamily C member 1	4.68	4.61
Q14534	*SQLE*	Squalene monooxygenase	3.51	4.55
O60664	*PLIN3*	Perilipin-3	2.05	4.54
Q9NP61	*ARFGAP3*	ADP-ribosylation factor GTPase-activating protein 3	3.11	4.52
P20290	*BTF3*	Transcription factor BTF3	2.15	4.32
O15270	*SPTLC2*	Serine palmitoyltransferase 2	3.48	4.17
P56962	*STX17*	Syntaxin-17	2.93	4.13
Q9UGP8	*SEC63*	Translocation protein SEC63 homolog	2.70	4.11
Q66K14	*TBC1D9B*	TBC1 domain family member 9B	3.47	4.09
O75330	*HMMR*	Hyaluronan mediated motility receptor	2.77	4.07
Q9UHR4	*BAIAP2L1*	Brain-specific angiogenesis inhibitor 1-associated protein 2-like protein 1	3.38	3.99
Q8NF37	*LPCAT1*	Lysophosphatidylcholine acyltransferase 1	2.36	3.98
Q5JSH3	*WDR44*	WD repeat-containing protein 44	2.39	3.97
Q69YH5	*CDCA2*	Cell division cycle-associated protein 2	3.79	3.95
Q6WKZ4	*RAB11FIP1*	Rab11 family-interacting protein 1	2.57	3.89
Q5SWX8	*ODR4*	Protein odr-4 homolog	2.63	3.85
Q8ND24	*RNF214*	RING finger protein 214	2.62	3.83
P51116	*FXR2*	Fragile X mental retardation syndrome-related protein 2	3.24	3.80
Q96CP6	*GRAMD1A*	GRAM domain-containing protein 1A	2.18	3.75
P82094	*TMF1*	TATA element modulatory factor	3.53	3.72
Q96IZ0	*PAWR*	PRKC apoptosis WT1 regulator protein	3.03	3.72
Q8NG31	*CASC5*	Protein CASC5	3.00	3.71
Q9BY89	*KIAA1671*	Uncharacterized protein KIAA1671	2.01	3.66
Q8WX93	*PALLD*	Palladin	2.17	3.65
Q9HBM0	*VEZT*	Vezatin	2.15	3.61
Q32MZ4	*LRRFIP1*	Leucine-rich repeat flightless-interacting protein 1	3.58	3.58
Q8N511	*TMEM199*	Transmembrane protein 199	2.63	3.57
P30519	*HMOX2*	Heme oxygenase 2	3.58	3.56
Q9P1Z2	*CALCOCO1*	Calcium-binding and coiled-coil domain-containing protein 1	2.77	3.56
O94830	*DDHD2*	Phospholipase DDHD2	3.06	3.55
P48651	*PTDSS1*	Phosphatidylserine synthase 1	2.04	3.52
Q96BW5	*PTER*	Phosphotriesterase-related protein	2.43	3.49
Q9HD26	*GOPC*	Golgi-associated PDZ and coiled-coil motif-containing protein	2.56	3.45
Q9BZF3	*OSBPL6*	Oxysterol-binding protein-related protein 6	2.91	3.45
P37198	*NUP62*	Nuclear pore glycoprotein p62	3.31	3.45
Q27J81	*INF2*	Inverted formin-2	2.07	3.43
Q16204	*CCDC6*	Coiled-coil domain-containing protein 6	2.54	3.43
Q99661	*KIF2C*	Kinesin-like protein KIF2C	3.19	3.38
Q00653	*NFKB2*	Nuclear factor NF-kappa-B p100 subunit	4.49	3.38
Q86Y07	*VRK2*	Serine/threonine-protein kinase VRK2	4.41	3.37
Q9UJY4	*GGA2*	ADP-ribosylation factor-binding protein GGA2	2.57	3.32
Q14807	*KIF22*	Kinesin-like protein KIF22	2.12	3.28
O95817	*BAG3*	BAG family molecular chaperone regulator 3	3.42	3.27
Q9H4H8	*FAM83D*	Protein FAM83D	2.49	3.26
Q14318	*FKBP8*	Peptidyl-prolyl cis-trans isomerase FKBP8	4.38	3.24
Q9Y5A7	*NUB1*	NEDD8 ultimate buster 1	2.18	3.23
Q8N6T3	*ARFGAP1*	ADP-ribosylation factor GTPase-activating protein 1	2.71	3.21
Q6ZSR9		Uncharacterized protein FLJ45252	2.14	3.20
Q9HC38	*GLOD4*	Glyoxalase domain-containing protein 4	3.16	3.20
Q12802	*AKAP13*	A-kinase anchor protein 13	3.47	3.19
Q9Y6A5	*TACC3*	Transforming acidic coiled-coil-containing protein 3	3.50	3.15
Q00577	*PURA*	Transcriptional activator protein Pur-alpha	2.72	3.14
Q8N2G8	*GHDC*	GH3 domain-containing protein	2.08	3.07
Q9BSD7	*NTPCR*	Cancer-related nucleoside-triphosphatase	2.78	3.05
Q8N3F8	*MICALL1*	MICAL-like protein 1	2.41	3.04
Q53EZ4	*CEP55*	Centrosomal protein of 55 kDa	2.29	3.04
Q9UNI6	*DUSP12*	Dual specificity protein phosphatase 12	2.50	3.04
Q9HD20	*ATP13A1*	Manganese-transporting ATPase 13A1	2.95	3.03
Q9BXB4	*OSBPL11*	Oxysterol-binding protein-related protein 11	2.07	3.03
O75170	*PPP6R2*	Serine/threonine-protein phosphatase 6 regulatory subunit 2	2.55	3.02
Q9NQW6	*ANLN*	Actin-binding protein anillin	2.13	3.02

Q96S59	*RANBP9*	Ran-binding protein 9	2.87	3.01
Q96B36	*AKT1S1*	Proline-rich AKT1 substrate 1	3.47	3.00
O60678	*PRMT3*	Protein arginine N-methyltransferase 3	2.12	2.99
Q9NQS7	*INCENP*	Inner centromere protein	3.22	2.97
Q5VV42	*CDKAL1*	Threonylcarbamoyladenosine tRNA methylthiotransferase	3.15	2.95
Q9Y4P3	*TBL2*	Transducin beta-like protein 2	2.99	2.95
Q96T51	*RUFY1*	RUN and FYVE domain-containing protein 1	2.02	2.94
Q8IWC1	*MAP7D3*	MAP7 domain-containing protein 3	3.87	2.94
Q9Y2D5	*AKAP2*	A-kinase anchor protein 2	3.15	2.94
Q9HAP2	*MLXIP*	MLX-interacting protein	4.55	2.93
O43303	*CCP110*	Centriolar coiled-coil protein of 110 kDa	2.09	2.93
O14531	*DPYSL4*	Dihydropyrimidinase-related protein 4	2.26	2.88
O95999	*BCL10*	B-cell lymphoma/leukemia 10	3.25	2.88
Q9BZE9	*ASPSCR1*	Tether containing UBX domain for GLUT4	3.27	2.87
Q08379	*GOLGA2*	Golgin subfamily A member 2	3.55	2.86
O75157	*TSC22D2*	TSC22 domain family protein 2	2.21	2.85
Q9NT62	*ATG3*	Ubiquitin-like-conjugating enzyme ATG3	2.14	2.84
O95197	*RTN3*	Reticulon-3	2.40	2.81
Q96SK2	*TMEM209*	Transmembrane protein 209	3.16	2.81
P18031	*PTPN1*	Tyrosine-protein phosphatase non-receptor type 1	2.09	2.80
O14976	*GAK*	Cyclin-G-associated kinase	3.80	2.78
Q16799	*RTN1*	Reticulon-1	2.12	2.77
Q9UJC3	*HOOK1*	Protein Hook homolog 1	3.56	2.76
P46821	*MAP1B*	Microtubule-associated protein 1B	2.58	2.75
O60566	*BUB1B*	Mitotic checkpoint serine/threonine-protein kinase BUB1 beta	2.58	2.74
Q9HDC5	*JPH1*	Junctophilin-1	2.75	2.73
Q15003	*NCAPH*	Condensin complex subunit 2	3.22	2.72
Q08378	*GOLGA3*	Golgin subfamily A member 3	2.84	2.71
Q8NBF2	*NHLRC2*	NHL repeat-containing protein 2	2.21	2.71
O94763	*URI1*	Unconventional prefoldin RPB5 interactor 1	2.73	2.69
P51148	*RAB5C*	Ras-related protein Rab-5C	2.29	2.68
O75475	*PSIP1*	PC4 and SFRS1-interacting protein	2.01	2.67
Q8NFH5	*NUP35*	Nucleoporin NUP53	2.31	2.67
Q04323	*UBXN1*	UBX domain-containing protein 1	2.90	2.65
Q7Z2Z2	*EFTUD1*	Elongation factor Tu GTP-binding domain-containing protein 1	2.39	2.65
Q99640	*PKMYT1*	Membrane-associated tyrosine- and threonine-specific cdc2-inhibitory kinase	2.94	2.65
Q8IXW5	*RPAP2*	Putative RNA polymerase II subunit B1 CTD phosphatase RPAP2	2.16	2.63
Q9C0E8	*LNP*	Protein lunapark	2.06	2.62
Q9HC52	*CBX8*	Chromobox protein homolog 8	4.39	2.61
Q16352	*INA*	Alpha-internexin	3.35	2.60
Q96GS4	*C17orf59*	Uncharacterized protein C17orf59	2.76	2.60
P20810	*CAST*	Calpastatin	2.11	2.60
Q92625	*ANKS1A*	Ankyrin repeat and SAM domain-containing protein 1A	2.68	2.59
Q9BSJ8	*ESYT1*	Extended synaptotagmin-1	3.29	2.59
P46109	*CRKL*	Crk-like protein	3.40	2.59
Q9Y4E8	*USP15*	Ubiquitin carboxyl-terminal hydrolase 15	2.36	2.58
Q8TBM8	*DNAJB14*	DnaJ homolog subfamily B member 14	2.08	2.57
Q8N1F8	*STK11IP*	Serine/threonine-protein kinase 11-interacting protein	2.62	2.57
Q92575	*UBXN4*	UBX domain-containing protein 4	2.74	2.56
Q8TEY7	*USP33*	Ubiquitin carboxyl-terminal hydrolase 33	3.61	2.56
Q7Z5L2	*R3HCC1L*	Coiled-coil domain-containing protein R3HCC1L	2.36	2.55
Q96II8	*LRCH3*	Leucine-rich repeat and calponin homology domain-containing protein 3	3.59	2.55
Q9NZT2	*OGFR*	Opioid growth factor receptor	2.71	2.54
Q9NRR5	*UBQLN4*	Ubiquilin-4	2.05	2.53
O76024	*WFS1*	Wolframin	3.25	2.52
Q9Y2W6	*TDRKH*	Tudor and KH domain-containing protein	2.96	2.51
P08240	*SRPR*	Signal recognition particle receptor subunit alpha	3.30	2.50
Q9Y2V2	*CARHSP1*	Calcium-regulated heat stable protein 1	2.97	2.49
Q9UKX7	*NUP50*	Nuclear pore complex protein Nup50	2.73	2.48
P51617	*IRAK1*	Interleukin-1 receptor-associated kinase 1	2.34	2.48
Q9UPQ9	*TNRC6B*	Trinucleotide repeat-containing gene 6B protein	2.10	2.47
Q7Z2K8	*GPRIN1*	G protein-regulated inducer of neurite outgrowth 1	2.58	2.46
Q5JRA6	*MIA3*	Melanoma inhibitory activity protein 3	3.87	2.43
P22059	*OSBP*	Oxysterol-binding protein 1	3.42	2.40
Q9Y679	*AUP1*	Ancient ubiquitous protein 1	3.19	2.40
Q9P0L0	*VAPA*	Vesicle-associated membrane protein-associated protein A	3.39	2.40
Q8TD19	*NEK9*	Serine/threonine-protein kinase Nek9	2.34	2.38
Q9HCU5	*PREB*	Prolactin regulatory element-binding protein	2.95	2.37
P50402	*EMD*	Emerin	4.16	2.35
Q15005	*SPCS2*	Signal peptidase complex subunit 2	3.07	2.35
P49069	*CAMLG*	Calcium signal-modulating cyclophilin ligand	3.94	2.35

Q8IZ21	*PHACTR4*	Phosphatase and actin regulator 4	2.68	2.34
Q9NYZ3	*GTSE1*	G2 and S phase-expressed protein 1	2.08	2.34
P29372	*MPG*	DNA-3-methyladenine glycosylase	4.56	2.34
Q96P47	*AGAP3*	Arf-GAP with GTPase, ANK repeat and PH domain-containing protein 3	2.63	2.33
Q9UGV2	*NDRG3*	Protein NDRG3	2.08	2.31
Q5T5U3	*ARHGAP21*	Rho GTPase-activating protein 21	2.90	2.31
Q8NEN9	*PDZD8*	PDZ domain-containing protein 8	2.93	2.31
Q6PJ69	*TRIM65*	Tripartite motif-containing protein 65	2.63	2.30
Q9BVQ7	*SPATA5L1*	Spermatogenesis-associated protein 5-like protein 1	2.71	2.30
P04035	*HMGCR*	3-hydroxy-3-methylglutaryl-coenzyme A reductase	3.52	2.29
Q9NZ52	*GGA3*	ADP-ribosylation factor-binding protein GGA3	2.03	2.29
Q99439	*CNN2*	Calponin-2	2.63	2.27
Q00587	*CDC42EP1*	Cdc42 effector protein 1	2.08	2.27
Q9NP72	*RAB18*	Ras-related protein Rab-18	3.40	2.27
Q86XL3	*ANKLE2*	Ankyrin repeat and LEM domain-containing protein 2	4.09	2.27
O75348	*ATP6V1G1*	V-type proton ATPase subunit G 1	3.85	2.26
Q12800	*TFCP2*	Alpha-globin transcription factor CP2	2.15	2.26
Q7Z434	*MAVS*	Mitochondrial antiviral-signaling protein	3.92	2.26
Q92615	*LARP4B*	La-related protein 4B	3.07	2.26
A1X283	*SH3PXD2B*	SH3 and PX domain-containing protein 2B	2.00	2.26
P53384	*NUBP1*	Cytosolic Fe-S cluster assembly factor NUBP1	4.81	2.23
Q9H2G2	*SLK*	STE20-like serine/threonine-protein kinase	3.05	2.23
Q8N0X7	*SPG20*	Spartin	3.20	2.23
O75410	*TACC1*	Transforming acidic coiled-coil-containing protein 1	2.21	2.22
Q15398	*DLGAP5*	Disks large-associated protein 5	2.52	2.22
Q99666	*RGPD5*	RANBP2-like and GRIP domain-containing protein 5/6	2.17	2.20
Q9Y4K3	*TRAF6*	TNF receptor-associated factor 6	2.62	2.19
Q5UIP0	*RIF1*	Telomere-associated protein RIF1	2.20	2.19
Q96KB5	*PBK*	Lymphokine-activated killer T-cell-originated protein kinase	5.06	2.18
Q69YQ0	*SPECC1L*	Cytospin-A	3.23	2.18
Q14694	*USP10*	Ubiquitin carboxyl-terminal hydrolase 10	2.93	2.18
P15170	*GSPT1*	Eukaryotic peptide chain release factor GTP-binding subunit ERF3A	3.56	2.18
O00233	*PSMD9*	26S proteasome non-ATPase regulatory subunit 9	2.83	2.17
P19174	*PLCG1*	1-phosphatidylinositol 4,5-bisphosphate phosphodiesterase gamma-1	2.74	2.17
Q96R06	*SPAG5*	Sperm-associated antigen 5	2.56	2.15
Q86UK7	*ZNF598*	Zinc finger protein 598	2.88	2.14
Q66K74	*MAP1S*	Microtubule-associated protein 1S	2.15	2.13
Q9NUQ3	*TXLNG*	Gamma-taxilin	2.61	2.12
Q9BTE3	*MCMBP*	Mini-chromosome maintenance complex-binding protein	2.63	2.12
Q9Y2G8	*DNAJC16*	DnaJ homolog subfamily C member 16	2.04	2.12
Q9P0U3	*SENP1*	Sentrin-specific protease 1	2.65	2.10
Q7L5N7	*LPCAT2*	Lysophosphatidylcholine acyltransferase 2	3.26	2.10
O94966	*USP19*	Ubiquitin carboxyl-terminal hydrolase 19	3.81	2.09
Q9H6U6	*BCAS3*	Breast carcinoma-amplified sequence 3	2.42	2.08
Q5T6F2	*UBAP2*	Ubiquitin-associated protein 2	3.41	2.08
Q9UL15	*BAG5*	BAG family molecular chaperone regulator 5	3.02	2.08
O00161	*SNAP23*	Synaptosomal-associated protein 23	2.65	2.07
Q16513	*PKN2*	Serine/threonine-protein kinase N2	2.16	2.07
P51153	*RAB13*	Ras-related protein Rab-13	2.51	2.06
P22681	*CBL*	E3 ubiquitin-protein ligase CBL	2.24	2.05
O75131	*CPNE3*	Copine-3	3.15	2.05
P16615	*ATP2A2*	Sarcoplasmic/endoplasmic reticulum calcium ATPase 2	3.07	2.04
O95140	*MFN2*	Mitofusin-2	2.82	2.03
O75663	*TIPRL*	TIP41-like protein	2.32	2.03
Q643R3	*LPCAT4*	Lysophospholipid acyltransferase LPCAT4	2.59	2.03
P98194	*ATP2C1*	Calcium-transporting ATPase type 2C member 1	2.28	2.02
Q9BZI7	*UPF3B*	Regulator of nonsense transcripts 3B	2.01	2.02
Q9Y5K6	*CD2AP*	CD2-associated protein	2.09	2.02
Q9Y2U8	*LEMD3*	Inner nuclear membrane protein Man1	3.95	2.01
Q9H7E9	*C8orf33*	UPF0488 protein C8orf33	2.43	2.01
Q92551	*IP6K1*	Inositol hexakisphosphate kinase 1	2.61	2.00
Q8TCU4	*ALMS1*	Alstrom syndrome protein 1	2.22	2.00
Q9Y277	*VDAC3*	Voltage-dependent anion-selective channel protein 3	3.70	2.00

Table VI-6: Proteins significantly outcompeted by a 10-fold excess of **QC** vs. 15 µM **DA-P3** in Hek293 cells.

Protein IDs	**Gene names**	**Protein names**	**-log$_{10}$(*p*-value)**	**log$_2$(enrichment)**
Q9Y6A5	*TACC3*	Transforming acidic coiled-coil-containing protein 3	3.56	6.91
Q9UJY4	*GGA2*	ADP-ribosylation factor-binding protein GGA2	3.43	6.04
Q8IWC1	*MAP7D3*	MAP7 domain-containing protein 3	2.14	6.01

Q32MZ4	*LRRFIP1*	Leucine-rich repeat flightless-interacting protein 1	4.71	6.00
O60664	*PLIN3*	Perilipin-3	2.91	5.94
P09132	*SRP19*	Signal recognition particle 19 kDa protein	2.75	5.86
O15270	*SPTLC2*	Serine palmitoyltransferase 2	2.09	5.60
Q9H773	*DCTPP1*	dCTP pyrophosphatase 1	3.15	5.57
Q6P2H3	*CEP85*	Centrosomal protein of 85 kDa	2.49	5.57
Q8ND24	*RNF214*	RING finger protein 214	3.95	5.54
Q7Z3T8	*ZFYVE16*	Zinc finger FYVE domain-containing protein 16	3.11	5.48
O75330	*HMMR*	Hyaluronan mediated motility receptor	3.00	5.38
Q2NKX8	*ERCC6L*	DNA excision repair protein ERCC-6-like	3.45	5.36
Q6WKZ4	*RAB11FIP1*	Rab11 family-interacting protein 1	2.37	5.31
Q9H019	*MTFR1L*	Mitochondrial fission regulator 1-like	3.72	5.23
O14976	*GAK*	Cyclin-G-associated kinase	2.65	5.19
O60566	*BUB1B*	Mitotic checkpoint serine/threonine-protein kinase BUB1 beta	4.42	5.17
Q6NUQ1	*RINT1*	RAD50-interacting protein 1	2.09	5.13
Q8WX93	*PALLD*	Palladin	2.05	5.11
P20810	*CAST*	Calpastatin	2.52	4.91
P46821	*MAP1B*	Microtubule-associated protein 1B	3.74	4.90
O95197	*RTN3*	Reticulon-3	2.65	4.88
Q9BZE9	*ASPSCR1*	Tether containing UBX domain for GLUT4	3.12	4.82
Q8N2K0	*ABHD12*	Monoacylglycerol lipase ABHD12	2.40	4.78
Q14534	*SQLE*	Squalene monooxygenase	3.33	4.77
O95817	*BAG3*	BAG family molecular chaperone regulator 3	5.14	4.74
Q96BW5	*PTER*	Phosphotriesterase-related protein	2.57	4.70
P49247	*RPIA*	Ribose-5-phosphate isomerase	2.35	4.69
Q86VQ1	*GLCCI1*	Glucocorticoid-induced transcript 1 protein	2.83	4.65
Q5SQN1	*SNAP47*	Synaptosomal-associated protein 47	3.20	4.64
P56962	*STX17*	Syntaxin-17	3.90	4.61
O94763	*URI1*	Unconventional prefoldin RPB5 interactor 1	3.10	4.60
Q96KC8	*DNAJC1*	DnaJ homolog subfamily C member 1	3.94	4.58
Q96S59	*RANBP9*	Ran-binding protein 9	3.38	4.48
Q969V6	*MKL1*	MKL/myocardin-like protein 1	2.20	4.47
Q16799	*RTN1*	Reticulon-1	4.88	4.40
Q96CP6	*GRAMD1A*	GRAM domain-containing protein 1A	2.01	4.38
Q9BZF3	*OSBPL6*	Oxysterol-binding protein-related protein 6	2.37	4.38
Q9NQW6	*ANLN*	Actin-binding protein anillin	2.48	4.34
Q14318	*FKBP8*	Peptidyl-prolyl cis-trans isomerase FKBP8	2.92	4.31
P40763	*STAT3*	Signal transducer and activator of transcription 3	2.20	4.31
Q5W0B1	*RNF219*	RING finger protein 219	2.07	4.29
P46109	*CRKL*	Crk-like protein	2.93	4.28
P82094	*TMF1*	TATA element modulatory factor	3.63	4.26
A1X283	*SH3PXD2B*	SH3 and PX domain-containing protein 2B	2.68	4.26
Q5VV42	*CDKAL1*	Threonylcarbamoyladenosine tRNA methylthiotransferase	2.55	4.25
Q9Y4P3	*TBL2*	Transducin beta-like protein 2	2.75	4.23
Q96GA3	*LTV1*	Protein LTV1 homolog	2.27	4.19
Q96P47	*AGAP3*	Arf-GAP with GTPase, ANK repeat and PH domain-containing protein 3	2.42	4.16
Q8TBM8	*DNAJB14*	DnaJ homolog subfamily B member 14	2.45	4.14
Q5JSH3	*WDR44*	WD repeat-containing protein 44	2.07	4.12
Q3KQU3	*MAP7D1*	MAP7 domain-containing protein 1	2.85	4.09
P32929	*CTH*	Cystathionine gamma-lyase	2.01	4.08
Q9BXB4	*OSBPL11*	Oxysterol-binding protein-related protein 11	2.42	4.07
P04035	*HMGCR*	3-hydroxy-3-methylglutaryl-coenzyme A reductase	3.56	4.06
Q9NW68	*BSDC1*	BSD domain-containing protein 1	3.12	4.06
Q9UL63	*MKLN1*	Muskelin	2.66	4.04
Q92575	*UBXN4*	UBX domain-containing protein 4	2.96	4.02
Q92615	*LARP4B*	La-related protein 4B	2.96	4.00
Q9HBM0	*VEZT*	Vezatin	2.42	4.00
Q66K74	*MAP1S*	Microtubule-associated protein 1S	3.71	3.98
Q9Y5A7	*NUB1*	NEDD8 ultimate buster 1	3.51	3.97
Q8NFH5	*NUP35*	Nucleoporin NUP53	2.63	3.97
Q96IZ0	*PAWR*	PRKC apoptosis WT1 regulator protein	2.76	3.96
Q9NP61	*ARFGAP3*	ADP-ribosylation factor GTPase-activating protein 3	2.14	3.96
Q96PC5	*MIA2*	Melanoma inhibitory activity protein 2	3.80	3.93
Q8N2G8	*GHDC*	GH3 domain-containing protein	2.74	3.92
Q8TD19	*NEK9*	Serine/threonine-protein kinase Nek9	2.47	3.90
O43303	*CCP110*	Centriolar coiled-coil protein of 110 kDa	3.26	3.86
Q9UHR4	*BAIAP2L1*	Brain-specific angiogenesis inhibitor 1-associated protein 2-like protein 1	2.73	3.84
Q12802	*AKAP13*	A-kinase anchor protein 13	2.98	3.84
Q08379	*GOLGA2*	Golgin subfamily A member 2	3.39	3.83
O75157	*TSC22D2*	TSC22 domain family protein 2	2.61	3.81
Q86XL3	*ANKLE2*	Ankyrin repeat and LEM domain-containing protein 2	2.89	3.81

Q15003	*NCAPH*	Condensin complex subunit 2	3.06	3.77
Q9UJC3	*HOOK1*	Protein Hook homolog 1	3.14	3.75
Q8NBF2	*NHLRC2*	NHL repeat-containing protein 2	3.34	3.74
Q00577	*PURA*	Transcriptional activator protein Pur-alpha	2.89	3.73
Q08378	*GOLGA3*	Golgin subfamily A member 3	3.35	3.72
O43683	*BUB1*	Mitotic checkpoint serine/threonine-protein kinase BUB1	2.94	3.69
Q9BSJ8	*ESYT1*	Extended synaptotagmin-1	2.89	3.68
P30519	*HMOX2*	Heme oxygenase 2	4.56	3.67
O75410	*TACC1*	Transforming acidic coiled-coil-containing protein 1	3.55	3.64
Q8IXW5	*RPAP2*	Putative RNA polymerase II subunit B1 CTD phosphatase RPAP2	2.26	3.64
P15170	*GSPT1*	Eukaryotic peptide chain release factor GTP-binding subunit ERF3A	3.66	3.61
P08240	*SRPR*	Signal recognition particle receptor subunit alpha	2.57	3.59
Q9HC38	*GLOD4*	Glyoxalase domain-containing protein 4	2.46	3.59
Q9UKA4	*AKAP11*	A-kinase anchor protein 11	2.19	3.57
Q96T51	*RUFY1*	RUN and FYVE domain-containing protein 1	2.49	3.55
P51116	*FXR2*	Fragile X mental retardation syndrome-related protein 2	2.99	3.52
Q5SWX8	*ODR4*	Protein odr-4 homolog	4.84	3.50
Q99661	*KIF2C*	Kinesin-like protein KIF2C	3.26	3.49
Q9NYZ3	*GTSE1*	G2 and S phase-expressed protein 1	2.20	3.46
O94830	*DDHD2*	Phospholipase DDHD2	2.66	3.46
O14531	*DPYSL4*	Dihydropyrimidinase-related protein 4	3.36	3.46
P18031	*PTPN1*	Tyrosine-protein phosphatase non-receptor type 1	2.20	3.43
Q00653	*NFKB2*	Nuclear factor NF-kappa-B p100 subunit	3.34	3.39
Q13596	*SNX1*	Sorting nexin-1	2.30	3.38
Q9Y4K3	*TRAF6*	TNF receptor-associated factor 6	2.78	3.38
Q9HD26	*GOPC*	Golgi-associated PDZ and coiled-coil motif-containing protein	3.30	3.35
P42566	*EPS15*	Epidermal growth factor receptor substrate 15	2.99	3.35
P22059	*OSBP*	Oxysterol-binding protein 1	2.61	3.34
Q9Y679	*AUP1*	Ancient ubiquitous protein 1	3.54	3.34
Q16512	*PKN1*	Serine/threonine-protein kinase N1	2.80	3.32
P37198	*NUP62*	Nuclear pore glycoprotein p62	3.13	3.32
Q69YH5	*CDCA2*	Cell division cycle-associated protein 2	2.86	3.32
Q7Z2K8	*GPRIN1*	G protein-regulated inducer of neurite outgrowth 1	2.64	3.31
Q9NUQ3	*TXLNG*	Gamma-taxilin	3.97	3.31
Q66K14	*TBC1D9B*	TBC1 domain family member 9B	2.11	3.30
Q9BY89	*KIAA1671*	Uncharacterized protein KIAA1671	2.03	3.29
P27816	*MAP4*	Microtubule-associated protein 4	2.93	3.29
Q9H4H8	*FAM83D*	Protein FAM83D	2.02	3.28
P19174	*PLCG1*	1-phosphatidylinositol 4,5-bisphosphate phosphodiesterase gamma-1	2.84	3.27
P48651	*PTDSS1*	Phosphatidylserine synthase 1	2.23	3.27
Q92625	*ANKS1A*	Ankyrin repeat and SAM domain-containing protein 1A	3.92	3.25
Q9UL15	*BAG5*	BAG family molecular chaperone regulator 5	4.28	3.24
Q9NRR5	*UBQLN4*	Ubiquilin-4	2.46	3.24
P19525	*EIF2AK2*	Interferon-induced, double-stranded RNA-activated protein kinase	2.50	3.23
Q15005	*SPCS2*	Signal peptidase complex subunit 2	4.61	3.21
Q9NZJ0	*DTL*	Denticleless protein homolog	2.68	3.20
Q14807	*KIF22*	Kinesin-like protein KIF22	2.16	3.19
P61758	*VBP1*	Prefoldin subunit 3	3.99	3.18
Q9NZT2	*OGFR*	Opioid growth factor receptor	2.59	3.18
O60547	*GMDS*	GDP-mannose 4,6 dehydratase	3.93	3.15
Q86Y07	*VRK2*	Serine/threonine-protein kinase VRK2	2.65	3.14
Q8TEY7	*USP33*	Ubiquitin carboxyl-terminal hydrolase 33	2.24	3.14
Q9UKX7	*NUP50*	Nuclear pore complex protein Nup50	3.33	3.13
Q9Y2D5	*AKAP2*	A-kinase anchor protein 2	2.82	3.13
P63151	*PPP2R2A*	Serine/threonine-protein phosphatase 2A 55 kDa regulatory subunit B alpha isoform	2.77	3.12
P53384	*NUBP1*	Cytosolic Fe-S cluster assembly factor NUBP1	4.72	3.11
Q9NT62	*ATG3*	Ubiquitin-like-conjugating enzyme ATG3	3.34	3.11
Q5T8D3	*ACBD5*	Acyl-CoA-binding domain-containing protein 5	2.46	3.10
Q5T5U3	*ARHGAP21*	Rho GTPase-activating protein 21	2.37	3.10
P51617	*IRAK1*	Interleukin-1 receptor-associated kinase 1	2.71	3.10
Q15398	*DLGAP5*	Disks large-associated protein 5	3.75	3.10
O95999	*BCL10*	B-cell lymphoma/leukemia 10	2.38	3.10
Q96C19	*EFHD2*	EF-hand domain-containing protein D2	2.75	3.09
Q96GS4	*C17orf59*	Uncharacterized protein C17orf59	2.92	3.09
Q96A49	*SYAP1*	Synapse-associated protein 1	2.22	3.09
Q8NFW8	*CMAS*	N-acylneuraminate cytidylyltransferase	2.20	3.07
Q14694	*USP10*	Ubiquitin carboxyl-terminal hydrolase 10	3.14	3.06
Q8N0X7	*SPG20*	Spartin	3.20	3.06
Q99666	*RGPD5*	RANBP2-like and GRIP domain-containing protein 5/6	3.96	3.05
Q9H2G2	*SLK*	STE20-like serine/threonine-protein kinase	3.03	3.04
Q9BQ70	*TCF25*	Transcription factor 25	2.89	3.02
Q9Y2G8	*DNAJC16*	DnaJ homolog subfamily C member 16	2.58	3.01

Q7Z4H7	*HAUS6*	HAUS augmin-like complex subunit 6	2.99	3.00
Q8N1F8	*STK11IP*	Serine/threonine-protein kinase 11-interacting protein	2.40	3.00
Q6PJG6	*BRAT1*	BRCA1-associated ATM activator 1	3.16	2.99
Q8WXE0	*CASKIN2*	Caskin-2	3.30	2.98
Q7Z434	*MAVS*	Mitochondrial antiviral-signaling protein	2.92	2.98
O94966	*USP19*	Ubiquitin carboxyl-terminal hydrolase 19	2.60	2.98
Q9BSD7	*NTPCR*	Cancer-related nucleoside-triphosphatase	2.12	2.94
O15027	*SEC16A*	Protein transport protein Sec16A	3.21	2.94
Q9HCU5	*PREB*	Prolactin regulatory element-binding protein	2.50	2.94
Q9NP72	*RAB18*	Ras-related protein Rab-18	2.76	2.93
Q92667	*AKAP1*	A-kinase anchor protein 1, mitochondrial	3.69	2.92
Q8N511	*TMEM199*	Transmembrane protein 199	3.60	2.91
Q96KB5	*PBK*	Lymphokine-activated killer T-cell-originated protein kinase	2.56	2.90
O00233	*PSMD9*	26S proteasome non-ATPase regulatory subunit 9	4.50	2.89
O60784	*TOM1*	Target of Myb protein 1	2.56	2.89
P49069	*CAMLG*	Calcium signal-modulating cyclophilin ligand	2.95	2.88
O95613	*PCNT*	Pericentrin	2.51	2.87
P50402	*EMD*	Emerin	3.68	2.86
Q9HDC5	*JPH1*	Junctophilin-1	3.15	2.85
Q8N573	*OXR1*	Oxidation resistance protein 1	2.11	2.82
Q96R06	*SPAG5*	Sperm-associated antigen 5	3.18	2.81
O95793	*STAU1*	Double-stranded RNA-binding protein Staufen homolog 1	2.21	2.80
Q9H7E9	*C8orf33*	UPF0488 protein C8orf33	3.07	2.80
Q99873	*PRMT1*	Protein arginine N-methyltransferase 1	2.06	2.79
Q9UBU6	*FAM8A1*	Protein FAM8A1	3.09	2.79
Q9P0U3	*SENP1*	Sentrin-specific protease 1	2.75	2.76
Q13615	*MTMR3*	Myotubularin-related protein 3	3.49	2.76
Q53EZ4	*CEP55*	Centrosomal protein of 55 kDa	4.79	2.75
Q9Y371	*SH3GLB1*	Endophilin-B1	2.66	2.74
Q8NB90	*SPATA5*	Spermatogenesis-associated protein 5	2.62	2.73
Q7Z2Z2	*EFTUD1*	Elongation factor Tu GTP-binding domain-containing protein 1	2.92	2.72
Q8N6M0	*OTUD6B*	OTU domain-containing protein 6B	2.01	2.71
Q14247	*CTTN*	Src substrate cortactin	3.95	2.71
Q9Y4E8	*USP15*	Ubiquitin carboxyl-terminal hydrolase 15	3.40	2.71
Q9Y4C1	*KDM3A*	Lysine-specific demethylase 3A	3.76	2.71
P49790	*NUP153*	Nuclear pore complex protein Nup153	3.64	2.70
Q9BYB4	*GNB1L*	Guanine nucleotide-binding protein subunit beta-like protein 1	2.57	2.70
Q9H4A3	*WNK1*	Serine/threonine-protein kinase WNK1	2.23	2.69
Q8NHV4	*NEDD1*	Protein NEDD1	2.22	2.69
Q9BZX2	*UCK2*	Uridine-cytidine kinase 2	2.25	2.68
O60427	*FADS1*	Fatty acid desaturase 1	3.67	2.68
Q96SU4	*OSBPL9*	Oxysterol-binding protein-related protein 9	4.14	2.67
Q8ND83	*SLAIN1*	SLAIN motif-containing protein 1	2.04	2.67
Q8IZ21	*PHACTR4*	Phosphatase and actin regulator 4	2.29	2.66
O75044	*SRGAP2*	SLIT-ROBO Rho GTPase-activating protein 2	2.34	2.65
P28290	*SSFA2*	Sperm-specific antigen 2	3.34	2.65
O75694	*NUP155*	Nuclear pore complex protein Nup155	2.18	2.64
Q9UGP4	*LIMD1*	LIM domain-containing protein 1	3.94	2.64
P48506	*GCLC*	Glutamate--cysteine ligase catalytic subunit	2.44	2.64
P20290	*BTF3*	Transcription factor BTF3	2.01	2.63
Q8N5G2	*TMEM57*	Macoilin	4.01	2.63
Q99567	*NUP88*	Nuclear pore complex protein Nup88	2.21	2.61
Q643R3	*LPCAT4*	Lysophospholipid acyltransferase LPCAT4	2.24	2.60
Q9Y277	*VDAC3*	Voltage-dependent anion-selective channel protein 3	3.73	2.59
O76024	*WFS1*	Wolframin	2.21	2.59
Q8WZA9	*IRGQ*	Immunity-related GTPase family Q protein	3.02	2.57
Q9UJW0	*DCTN4*	Dynactin subunit 4	2.67	2.56
O15269	*SPTLC1*	Serine palmitoyltransferase 1	2.52	2.54
O43379	*WDR62*	WD repeat-containing protein 62	2.16	2.53
Q9H6T3	*RPAP3*	RNA polymerase II-associated protein 3	2.46	2.51
Q15654	*TRIP6*	Thyroid receptor-interacting protein 6	3.18	2.51
Q9BTE3	*MCMBP*	Mini-chromosome maintenance complex-binding protein	4.33	2.50
Q6UVJ0	*SASS6*	Spindle assembly abnormal protein 6 homolog	3.70	2.50
Q9UBF8	*PI4KB*	Phosphatidylinositol 4-kinase beta	2.40	2.47
Q9Y2U8	*LEMD3*	Inner nuclear membrane protein Man1	2.97	2.45
Q8NHH9	*ATL2*	Atlastin-2	2.32	2.45
Q8IYS1	*PM20D2*	Peptidase M20 domain-containing protein 2	2.62	2.44
P51858	*HDGF*	Hepatoma-derived growth factor	2.51	2.44
P49585	*PCYT1A*	Choline-phosphate cytidylyltransferase A	2.87	2.42
Q9Y2Z0	*SUGT1*	Suppressor of G2 allele of SKP1 homolog	2.18	2.41
Q99961	*SH3GL1*	Endophilin-A2	2.99	2.41
Q6PKG0	*LARP1*	La-related protein 1	3.49	2.41
Q9P2E9	*RRBP1*	Ribosome-binding protein 1	3.01	2.41

Q9H910	*HN1L*	Hematological and neurological expressed 1-like protein	2.15	2.40
P06753	*TPM3*	Tropomyosin alpha-3 chain	2.33	2.40
O00161	*SNAP23*	Synaptosomal-associated protein 23	2.82	2.40
Q9Y2W6	*TDRKH*	Tudor and KH domain-containing protein	2.63	2.39
Q71RC2	*LARP4*	La-related protein 4	5.50	2.38
Q96F86	*EDC3*	Enhancer of mRNA-decapping protein 3	2.57	2.37
Q8IW35	*CEP97*	Centrosomal protein of 97 kDa	2.42	2.37
Q06124	*PTPN11*	Tyrosine-protein phosphatase non-receptor type 11	3.53	2.37
Q9C0C9	*UBE2O*	E2/E3 hybrid ubiquitin-protein ligase UBE2O	3.20	2.35
Q01970	*PLCB3*	1-phosphatidylinositol 4,5-bisphosphate phosphodiesterase beta-3	2.29	2.35
Q9BVQ7	*SPATA5L1*	Spermatogenesis-associated protein 5-like protein 1	2.36	2.35
Q15653	*NFKBIB*	NF-kappa-B inhibitor beta	2.97	2.34
Q9H6U6	*BCAS3*	Breast carcinoma-amplified sequence 3	2.54	2.33
Q86V48	*LUZP1*	Leucine zipper protein 1	2.67	2.33
Q92551	*IP6K1*	Inositol hexakisphosphate kinase 1	3.11	2.33
Q8TC07	*TBC1D15*	TBC1 domain family member 15	2.03	2.33
Q9H0B6	*KLC2*	Kinesin light chain 2	2.43	2.33
A6NDG6	*PGP*	Phosphoglycolate phosphatase	2.92	2.33
A8CG34	*POM121C*	Nuclear envelope pore membrane protein POM 121C	3.09	2.32
Q15027	*ACAP1*	Arf-GAP with coiled-coil, ANK repeat and PH domain-containing protein 1	2.84	2.32
P42166	*TMPO*	Lamina-associated polypeptide 2, isoform alpha	2.02	2.30
P48507	*GCLM*	Glutamate--cysteine ligase regulatory subunit	2.39	2.29
P48634	*PRRC2A*	Protein PRRC2A	2.40	2.29
Q99614	*TTC1*	Tetratricopeptide repeat protein 1	2.01	2.29
Q9NZZ3	*CHMP5*	Charged multivesicular body protein 5	3.92	2.29
Q9Y520	*PRRC2C*	Protein PRRC2C	3.15	2.29
Q9H0W8	*SMG9*	Protein SMG9	2.45	2.28
P0DN79	*CBS*	Cystathionine beta-synthase	3.20	2.28
P00390	*GSR*	Glutathione reductase, mitochondrial	2.03	2.28
O95292	*VAPB*	Vesicle-associated membrane protein-associated protein B/C	3.32	2.28
Q9NPH2	*ISYNA1*	Inositol-3-phosphate synthase 1	2.24	2.27
Q9UGV2	*NDRG3*	Protein NDRG3	4.22	2.26
Q15276	*RABEP1*	Rab GTPase-binding effector protein 1	2.10	2.25
O95486	*SEC24A*	Protein transport protein Sec24A	2.73	2.24
O75179	*ANKRD17*	Ankyrin repeat domain-containing protein 17	2.12	2.23
O75348	*ATP6V1G1*	V-type proton ATPase subunit G 1	2.46	2.23
P60468	*SEC61B*	Protein transport protein Sec61 subunit beta	5.41	2.22
Q15477	*SKIV2L*	Helicase SKI2W	2.14	2.22
Q8IV63	*VRK3*	Inactive serine/threonine-protein kinase VRK3	2.65	2.22
Q9NQX3	*GPHN*	Gephyrin	2.22	2.22
Q02833	*RASSF7*	Ras association domain-containing protein 7	2.68	2.22
A0AVT1	*UBA6*	Ubiquitin-like modifier-activating enzyme 6	2.46	2.19
Q9NZL4	*HSPBP1*	Hsp70-binding protein 1	2.26	2.17
Q7L5N7	*LPCAT2*	Lysophosphatidylcholine acyltransferase 2	2.76	2.17
Q9BVS4	*RIOK2*	Serine/threonine-protein kinase RIO2	2.35	2.16
P02545	*LMNA*	Prelamin-A/C	3.79	2.15
O43432	*EIF4G3*	Eukaryotic translation initiation factor 4 gamma 3	2.07	2.15
P14635	*CCNB1*	G2/mitotic-specific cyclin-B1	3.22	2.14
Q9UPY3	*DICER1*	Endoribonuclease Dicer	2.41	2.14
Q9NVG8	*TBC1D13*	TBC1 domain family member 13	2.57	2.13
Q8WWM7	*ATXN2L*	Ataxin-2-like protein	2.89	2.11
Q8WWK9	*CKAP2*	Cytoskeleton-associated protein 2	2.38	2.10
P52732	*KIF11*	Kinesin-like protein KIF11	2.43	2.10
Q9NWV8	*BABAM1*	BRISC and BRCA1-A complex member 1	3.85	2.09
Q9UNY4	*TTF2*	Transcription termination factor 2	2.55	2.08
Q15154	*PCM1*	Pericentriolar material 1 protein	3.06	2.08
Q15365	*PCBP1*	Poly(rC)-binding protein 1	2.48	2.08
Q14BN4	*SLMAP*	Sarcolemmal membrane-associated protein	3.21	2.06
Q9Y3C8	*UFC1*	Ubiquitin-fold modifier-conjugating enzyme 1	2.82	2.06
P16615	*ATP2A2*	Sarcoplasmic/endoplasmic reticulum calcium ATPase 2	2.29	2.06
O00170	*AIP*	AH receptor-interacting protein	2.69	2.05
Q9HBM1	*SPC25*	Kinetochore protein Spc25	2.55	2.05
Q9UNF1	*MAGED2*	Melanoma-associated antigen D2	2.24	2.04
Q12756	*KIF1A*	Kinesin-like protein KIF1A	2.26	2.03
Q69YQ0	*SPECC1L*	Cytospin-A	2.79	2.03
O95905	*ECD*	Protein SGT1	2.86	2.03
Q9UL46	*PSME2*	Proteasome activator complex subunit 2	2.40	2.02

Table VI-7: Proteins significantly outcompeted by a 10-fold excess of **LU** vs. 15 µM **DA-P3** in Hek293 cells.

Protein IDs	Gene names	Protein names	-log$_{10}$(*p*-value)	log$_2$(enrichment)
Q8N2K0	*ABHD12*	Monoacylglycerol lipase ABHD12	2.93	7.26
Q32MZ4	*LRRFIP1*	Leucine-rich repeat flightless-interacting protein 1	3.19	6.89
Q9Y6A5	*TACC3*	Transforming acidic coiled-coil-containing protein 3	3.47	6.58
Q6P2H3	*CEP85*	Centrosomal protein of 85 kDa	5.03	6.32
Q8IWZ3	*ANKHD1*	Ankyrin repeat and KH domain-containing protein 1	2.99	6.24
Q8IWC1	*MAP7D3*	MAP7 domain-containing protein 3	2.34	6.16
P46821	*MAP1B*	Microtubule-associated protein 1B	3.29	6.10
O95817	*BAG3*	BAG family molecular chaperone regulator 3	2.24	6.08
Q6NUQ1	*RINT1*	RAD50-interacting protein 1	2.61	5.95
O60566	*BUB1B*	Mitotic checkpoint serine/threonine-protein kinase BUB1 beta	5.00	5.88
O15270	*SPTLC2*	Serine palmitoyltransferase 2	2.22	5.82
P40763	*STAT3*	Signal transducer and activator of transcription 3	2.63	5.65
Q16204	*CCDC6*	Coiled-coil domain-containing protein 6	2.53	5.37
P56962	*STX17*	Syntaxin-17	3.48	5.36
Q5SQN1	*SNAP47*	Synaptosomal-associated protein 47	3.03	5.35
Q8ND24	*RNF214*	RING finger protein 214	2.23	5.29
O75410	*TACC1*	Transforming acidic coiled-coil-containing protein 1	3.25	5.22
Q96GA3	*LTV1*	Protein LTV1 homolog	2.84	5.19
Q2NKX8	*ERCC6L*	DNA excision repair protein ERCC-6-like	3.84	5.18
Q96P47	*AGAP3*	Arf-GAP with GTPase, ANK repeat and PH domain-containing protein 3	3.46	5.03
O14976	*GAK*	Cyclin-G-associated kinase	2.19	4.97
P82094	*TMF1*	TATA element modulatory factor	2.98	4.95
Q15003	*NCAPH*	Condensin complex subunit 2	2.10	4.95
Q66K74	*MAP1S*	Microtubule-associated protein 1S	3.13	4.93
O14531	*DPYSL4*	Dihydropyrimidinase-related protein 4	2.73	4.89
P27816	*MAP4*	Microtubule-associated protein 4	2.09	4.89
Q8TD19	*NEK9*	Serine/threonine-protein kinase Nek9	2.06	4.87
O95197	*RTN3*	Reticulon-3	2.86	4.84
P04035	*HMGCR*	3-hydroxy-3-methylglutaryl-coenzyme A reductase	2.79	4.73
Q9HC38	*GLOD4*	Glyoxalase domain-containing protein 4	3.19	4.71
Q5VV42	*CDKAL1*	Threonylcarbamoyladenosine tRNA methylthiotransferase	3.88	4.62
Q9UJC3	*HOOK1*	Protein Hook homolog 1	2.72	4.59
Q99661	*KIF2C*	Kinesin-like protein KIF2C	2.75	4.58
Q00577	*PURA*	Transcriptional activator protein Pur-alpha	2.48	4.57
Q5JSZ5	*PRRC2B*	Protein PRRC2B	2.66	4.57
Q9BZE9	*ASPSCR1*	Tether containing UBX domain for GLUT4	3.77	4.53
Q96S59	*RANBP9*	Ran-binding protein 9	3.48	4.48
Q9UHR4	*BAIAP2L1*	Brain-specific angiogenesis inhibitor 1-associated protein 2-like protein 1	2.88	4.48
P46109	*CRKL*	Crk-like protein	2.77	4.45
Q9Y5A7	*NUB1*	NEDD8 ultimate buster 1	3.63	4.43
Q9BXB4	*OSBPL11*	Oxysterol-binding protein-related protein 11	2.43	4.38
Q9Y5T5	*USP16*	Ubiquitin carboxyl-terminal hydrolase 16	2.03	4.36
P19525	*EIF2AK2*	Interferon-induced, double-stranded RNA-activated protein kinase	2.65	4.31
P22059	*OSBP*	Oxysterol-binding protein 1	3.34	4.25
O43303	*CCP110*	Centriolar coiled-coil protein of 110 kDa	2.72	4.23
Q9NUQ3	*TXLNG*	Gamma-taxilin	2.25	4.21
Q9NT62	*ATG3*	Ubiquitin-like-conjugating enzyme ATG3	2.09	4.11
P51116	*FXR2*	Fragile X mental retardation syndrome-related protein 2	2.21	4.01
Q9UJW0	*DCTN4*	Dynactin subunit 4	4.41	4.00
O60343	*TBC1D4*	TBC1 domain family member 4	3.97	3.98
Q9H9A6	*LRRC40*	Leucine-rich repeat-containing protein 40	3.36	3.93
Q9NYZ3	*GTSE1*	G2 and S phase-expressed protein 1	2.35	3.91
Q8IZ21	*PHACTR4*	Phosphatase and actin regulator 4	3.03	3.87
Q9HD26	*GOPC*	Golgi-associated PDZ and coiled-coil motif-containing protein	2.43	3.87
P63151	*PPP2R2A*	Serine/threonine-protein phosphatase 2A 55 kDa regulatory subunit B alpha isoform	3.03	3.85
Q9BSJ8	*ESYT1*	Extended synaptotagmin-1	3.62	3.85
Q9NQ88	*TIGAR*	Fructose-2,6-bisphosphatase TIGAR	2.22	3.83
Q15005	*SPCS2*	Signal peptidase complex subunit 2	2.74	3.83
Q7Z2Z2	*EFTUD1*	Elongation factor Tu GTP-binding domain-containing protein 1	2.01	3.82
Q96PC5	*MIA2*	Melanoma inhibitory activity protein 2	3.18	3.82
Q8WZA9	*IRGQ*	Immunity-related GTPase family Q protein	3.44	3.76
Q8N0X7	*SPG20*	Spartin	3.41	3.73
Q8NBF2	*NHLRC2*	NHL repeat-containing protein 2	2.42	3.71
Q9H2G2	*SLK*	STE20-like serine/threonine-protein kinase	2.19	3.68
Q9BZX2	*UCK2*	Uridine-cytidine kinase 2	2.86	3.66
Q96C19	*EFHD2*	EF-hand domain-containing protein D2	2.23	3.63
P19174	*PLCG1*	1-phosphatidylinositol 4,5-bisphosphate phosphodiesterase gamma-1	3.49	3.63

Q9Y4E8	*USP15*	Ubiquitin carboxyl-terminal hydrolase 15	3.25	3.63
Q99961	*SH3GL1*	Endophilin-A2	2.79	3.62
A0MZ66	*KIAA1598*	Shootin-1	3.64	3.60
Q08378	*GOLGA3*	Golgin subfamily A member 3	2.32	3.59
Q8NFH5	*NUP35*	Nucleoporin NUP53	2.74	3.59
Q92615	*LARP4B*	La-related protein 4B	2.83	3.55
P29372	*MPG*	DNA-3-methyladenine glycosylase	3.19	3.52
Q04323	*UBXN1*	UBX domain-containing protein 1	2.32	3.52
Q9BQA1	*WDR77*	Methylosome protein 50	2.11	3.50
P98194	*ATP2C1*	Calcium-transporting ATPase type 2C member 1	2.87	3.49
O95793	*STAU1*	Double-stranded RNA-binding protein Staufen homolog 1	2.29	3.47
Q86XL3	*ANKLE2*	Ankyrin repeat and LEM domain-containing protein 2	4.17	3.47
Q96KB5	*PBK*	Lymphokine-activated killer T-cell-originated protein kinase	3.19	3.47
Q13596	*SNX1*	Sorting nexin-1	2.62	3.44
Q15654	*TRIP6*	Thyroid receptor-interacting protein 6	2.09	3.44
P08240	*SRPR*	Signal recognition particle receptor subunit alpha	3.86	3.44
Q9UGV2	*NDRG3*	Protein NDRG3	3.72	3.42
Q15417	*CNN3*	Calponin-3	3.25	3.42
Q9Y679	*AUP1*	Ancient ubiquitous protein 1	4.96	3.41
O15027	*SEC16A*	Protein transport protein Sec16A	3.18	3.41
Q14318	*FKBP8*	Peptidyl-prolyl cis-trans isomerase FKBP8	2.67	3.39
Q9H6T3	*RPAP3*	RNA polymerase II-associated protein 3	3.21	3.36
P52888	*THOP1*	Thimet oligopeptidase	2.69	3.36
P51617	*IRAK1*	Interleukin-1 receptor-associated kinase 1	3.53	3.35
Q9NQX3	*GPHN*	Gephyrin	2.90	3.34
P0DN79	*CBS*	Cystathionine beta-synthase	2.20	3.34
Q9BTE3	*MCMBP*	Mini-chromosome maintenance complex-binding protein	3.83	3.33
Q86VQ1	*GLCCI1*	Glucocorticoid-induced transcript 1 protein	2.07	3.33
Q9P0U3	*SENP1*	Sentrin-specific protease 1	2.42	3.29
P12081	*HARS*	Histidine--tRNA ligase, cytoplasmic	2.37	3.29
P04080	*CSTB*	Cystatin-B	2.40	3.27
P28290	*SSFA2*	Sperm-specific antigen 2	2.75	3.27
A6NDG6	*PGP*	Phosphoglycolate phosphatase	2.47	3.27
Q96SK2	*TMEM209*	Transmembrane protein 209	2.53	3.25
O14965	*AURKA*	Aurora kinase A	2.20	3.23
O95336	*PGLS*	6-phosphogluconolactonase	2.40	3.21
Q9BQ70	*TCF25*	Transcription factor 25	3.62	3.20
Q14694	*USP10*	Ubiquitin carboxyl-terminal hydrolase 10	2.82	3.19
A0AVT1	*UBA6*	Ubiquitin-like modifier-activating enzyme 6	2.80	3.16
Q5JRA6	*MIA3*	Melanoma inhibitory activity protein 3	3.74	3.16
Q8IY17	*PNPLA6*	Neuropathy target esterase	2.81	3.15
Q9UNF1	*MAGED2*	Melanoma-associated antigen D2	2.29	3.14
Q16513	*PKN2*	Serine/threonine-protein kinase N2	3.73	3.14
P11766	*ADH5*	Alcohol dehydrogenase class-3	2.11	3.12
Q9UI30	*TRMT112*	Multifunctional methyltransferase subunit TRM112-like protein	3.08	3.12
Q9UI10	*EIF2B4*	Translation initiation factor eIF-2B subunit delta	2.38	3.11
Q9C0C9	*UBE2O*	E2/E3 hybrid ubiquitin-protein ligase UBE2O	3.67	3.09
P48507	*GCLM*	Glutamate--cysteine ligase regulatory subunit	2.56	3.08
Q8IW35	*CEP97*	Centrosomal protein of 97 kDa	2.51	3.07
Q69YH5	*CDCA2*	Cell division cycle-associated protein 2	2.10	3.05
Q9UL46	*PSME2*	Proteasome activator complex subunit 2	4.01	3.03
Q06124	*PTPN11*	Tyrosine-protein phosphatase non-receptor type 11	3.32	3.03
P54646	*PRKAA2*	5-AMP-activated protein kinase catalytic subunit alpha-2	2.37	3.02
Q9UJY5	*GGA1*	ADP-ribosylation factor-binding protein GGA1	3.04	3.01
Q12756	*KIF1A*	Kinesin-like protein KIF1A	2.00	3.01
Q8WU90	*ZC3H15*	Zinc finger CCCH domain-containing protein 15	2.29	3.00
P53384	*NUBP1*	Cytosolic Fe-S cluster assembly factor NUBP1	3.95	2.99
Q8N5G2	*TMEM57*	Macoilin	2.70	2.98
Q5T8D3	*ACBD5*	Acyl-CoA-binding domain-containing protein 5	2.52	2.96
Q9NZZ3	*CHMP5*	Charged multivesicular body protein 5	3.39	2.95
Q9NSV4	*DIAPH3*	Protein diaphanous homolog 3	2.78	2.94
Q9NUL3	*STAU2*	Double-stranded RNA-binding protein Staufen homolog 2	4.48	2.92
A0A087X1C1	*TMSB15B*	Thymosin beta-15B	2.01	2.90
Q99567	*NUP88*	Nuclear pore complex protein Nup88	2.61	2.88
Q14247	*CTTN*	Src substrate cortactin	3.16	2.87
O94966	*USP19*	Ubiquitin carboxyl-terminal hydrolase 19	4.07	2.85
P37198	*NUP62*	Nuclear pore glycoprotein p62	2.80	2.84
O43379	*WDR62*	WD repeat-containing protein 62	2.69	2.82
P55957	*BID*	BH3-interacting domain death agonist	4.17	2.78
P35080	*PFN2*	Profilin-2	3.02	2.77
O15355	*PPM1G*	Protein phosphatase 1G	3.41	2.76
Q8WWM7	*ATXN2L*	Ataxin-2-like protein	2.60	2.74

Q9ULT8	*HECTD1*	E3 ubiquitin-protein ligase HECTD1	2.65	2.73
Q86V48	*LUZP1*	Leucine zipper protein 1	2.51	2.72
Q9NPH2	*ISYNA1*	Inositol-3-phosphate synthase 1	4.08	2.72
Q99614	*TTC1*	Tetratricopeptide repeat protein 1	2.63	2.71
Q9NZL4	*HSPBP1*	Hsp70-binding protein 1	2.32	2.70
Q9UBP0	*SPAST*	Spastin	2.01	2.70
O00161	*SNAP23*	Synaptosomal-associated protein 23	2.04	2.70
P23921	*RRM1*	Ribonucleoside-diphosphate reductase large subunit	2.64	2.68
Q14807	*KIF22*	Kinesin-like protein KIF22	2.71	2.68
O95801	*TTC4*	Tetratricopeptide repeat protein 4	3.53	2.67
E7EVH7	*KLC1*	Kinesin light chain 1	2.48	2.64
P54105	*CLNS1A*	Methylosome subunit pICln	2.31	2.64
Q9Y3C8	*UFC1*	Ubiquitin-fold modifier-conjugating enzyme 1	2.05	2.64
Q96F86	*EDC3*	Enhancer of mRNA-decapping protein 3	3.31	2.59
Q96A49	*SYAP1*	Synapse-associated protein 1	2.07	2.59
Q8TCG1	*KIAA1524*	Protein CIP2A	2.26	2.57
Q5SW79	*CEP170*	Centrosomal protein of 170 kDa	2.13	2.56
Q15027	*ACAP1*	Arf-GAP with coiled-coil, ANK repeat and PH domain-containing protein 1	2.22	2.55
Q99873	*PRMT1*	Protein arginine N-methyltransferase 1	3.37	2.54
Q9UKX7	*NUP50*	Nuclear pore complex protein Nup50	3.79	2.53
Q9UHD8	*Sept9*	Septin-9	2.90	2.51
P41227	*NAA10*	N-alpha-acetyltransferase 10	2.46	2.51
Q6PKG0	*LARP1*	La-related protein 1	2.66	2.50
Q14C86	*GAPVD1*	GTPase-activating protein and VPS9 domain-containing protein 1	2.21	2.48
Q8NEN9	*PDZD8*	PDZ domain-containing protein 8	2.22	2.48
P31153	*MAT2A*	S-adenosylmethionine synthase isoform type-2	4.79	2.47
Q96IW7	*SEC22A*	Vesicle-trafficking protein SEC22a	2.17	2.47
Q7Z5L2	*R3HCC1L*	Coiled-coil domain-containing protein R3HCC1L	2.14	2.46
Q71RC2	*LARP4*	La-related protein 4	4.62	2.45
Q96SU4	*OSBPL9*	Oxysterol-binding protein-related protein 9	2.91	2.43
P14635	*CCNB1*	G2/mitotic-specific cyclin-B1	3.91	2.41
Q14738	*PPP2R5D*	Serine/threonine-protein phosphatase 2A 56 kDa regulatory subunit delta isoform	2.90	2.41
O95347	*SMC2*	Structural maintenance of chromosomes protein 2	3.56	2.40
Q9Y520	*PRRC2C*	Protein PRRC2C	2.65	2.40
O95905	*ECD*	Protein SGT1	2.28	2.40
P00390	*GSR*	Glutathione reductase, mitochondrial	2.76	2.39
Q9Y696	*CLIC4*	Chloride intracellular channel protein 4	3.37	2.39
O00233	*PSMD9*	26S proteasome non-ATPase regulatory subunit 9	2.66	2.38
O75663	*TIPRL*	TIP41-like protein	2.20	2.37
Q9H6S0	*YTHDC2*	Probable ATP-dependent RNA helicase YTHDC2	4.08	2.36
Q15334	*LLGL1*	Lethal(2) giant larvae protein homolog 1	3.15	2.34
Q96SB4	*SRPK1*	SRSF protein kinase 1	2.84	2.34
O43583	*DENR*	Density-regulated protein	2.21	2.33
O75122	*CLASP2*	CLIP-associating protein 2	2.12	2.31
P01893	*HLA-H*	Putative HLA class I histocompatibility antigen, alpha chain H	2.70	2.29
Q15021	*NCAPD2*	Condensin complex subunit 1	3.93	2.29
P60468	*SEC61B*	Protein transport protein Sec61 subunit beta	2.40	2.29
Q9Y5A9	*YTHDF2*	YTH domain-containing family protein 2	2.15	2.27
Q9NSD9	*FARSB*	Phenylalanine--tRNA ligase beta subunit	2.18	2.25
P48634	*PRRC2A*	Protein PRRC2A	2.33	2.25
Q01433	*AMPD2*	AMP deaminase 2	2.58	2.25
Q9UBU6	*FAM8A1*	Protein FAM8A1	2.95	2.23
Q53GS7	*GLE1*	Nucleoporin GLE1	2.58	2.21
P50851	*LRBA*	Lipopolysaccharide-responsive and beige-like anchor protein	2.59	2.21
Q9H3K6	*BOLA2*	BolA-like protein 2	2.54	2.21
Q9P2E9	*RRBP1*	Ribosome-binding protein 1	4.88	2.21
P49915	*GMPS*	GMP synthase [glutamine-hydrolyzing]	2.37	2.21
A0FGR8	*ESYT2*	Extended synaptotagmin-2	3.09	2.20
Q8IV63	*VRK3*	Inactive serine/threonine-protein kinase VRK3	2.22	2.20
Q06210	*GFPT1*	Glutamine--fructose-6-phosphate aminotransferase [isomerizing] 1	2.46	2.19
Q13045	*FLII*	Protein flightless-1 homolog	2.22	2.19
Q96H79	*ZC3HAV1L*	Zinc finger CCCH-type antiviral protein 1-like	2.29	2.19
Q86WB0	*ZC3HC1*	Nuclear-interacting partner of ALK	2.07	2.18
O95163	*IKBKAP*	Elongator complex protein 1	2.85	2.18
O14545	*TRAFD1*	TRAF-type zinc finger domain-containing protein 1	2.85	2.17
P22102	*GART*	Trifunctional purine biosynthetic protein adenosine-3	2.57	2.16
Q96T76	*MMS19*	MMS19 nucleotide excision repair protein homolog	2.67	2.13
P45984	*MAPK9*	Mitogen-activated protein kinase 9	2.96	2.12
O43396	*TXNL1*	Thioredoxin-like protein 1	4.12	2.12
Q05682	*CALD1*	Caldesmon	2.66	2.11
Q6IA86	*ELP2*	Elongator complex protein 2	2.79	2.11

Q9H4L5	*OSBPL3*	Oxysterol-binding protein-related protein 3	2.31	2.11
Q00341	*HDLBP*	Vigilin	2.51	2.10
P13807	*GYS1*	Glycogen [starch] synthase, muscle	2.07	2.09
Q96PZ0	*PUS7*	Pseudouridylate synthase 7 homolog	2.24	2.08
O00170	*AIP*	AH receptor-interacting protein	2.84	2.08
Q99543	*DNAJC2*	DnaJ homolog subfamily C member 2	2.59	2.08
Q9Y5Y2	*NUBP2*	Cytosolic Fe-S cluster assembly factor NUBP2	2.47	2.06
O76024	*WFS1*	Wolframin	2.21	2.06
Q9Y605	*MRFAP1*	MORF4 family-associated protein 1	2.01	2.05
P60660	*MYL6*	Myosin light polypeptide 6	2.34	2.02
O75821	*EIF3G*	Eukaryotic translation initiation factor 3 subunit G	2.66	2.01

Table VI-8: Proteins significantly outcompeted by a 10-fold excess of **EG** vs. 15 µM **DA-P3** in Hek293 cells.

Protein IDs	**Gene names**	**Protein names**	**-log$_{10}$(*p*-value)**	**log$_2$(enrichment)**
Q9Y6A5	*TACC3*	Transforming acidic coiled-coil-containing protein 3	2.61	7.64
Q8TD19	*NEK9*	Serine/threonine-protein kinase Nek9	3.30	7.04
P40763	*STAT3*	Signal transducer and activator of transcription 3	4.58	6.71
P09132	*SRP19*	Signal recognition particle 19 kDa protein	2.81	6.59
Q16204	*CCDC6*	Coiled-coil domain-containing protein 6	2.49	6.50
P15170	*GSPT1*	Eukaryotic peptide chain release factor GTP-binding subunit ERF3A	2.02	6.40
Q15003	*NCAPH*	Condensin complex subunit 2	3.53	6.27
Q14694	*USP10*	Ubiquitin carboxyl-terminal hydrolase 10	2.89	6.24
Q96GA3	*LTV1*	Protein LTV1 homolog	4.08	6.09
Q8IWZ3	*ANKHD1*	Ankyrin repeat and KH domain-containing protein 1	2.71	5.54
O95817	*BAG3*	BAG family molecular chaperone regulator 3	2.52	5.54
P19174	*PLCG1*	1-phosphatidylinositol 4,5-bisphosphate phosphodiesterase gamma-1	5.47	5.53
Q9NT62	*ATG3*	Ubiquitin-like-conjugating enzyme ATG3	4.09	5.52
Q9ULT8	*HECTD1*	E3 ubiquitin-protein ligase HECTD1	2.42	5.36
Q9NQW6	*ANLN*	Actin-binding protein anillin	3.01	5.32
A0MZ66	*KIAA1598*	Shootin-1	2.56	5.32
Q9HC38	*GLOD4*	Glyoxalase domain-containing protein 4	3.55	5.31
P61758	*VBP1*	Prefoldin subunit 3	3.35	5.29
Q96C19	*EFHD2*	EF-hand domain-containing protein D2	2.47	5.22
P52888	*THOP1*	Thimet oligopeptidase	2.87	5.17
Q96CX2	*KCTD12*	BTB/POZ domain-containing protein KCTD12	3.21	5.14
Q8IXW5	*RPAP2*	Putative RNA polymerase II subunit B1 CTD phosphatase RPAP2	2.26	5.12
Q9UNF1	*MAGED2*	Melanoma-associated antigen D2	2.08	5.11
Q9Y371	*SH3GLB1*	Endophilin-B1	2.40	5.05
A0AVT1	*UBA6*	Ubiquitin-like modifier-activating enzyme 6	2.50	5.03
P20810	*CAST*	Calpastatin	3.60	4.97
Q12756	*KIF1A*	Kinesin-like protein KIF1A	4.07	4.90
Q96P47	*AGAP3*	Arf-GAP with GTPase, ANK repeat and PH domain-containing protein 3	3.11	4.88
Q9UKA4	*AKAP11*	A-kinase anchor protein 11	2.03	4.88
P0DN79	*CBS*	Cystathionine beta-synthase	2.32	4.83
P04035	*HMGCR*	3-hydroxy-3-methylglutaryl-coenzyme A reductase	2.02	4.77
P46109	*CRKL*	Crk-like protein	2.19	4.68
Q9UGP4	*LIMD1*	LIM domain-containing protein 1	3.13	4.68
P51617	*IRAK1*	Interleukin-1 receptor-associated kinase 1	3.06	4.66
Q99661	*KIF2C*	Kinesin-like protein KIF2C	3.67	4.58
Q9H3K6	*BOLA2*	BolA-like protein 2	2.21	4.56
A1X283	*SH3PXD2B*	SH3 and PX domain-containing protein 2B	2.24	4.52
O43303	*CCP110*	Centriolar coiled-coil protein of 110 kDa	4.60	4.48
Q9BTE3	*MCMBP*	Mini-chromosome maintenance complex-binding protein	2.97	4.44
P17812	*CTPS1*	CTP synthase 1	2.99	4.44
Q9BZE9	*ASPSCR1*	Tether containing UBX domain for GLUT4	3.56	4.41
Q8TC07	*TBC1D15*	TBC1 domain family member 15	2.35	4.35
Q8N6T3	*ARFGAP1*	ADP-ribosylation factor GTPase-activating protein 1	2.67	4.33
P12081	*HARS*	Histidine--tRNA ligase, cytoplasmic	3.92	4.32
Q96S59	*RANBP9*	Ran-binding protein 9	2.07	4.30
Q00577	*PURA*	Transcriptional activator protein Pur-alpha	2.26	4.29
Q8IWC1	*MAP7D3*	MAP7 domain-containing protein 3	4.54	4.28
Q92616	*GCN1L1*	Translational activator GCN1	2.99	4.27
O94966	*USP19*	Ubiquitin carboxyl-terminal hydrolase 19	3.84	4.22
P27816	*MAP4*	Microtubule-associated protein 4	3.41	4.15
Q5JSZ5	*PRRC2B*	Protein PRRC2B	3.00	4.13
Q8N2K0	*ABHD12*	Monoacylglycerol lipase ABHD12	2.09	4.11
O60271	*SPAG9*	C-Jun-amino-terminal kinase-interacting protein 4	4.58	4.09
A6NDG6	*PGP*	Phosphoglycolate phosphatase	2.48	4.07
P82094	*TMF1*	TATA element modulatory factor	3.49	4.06

O95197	*RTN3*	Reticulon-3	2.21	4.04
P49588	*AARS*	Alanine--tRNA ligase, cytoplasmic	2.16	4.02
Q9NUQ3	*TXLNG*	Gamma-taxilin	3.43	3.99
Q9Y2Z0	*SUGT1*	Suppressor of G2 allele of SKP1 homolog	2.86	3.93
P41227	*NAA10*	N-alpha-acetyltransferase 10	3.91	3.92
Q9H9A6	*LRRC40*	Leucine-rich repeat-containing protein 40	2.25	3.92
Q9C0C9	*UBE2O*	E2/E3 hybrid ubiquitin-protein ligase UBE2O	2.86	3.89
O95816	*BAG2*	BAG family molecular chaperone regulator 2	2.04	3.88
Q7Z6Z7	*HUWE1*	E3 ubiquitin-protein ligase HUWE1	2.80	3.86
Q06124	*PTPN11*	Tyrosine-protein phosphatase non-receptor type 11	3.95	3.86
Q3KQU3	*MAP7D1*	MAP7 domain-containing protein 1	3.55	3.86
Q15154	*PCM1*	Pericentriolar material 1 protein	4.07	3.84
Q8IZ21	*PHACTR4*	Phosphatase and actin regulator 4	3.17	3.81
P04080	*CSTB*	Cystatin-B	3.18	3.81
Q8TEQ6	*GEMIN5*	Gem-associated protein 5	2.87	3.80
Q5T4S7	*UBR4*	E3 ubiquitin-protein ligase UBR4	2.56	3.79
O60610	*DIAPH1*	Protein diaphanous homolog 1	4.05	3.76
O95163	*IKBKAP*	Elongator complex protein 1	2.04	3.73
A0A087X1C1	*TMSB15B*	Thymosin beta-15B	2.12	3.68
Q8WZA9	*IRGQ*	Immunity-related GTPase family Q protein	3.41	3.68
Q9NYZ3	*GTSE1*	G2 and S phase-expressed protein 1	2.69	3.67
Q8N0X7	*SPG20*	Spartin	3.47	3.66
O60256	*PRPSAP2*	Phosphoribosyl pyrophosphate synthase-associated protein 2	3.01	3.64
Q13131	*PRKAA1*	5-AMP-activated protein kinase catalytic subunit alpha-1	2.02	3.63
P53384	*NUBP1*	Cytosolic Fe-S cluster assembly factor NUBP1	3.06	3.60
P42345	*MTOR*	Serine/threonine-protein kinase mTOR	2.46	3.60
Q9NZL4	*HSPBP1*	Hsp70-binding protein 1	2.37	3.60
O95613	*PCNT*	Pericentrin	2.30	3.58
O15121	*DEGS1*	Sphingolipid delta(4)-desaturase DES1	2.26	3.58
Q9H6S0	*YTHDC2*	Probable ATP-dependent RNA helicase YTHDC2	4.37	3.55
P49915	*GMPS*	GMP synthase [glutamine-hydrolyzing]	2.06	3.54
Q9NPH2	*ISYNA1*	Inositol-3-phosphate synthase 1	3.10	3.54
Q14166	*TTLL12*	Tubulin--tyrosine ligase-like protein 12	2.19	3.53
Q9BQ70	*TCF25*	Transcription factor 25	2.26	3.52
Q13085	*ACACA*	Acetyl-CoA carboxylase 1	2.15	3.52
Q13370	*PDE3B*	cGMP-inhibited 3,5-cyclic phosphodiesterase B	2.55	3.48
O75821	*EIF3G*	Eukaryotic translation initiation factor 3 subunit G	3.18	3.48
P52565	*ARHGDIA*	Rho GDP-dissociation inhibitor 1	2.95	3.47
Q9BZX2	*UCK2*	Uridine-cytidine kinase 2	2.10	3.46
O75153	*CLUH*	Clustered mitochondria protein homolog	2.59	3.44
Q14738	*PPP2R5D*	Serine/threonine-protein phosphatase 2A 56 kDa regulatory subunit delta isoform	4.99	3.43
Q5T5U3	*ARHGAP21*	Rho GTPase-activating protein 21	3.22	3.40
Q9H7E9	*C8orf33*	UPF0488 protein C8orf33	3.80	3.39
Q6FI81	*CIAPIN1*	Anamorsin	4.64	3.37
Q6WKZ4	*RAB11FIP1*	Rab11 family-interacting protein 1	2.01	3.37
Q15417	*CNN3*	Calponin-3	2.34	3.36
P30520	*ADSS*	Adenylosuccinate synthetase isozyme 2	2.23	3.35
Q9UHD1	*CHORDC1*	Cysteine and histidine-rich domain-containing protein 1	2.46	3.35
Q8N2G8	*GHDC*	GH3 domain-containing protein	2.33	3.35
Q16799	*RTN1*	Reticulon-1	3.44	3.35
P49327	*FASN*	Fatty acid synthase	2.53	3.34
Q8TEX9	*IPO4*	Importin-4	3.50	3.34
Q01433	*AMPD2*	AMP deaminase 2	2.72	3.32
Q8N3C0	*ASCC3*	Activating signal cointegrator 1 complex subunit 3	3.38	3.32
P52732	*KIF11*	Kinesin-like protein KIF11	3.56	3.30
Q08378	*GOLGA3*	Golgin subfamily A member 3	2.95	3.30
Q06203	*PPAT*	Amidophosphoribosyltransferase	3.47	3.30
O00170	*AIP*	AH receptor-interacting protein	2.41	3.30
P56962	*STX17*	Syntaxin-17	2.36	3.28
P19525	*EIF2AK2*	Interferon-induced, double-stranded RNA-activated protein kinase	2.10	3.28
P53992	*SEC24C*	Protein transport protein Sec24C	2.14	3.27
P35573	*AGL*	Glycogen debranching enzyme	4.10	3.27
P14735	*IDE*	Insulin-degrading enzyme	2.81	3.26
Q8NHV4	*NEDD1*	Protein NEDD1	2.89	3.25
Q06210	*GFPT1*	Glutamine--fructose-6-phosphate aminotransferase [isomerizing] 1	2.65	3.25
Q5VV42	*CDKAL1*	Threonylcarbamoyladenosine tRNA methylthiotransferase	3.54	3.25
Q99543	*DNAJC2*	DnaJ homolog subfamily C member 2	3.21	3.22
Q9UL46	*PSME2*	Proteasome activator complex subunit 2	2.26	3.22
Q96A49	*SYAP1*	Synapse-associated protein 1	2.44	3.22
Q9BV44	*THUMPD3*	THUMP domain-containing protein 3	3.33	3.21
P54105	*CLNS1A*	Methylosome subunit pICln	2.57	3.20

Q9HB20	*PLEKHA3*	Pleckstrin homology domain-containing family A member 3	2.33	3.20
P51570	*GALK1*	Galactokinase	2.63	3.19
O14929	*HAT1*	Histone acetyltransferase type B catalytic subunit	2.11	3.17
Q9UGV2	*NDRG3*	Protein NDRG3	3.09	3.17
P48507	*GCLM*	Glutamate--cysteine ligase regulatory subunit	3.54	3.16
O00410	*IPO5*	Importin-5	2.51	3.15
O14744	*PRMT5*	Protein arginine N-methyltransferase 5	2.34	3.15
Q8IYS1	*PM20D2*	Peptidase M20 domain-containing protein 2	2.78	3.13
Q8WWM7	*ATXN2L*	Ataxin-2-like protein	2.52	3.12
O95801	*TTC4*	Tetratricopeptide repeat protein 4	2.51	3.11
O75410	*TACC1*	Transforming acidic coiled-coil-containing protein 1	3.66	3.10
Q8ND83	*SLAIN1*	SLAIN motif-containing protein 1	2.45	3.09
Q99961	*SH3GL1*	Endophilin-A2	2.79	3.05
Q9Y266	*NUDC*	Nuclear migration protein nudC	2.69	3.03
Q99873	*PRMT1*	Protein arginine N-methyltransferase 1	2.34	3.01
Q92615	*LARP4B*	La-related protein 4B	2.01	2.99
Q00341	*HDLBP*	Vigilin	2.48	2.97
P53618	*COPB1*	Coatomer subunit beta	3.01	2.96
Q9H8Y5	*ANKZF1*	Ankyrin repeat and zinc finger domain-containing protein 1	2.35	2.96
P56192	*MARS*	Methionine--tRNA ligase, cytoplasmic	2.04	2.95
Q99614	*TTC1*	Tetratricopeptide repeat protein 1	3.17	2.95
Q96RS6	*NUDCD1*	NudC domain-containing protein 1	3.11	2.94
P45974	*USP5*	Ubiquitin carboxyl-terminal hydrolase 5	2.33	2.94
Q9NSV4	*DIAPH3*	Protein diaphanous homolog 3	2.29	2.93
Q2M1P5	*KIF7*	Kinesin-like protein KIF7	2.14	2.92
O15067	*PFAS*	Phosphoribosylformylglycinamidine synthase	2.21	2.92
Q6PKG0	*LARP1*	La-related protein 1	2.97	2.91
P22061	*PCMT1*	Protein-L-isoaspartate(D-aspartate) O-methyltransferase	2.64	2.91
O15344	*MID1*	E3 ubiquitin-protein ligase Midline-1	2.31	2.90
P53396	*ACLY*	ATP-citrate synthase	2.69	2.90
E7EVH7	*KLC1*	Kinesin light chain 1	2.57	2.89
Q04760	*GLO1*	Lactoylglutathione lyase	2.46	2.87
Q9UBT2	*UBA2*	SUMO-activating enzyme subunit 2	3.12	2.86
O00299	*CLIC1*	Chloride intracellular channel protein 1	2.07	2.84
Q9ULX3	*NOB1*	RNA-binding protein NOB1	2.06	2.82
Q9P1Y5	*CAMSAP3*	Calmodulin-regulated spectrin-associated protein 3	2.23	2.81
P19784	*CSNK2A2*	Casein kinase II subunit alpha	2.47	2.78
P53041	*PPP5C*	Serine/threonine-protein phosphatase 5	2.04	2.78
O60763	*USO1*	General vesicular transport factor p115	3.10	2.76
O95373	*IPO7*	Importin-7	2.21	2.75
Q9UNH7	*SNX6*	Sorting nexin-6	2.46	2.75
O95757	*HSPA4L*	Heat shock 70 kDa protein 4L	2.21	2.73
O75122	*CLASP2*	CLIP-associating protein 2	3.05	2.72
P61088	*UBE2N*	Ubiquitin-conjugating enzyme E2 N	2.10	2.70
Q15181	*PPA1*	Inorganic pyrophosphatase	3.32	2.68
Q5SWX8	*ODR4*	Protein odr-4 homolog	2.88	2.67
P30153	*PPP2R1A*	Serine/threonine-protein phosphatase 2A 65 kDa regulatory subunit A alpha isoform	2.25	2.65
Q96SU4	*OSBPL9*	Oxysterol-binding protein-related protein 9	3.09	2.65
P20290	*BTF3*	Transcription factor BTF3	2.69	2.65
Q9UI10	*EIF2B4*	Translation initiation factor eIF-2B subunit delta	2.17	2.62
Q9H910	*HN1L*	Hematological and neurological expressed 1-like protein	2.41	2.62
P20618	*PSMB1*	Proteasome subunit beta type-1	2.85	2.62
Q14318	*FKBP8*	Peptidyl-prolyl cis-trans isomerase FKBP8	2.28	2.61
P26641	*EEF1G*	Elongation factor 1-gamma	2.13	2.61
Q92538	*GBF1*	Golgi-specific brefeldin A-resistance guanine nucleotide exchange factor 1	3.80	2.60
P25786	*PSMA1*	Proteasome subunit alpha type-1	2.22	2.58
P07737	*PFN1*	Profilin-1	3.14	2.58
P27348	*YWHAQ*	14-3-3 protein theta	2.12	2.57
P14635	*CCNB1*	G2/mitotic-specific cyclin-B1	3.91	2.56
Q9BSJ8	*ESYT1*	Extended synaptotagmin-1	3.47	2.55
P61970	*NUTF2*	Nuclear transport factor 2	3.36	2.55
P11172	*UMPS*	Uridine 5-monophosphate synthase	2.68	2.55
Q9NRL3	*STRN4*	Striatin-4	2.10	2.54
Q9Y617	*PSAT1*	Phosphoserine aminotransferase	2.64	2.53
Q96HC4	*PDLIM5*	PDZ and LIM domain protein 5	3.75	2.53
Q9Y679	*AUP1*	Ancient ubiquitous protein 1	2.10	2.53
Q14671	*PUM1*	Pumilio homolog 1	2.16	2.53
Q9NZB2	*FAM120A*	Constitutive coactivator of PPAR-gamma-like protein 1	2.05	2.53
Q9HAV4	*XPO5*	Exportin-5	3.55	2.53
P54136	*RARS*	Arginine--tRNA ligase, cytoplasmic	2.92	2.52
O95456	*PSMG1*	Proteasome assembly chaperone 1	2.93	2.52

P00492	*HPRT1*	Hypoxanthine-guanine phosphoribosyltransferase	2.35	2.52
P35080	*PFN2*	Profilin-2	2.20	2.51
P48634	*PRRC2A*	Protein PRRC2A	2.09	2.51
Q9Y520	*PRRC2C*	Protein PRRC2C	3.76	2.51
Q92551	*IP6K1*	Inositol hexakisphosphate kinase 1	2.26	2.49
O75116	*ROCK2*	Rho-associated protein kinase 2	2.52	2.48
Q9Y2D5	*AKAP2*	A-kinase anchor protein 2	2.53	2.48
P31939	*ATIC*	Bifunctional purine biosynthesis protein PURH	2.29	2.47
Q8NEN9	*PDZD8*	PDZ domain-containing protein 8	2.42	2.46
P61081	*UBE2M*	NEDD8-conjugating enzyme Ubc12	3.02	2.46
P10768	*ESD*	S-formylglutathione hydrolase	2.16	2.46
Q96GS4	*C17orf59*	Uncharacterized protein C17orf59	2.04	2.45
P60174	*TPI1*	Triosephosphate isomerase	2.05	2.45
O43175	*PHGDH*	D-3-phosphoglycerate dehydrogenase	2.24	2.44
Q9UBB4	*ATXN10*	Ataxin-10	2.44	2.44
P30519	*HMOX2*	Heme oxygenase 2	5.24	2.44
P06733	*ENO1*	Alpha-enolase	2.36	2.43
O95433	*AHSA1*	Activator of 90 kDa heat shock protein ATPase homolog 1	3.02	2.43
Q15005	*SPCS2*	Signal peptidase complex subunit 2	3.88	2.39
Q9UPT5	*EXOC7*	Exocyst complex component 7	2.55	2.39
P61201	*COPS2*	COP9 signalosome complex subunit 2	2.57	2.38
P37198	*NUP62*	Nuclear pore glycoprotein p62	3.10	2.38
Q9BY32	*ITPA*	Inosine triphosphate pyrophosphatase	3.18	2.37
O14545	*TRAFD1*	TRAF-type zinc finger domain-containing protein 1	2.58	2.36
P28074	*PSMB5*	Proteasome subunit beta type-5	2.83	2.35
Q9UKX7	*NUP50*	Nuclear pore complex protein Nup50	2.68	2.34
Q9Y3C8	*UFC1*	Ubiquitin-fold modifier-conjugating enzyme 1	2.38	2.34
P13797	*PLS3*	Plastin-3	2.56	2.34
Q16513	*PKN2*	Serine/threonine-protein kinase N2	3.28	2.32
P13639	*EEF2*	Elongation factor 2	2.55	2.32
P43487	*RANBP1*	Ran-specific GTPase-activating protein	2.75	2.31
Q13310	*PABPC4*	Polyadenylate-binding protein 4	2.54	2.31
P61221	*ABCE1*	ATP-binding cassette sub-family E member 1	2.59	2.30
P17858	*PFKL*	ATP-dependent 6-phosphofructokinase, liver type	2.61	2.28
Q15027	*ACAP1*	Arf-GAP with coiled-coil, ANK repeat and PH domain-containing protein 1	2.37	2.28
Q9UEG4	*ZNF629*	Zinc finger protein 629	2.63	2.27
Q9Y3F4	*STRAP*	Serine-threonine kinase receptor-associated protein	2.25	2.26
Q9UHV9	*PFDN2*	Prefoldin subunit 2	2.43	2.23
Q16637	*SMN1*	Survival motor neuron protein	2.76	2.23
Q9NPI6	*DCP1A*	mRNA-decapping enzyme 1A	2.06	2.23
Q99700	*ATXN2*	Ataxin-2	2.24	2.23
P04049	*RAF1*	RAF proto-oncogene serine/threonine-protein kinase	2.21	2.23
P41240	*CSK*	Tyrosine-protein kinase CSK	3.08	2.22
P00558	*PGK1*	Phosphoglycerate kinase 1	2.24	2.22
O43592	*XPOT*	Exportin-T	2.21	2.22
Q00688	*FKBP3*	Peptidyl-prolyl cis-trans isomerase FKBP3	2.03	2.22
A2RTX5	*TARSL2*	Probable threonine--tRNA ligase 2, cytoplasmic	2.55	2.21
Q96CP2	*FLYWCH2*	FLYWCH family member 2	2.36	2.21
P68363	*TUBA1B*	Tubulin alpha-1B chain	2.41	2.20
Q9P0U3	*SENP1*	Sentrin-specific protease 1	2.57	2.20
P60842	*EIF4A1*	Eukaryotic initiation factor 4A-I	2.16	2.20
Q00169	*PITPNA*	Phosphatidylinositol transfer protein alpha isoform	3.45	2.18
O76003	*GLRX3*	Glutaredoxin-3	2.68	2.16
Q86V48	*LUZP1*	Leucine zipper protein 1	2.86	2.16
Q71RC2	*LARP4*	La-related protein 4	3.00	2.16
O76024	*WFS1*	Wolframin	2.54	2.15
Q8NFW8	*CMAS*	N-acylneuraminate cytidylyltransferase	2.81	2.15
O94992	*HEXIM1*	Protein HEXIM1	2.32	2.14
Q8IYI6	*EXOC8*	Exocyst complex component 8	2.49	2.14
P08238	*HSP90AB1*	Heat shock protein HSP 90-beta	2.17	2.14
O43583	*DENR*	Density-regulated protein	2.35	2.13
Q13613	*MTMR1*	Myotubularin-related protein 1	2.38	2.12
Q96T76	*MMS19*	MMS19 nucleotide excision repair protein homolog	3.98	2.11
O43264	*ZW10*	Centromere/kinetochore protein zw10 homolog	2.50	2.10
P37802	*TAGLN2*	Transgelin-2	2.26	2.10
Q14247	*CTTN*	Src substrate cortactin	2.13	2.09
Q00535	*CDK5*	Cyclin-dependent-like kinase 5	2.87	2.09
Q96KC8	*DNAJC1*	DnaJ homolog subfamily C member 1	2.01	2.08
O60879	*DIAPH2*	Protein diaphanous homolog 2	3.11	2.08
Q504Q3	*PAN2*	PAB-dependent poly(A)-specific ribonuclease subunit PAN2	2.21	2.08
P09936	*UCHL1*	Ubiquitin carboxyl-terminal hydrolase isozyme L1	2.97	2.07
Q9BRA2	*TXNDC17*	Thioredoxin domain-containing protein 17	2.06	2.06

P04406	*GAPDH*	Glyceraldehyde-3-phosphate dehydrogenase	3.09	2.06
Q15819	*UBE2V2*	Ubiquitin-conjugating enzyme E2 variant 2	2.58	2.06
Q9UBE0	*SAE1*	SUMO-activating enzyme subunit 1	2.73	2.05
P50990	*CCT8*	T-complex protein 1 subunit theta	2.55	2.05
Q92667	*AKAP1*	A-kinase anchor protein 1, mitochondrial	3.09	2.03
P19623	*SRM*	Spermidine synthase	2.02	2.03
Q15042	*RAB3GAP1*	Rab3 GTPase-activating protein catalytic subunit	2.12	2.02
P61513	*RPL37A*	60S ribosomal protein L37a	2.56	2.01
P60900	*PSMA6*	Proteasome subunit alpha type-6	3.13	2.01
P62937	*PPIA*	Peptidyl-prolyl cis-trans isomerase A	5.08	2.01
Q9Y450	*HBS1L*	HBS1-like protein	3.14	2.01
Q14554	*PDIA5*	Protein disulfide-isomerase A5	2.11	2.00

Table VI-9: Proteins significantly outcompeted by a 10-fold excess of **OL** vs. 15 µM **DA-P3** in Hek293 cells.

Protein IDs	**Gene names**	**Protein names**	**-log$_{10}$(*p*-value)**	**log$_2$(enrichment)**
O75330	*HMMR*	Hyaluronan mediated motility receptor	2.58	5.31
Q16204	*CCDC6*	Coiled-coil domain-containing protein 6	2.82	5.00
P46821	*MAP1B*	Microtubule-associated protein 1B	2.77	4.90
Q6NUQ1	*RINT1*	RAD50-interacting protein 1	2.56	4.84
Q9BXB4	*OSBPL11*	Oxysterol-binding protein-related protein 11	2.00	4.83
Q00653	*NFKB2*	Nuclear factor NF-kappa-B p100 subunit	3.18	4.30
O60343	*TBC1D4*	TBC1 domain family member 4	2.46	4.21
Q8WX93	*PALLD*	Palladin	2.51	4.06
P35237	*SERPINB6*	Serpin B6	2.08	3.97
Q8ND24	*RNF214*	RING finger protein 214	2.08	3.95
Q7Z4H7	*HAUS6*	HAUS augmin-like complex subunit 6	2.94	3.93
P30519	*HMOX2*	Heme oxygenase 2	2.37	3.91
O43353	*RIPK2*	Receptor-interacting serine/threonine-protein kinase 2	2.04	3.89
Q66K14	*TBC1D9B*	TBC1 domain family member 9B	3.28	3.88
Q8NBF2	*NHLRC2*	NHL repeat-containing protein 2	3.00	3.88
P56962	*STX17*	Syntaxin-17	2.38	3.77
Q7Z3T8	*ZFYVE16*	Zinc finger FYVE domain-containing protein 16	2.34	3.77
A1X283	*SH3PXD2B*	SH3 and PX domain-containing protein 2B	2.32	3.76
Q8TD19	*NEK9*	Serine/threonine-protein kinase Nek9	2.65	3.75
Q9UPQ9	*TNRC6B*	Trinucleotide repeat-containing gene 6B protein	2.92	3.65
P40763	*STAT3*	Signal transducer and activator of transcription 3	3.61	3.64
P19525	*EIF2AK2*	Interferon-induced, double-stranded RNA-activated protein kinase	2.37	3.61
Q8IXW5	*RPAP2*	Putative RNA polymerase II subunit B1 CTD phosphatase RPAP2	2.76	3.60
O95817	*BAG3*	BAG family molecular chaperone regulator 3	4.59	3.58
Q7Z2Z2	*EFTUD1*	Elongation factor Tu GTP-binding domain-containing protein 1	3.30	3.57
P09132	*SRP19*	Signal recognition particle 19 kDa protein	2.14	3.54
Q9UBF8	*PI4KB*	Phosphatidylinositol 4-kinase beta	2.77	3.53
O60547	*GMDS*	GDP-mannose 4,6 dehydratase	4.53	3.51
P15170	*GSPT1*	Eukaryotic peptide chain release factor GTP-binding subunit ERF3A	3.02	3.50
Q9NZT2	*OGFR*	Opioid growth factor receptor	2.66	3.50
Q8N6T3	*ARFGAP1*	ADP-ribosylation factor GTPase-activating protein 1	2.33	3.48
Q96GA3	*LTV1*	Protein LTV1 homolog	2.42	3.48
O94830	*DDHD2*	Phospholipase DDHD2	2.42	3.44
Q9Y4K3	*TRAF6*	TNF receptor-associated factor 6	4.03	3.42
P22059	*OSBP*	Oxysterol-binding protein 1	2.46	3.41
Q66K74	*MAP1S*	Microtubule-associated protein 1S	2.62	3.40
P51617	*IRAK1*	Interleukin-1 receptor-associated kinase 1	2.98	3.38
Q8IWC1	*MAP7D3*	MAP7 domain-containing protein 3	2.57	3.38
Q9BZX2	*UCK2*	Uridine-cytidine kinase 2	2.67	3.37
Q9H910	*HN1L*	Hematological and neurological expressed 1-like protein	2.08	3.36
Q96P47	*AGAP3*	Arf-GAP with GTPase, ANK repeat and PH domain-containing protein 3	3.25	3.36
Q96KB5	*PBK*	Lymphokine-activated killer T-cell-originated protein kinase	4.24	3.36
O75170	*PPP6R2*	Serine/threonine-protein phosphatase 6 regulatory subunit 2	3.05	3.35
Q9NT62	*ATG3*	Ubiquitin-like-conjugating enzyme ATG3	3.60	3.33
Q8TBM8	*DNAJB14*	DnaJ homolog subfamily B member 14	2.10	3.33
Q92625	*ANKS1A*	Ankyrin repeat and SAM domain-containing protein 1A	2.53	3.31
O15121	*DEGS1*	Sphingolipid delta(4)-desaturase DES1	2.45	3.31
Q5SQN1	*SNAP47*	Synaptosomal-associated protein 47	2.23	3.29
Q9UNY4	*TTF2*	Transcription termination factor 2	3.05	3.24
Q9NQ88	*TIGAR*	Fructose-2,6-bisphosphatase TIGAR	2.29	3.23
Q6P1Q9	*METTL2B*	Methyltransferase-like protein 2B	2.79	3.22
P19174	*PLCG1*	1-phosphatidylinositol 4,5-bisphosphate phosphodiesterase gamma-1	2.35	3.21
Q9NPH2	*ISYNA1*	Inositol-3-phosphate synthase 1	3.00	3.19
Q9Y5T5	*USP16*	Ubiquitin carboxyl-terminal hydrolase 16	2.42	3.19

Q9UL63	*MKLN1*	Muskelin	2.36	3.16
Q9HD26	*GOPC*	Golgi-associated PDZ and coiled-coil motif-containing protein	3.35	3.12
O43303	*CCP110*	Centriolar coiled-coil protein of 110 kDa	2.74	3.09
Q969V6	*MKL1*	MKL/myocardin-like protein 1	2.68	3.08
Q9NQW6	*ANLN*	Actin-binding protein anillin	2.08	3.07
A0MZ66	*KIAA1598*	Shootin-1	2.56	3.07
Q96SK2	*TMEM209*	Transmembrane protein 209	2.09	3.06
Q5T5U3	*ARHGAP21*	Rho GTPase-activating protein 21	2.03	3.06
Q15003	*NCAPH*	Condensin complex subunit 2	4.25	3.02
O14976	*GAK*	Cyclin-G-associated kinase	2.01	2.99
Q9H6T3	*RPAP3*	RNA polymerase II-associated protein 3	3.05	2.97
Q5SWX8	*ODR4*	Protein odr-4 homolog	2.34	2.93
Q86UK7	*ZNF598*	Zinc finger protein 598	2.27	2.90
P13807	*GYS1*	Glycogen [starch] synthase, muscle	3.41	2.88
P48506	*GCLC*	Glutamate--cysteine ligase catalytic subunit	2.32	2.87
Q7Z5L2	*R3HCC1L*	Coiled-coil domain-containing protein R3HCC1L	2.69	2.87
Q5T6F2	*UBAP2*	Ubiquitin-associated protein 2	2.70	2.86
Q9NW68	*BSDC1*	BSD domain-containing protein 1	2.11	2.84
O43683	*BUB1*	Mitotic checkpoint serine/threonine-protein kinase BUB1	2.21	2.81
Q9Y2V2	*CARHSP1*	Calcium-regulated heat stable protein 1	2.69	2.81
Q96CX2	*KCTD12*	BTB/POZ domain-containing protein KCTD12	3.52	2.80
Q14694	*USP10*	Ubiquitin carboxyl-terminal hydrolase 10	2.13	2.79
Q69YQ0	*SPECC1L*	Cytospin-A	3.29	2.79
Q8N573	*OXR1*	Oxidation resistance protein 1	2.49	2.77
O00178	*GTPBP1*	GTP-binding protein 1	2.69	2.76
O95336	*PGLS*	6-phosphogluconolactonase	3.03	2.76
O43396	*TXNL1*	Thioredoxin-like protein 1	2.44	2.76
Q8WZA9	*IRGQ*	Immunity-related GTPase family Q protein	2.96	2.74
Q96R06	*SPAG5*	Sperm-associated antigen 5	3.36	2.73
P0DN79	*CBS*	Cystathionine beta-synthase	3.11	2.72
O95793	*STAU1*	Double-stranded RNA-binding protein Staufen homolog 1	3.27	2.69
Q9NQX3	*GPHN*	Gephyrin	2.98	2.68
Q9H019	*MTFR1L*	Mitochondrial fission regulator 1-like	2.13	2.67
P53384	*NUBP1*	Cytosolic Fe-S cluster assembly factor NUBP1	3.42	2.66
O43318	*MAP3K7*	Mitogen-activated protein kinase kinase kinase 7	2.80	2.65
Q6PJG6	*BRAT1*	BRCA1-associated ATM activator 1	2.49	2.63
Q5JSZ5	*PRRC2B*	Protein PRRC2B	3.44	2.63
Q16352	*INA*	Alpha-internexin	2.24	2.63
Q13596	*SNX1*	Sorting nexin-1	2.63	2.63
Q9H3K6	*BOLA2*	BolA-like protein 2	2.88	2.61
Q9HDC5	*JPH1*	Junctophilin-1	2.24	2.60
Q15417	*CNN3*	Calponin-3	2.91	2.60
P04035	*HMGCR*	3-hydroxy-3-methylglutaryl-coenzyme A reductase	2.43	2.59
Q9NUQ3	*TXLNG*	Gamma-taxilin	3.68	2.58
Q9C0C9	*UBE2O*	E2/E3 hybrid ubiquitin-protein ligase UBE2O	3.02	2.58
P17812	*CTPS1*	CTP synthase 1	2.41	2.58
Q86VQ1	*GLCCI1*	Glucocorticoid-induced transcript 1 protein	2.06	2.57
Q8ND83	*SLAIN1*	SLAIN motif-containing protein 1	2.15	2.57
Q9NYZ3	*GTSE1*	G2 and S phase-expressed protein 1	2.45	2.56
Q86WB0	*ZC3HC1*	Nuclear-interacting partner of ALK	3.24	2.54
P20839	*IMPDH1*	Inosine-5-monophosphate dehydrogenase 1	2.24	2.54
Q92551	*IP6K1*	Inositol hexakisphosphate kinase 1	2.55	2.54
O60610	*DIAPH1*	Protein diaphanous homolog 1	2.05	2.53
Q9UGP4	*LIMD1*	LIM domain-containing protein 1	3.41	2.53
Q9BWH6	*RPAP1*	RNA polymerase II-associated protein 1	2.04	2.51
O75122	*CLASP2*	CLIP-associating protein 2	3.09	2.50
Q9UNF1	*MAGED2*	Melanoma-associated antigen D2	3.98	2.48
Q5TAX3	*ZCCHC11*	Terminal uridylyltransferase 4	2.14	2.47
Q9UJW0	*DCTN4*	Dynactin subunit 4	3.15	2.47
P27816	*MAP4*	Microtubule-associated protein 4	3.38	2.46
P52732	*KIF11*	Kinesin-like protein KIF11	2.93	2.44
Q14C86	*GAPVD1*	GTPase-activating protein and VPS9 domain-containing protein 1	2.71	2.44
P12081	*HARS*	Histidine--tRNA ligase, cytoplasmic	2.10	2.43
Q9BTE3	*MCMBP*	Mini-chromosome maintenance complex-binding protein	3.37	2.42
Q9H7E9	*C8orf33*	UPF0488 protein C8orf33	5.72	2.41
Q9NP72	*RAB18*	Ras-related protein Rab-18	2.40	2.41
O43379	*WDR62*	WD repeat-containing protein 62	2.28	2.40
Q9BSJ8	*ESYT1*	Extended synaptotagmin-1	2.24	2.40
Q9UPY3	*DICER1*	Endoribonuclease Dicer	2.47	2.40
Q9P1Z2	*CALCOCO1*	Calcium-binding and coiled-coil domain-containing protein 1	2.49	2.39
Q8N2G8	*GHDC*	GH3 domain-containing protein	2.38	2.37
Q9H4A3	*WNK1*	Serine/threonine-protein kinase WNK1	2.16	2.37
O75410	*TACC1*	Transforming acidic coiled-coil-containing protein 1	3.04	2.37

Q5T4S7	*UBR4*	E3 ubiquitin-protein ligase UBR4	2.06	2.37
O75663	*TIPRL*	TIP41-like protein	3.05	2.35
Q15654	*TRIP6*	Thyroid receptor-interacting protein 6	2.36	2.34
Q8TEW0	*PARD3*	Partitioning defective 3 homolog	2.07	2.34
O95163	*IKBKAP*	Elongator complex protein 1	2.06	2.33
Q06124	*PTPN11*	Tyrosine-protein phosphatase non-receptor type 11	4.43	2.33
P61758	*VBP1*	Prefoldin subunit 3	3.06	2.33
Q9H2G2	*SLK*	STE20-like serine/threonine-protein kinase	2.68	2.30
Q8TC07	*TBC1D15*	TBC1 domain family member 15	2.43	2.30
A0AVT1	*UBA6*	Ubiquitin-like modifier-activating enzyme 6	3.74	2.30
Q96IZ0	*PAWR*	PRKC apoptosis WT1 regulator protein	2.27	2.29
Q9BVS4	*RIOK2*	Serine/threonine-protein kinase RIO2	3.49	2.28
P28290	*SSFA2*	Sperm-specific antigen 2	2.45	2.27
Q15005	*SPCS2*	Signal peptidase complex subunit 2	3.30	2.26
Q96SB4	*SRPK1*	SRSF protein kinase 1	2.03	2.25
P54105	*CLNS1A*	Methylosome subunit pICln	2.32	2.23
Q16799	*RTN1*	Reticulon-1	3.69	2.22
Q5H9R7	*PPP6R3*	Serine/threonine-protein phosphatase 6 regulatory subunit 3	2.40	2.20
E7EVH7	*KLC1*	Kinesin light chain 1	2.37	2.20
Q14247	*CTTN*	Src substrate cortactin	2.99	2.20
Q8TEQ6	*GEMIN5*	Gem-associated protein 5	2.08	2.19
Q06210	*GFPT1*	Glutamine--fructose-6-phosphate aminotransferase [isomerizing] 1	2.14	2.19
Q9UJY5	*GGA1*	ADP-ribosylation factor-binding protein GGA1	2.87	2.18
Q9H9A6	*LRRC40*	Leucine-rich repeat-containing protein 40	3.01	2.18
Q9UGV2	*NDRG3*	Protein NDRG3	2.22	2.16
Q9BV44	*THUMPD3*	THUMP domain-containing protein 3	3.60	2.15
P41227	*NAA10*	N-alpha-acetyltransferase 10	2.45	2.12
P04080	*CSTB*	Cystatin-B	2.76	2.11
O76024	*WFS1*	Wolframin	3.23	2.11
Q53EZ4	*CEP55*	Centrosomal protein of 55 kDa	2.46	2.10
A6NDG6	*PGP*	Phosphoglycolate phosphatase	2.40	2.10
O94967	*WDR47*	WD repeat-containing protein 47	2.49	2.10
Q8WWM7	*ATXN2L*	Ataxin-2-like protein	3.43	2.09
Q8TEA1	*NSUN6*	Putative methyltransferase NSUN6	2.22	2.09
Q14738	*PPP2R5D*	Serine/threonine-protein phosphatase 2A 56 kDa regulatory subunit delta isoform	3.57	2.09
Q9H0B6	*KLC2*	Kinesin light chain 2	3.55	2.07
Q9BYB4	*GNB1L*	Guanine nucleotide-binding protein subunit beta-like protein 1	2.02	2.07
Q8N9N8	*EIF1AD*	Probable RNA-binding protein EIF1AD	2.13	2.07
Q9Y4K4	*MAP4K5*	Mitogen-activated protein kinase kinase kinase kinase 5	2.29	2.07
O00233	*PSMD9*	26S proteasome non-ATPase regulatory subunit 9	2.55	2.06
Q96II8	*LRCH3*	Leucine-rich repeat and calponin homology domain-containing protein 3	2.16	2.05
P48634	*PRRC2A*	Protein PRRC2A	2.46	2.05
Q14534	*SQLE*	Squalene monooxygenase	2.07	2.05
Q8IW35	*CEP97*	Centrosomal protein of 97 kDa	2.86	2.04
P23921	*RRM1*	Ribonucleoside-diphosphate reductase large subunit	3.98	2.04
O95801	*TTC4*	Tetratricopeptide repeat protein 4	3.12	2.04
P08243	*ASNS*	Asparagine synthetase [glutamine-hydrolyzing]	2.46	2.04
Q9Y2U8	*LEMD3*	Inner nuclear membrane protein Man1	2.32	2.04
O43164	*PJA2*	E3 ubiquitin-protein ligase Praja-2	2.60	2.02
Q6P158	*DHX57*	Putative ATP-dependent RNA helicase DHX57	2.44	2.01
P55786	*NPEPPS*	Puromycin-sensitive aminopeptidase	3.12	2.00
Q96GS4	*C17orf59*	Uncharacterized protein C17orf59	3.21	2.00
P28161	*GSTM2*	Glutathione S-transferase Mu 2	2.74	2.00

Table VI-10: Proteins significantly outcompeted by a 10-fold excess of **CP** vs. 15 µM **DA-P3** in Hek293 cells.

Protein IDs	**Gene names**	**Protein names**	**-log$_{10}$(*p*-value)**	**log$_2$(enrichment)**
Q16204	*CCDC6*	Coiled-coil domain-containing protein 6	4.78	6.80
O15270	*SPTLC2*	Serine palmitoyltransferase 2	2.36	6.76
Q5JRA6	*MIA3*	Melanoma inhibitory activity protein 3	4.17	6.65
P22059	*OSBP*	Oxysterol-binding protein 1	2.18	6.38
Q6P2H3	*CEP85*	Centrosomal protein of 85 kDa	4.23	6.37
O60566	*BUB1B*	Mitotic checkpoint serine/threonine-protein kinase BUB1 beta	3.02	6.11
Q86XL3	*ANKLE2*	Ankyrin repeat and LEM domain-containing protein 2	2.31	6.08
O95817	*BAG3*	BAG family molecular chaperone regulator 3	3.23	5.98
Q9NQS7	*INCENP*	Inner centromere protein	4.92	5.92
O75330	*HMMR*	Hyaluronan mediated motility receptor	2.80	5.84
Q8IWC1	*MAP7D3*	MAP7 domain-containing protein 3	2.89	5.80
Q7Z3T8	*ZFYVE16*	Zinc finger FYVE domain-containing protein 16	2.29	5.64
P29372	*MPG*	DNA-3-methyladenine glycosylase	2.58	5.52
P46821	*MAP1B*	Microtubule-associated protein 1B	2.70	5.47

O60664	*PLIN3*	Perilipin-3	2.32	5.44
Q92575	*UBXN4*	UBX domain-containing protein 4	3.61	5.43
Q5VV42	*CDKAL1*	Threonylcarbamoyladenosine tRNA methylthiotransferase	2.91	5.41
Q9Y4P3	*TBL2*	Transducin beta-like protein 2	3.01	5.31
P48634	*PRRC2A*	Protein PRRC2A	2.01	5.25
P82094	*TMF1*	TATA element modulatory factor	2.58	5.25
Q86UK7	*ZNF598*	Zinc finger protein 598	2.77	5.19
Q96KC8	*DNAJC1*	DnaJ homolog subfamily C member 1	4.28	5.18
Q92615	*LARP4B*	La-related protein 4B	2.40	5.12
Q14694	*USP10*	Ubiquitin carboxyl-terminal hydrolase 10	2.42	5.01
Q8N2K0	*ABHD12*	Monoacylglycerol lipase ABHD12	2.59	4.97
Q9UJC3	*HOOK1*	Protein Hook homolog 1	3.45	4.93
Q14807	*KIF22*	Kinesin-like protein KIF22	2.69	4.87
Q8ND24	*RNF214*	RING finger protein 214	3.98	4.86
Q96P47	*AGAP3*	Arf-GAP with GTPase, ANK repeat and PH domain-containing protein 3	2.91	4.84
Q8NFH5	*NUP35*	Nucleoporin NUP53	3.25	4.83
Q96R06	*SPAG5*	Sperm-associated antigen 5	2.91	4.81
Q96GA3	*LTV1*	Protein LTV1 homolog	3.54	4.81
Q96PC5	*MIA2*	Melanoma inhibitory activity protein 2	2.59	4.79
Q8WXH0	*SYNE2*	Nesprin-2	2.25	4.77
P56962	*STX17*	Syntaxin-17	2.93	4.76
Q66K74	*MAP1S*	Microtubule-associated protein 1S	3.72	4.68
Q8NBF2	*NHLRC2*	NHL repeat-containing protein 2	2.39	4.67
O14976	*GAK*	Cyclin-G-associated kinase	2.28	4.61
Q8IY17	*PNPLA6*	Neuropathy target esterase	2.35	4.59
Q9BZE9	*ASPSCR1*	Tether containing UBX domain for GLUT4	2.39	4.55
Q32MZ4	*LRRFIP1*	Leucine-rich repeat flightless-interacting protein 1	2.22	4.54
Q16799	*RTN1*	Reticulon-1	3.65	4.53
P09132	*SRP19*	Signal recognition particle 19 kDa protein	3.47	4.53
Q7Z4H7	*HAUS6*	HAUS augmin-like complex subunit 6	3.48	4.53
Q8WU90	*ZC3H15*	Zinc finger CCCH domain-containing protein 15	2.50	4.42
P40763	*STAT3*	Signal transducer and activator of transcription 3	4.10	4.41
P19174	*PLCG1*	1-phosphatidylinositol 4,5-bisphosphate phosphodiesterase gamma-1	2.76	4.22
P04035	*HMGCR*	3-hydroxy-3-methylglutaryl-coenzyme A reductase	5.10	4.22
Q9UHR4	*BAIAP2L1*	Brain-specific angiogenesis inhibitor 1-associated protein 2-like protein 1	2.97	4.19
P51148	*RAB5C*	Ras-related protein Rab-5C	2.25	4.15
A0MZ66	*KIAA1598*	Shootin-1	2.48	4.13
Q66K14	*TBC1D9B*	TBC1 domain family member 9B	2.37	4.09
Q8WX93	*PALLD*	Palladin	2.17	4.04
Q9UL15	*BAG5*	BAG family molecular chaperone regulator 5	2.96	4.03
Q13111	*CHAF1A*	Chromatin assembly factor 1 subunit A	2.74	4.02
Q5JSH3	*WDR44*	WD repeat-containing protein 44	2.50	4.02
O14965	*AURKA*	Aurora kinase A	2.55	4.02
P49137	*MAPKAPK2*	MAP kinase-activated protein kinase 2	2.56	3.96
Q9UL63	*MKLN1*	Muskelin	2.42	3.95
Q6P1Q9	*METTL2B*	Methyltransferase-like protein 2B	2.46	3.94
Q96SK2	*TMEM209*	Transmembrane protein 209	3.27	3.93
Q9BZF3	*OSBPL6*	Oxysterol-binding protein-related protein 6	2.78	3.89
P46109	*CRKL*	Crk-like protein	4.54	3.85
Q9BSJ8	*ESYT1*	Extended synaptotagmin-1	5.55	3.85
O60610	*DIAPH1*	Protein diaphanous homolog 1	2.32	3.82
P37198	*NUP62*	Nuclear pore glycoprotein p62	2.14	3.81
P20290	*BTF3*	Transcription factor BTF3	2.83	3.80
O95793	*STAU1*	Double-stranded RNA-binding protein Staufen homolog 1	2.97	3.80
Q5T6F2	*UBAP2*	Ubiquitin-associated protein 2	2.74	3.77
Q9UPQ9	*TNRC6B*	Trinucleotide repeat-containing gene 6B protein	2.15	3.76
O43303	*CCP110*	Centriolar coiled-coil protein of 110 kDa	2.75	3.72
P19525	*EIF2AK2*	Interferon-induced, double-stranded RNA-activated protein kinase	2.69	3.72
Q69YH5	*CDCA2*	Cell division cycle-associated protein 2	2.23	3.70
Q9NT62	*ATG3*	Ubiquitin-like-conjugating enzyme ATG3	3.46	3.69
Q99661	*KIF2C*	Kinesin-like protein KIF2C	3.29	3.68
Q6WKZ4	*RAB11FIP1*	Rab11 family-interacting protein 1	4.16	3.67
Q8NHH9	*ATL2*	Atlastin-2	3.47	3.66
Q8TD19	*NEK9*	Serine/threonine-protein kinase Nek9	3.58	3.65
P61160	*ACTR2*	Actin-related protein 2	2.46	3.64
Q9BZX2	*UCK2*	Uridine-cytidine kinase 2	3.24	3.64
Q9H019	*MTFR1L*	Mitochondrial fission regulator 1-like	2.68	3.61
O14531	*DPYSL4*	Dihydropyrimidinase-related protein 4	2.67	3.59
O60318	*MCM3AP*	Germinal-center associated nuclear protein	2.76	3.59
O43683	*BUB1*	Mitotic checkpoint serine/threonine-protein kinase BUB1	2.28	3.56

Q4VCS5	*AMOT*	Angiomotin	2.39	3.56
Q15003	*NCAPH*	Condensin complex subunit 2	3.21	3.53
P16615	*ATP2A2*	Sarcoplasmic/endoplasmic reticulum calcium ATPase 2	3.08	3.47
Q8IWZ3	*ANKHD1*	Ankyrin repeat and KH domain-containing protein 1	2.69	3.46
P31153	*MAT2A*	S-adenosylmethionine synthase isoform type-2	2.98	3.45
Q8WZA9	*IRGQ*	Immunity-related GTPase family Q protein	2.91	3.43
Q9HCU5	*PREB*	Prolactin regulatory element-binding protein	2.12	3.43
Q9BVS4	*RIOK2*	Serine/threonine-protein kinase RIO2	3.01	3.39
Q5SWX8	*ODR4*	Protein odr-4 homolog	3.52	3.39
Q9Y5A7	*NUB1*	NEDD8 ultimate buster 1	3.29	3.36
Q9NZZ3	*CHMP5*	Charged multivesicular body protein 5	2.09	3.33
O75410	*TACC1*	Transforming acidic coiled-coil-containing protein 1	3.33	3.32
Q9ULX3	*NOB1*	RNA-binding protein NOB1	2.54	3.31
Q14318	*FKBP8*	Peptidyl-prolyl cis-trans isomerase FKBP8	2.30	3.30
P09211	*GSTP1*	Glutathione S-transferase P	3.53	3.29
O75044	*SRGAP2*	SLIT-ROBO Rho GTPase-activating protein 2	2.09	3.29
Q8N2G8	*GHDC*	GH3 domain-containing protein	3.35	3.27
Q99873	*PRMT1*	Protein arginine N-methyltransferase 1	2.28	3.25
Q12756	*KIF1A*	Kinesin-like protein KIF1A	2.93	3.23
Q15417	*CNN3*	Calponin-3	3.45	3.20
P42166	*TMPO*	Lamina-associated polypeptide 2, isoform alpha	2.39	3.17
Q14C86	*GAPVD1*	GTPase-activating protein and VPS9 domain-containing protein 1	2.45	3.16
P20810	*CAST*	Calpastatin	2.91	3.16
Q15654	*TRIP6*	Thyroid receptor-interacting protein 6	2.03	3.15
Q9HBM0	*VEZT*	Vezatin	2.22	3.14
Q9H6S0	*YTHDC2*	Probable ATP-dependent RNA helicase YTHDC2	2.67	3.13
Q08378	*GOLGA3*	Golgin subfamily A member 3	2.77	3.11
O00233	*PSMD9*	26S proteasome non-ATPase regulatory subunit 9	3.11	3.10
Q9UNY4	*TTF2*	Transcription termination factor 2	2.74	3.06
P51617	*IRAK1*	Interleukin-1 receptor-associated kinase 1	2.30	3.04
P02545	*LMNA*	Prelamin-A/C	2.30	3.02
Q9NRG9	*AAAS*	Aladin	2.22	2.98
Q8N0X7	*SPG20*	Spartin	2.22	2.97
Q99640	*PKMYT1*	Membrane-associated tyrosine- and threonine-specific cdc2-inhibitory kinase	2.34	2.96
Q92667	*AKAP1*	A-kinase anchor protein 1, mitochondrial	2.07	2.96
Q9Y266	*NUDC*	Nuclear migration protein nudC	2.71	2.95
Q7Z2Z2	*EFTUD1*	Elongation factor Tu GTP-binding domain-containing protein 1	3.18	2.94
O43491	*EPB41L2*	Band 4.1-like protein 2	2.77	2.89
P50402	*EMD*	Emerin	3.79	2.88
Q5T8D3	*ACBD5*	Acyl-CoA-binding domain-containing protein 5	2.10	2.85
Q14126	*DSG2*	Desmoglein-2	3.27	2.84
Q71RC2	*LARP4*	La-related protein 4	2.21	2.82
P49792	*RANBP2*	E3 SUMO-protein ligase RanBP2	2.58	2.81
P49069	*CAMLG*	Calcium signal-modulating cyclophilin ligand	2.32	2.79
Q9H2G2	*SLK*	STE20-like serine/threonine-protein kinase	2.35	2.79
Q53GS7	*GLE1*	Nucleoporin GLE1	2.55	2.76
O75475	*PSIP1*	PC4 and SFRS1-interacting protein	2.82	2.76
P13804	*ETFA*	Electron transfer flavoprotein subunit alpha, mitochondrial	2.17	2.74
Q6PKG0	*LARP1*	La-related protein 1	3.47	2.74
Q96F86	*EDC3*	Enhancer of mRNA-decapping protein 3	3.95	2.73
Q8N1F8	*STK11IP*	Serine/threonine-protein kinase 11-interacting protein	2.68	2.73
O95336	*PGLS*	6-phosphogluconolactonase	3.00	2.72
Q9Y277	*VDAC3*	Voltage-dependent anion-selective channel protein 3	2.67	2.72
Q9Y5X3	*SNX5*	Sorting nexin-5	2.31	2.71
Q92545	*TMEM131*	Transmembrane protein 131	2.29	2.71
Q9Y2U8	*LEMD3*	Inner nuclear membrane protein Man1	2.51	2.68
Q9UGP4	*LIMD1*	LIM domain-containing protein 1	2.92	2.68
Q9Y613	*FHOD1*	FH1/FH2 domain-containing protein 1	2.37	2.68
Q15005	*SPCS2*	Signal peptidase complex subunit 2	5.00	2.67
Q5JSZ5	*PRRC2B*	Protein PRRC2B	2.64	2.67
P18850	*ATF6*	Cyclic AMP-dependent transcription factor ATF-6 alpha	3.12	2.62
Q13310	*PABPC4*	Polyadenylate-binding protein 4	3.29	2.62
P54105	*CLNS1A*	Methylosome subunit pICln	2.68	2.58
Q9HDC5	*JPH1*	Junctophilin-1	2.50	2.55
P49721	*PSMB2*	Proteasome subunit beta type-2	3.30	2.54
Q7Z2K8	*GPRIN1*	G protein-regulated inducer of neurite outgrowth 1	2.24	2.53
P35659	*DEK*	Protein DEK	4.25	2.52
O75694	*NUP155*	Nuclear pore complex protein Nup155	2.76	2.50
Q8N573	*OXR1*	Oxidation resistance protein 1	2.55	2.48
P27816	*MAP4*	Microtubule-associated protein 4	3.67	2.48
P11171	*EPB41*	Protein 4.1	2.20	2.47
A8CG34	*POM121C*	Nuclear envelope pore membrane protein POM 121C	2.35	2.46

O75083	*WDR1*	WD repeat-containing protein 1	2.01	2.44
Q8NHV4	*NEDD1*	Protein NEDD1	2.56	2.44
Q9BZF1	*OSBPL8*	Oxysterol-binding protein-related protein 8	2.05	2.42
Q3KQU3	*MAP7D1*	MAP7 domain-containing protein 1	2.15	2.41
P01891	*HLA-A*	HLA class I histocompatibility antigen, A-68 alpha chain	2.25	2.38
O15344	*MID1*	E3 ubiquitin-protein ligase Midline-1	2.56	2.37
O95757	*HSPA4L*	Heat shock 70 kDa protein 4L	3.77	2.37
Q8WWM7	*ATXN2L*	Ataxin-2-like protein	4.21	2.36
Q96AG4	*LRRC59*	Leucine-rich repeat-containing protein 59	2.57	2.36
O14802	*POLR3A*	DNA-directed RNA polymerase III subunit RPC1	2.13	2.36
Q9BTE3	*MCMBP*	Mini-chromosome maintenance complex-binding protein	2.56	2.34
Q8N3C0	*ASCC3*	Activating signal cointegrator 1 complex subunit 3	2.56	2.33
Q99614	*TTC1*	Tetratricopeptide repeat protein 1	3.48	2.33
Q99961	*SH3GL1*	Endophilin-A2	2.66	2.33
P17858	*PFKL*	ATP-dependent 6-phosphofructokinase, liver type	2.53	2.30
Q9UGV2	*NDRG3*	Protein NDRG3	2.42	2.30
O43264	*ZW10*	Centromere/kinetochore protein zw10 homolog	2.03	2.30
O76003	*GLRX3*	Glutaredoxin-3	3.52	2.30
O76024	*WFS1*	Wolframin	2.62	2.30
O43318	*MAP3K7*	Mitogen-activated protein kinase kinase kinase 7	2.87	2.25
Q8WYP5	*AHCTF1*	Protein ELYS	3.25	2.24
P41250	*GARS*	Glycine--tRNA ligase	2.43	2.21
Q96T17	*MAP7D2*	MAP7 domain-containing protein 2	2.99	2.19
Q9H0B6	*KLC2*	Kinesin light chain 2	2.62	2.18
Q8IW35	*CEP97*	Centrosomal protein of 97 kDa	2.22	2.17
Q13283	*G3BP1*	Ras GTPase-activating protein-binding protein 1	2.32	2.16
P28290	*SSFA2*	Sperm-specific antigen 2	2.41	2.16
Q96CX2	*KCTD12*	BTB/POZ domain-containing protein KCTD12	2.19	2.16
P57740	*NUP107*	Nuclear pore complex protein Nup107	3.66	2.15
P51114	*FXR1*	Fragile X mental retardation syndrome-related protein 1	2.70	2.14
Q6PJG6	*BRAT1*	BRCA1-associated ATM activator 1	2.24	2.13
Q5UCC4	*EMC10*	ER membrane protein complex subunit 10	2.64	2.13
O43432	*EIF4G3*	Eukaryotic translation initiation factor 4 gamma 3	2.74	2.13
Q643R3	*LPCAT4*	Lysophospholipid acyltransferase LPCAT4	2.35	2.09
P11216	*PYGB*	Glycogen phosphorylase, brain form	2.11	2.08
P98194	*ATP2C1*	Calcium-transporting ATPase type 2C member 1	3.36	2.07
P08758	*ANXA5*	Annexin A5	2.97	2.04
O00161	*SNAP23*	Synaptosomal-associated protein 23	3.15	2.03
P53384	*NUBP1*	Cytosolic Fe-S cluster assembly factor NUBP1	2.49	2.03
Q9Y5Y2	*NUBP2*	Cytosolic Fe-S cluster assembly factor NUBP2	2.47	2.03
P52888	*THOP1*	Thimet oligopeptidase	2.58	2.02
Q02241	*KIF23*	Kinesin-like protein KIF23	2.83	2.02
Q9H4A3	*WNK1*	Serine/threonine-protein kinase WNK1	2.37	2.00